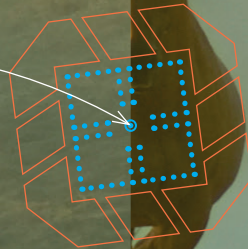




Immunity Unchained

Immune cells called T cells scavenge our body for cancerous cells and destroy them to prevent further spread of malignant disease. However, tumors are capable of escaping immune responses by restraining T-cell immunity at multiple sites in the body. The next frontier in cancer immunotherapy aims to dissect the modes of immune resistance to cancer therapy and design effective combination treatments to 'unchain' T-cell immunity and improve cancer survival.



Immunity Unchained

f. Dammeijer

IMPROVING CANCER
IMMUNOTHERAPY
BY TARGETING
THE TUMOR
MACRO-ENVIRONMENT

Immunity Unchained

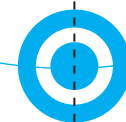
f. Dammeijer

DINSDAG 5 OKTOBER 2021 / 15.30 UUR

Erasmus MC
Professor Andries Querido zaal
Wytemaweg 80, Rotterdam
Nederland

INVITATIE
VOOR HET BIJWONEN VAN DE
OPENBARE VERDEDIGING VAN
HET PROEFSCHRIFT:
Immunity Unchained





Immunity Unchained
IMPROVING CANCER
IMMUNOTHERAPY
BY TARGETING
THE TUMOR
MACRO-ENVIRONMENT

F.H.W.P. DAMMEIJER
Stroveer 139, NL-3032 GB Rotterdam
T +31 6 38 55 16 20
f.dammeijer@erasmusmc.nl



Immunity Unchained


IMPROVING CANCER
IMMUNOTHERAPY
BY TARGETING THE TUMOR
MACRO-ENVIRONMENT



J. Dammeijer



**Immunity Unchained: Improving Cancer Immunotherapy
by targeting the Tumor Macro-Environment.**
ISBN: 978-94-6416-759-7

Cover-design and lay-out: Bureau Thiery  letje Thiery
Venlo, the Netherlands.
Print: Ridderprint, the Netherlands, www.ridderprint.nl

© **f. Dammeijer**

Rotterdam, the Netherlands, 2021.

All rights reserved. No parts of this thesis may be reproduced, stored in a retrieval system of any nature, or transmitted in any form or by any means, without permission of the author, or when appropriate, of the publishers of the publication.



Immunity Unchained

*Improving Cancer Immunotherapy
by targeting the Tumor Macro-Environment*

Het immuunsysteem ontketend

*Verbeteren van immuuntherapie bij kanker door
het moduleren van de tumor macro-omgeving*

Proefschrift



ter verkrijging van de graad van doctor aan de
Erasmus Universiteit Rotterdam
op gezag van de
rector magnificus

Prof. dr. A.L. Bredenoord

en volgens besluit van het College voor Promoties.
De openbare verdediging zal plaatsvinden op

dinsdag 5 oktober 2021 om 15.30 uur

door

Floris Hendrikus Wilhelmus Petrus Dammeijer

geboren te Maastricht

Erasmus University Rotterdam

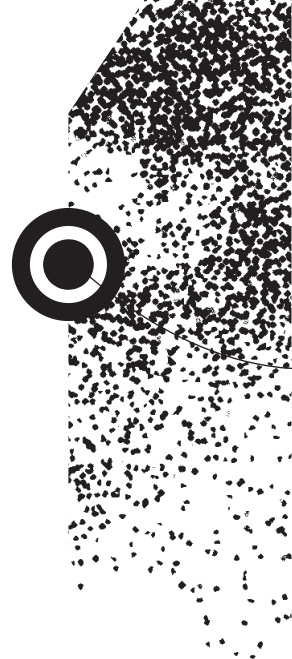


TABLE OF CONTENTS

PROMOTIECOMMISSIE

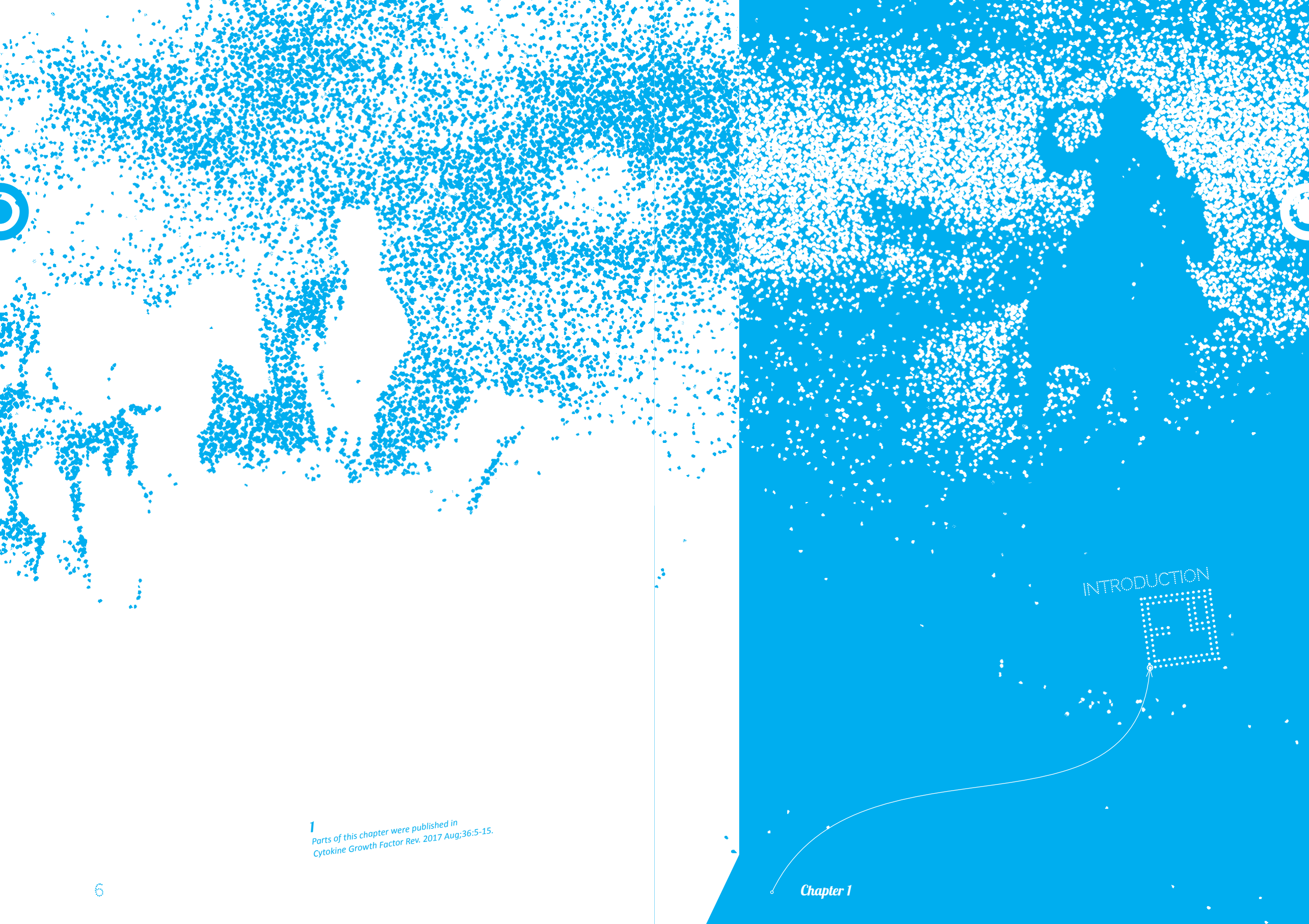
Promotoren

prof. dr. J.G.J.V. Aerts
prof. dr. R.W. Hendriks
prof. dr. T. van Hall


Overige leden

prof. dr. J.E.M.A. Debets
prof. dr. T.D. de Gruijl
dr. P.S. Adusumilli

Chapter 1	Introduction.	7
	<i>Parts of this chapter were published in Cytokine Growth Factor Rev. 2017 Aug;36:5-15.</i>	
PART A	NOVEL IMMUNOLOGICAL INSIGHTS INTO CHEMOTHERAPY AND IMMUNE-CHECKPOINT BLOCKADE	
Chapter 2	The PD-1/PD-L1-checkpoint restrains T-cell immunity in tumor-draining lymph nodes.	37
	<i>Cancer Cell. 2020 Nov 9;38(5):685-700.e8.</i>	
Chapter 3	Immune monitoring in mesothelioma patients identifies novel immune-modulatory functions of gemcitabine associating with clinical response.	83
	<i>EBioMedicine. 2020 Dec 22:103160.</i>	
PART B	IMPROVING THE EFFICACY OF CANCER VACCINES FOR SOLID TUMORS BY COMBINATION IMMUNOTHERAPY	
Chapter 4	The efficacy of tumor vaccines and cellular immunotherapies in non-small cell lung cancer: a systematic review and meta-analysis.	113
	<i>J Clin Oncol. 2016 Sep 10;34(26):3204-12.</i>	
Chapter 5	Depletion of tumor-associated macrophages with a CSF-1R kinase inhibitor enhances anti-tumor immunity and survival induced by dendritic cell immunotherapy.	139
	<i>Cancer Immunology Research. 2017 Jul;5(7):535-546.</i>	
Chapter 6	Dendritic cell vaccination and CD40-agonist combination therapy licenses T cell-dependent antitumor immunity in a pancreatic carcinoma murine model.	171
	<i>J Immunother Cancer. 2020 Jul;8(2):e000772.</i>	
Chapter 7	Low-dose JAK3-inhibition improves anti-tumor T-cell immunity and immunotherapy efficacy.	215
	<i>Submitted.</i>	
Chapter 8	Discussion.	245
Appendices	English Summary	269
	Nederlandse Samenvatting	277
	Dankwoord	285
	List of Publications	291
	About the Author	295
	About the Cover	301



1
Parts of this chapter were published in
Cytokine Growth Factor Rev. 2017 Aug;36:5-15.

INTRODUCTION


INTRODUCTION

Tumors are characterized by a complex ecology of neoplastic and non-neoplastic cells contributing to cancer evolution¹. Leukocytes are the major non-neoplastic cell population in cancer and were identified as early as 1986 by Dvorak describing tumors to be reminiscent of ‘wounds that never heal’². Since this observation, our knowledge of the interplay between cancer and immune cells has increased tremendously, culminating in the development and widespread implementation of cancer immunotherapy. Although a wide variety of cancer types are currently treated with immunotherapy, a majority of patients does not respond durably and inevitably develops disease recurrence³. The mechanisms underlying primary or acquired resistance in these patients are incompletely understood, nor do we understand why some patients show exceptional responses or even complete disease resolution. This introductory chapter will highlight recent concepts in tumor immunology that have emerged in the past decade that form the basis for future investigations aiming to improve immunotherapy efficacy. Finally, an outline of the thesis will be presented.

Hallmarks of cancer; the next generation.

Many years, cancer was considered a tumor-cell autonomous process resulting from a step-wise acquisition of mutations driving uncontrolled cell division⁴. At the start of the new millennium, Hanahan and Weinberg published their epitome entitled ‘the hallmarks of cancer’, dissecting the tumor cell traits required to drive neoplastic transformation and growth⁵. The work summarized in their review included the fundamental discoveries of targeted therapies such as antibodies (e.g. anti-VEGF) and small molecule inhibitors (e.g. EGFR-inhibitors) providing modes of precision medicine which were different from the existing modes of cancer treatment (Fig. 1A). The biological underpinnings of carcinogenesis proposed by Hanahan and Weinberg were updated a decade later, including the ‘emerging’ hallmarks of avoiding immune destruction by tumors and deregulation of cellular energetics fueling tumor growth⁶ (Fig. 1B).

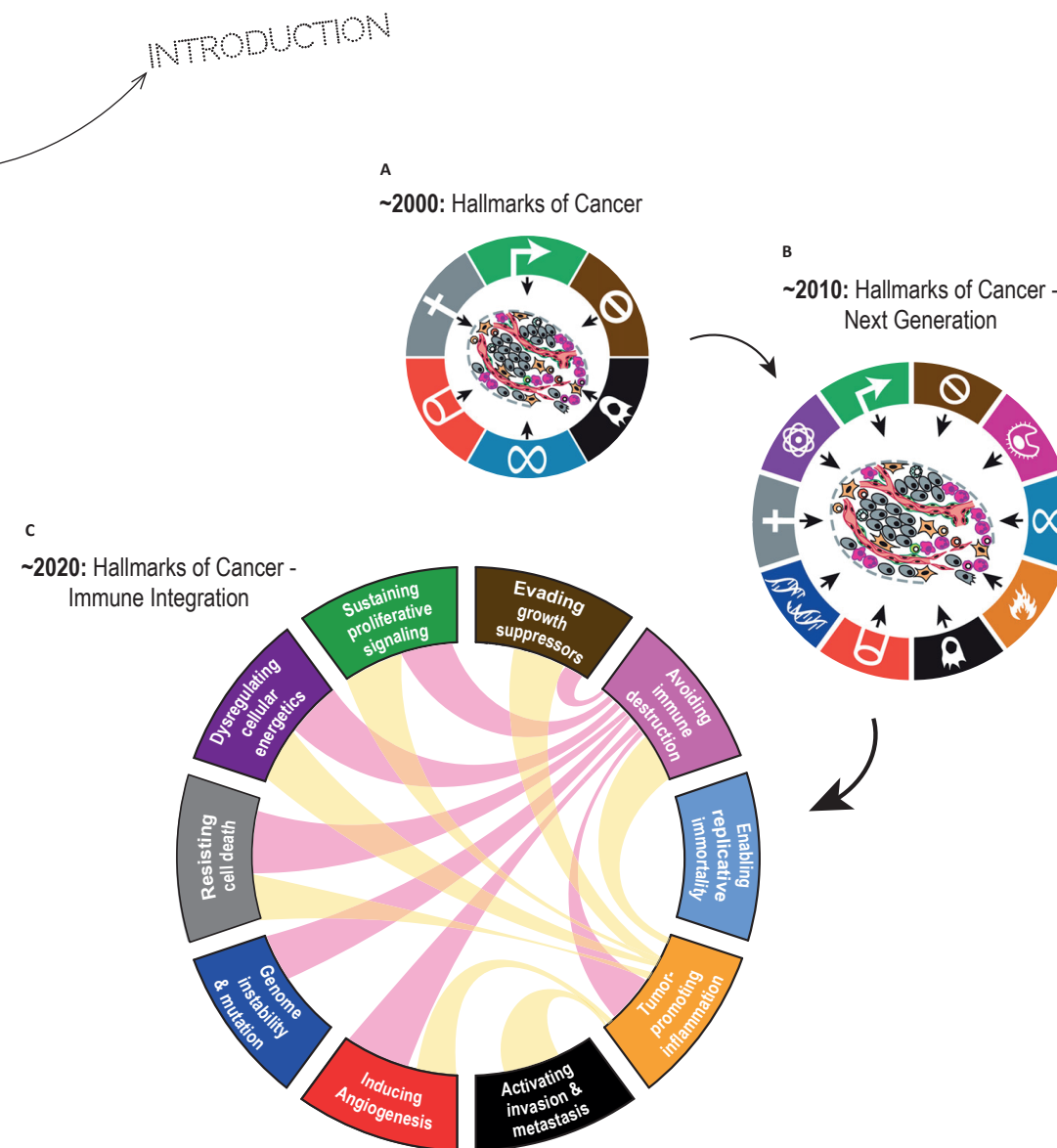


Figure 1. Immune escape and tumor-promoting inflammation as critical hallmarks of cancer formation and progression. (A) Oncogenesis results from a stepwise accumulation genetic alterations in a tumor-promoting environment, summarized by Hanahan & Weinberg, *Cell* in 2000. (B) In the following decades, more hallmarks were identified and subsequently included establishing a complex tumor microenvironment consisting of tumor- and non-tumor cells aiding cancer growth (Hanahan & Weinberg, *Cell* 2011). (C) In recent years, mechanisms underlying immune-escape (purple) and pro-tumoral inflammatory responses (yellow) were found to result from the same hallmarks inducing neoplastic growth.

Some of these traits had been identified nearly a century earlier, i.e. loss of antigen-presenting machinery in cancers during steady state and following immunotherapy^{7,8}, and aerobic glycolysis in the presence of sufficient oxygen⁹. However, their contribution to carcinogenesis has only been appreciated over the recent years. In addition, tumor-promoting inflammation was added as an 'enabling' characteristic, stemming from observations from chronic viral (e.g. HBV-associated hepatitis) and bacterial (e.g. helicobacter pylori-mediated gastritis) infections that are known to fuel neoplasia. Besides direct mutagenic properties of particular microorganisms, chronic production of pro-inflammatory cytokines and reactive-oxygen species (ROS) by immune cells has been found to promote cancer formation, revealing the paradoxical role of leukocytes in cancer (Fig 2)¹⁰⁻¹².

INTRODUCTION

Hallmarks of cancer revisited: towards immune integration.

Currently, our knowledge of the interplay between cancer and our immune system has expanded immensely, culminating in the widespread application of **immune checkpoint blockade** (ICB) immunotherapy for a wide variety of cancers (Box 1)¹³. But how do immune cells and cancer cells interrelate? Fundamental to our understanding of cancer immunity were experiments performed by the groups of Lloyd J. Old and Robert D. Schreiber, showing that mice deficient for critical lymphocyte effector molecules e.g. perforin and interferon-gamma (IFN- γ) were more susceptible to cancer induction^{14,15}. These findings provided scientific evidence for the cancer immunoediting hypothesis, stating that the immune system continuously monitors the host for (pre-)cancerous cells and eliminates them¹⁶. Alternatively, if the immune response is thwarted by escape mechanisms, cancer formation ensues and ultimately becomes clinically apparent.

Box 1: IMMUNE CHECKPOINT BLOCKADE (ICB) is a form of immunotherapy where antagonistic antibodies aimed at *immune checkpoints* on lymphocytes are used to promote anti-tumor immune responses. Immune checkpoints are generally co-inhibitory receptors (e.g. CTLA-4, PD-1) expressed on antigen-experienced effector T cells that restrain full-fledged T-cell activation after antigenic stimulation. When inhibitory receptors are blocked, T-cell activation is induced resulting in tumor responses in a subset of cancer patients. ICB antibodies are first- or second line treatment for a wide variety of malignancies including metastatic melanoma, non-small cell lung cancer (NSCLC) and renal cancer.

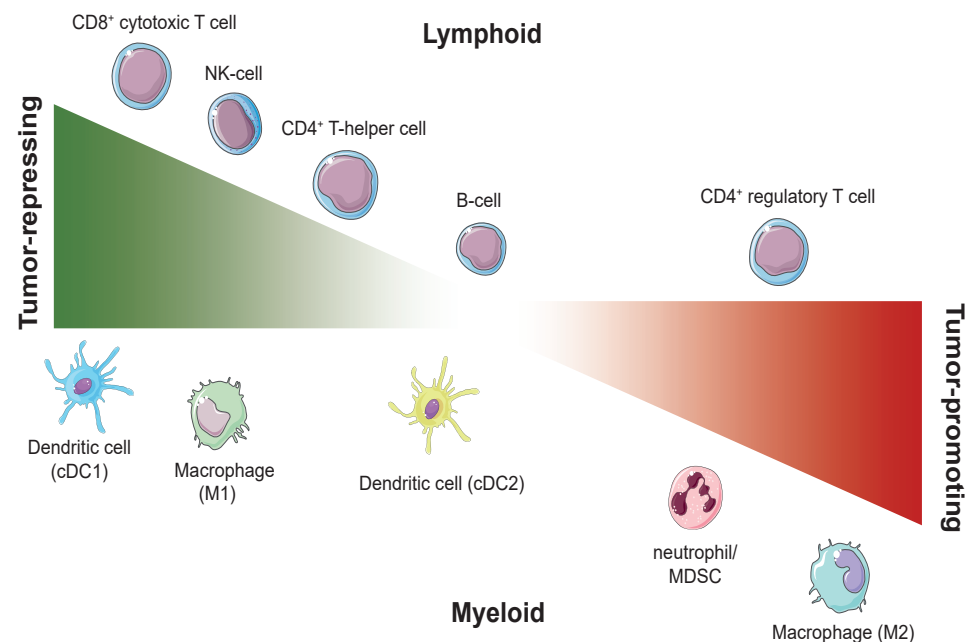


Figure 2. Leukocyte complexity in cancer. Leukocyte subtypes affect cancer differently, some promoting tumor formation and associating with poor prognosis (right), and others having potent anti-tumor functions hence correlating with improved disease outcome (left). Cells were plotted on the spectrum based on meta-analyses summarizing the associations of different immune cells with clinical outcome in a wide variety of tumor types (Bruni et al, Nature Reviews Cancer 2020, Fridman et al. Nature Reviews Clinical Oncology 2017).

The underlying pathophysiology of these processes has been studied in pre-clinical tumor models with each model carrying obvious limitations preventing full translation to the human setting¹⁷. However, recent findings suggest immunoediting to occur in humans. One of the most robust observations extending to nearly all cancer types concerns the association between a high tumor CD8⁺ lymphocyte (TIL) infiltrate and improved disease prognosis¹¹. Early work by Galon and colleagues established a CD8⁺ T-cell signature in human colorectal cancer (CRC) to be more predictive of patient outcome than current gold-standard staging methods such as the TNM-criteria¹⁸. Although many of these T cells could later be identified as bystander cells, a subset of T-cell clonotypes recognized tumor neo-antigens that resulted from immunogenic mutations acquired during oncogenesis^{19,20}. These cells could then be harvested and expanded *in vitro*, followed by intravenous administration yielding strong and durable clinical responses in a subset of metastatic CRC patients^{21,22}. More descriptive studies of human cancer have utilized recent advances in next-generation sequencing and bioinformatics to show extensive intratumoral heterogeneity that correlated with immune infiltration, identifying signs of immunoediting

and tumoral immune cell evasion in treatment-naïve patient tumors²³⁻²⁵. Recently, regressing in-situ lung carcinomas were found to harbor increased pro-inflammatory CD8⁺ T-cell frequencies compared to lesions progressing to overt cancer²⁶. These observations substantiate the hypothesis that the immune system offers a barrier to tumor outgrowth and that this safeguard mechanisms seems to be compromised in patients who develop cancer. A major question that remains to be answered is what drives immune evasion in these patients, and how can their immune system be coerced to control cancer growth instead of promoting it?

The yin and yang of cancer immune evasion and inflammation.

Recent discoveries have shed light on modes of immune evasion and inflammation in cancer, identifying key hallmarks driving cancer-immune interactions. Integrating these hallmarks rather than assessing their individual role in oncogenesis appears to be the most important recent discovery in oncology, providing a platform for future research into immunotherapy failure and combination treatments (Fig. 1C). One major cause of immune evasion appears to be the total absence of TILs referred to as the 'immune-deserted' tumor phenotype or in case of lack of sufficient infiltration of T cells in tumor nests, 'immune-exclusion'²⁷. What drives these phenotypes that inherently prevent patients to respond to current immunotherapies?

Essential to anti-tumor T-cell immunity is the presence of activated antigen-presenting cells (APCs) and subsequent trafficking of T cells to the tumor site. Seminal discoveries have identified conventional dendritic cells (cDCs), specifically type 1 cDCs (cDC1s), to be well equipped for (cross-) presenting antigen to anti-tumor CD8⁺ T cells, and that a lack of these cells in the tumor microenvironment (TME) drives immune desertification²⁸⁻³². The search for molecular drivers responsible for cDC1- and consequent T-cell paucity from tumors lead back to the same oncogenic pathways critical for sustaining tumor cell proliferation, one of the first hallmarks to be identified previously (Fig. 3). For example, increased activity of key oncogenic pathways such as the Wnt/ β -catenin-pathway led to decreased chemokine (C-C motif) ligand 4 (CCL4)-production in tumors preventing attraction of chemokine receptor 5 (CCR5)⁺ cDC1s leading to T-cell exclusion in melanoma³³. These findings were later extended to numerous other tumor types, and several other signaling pathways such as the Notch-, and Myc-pathways which were similarly found to subvert TIL-presence, albeit through different mechanisms³⁴⁻³⁶. Alternatively, silencing of tumor-suppressor genes giving way to unrestrained tumor cell proliferation could similarly result in immune evasion as documented for phosphatase and tensin homolog (PTEN)-mutated cancers³⁷. Taken together, these findings illustrate that driver mutations in oncogenic pathways have multiple pleiotropic roles in cancer formation which in part are dependent on eliciting immune evasion.

INTRODUCTION

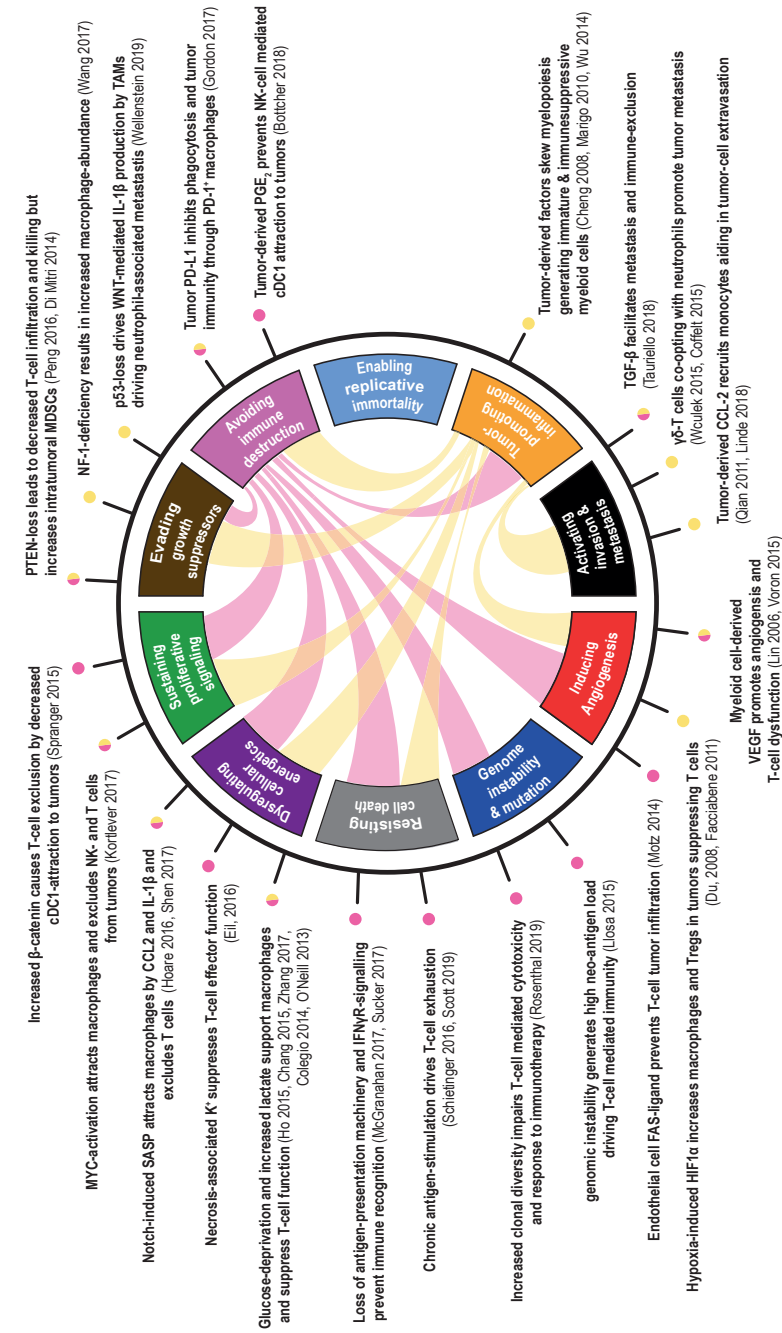
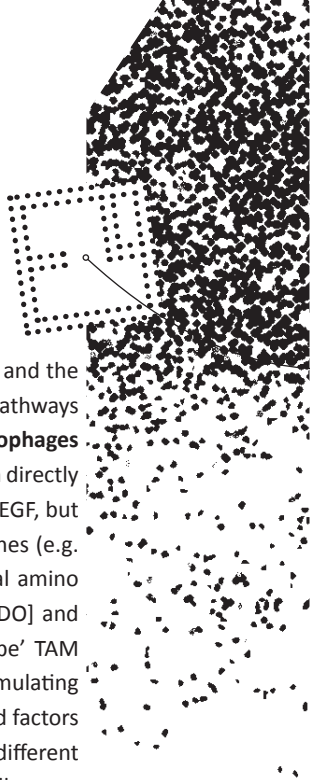


Figure 3. Hallmark mechanisms sculpting the immune contexture in cancer. The immune system integrated within the hallmarks of cancer derived from Fig. 1 including key examples with references how immune escape (purple spheres) or tumor-promoting inflammation (yellow spheres) is achieved. Purple and yellow roadways project mechanisms pertaining to a specific hallmark that also affect immune escape and tumor-promoting inflammation, respectively.



In addition to the inhibitory effects of certain cancer cell mutations on TILs and the APCs licensing TIL-activity, mutations in key oncogenic and tumor-suppressor pathways favor immune suppressive myeloid cells, typified by **tumor-associated macrophages** (TAMs, box 2), and T-regulatory cells (Tregs) entering the TME (Fig. 3)³⁸⁻⁴⁰. TAMs can directly nurture tumor growth by providing growth- and pro-angiogenic factors such as VEGF, but also silence T-cell activity through the production of immune-suppressive cytokines (e.g. IL-10), co-inhibitory ligand expression (e.g. PD-L1) and the depletion of essential amino acids such as tryptophan and arginine (through indoleamine 2,3-dioxygenase [IDO] and arginase, respectively)⁴¹. Polarization to this immune-suppressive 'M2-phenotype' TAM again relies in part on tumor-cell derived factors such as macrophage-colony stimulating factor (M-CSF), high lactate in the presence of hypoxia and non-tumor cell-derived factors such as antibodies and Th2-cytokines⁴¹⁻⁴³. More interconnections between the different hallmarks were established when the same immune suppressive myeloid cells were found to foster metastasis by facilitating tumor-cell extravasation and priming of the pre-metastatic niche in breast cancer⁴⁴⁻⁴⁷. This phenomenon similarly shared a genetic origin through the inactivation of tumor suppressor gene p53 which besides sensing deleterious DNA-damage, promoted the production of IL-1 β in the TME driving neutrophil-mediated distant metastasis⁴⁸. In addition to creating a favorable (pre-) metastatic microenvironment, neutrophils have been found to directly associate with circulating tumor cells (CTC) in the circulation, acting as chaperones by inducing CTC-cell cycle progression increasing metastatic potential⁴⁹.

Box 2: TUMOR ASSOCIATED MACROPHAGES (TAM) are a subset of myeloid cells present to varying degrees in the tumor microenvironment. TAMs originate from circulating monocytes or from local tissue-resident precursor cells seeded during embryogenesis and exhibit widely distinct profiles depending on environmental cues. A simplified model has been proposed dividing TAMs in a pro-inflammatory anti-tumor 'M1' phenotype, and an alternatively activated/immune suppressive 'M2' phenotype. Rather than the proposed M1/M2 dichotomy, a spectrum of phenotypes exists that can be therapeutically targeted to improve anti-tumor immune responses.

These findings exemplify that hallmarks first described as stand-alone contributors to cancer strongly associate with either immune evasion and/or tumor-promoting inflammation (Fig. 3). Future research will likely strengthen these interactions, offering valuable insights for the development of multi-purpose or combination targeted therapy.

INTRODUCTION

T-cell exhaustion and the tug-of-war between T cells and cancer.

In case tumors are successfully seeded by anti-tumor T cells, so-called 'inflamed' phenotype, tumor progression may be delayed but eventually ensues in the majority of patients through external immune suppression (e.g. by TAMs, Tregs) and a T-cell intrinsic process called T-cell exhaustion⁵⁰. T-cell exhaustion was first characterized in chronic viral infections and was subsequently found to exist in tumors as well, with TILs resembling their antiviral counterparts on both the transcriptomic and phenotypic level⁵¹. Greenberg and colleagues identified *in vivo* chronic tumor-antigen stimulation through the T-cell receptor (TCR) to be primarily responsible for driving the exhausted phenotype already early during tumorigenesis⁵². Since then, progress has been made to dissect the molecular drivers of T-cell exhaustion, identifying multiple transcription factors which when abundant foster the exhausted phenotype (e.g. high Eomes/T-bet and NFAT/AP-1 ratios)^{51,53}. Besides transcriptional rewiring following persistent TCR-stimulation, many other factors have been identified to attenuate T-cell exhaustion including persistent inhibitory receptor (e.g. PD-1, TIM-3) and cytokine receptor (IL-10, TGF- β , IL-2) signaling and lack of CD4⁺ T-cell help during the priming phase^{51,54,55}. More recently, the transcription factor TOX was identified to epigenetically imprint CD8⁺ T cells for the exhausted T-cell fate, repressing effector-modules but increasing T-cell persistence during continuous antigen challenge^{56,57}. Intriguingly, genetic ablation of TOX improved T-cell effector function (e.g. increased IFN- γ and TNF- α) but came at the expense of decreasing cell frequencies through enhanced cell death by effector-like T cells⁵⁷. These findings illustrate the importance of the exhaustion program in preventing immunopathology while providing some protective anti-tumor efficacy, elucidating why the mere presence of CD8⁺ TILs bears positive predictive value in solid tumors. Reciprocally, depleting exhausted CD8⁺ T cells in cancer and chronic viral infection, accelerates tumor progression and increases viral load, respectively^{11,58}.

In contrast to PD-1-high expressing exhausted T cells, an intermediate PD-1⁺ precursor-exhausted T-cell has been identified expressing TCF-1 and CXCR5, generating PD-1_{hi} exhausted-T-cell progeny following chronic antigen stimulation^{59,60}. This population was found to be responsible for the proliferative burst of T cells observed following anti-PD-1 immunotherapy which controlled tumor growth^{61,62}. While the exact origins and developmental requirements of these precursor cells remain largely unclear, TCF-1⁺ precursor-exhausted T cells were recently detected in APC-rich intratumoral niches. The presence of these precursor T cells correlated with increased TIL-infiltration and improved progression-free survival (PFS) following surgery⁶³. Although still immature, these findings suggest that the presence of precursor-exhausted T cells in cancer could dictate (ICB-) immunotherapy efficacy. Future immunotherapies aimed at enhancing TCF-1⁺ PD-1⁺ precursor T cells while preventing subsequent TOX-driven terminal exhaustion, could durably amplify anti-tumor immune responses.

Targeting exhaustion to give T cells the upper hand.

The generation of ICB antibodies to known targets of exhaustion including PD-1 and CTLA-4 lead to a revolution in the treatment of cancer and was honored with the Nobel Prize in Physiology or Medicine in 2018 for its discovery⁶⁴. The use of these blocking antibodies has further increased for a wide variety of cancer types, extending to earlier stage of disease to optimally impact survival⁶⁵⁻⁶⁷. As ICBs carry significant toxicities and costs, much effort has gone into biomarker discovery, identifying patients likely to respond to ICB-therapy from those who may require other treatments⁶⁸. These studies identified high inhibitory ligand-expression (e.g. PD-L1), high tumor mutational burden (TMB) and a T-cell inflamed tumor phenotype to correlate with increased response to ICBs but could either not be confirmed in later validation studies or lacked enough discriminatory power to deny treatment in the clinic^{69,70}. As the search for effective biomarkers continuous, numerous clinical trials have set out to increase the number of durable responders to ICB-treatments sometimes lacking clear pre-clinical rationales. What drives resistance to ICB-treatments, and how do these mechanisms relate to the modes of immune evasion mentioned earlier?

Clinical observations during ICB-therapy have recognized two types of resistance: primary resistance which ensues early after treatment and secondary resistance which occurs following initial treatment response after which tumors progress (Fig. 4)³. As ICBs aim to activate pre-existing immune responses, primary progression or lack of response occurs when tumors lack sufficient TIL-infiltrates (e.g. due to low tumor immunogenicity or obstruction of trafficking) or from any other mechanism described earlier (Fig. 3). In contrast to tumor-intrinsic or extrinsic factors impeding T-cell immunity at baseline, secondary progression involves a highly dynamic process where tumors respond initially but selection pressure drives immune-resistant tumor clones (e.g. through loss of antigen-presentation machinery, epigenetic repression of antigens and interferon resistance)^{23,71-73}. Moreover, ICB-mediated T-cell reinvigoration does not seem infinite, and terminal T-cell differentiation or upregulation of alternative checkpoints (e.g. TIM-3, LAG-3 or TIGIT) could cease ICB-efficacy eventually^{74,75}. An improved understanding of the mechanisms underlying the lack or loss of response to immunotherapy in individual patients could offer a more personalized approach allocating the right treatment to the right patient improving immunotherapy efficacy.

From micro- to tumor macroenvironment.

Most research has focused on the immune contexture of the tumor microenvironment, uncovering novel targets for immunotherapy or biomarkers predicting response⁷⁶. Although these investigations have launched the field to where it is now, new breakthroughs in solid tumors are still anticipated with ICB-combination efficacy being limited to some but not all cancer types⁷⁷⁻⁷⁹. For example, whereas combination immunotherapy using PD-1-

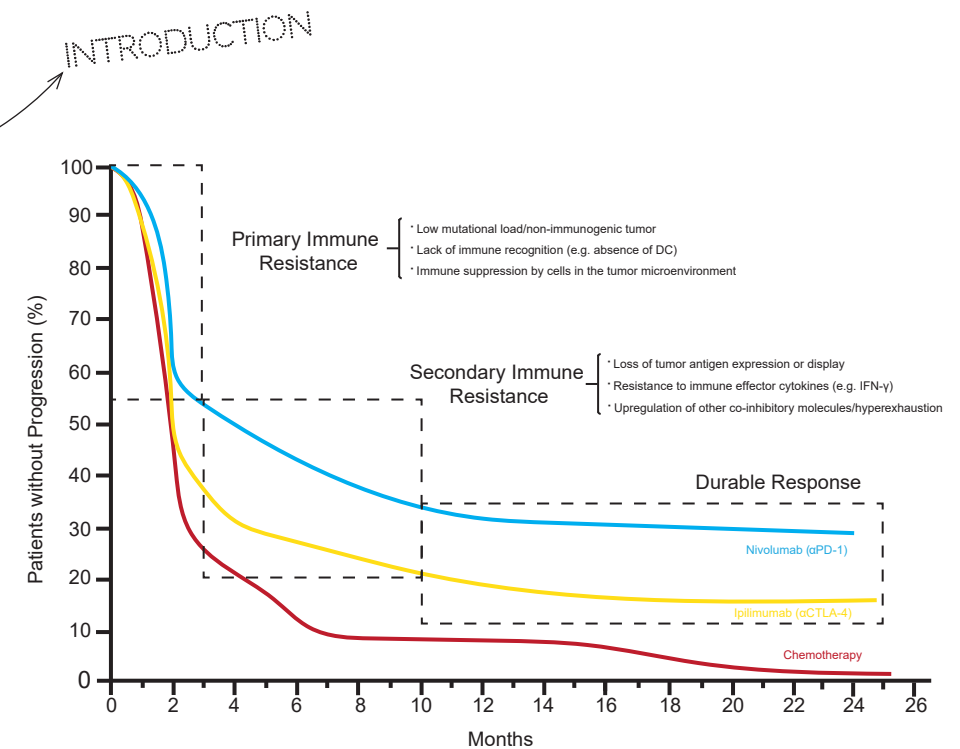


Figure 4. Immunotherapy extends time to disease progression but resistance ensues in a majority of patients. Kaplan-meier curves illustrating time to disease progression in metastatic melanoma patients treated with anti-PD-1 (blue) and anti-CTLA-4 (yellow) immune checkpoint blockade (ICB) therapy compared to conventional chemotherapy (red). Resistance to ICB can be subdivided into primary resistance when no initial response is achieved, and secondary resistance in case effective responses are non-durable. Figure derived from *Dammeijer & Lau et al., Cytokine and growth factors reviews 2017*.

blocking antibodies and IDO-inhibition would be expected to synergize based on TME-analysis, recent phase III trial results have been disappointing⁸⁰. Until now, only tumoral PD-L1 expression has been implemented in standard patient care for a limited number of tumor types including squamous non-small cell lung cancer (NSCLC). Although many late phase clinical trials are still underway and biomarkers are constantly being refined (e.g. by correcting for tumor purity in TMB, or adding tumor load to the frequency of circulating PD-1⁺ proliferating T cells), novel insights into the mechanisms of immune exclusion and successful anti-tumor immunity are warranted to optimally stratify patients^{81,82}.

Besides discovering modes of immune evasion or tumor-promoting inflammation in the tumor *microenvironment*, recent studies have widened the scope to non-tumor sites including lymphoid organs such as the spleen, bone marrow and **tumor-draining lymph nodes** (TDLNs, box 3)⁸³. By doing so a new paradigm emerged that extends beyond the tumor *microenvironment*; coined the *macroenvironment*. Corrupting the tumor macroenvironment through production of e.g. soluble mediators (cytokines, metabolites)

tumors effectively silence systemic anti-tumor immune responses, preventing durable immunotherapy benefit (Fig. 5). This model aligns with observations showing that certain immune-evading mechanisms seem to affect the host systemically besides providing only local suppression in the tumor microenvironment. An important systemic effect evoked by solid tumors is the premature release of immature neutrophils (also known as myeloid-derived suppressor cells; MDSC) from the bone marrow⁸⁴. Soluble components derived from the tumor microenvironment co-opt a stress-induced myelopoiesis pathway which offers protection in acute infections, but is detrimental to anti-tumor immunity⁸⁵. Several factors including damage-associated molecular patterns (DAMPs) and cytokines released by tumors were found to expand and halt maturation of granulocytic and monocytic precursors, at the expense of DC-progenitors⁸⁶⁻⁸⁸. This was shown to be dependent on STAT3- and RORC-mediated expression of C/EBP β in myeloid cells which upon arrested development seeded the tumor site to suppress T cells^{89,90}. Not only the bone marrow is involved in this process, but the spleen has been similarly documented to serve as an extramedullary hematopoietic site in solid cancers with myeloid progenitors seeding the spleen providing a reservoir for immature neutrophils^{91,92}. Myeloid progenitor- and hematopoietic stem cells (HSC) accumulated in the spleen through angiotensin production by NSCLC tumors inducing upregulation of a receptor called S1P1, which is involved in cell-retention. This in turn spawned monocytes and eventually macrophages to halt anti-tumor immunity⁹³. Intriguingly, the same S1P/S1P1-axis was responsible for trapping circulating T cells in the bone marrow in case of intracranial tumors, thereby causing immune-exclusion through still unresolved soluble mediators⁹⁴. These findings illustrate that tumors not only manipulate T-cell responses locally, but also systemically, warranting multi-organ assessment during tumorigenesis and immunotherapy to uncover new modes of immune-resistance⁹³.

Box 3: TUMOR-DRAINING LYMPH NODES (TDLNs) are lymphoid organs draining the TME through lymphatics transporting soluble molecules and immune cells including tumor antigens and dendritic cells, respectively. In TDLNs, dendritic cells prime anti-tumor T cells which then proliferate and traffic to the tumor site. Their direct exposure to the TME, however, also poses a threat as TDLNs are the most frequent site of tumor metastasis significantly impacting patient survival. For some malignancies TDLN location can be accurately determined using perioperative administration of radioactive probes and/or dyes at the tumor site (e.g. in melanoma and breast carcinoma).

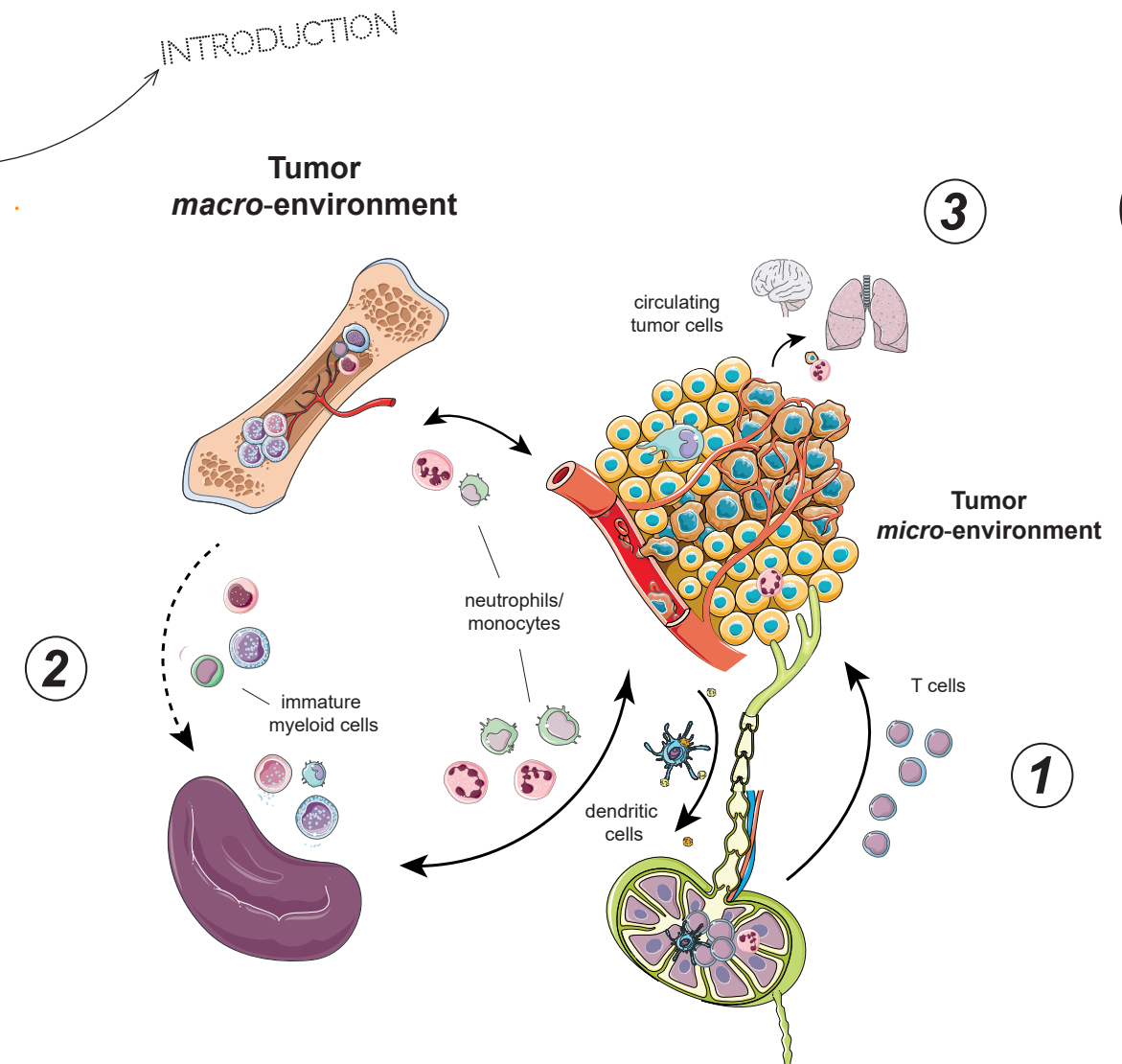


Figure 5. The concept of a tumor macroenvironment recapitulates the systemic immune response to cancer. The tumor macroenvironment consists of multiple tissues in the human body that are connected to the tumor (microenvironment; TME) through blood and lymphoid vessels. **(1)** Antigen-presenting cells (APCs) migrate from the TME to the tumor-draining lymph node (TDLN) where they prime cognate anti-tumor T cells that in turn infiltrate the TME and lyse tumor cells. **(2)** This process may be perturbed by soluble and cell-contact dependent factors corrupting TDLNs and other secondary lymphoid organs (SLOs), resulting in a systemically immune suppressed state. **(3)** Concurrently, immune cells facilitate further primary tumor progression but also promote and seed the pre-metastatic niche leading to cancer cell dissemination.

The TLDN as a central hub for anti-tumor immune response generation.

Whereas the spleen and bone marrow mainly support immune suppressive cells, TDLNs are most strategically exposed to tumor antigens and migratory APCs that prime T cells to cancer antigens⁹⁵. Recent data have shown that the immune contexture of the TDLN is crucial for dictating the magnitude and the anti-tumor properties of primed T cells, uncovering a major role for myeloid cells. As shown earlier, Batf3-dependent cDC1s are crucial for presenting tumor-antigens to CD8⁺ T cells, although other DC-subsets have been ascribed similar properties as well⁹⁶⁻⁹⁹. Elegant experiments performed by the Krummel group showed that cDC1s were quintessential for anti-cancer immunity by delivering and sharing antigen among other DCs in the TDLN, followed by the subsequent priming of CD8⁺ T cells capable of invading tumors^{99,100}. Moreover, exogenous administration of the main cDC1 growth factor FLT3-ligand increased intratumoral cDC1s and CD8⁺ T cells and further amplified anti-PD-L1 ICB-treatment in mice¹⁰¹. These findings underline the importance of initial DC-infiltration, tumor-cell phagocytosis and activation in tumors followed by trafficking to and priming of T cells in the TDLN, but also exposes several critical steps in which the immune response to cancer can be sabotaged.

Considering the plethora of myeloid cell subsets in TDLNs during steady state, a division of labor likely exists with different cell types promoting or suppressing effective T-cell responses. cDC2s are well known for their priming capacity of CD4⁺ T-cells, which display anti-tumor functions and are known to be critical for providing T-cell help during CD8⁺ T-cell priming^{102,103}. This process of 'licensing' was shown to be crucial for tissue invasive capacity and effector function of CD8⁺ T-cells and involved co-stimulation through CD27-CD70, CD40-ligand (CD40L)-CD40 and the presence of IL-21^{54,104,105}. In addition, a subset of CD11b⁺ cells was found to be strategically localized amidst CD169⁺ subcapsular sinus macrophages (SSMs), sampling lymph-borne particulate antigens and presenting them before migratory cDCs arrived¹⁰⁶. Reminiscent of the tumor microenvironment, TDLNs may harbor immune suppressive cells such as neutrophils which suppress DC-induced anti-tumor CD8⁺ T cells in the TDLN¹⁰⁷. TDLN macrophages are highly versatile and heterogeneous and have different roles in immune homeostasis based on their localization and surface receptors¹⁰⁸. CD169 (Siglec-1)-expressing SSMs are LN-resident cells lining the subcapsular floor where their protrusions take up draining particles including apoptotic tumor cells and present antigen to B- and T cells¹⁰⁹⁻¹¹². The Pittet group discovered an ingenious mechanism how SSMs suppress melanoma formation by preventing tumor exosomes from reaching SSM-neighboring B cells that would otherwise produce tumor-specific antibodies in response to draining exosomes, potentially polarizing suppressive (M2) TAMs¹¹³. These findings only begin to uncover the importance of TDLN-biology in anti-tumor immunity with still many processes (e.g. the interplay between immune cells and TDLN-metastasis) remaining to be uncovered.

INTRODUCTION

DC-immunotherapy as a way to circumvent aberrant T-cell priming.

In contrast to promoting anti-tumor T-cell immunity, DCs may be actively 'tolerized' by tumor-derived factors including TGF- β , VEGF, PGE₂ and Wnt-proteins to produce inhibitory molecules such as IL-10 and IDO while decreasing IL-12, thereby preferentially inducing Tregs over effector T cells¹¹⁴⁻¹¹⁷. This and a lack of T-cell priming altogether sparked the development of DC-immunotherapy, whereby DCs are directly obtained or matured from monocytes in blood, exposed to tumor-antigens and activated *in vitro* after which they are injected in the patient^{28,118,119}. Upon administration, these cells then migrate to the lymph node where they are able to generate vaccine-specific T-cells and clinical responses in a subset of patients with different tumor types¹²⁰⁻¹²³. Novel approaches applying different DC-subsets (with different functional properties, as discussed earlier), changes in antigen composition and combinations with other forms of treatment including ICB will likely improve response rates in the future^{118,119,124,125}. Alternatively, cancer vaccines provide an 'of the shelf'-approach consisting of tumor-peptide(s) or lysate combined with an adjuvant which after injection requires endogenous DCs to process and present antigen^{126,127}. Although large phase III trials with off-the-shelf peptide vaccines have failed to significantly improve survival in metastatic cancer patients, treatment of premalignant lesions and the development of personalized neo-epitope vaccines has showed potential¹²⁸⁻¹³¹. Similar to DC-therapy, combining vaccines with ICB or conventional modalities such as specific chemotherapies may equally elicit stronger tumor responses^{132,133}. These clinical studies have shown that peptide- and DC-vaccination can safely circumvent ineffective antigen presentation and T-cell priming in the TDLN. However, as immunological responses do not necessarily evoke clinical responses, both systemic and local immunosuppressive mechanisms in the tumor may inevitably curb effective anti-tumor immunity.

Other cancer therapies affecting the tumor macroenvironment.

Immunotherapies such as adoptive T-cell transfer, ICB and (DC-) vaccination aim to induce or propagate anti-tumor immunity, each acting at different phases of the immune response at varying locations in the tumor macroenvironment (Fig. 6). Conventional cancer treatments such as chemotherapy and targeted therapy were principally designed to target tumor cell proliferation but have been found to act much broader, also affecting immune cells. Notably, several widely used chemotherapies such as cisplatin, gemcitabine and doxorubicin lack complete clinical activity in T-cell deficient mice, underscoring the importance of therapy-induced T-cell immunity and testing anticancer drugs in appropriate preclinical models¹³⁴⁻¹³⁶.

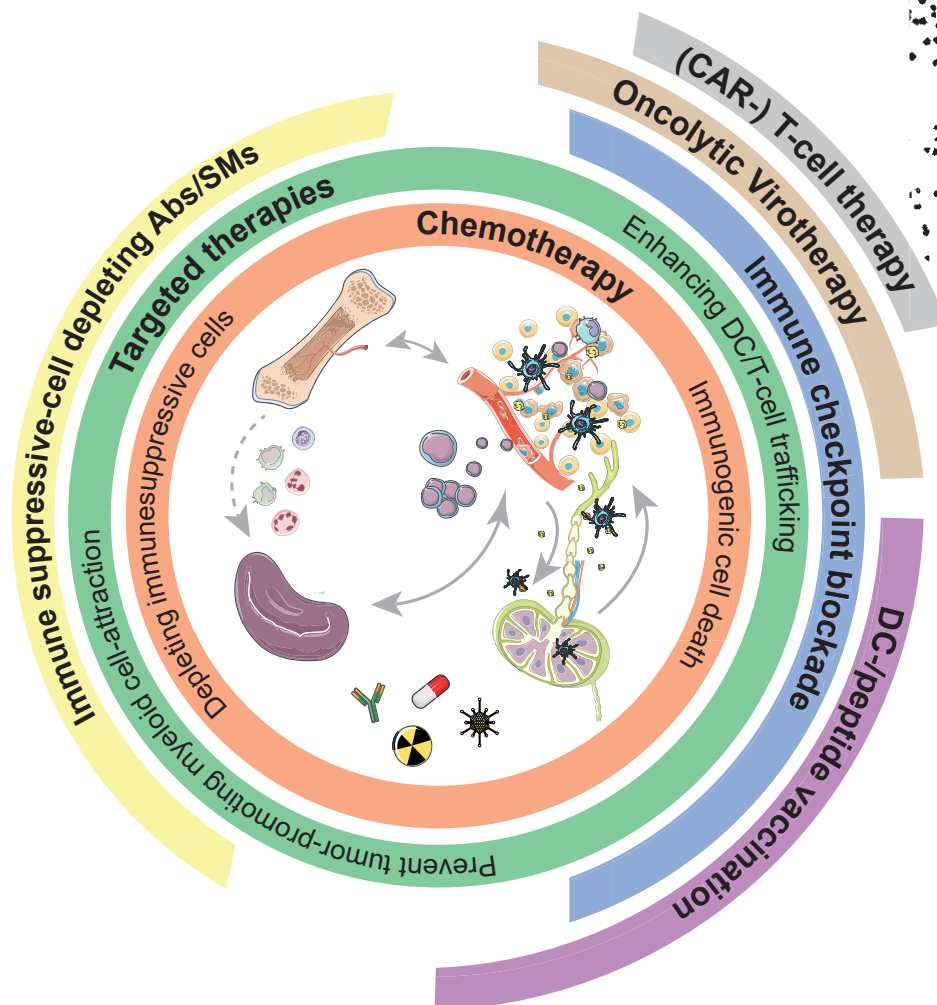


Figure 6. Immunotherapies can act at different sites of the tumor macroenvironment. Different immunotherapies including several immunogenic forms of chemo- and targeted therapies modulate existing or induce novel anti-tumor immune responses to induce tumor regression. As these therapies impact specific components of the tumor macroenvironment, effective immunotherapy may be achieved by rationally combining multiple modalities based on macroenvironment composition.

INTRODUCTION

Having established the contribution of the tumor macroenvironment to anti-tumor immunity, we are challenged by an increasing complexity when studying drug pharmacodynamics. One drug effect may amplify or counteract another, depending on the phase of the immune response. This was illustrated by the use of mammalian targets of rapamycin (mTOR)-inhibitors in cancer, which are aimed at targeting constitutive PI3-kinase (PI3K)-signaling in tumor cells. Administration of the drug *before* T-cell immune response generation, however, promoted Treg-expansion which dampened the anti-tumor response. Administering the drug *after* T-cells were primed, preferentially induced anti-tumor effector cells¹³⁷. Similarly, whereas intratumoral application of optimized IL-2 followed by systemic interferon-alpha (IFN- α) 48 hours later cured all tumor-bearing mice, concurrent administration of the two drugs failed to do so¹³⁸. As IFN- α is a strong activator of DCs, too early maturation resulted in DCs being unable to take up antigen and traffic to the TDLN after IL-2-therapy induced local immune destruction in the tumor.

Besides timing of treatment, dosing has become increasingly important with several small molecule inhibitors, cytokines and chemotherapies improving effector T-cell phenotype when administered at low, but not higher doses. For example, low-dose cyclophosphamide was shown to improve anti-tumor immunity in mice and patients through selective depletion of Tregs, but when given at high doses also effector T cells were decreased abrogating the immune-modulatory benefit^{139,140}. In addition to dosing, drug specificity should be considered. Small molecules including tyrosine kinase inhibitors may display previously unconsidered off-target effects with potentially detrimental effects on tumor immunity¹⁴¹. E.g. imatinib mesylate (Gleevec) is a tyrosine kinase inhibitor used in several malignancies including gastrointestinal stromal tumors (GIST) where it inhibits oncogenic KIT-signaling¹⁴². Although tumor cells responded to imatinib, cDC1s and therefore CD8⁺ T cells were scarce in imatinib-treated tumors which was found to be due to drug-induced GM-CSF deficiency preventing cDC1-accumulation¹⁴³.

Finally, a rational design of combination therapies aimed at different non-redundant pathways in the tumor macroenvironment may induce synergy and sensitize non-responding patients to immunotherapy¹⁴⁴. Although PD-1 and CTLA-4 are regarded to act at different phases of the immune response (i.e. at the effector site and the lymph node, respectively), the receptors can be co-expressed on T cells causing combination ICB to induce activation-induced cell death abrogating clinical benefit¹⁴⁵. Paradoxically, targeting the MEK-pathway in cancer using a MAPK-inhibitor did not hinder antigen-induced T-cell activation and proliferation but rather prevented activation-induced cell death, potentiating anti-PD-L1 immunotherapy¹⁴⁶. These findings illustrate both the challenges and opportunities of developing effective combination immunotherapy for solid cancers and demand a better understanding of the tumor macroenvironment in order to improve therapeutic strategies and eventually patient lives.

Methods to study the tumor macroenvironment.

Studying all assets of the tumor macroenvironment and their response to treatment in metastatic cancer patients is difficult for both technical and ethical reasons. With current *in vitro* model systems (e.g. organoids) lacking the cellular and architectural complexity of a solid tumor TME, let alone a macroenvironment, immune-competent animal models remain essential for studying cancer evolution and novel targets for therapy^{147,148}. Transplantable tumor cell lines in syngeneic mice are most often used because they allow for high-volume, easy to monitor and consistent tumor inoculation and follow-up. This is in contrast to genetically-modified spontaneous tumor models (GEMM; e.g. KPC pancreatic- or KP lung adenocarcinoma) which develop and metastasize in weeks/months, better reflecting the patient setting as compared to the rapid growth kinetics of transplantable models¹⁴⁹. GEMMs, however, are often characterized by a ultra-low frequency of neo-antigens as opposed to most human cancers and carcinogen-induced mouse models (e.g. MCA sarcoma model)^{150,151}. These examples highlight that depending on the research question and cancer type investigated, the appropriate set of models should be selected to optimally reflect the patient setting. As site of tumor cell injection has been found to determine TME composition, orthotopic rather than heterotopic (e.g. subcutaneous) injection should be considered whenever possible¹⁵²⁻¹⁵⁴. Also, in order to mimic inter-patient heterogeneity, multiple tumor models of the same histology but in different mouse strains (e.g. AB1 [BALB/c], AE17 [C57BL/6] and AC29 [CBA/J] in mesothelioma) may be used to increase validity and translatability of findings.

Although tissues of the tumor macroenvironment from patients is limited, tumor and (TD)LN are often available at early-disease stage post-surgery allowing for comprehensive live cell phenotyping or imaging. With several immunotherapies now being tested in the neo-adjuvant setting, explanted tissues are valuable in dissecting the prerequisites of immunotherapy efficacy, e.g. in the setting of (combination) ICB¹⁵⁵⁻¹⁵⁷. In the metastatic setting, peripheral blood or repeated tumor biopsies before, during and after immunotherapy administration can shed light on both the systemic and local anti-tumor immune response, respectively¹⁵⁸. In the end, integrating and validating the findings from translational preclinical mouse models with cancer patient tissues remains essential for future immunotherapy development.

Aims and outline of this thesis.

In the previous paragraphs several concepts pertaining to the tumor macroenvironment and anti-tumor immunity were introduced. Current anticancer therapies aim to improve different aspects of defective anti-tumor immunity but only a minority of patients respond durably. For many of these therapies depicted in figure 6 the exact modes of action, however, remain largely unknown. Furthermore, it is unclear which treatment

INTRODUCTION

combinations provide maximum synergy and would therefore be most eligible for clinical testing. By interrogating all available features of the tumor macroenvironment before, after and during treatment, we aim to identify novel mechanisms and treatment combinations that may aid in better immunotherapy design and allocation. Essential for this is to investigate whether existing immunotherapies have effects beyond their perceived target cell and location. To achieve this, a wide range of translational preclinical mouse models are employed enabling the precise targeting of specific molecules, cells or sites, identifying the prerequisites of effective anti-tumor immunity. Furthermore, we use patient-derived tumor, blood and lymph node materials with coupled clinical data to extend the obtained insights to the patient setting, potentially discovering novel biomarkers associating with response.

ICB and chemotherapy are the most frequently used treatments in solid cancer patients but responses are highly variable, ranging from durable partial or even complete tumor responses in a small subset of patients with the majority of patients responding temporarily or not at all. Much research has focused on how these treatments impact the TME or vice versa, and whether response to treatment can be predicted from T-cell phenotype in peripheral blood of patients. The exact modes of action, however, remain largely unknown. Comprehensive studies of not only T cells but multiple leukocyte lineages throughout the tumor macroenvironment could yield novel insights into the mechanism of action of treatments, which is critical for future immunotherapy optimization. In **Part A** of this thesis, novel modes of actions from two commonly systemically administered drugs are described, the first being PD-L1-checkpoint blockade (*Chapter 2*) and secondly gemcitabine chemotherapy (*Chapter 3*).

Anti-PD-1/PD-L1 immunotherapy is widely believed to re-invigorate PD-1⁺ exhausted tumor-infiltrating T cells but paradoxically, the degree of PD-L1 or PD-1 expression in the TME has only limited predictive value. To study this contradiction and assess whether other macroenvironmental sites such as TDLNs are involved, we assessed TDLNs of mice and patients for PD-1/PD-L1-axis activity in **Chapter 2**. To establish whether PD-L1 in TDLNs is involved in suppressing anti-tumor T-cell immunity, we specifically targeted TDLNs using a specialized injection technique. Additionally, we blocked T-cell egress from the TDLN using FTY720 to observe whether anti-PD-L1-derived responses were abrogated.

Besides directly targeting immune-inhibitory or stimulatory receptors on the T-cell membrane, certain chemotherapeutic drugs have been found to modulate receptor expression or enhance tumor cell immunogenicity *in vitro*, which could promote anti-tumor immunity¹⁵⁹. Whether these changes occur *in vivo* and correlate with treatment benefit remains unknown. In **Chapter 3**, we analyzed whether the commonly administered drug gemcitabine is capable of inducing or modulating circulating T- and NK-cells and whether this relates to effects of the drug on myeloid cells in patient blood. To this end we made

use of freshly harvested and processed MDSCs and stored peripheral-blood mononuclear cells (PBMCs) from the NVALT19-study evaluating the efficacy of maintenance gemcitabine treatment in mesothelioma patients¹⁶⁰. Measured immune parameters were correlated with clinical outcome yielding potential cues for biomarker-development.

Chemotherapy and immune-checkpoint blockade therapy generally affect the entire tumor macroenvironment, inducing a broad immune response at the expense of considerable toxicity. Cancer vaccines specifically act on (secondary) lymphoid organs, inducing a tumor-specific response without off-target toxicity¹²⁶. However, vaccine monotherapy is often insufficient to induce clinically meaningful responses in metastatic cancer, limiting its applicability in the clinic. By studying how vaccines affect the tumor macroenvironment, can we boost efficacy by rationally introducing partner drugs while preserving safety? **Part B** of this thesis focusses on improving cancer vaccine efficacy by rewiring immune suppressive cells in the tumor macroenvironment through combination immunotherapy. **Chapter 4** provides a systematically acquired overview and combined analysis of existing cellular- and peptide vaccine approaches in NSCLC. Moreover, meta-analyses was performed to assess efficacy of pooled peptide vaccine and cellular immunotherapies prioritizing which approach should be preferred.

Macrophages are present at all sites of the tumor macroenvironment frequently exhibiting potent immune suppressive phenotypes inhibiting T-cell functionality and promoting cancer desmoplasia and angiogenesis¹⁶¹. In **Chapters 5 & 6**, we attempted to improve DC-vaccination efficacy in mesothelioma- and the poorly immunogenic pancreatic cancer mouse model by targeting macrophages, either by depletion (via M-CSFR-inhibition, *Chapter 5*) or repolarization (using a CD40-agonist, *Chapter 6*). Safety and efficacy were monitored and we assessed immune responses in blood, tumor and lymphoid organs to evaluate whether systemic immunity was improved in the setting of combination immunotherapy.

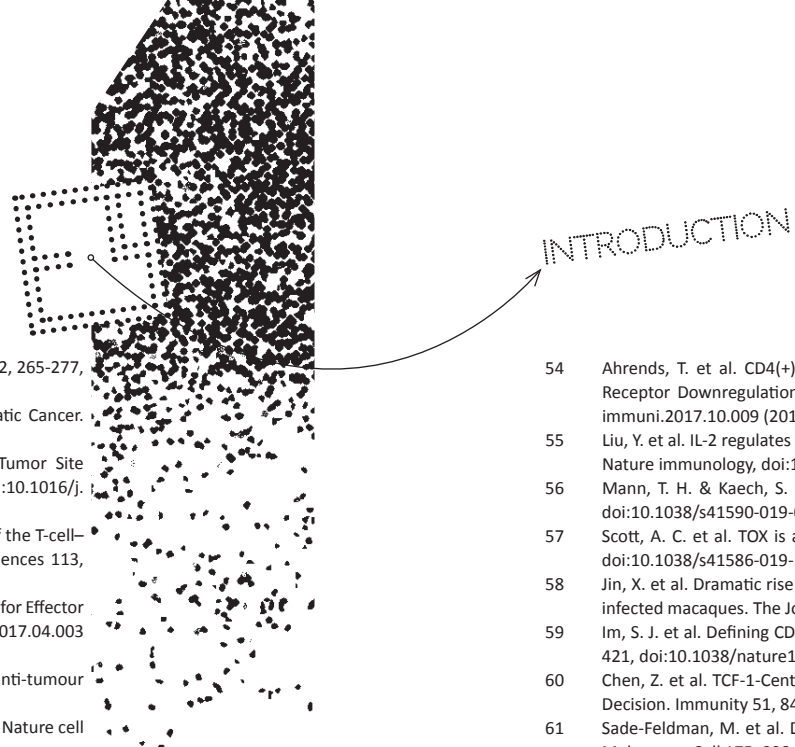
T-cell exhaustion may be another obstacle in cancer vaccine efficacy, hampering durable and effective anti-tumor immune responses. Cytokines and associated signaling molecules may have opposing functions on T-cell phenotype depending on the timing and context within the tumor macroenvironment. IL-2 is crucial for T-cell expansion following priming and survival during the effector phase¹⁶². However, excessive IL-2 could be deleterious for memory formation, or even induce exhaustion depending on the composition of the IL-2-receptor (IL-2R) being expressed^{55,163,164}. In **Chapter 7**, we temporally inhibited downstream IL-2R-expression by inhibiting Janus Kinase 3 (JAK3), aiming to improve vaccine-induced memory T-cell responses in solid tumor mouse models.

Finally, **Chapter 8** discusses the collected findings in the context of the currently available literature and proposes novel avenues for future research.

INTRODUCTION

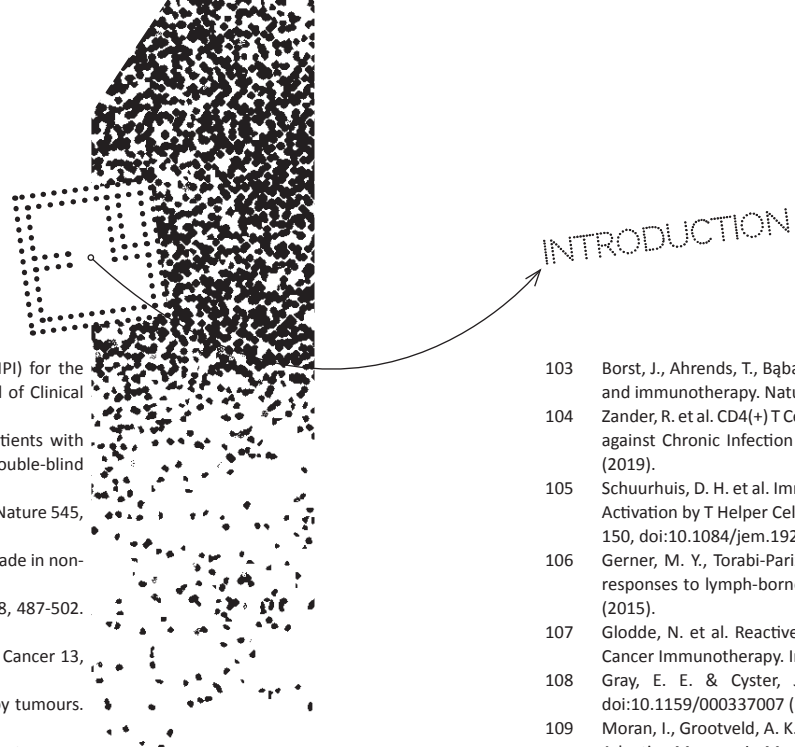
REFERENCES

- Weinberg, R. A. *The Biology of Cancer*. 2 edn, (Garland Science, 2014).
- Dvorak, H. F. Tumors: wounds that do not heal. Similarities between tumor stroma generation and wound healing. *The New England journal of medicine* 315, 1650-1659, doi:10.1056/nejm198612253152606 (1986).
- Dammeijer, F., Lau, S. P., van Eijck, C. H. J., van der Burg, S. H. & Aerts, J. Rationally combining immunotherapies to improve efficacy of immune checkpoint blockade in solid tumors. *Cytokine & growth factor reviews*, doi:10.1016/j.cytogfr.2017.06.011 (2017).
- Vogelstein, B. et al. Genetic Alterations during Colorectal-Tumor Development. *New England Journal of Medicine* 319, 525-532, doi:10.1056/NEJM198809013190901 (1988).
- Hanahan, D. & Weinberg, R. A. The hallmarks of cancer. *Cell* 100, 57-70 (2000).
- Hanahan, D. & Weinberg, R. A. Hallmarks of cancer: the next generation. *Cell* 144, 646-674, doi:10.1016/j.cell.2011.02.013 (2011).
- Restifo, N. P. et al. Loss of functional beta 2-microglobulin in metastatic melanomas from five patients receiving immunotherapy. *Journal of the National Cancer Institute* 88, 100-108 (1996).
- Holden, C. A., Shaw, M., McKee, P. H., Sanderson, A. R. & MacDonald, D. M. Loss of membrane B2 microglobulin in eccrine porocarcinoma. Its association with the histopathologic and clinical criteria of malignancy. *Arch Dermatol* 120, 732-735 (1984).
- Warburg, O., Wind, F. & Negelein, E. The Metabolism of Tumors in the Body. *J Gen Physiol* 8, 519-530 (1927).
- Grivennikov, S. I., Greten, F. R. & Karin, M. Immunity, inflammation, and cancer. *Cell* 140, 883-899 (2010).
- Fridman, W. H., Zitvogel, L., Sautès-Fridman, C. & Kroemer, G. The immune contexture in cancer prognosis and treatment. *Nature Reviews Clinical Oncology* 14, 717-734, doi:10.1038/nrclinonc.2017.101 (2017).
- Bruni, D., Angell, H. K. & Galon, J. The immune contexture and Immunoscore in cancer prognosis and therapeutic efficacy. *Nature Reviews Cancer* 20, 662-680, doi:10.1038/s41568-020-0285-7 (2020).
- Ribas, A. & Wolchok, J. D. Cancer immunotherapy using checkpoint blockade. *Science* 359, 1350-1355 (2018).
- Dighe, A. S., Richards, E., Old, L. J. & Schreiber, R. D. Enhanced in vivo growth and resistance to rejection of tumor cells expressing dominant negative IFN γ receptors. *Immunity* 1, 447-456, doi:https://doi.org/10.1016/1074-7613(94)90087-6 (1994).
- Smyth, M. J. et al. Perforin-mediated cytotoxicity is critical for surveillance of spontaneous lymphoma. *The Journal of experimental medicine* 192, 755-760, doi:10.1084/jem.192.5.755 (2000).
- Dunn, G. P., Old, L. J. & Schreiber, R. D. The immunobiology of cancer immunosurveillance and immunoediting. *Immunity* 21, 137-148, doi:10.1016/j.immuni.2004.07.017 (2004).
- Zitvogel, L., Pitt, J. M., Daillere, R., Smyth, M. J. & Kroemer, G. Mouse models in oncoimmunology. *Nature reviews. Cancer* 16, 759-773, doi:10.1038/nrc.2016.91 (2016).
- Galon, J. et al. Type, density, and location of immune cells within human colorectal tumors predict clinical outcome. *Science* 313, 1960-1964, doi:10.1126/science.1129139 (2006).
- Schumacher, T. N. & Schreiber, R. D. Neoantigens in cancer immunotherapy. *Science* 348, 69-74, doi:10.1126/science.aaa4971 (2015).
- Scheper, W. et al. Low and variable tumor reactivity of the intratumoral TCR repertoire in human cancers. 25, 89-94, doi:10.1038/s41591-018-0266-5 (2019).
- Rosenberg, S. A. & Restifo, N. P. Adoptive cell transfer as personalized immunotherapy for human cancer. *Science* 348, 62-68, doi:10.1126/science.aaa4967 (2015).
- Tran, E. et al. Cancer immunotherapy based on mutation-specific CD4 $^{+}$ T cells in a patient with epithelial cancer. *Science* 344, 641-645, doi:10.1126/science.1251102 (2014).
- Rosenthal, R. et al. Neoantigen-directed immune escape in lung cancer evolution. *Nature* 567, 479-485, doi:10.1038/s41586-019-1032-7 (2019).
- Rooney, M. S., Shukla, S. A., Wu, C. J., Getz, G. & Hacohen, N. Molecular and genetic properties of tumors associated with local immune cytolytic activity. *Cell* 160, 48-61, doi:10.1016/j.cell.2014.12.033 (2015).
- Angelova, M. et al. Evolution of Metastases in Space and Time under Immune Selection. *Cell* 175, 751-765, e716, doi:10.1016/j.cell.2018.09.018 (2018).
- Pennycuik, A. et al. Immune Surveillance in Clinical Regression of Preinvasive Squamous Cell Lung Cancer. *Cancer Discovery* 10, 1489, doi:10.1158/2159-8290.CD-19-1366 (2020).
- Galon, J. & Bruni, D. Approaches to treat immune hot, altered and cold tumours with combination immunotherapies. *Nat Rev Drug Discov* 18, 197-218, doi:10.1038/s41573-018-0007-y (2019).



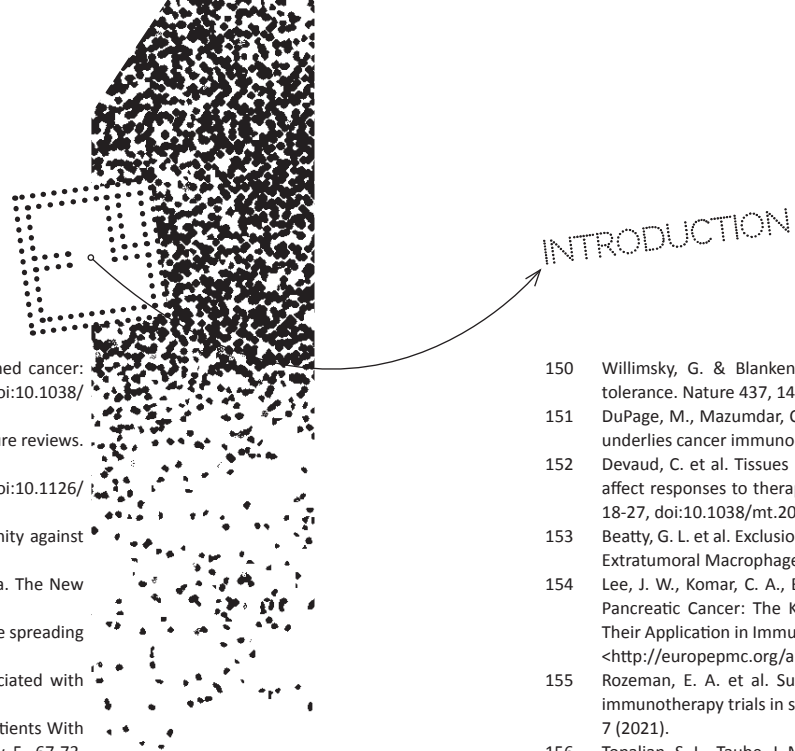
INTRODUCTION

- 28 Palucka, K. & Banchereau, J. Cancer immunotherapy via dendritic cells. *Nature reviews. Cancer* 12, 265-277, doi:10.1038/nrc3258 (2012).
- 29 Hegde, S. et al. Dendritic Cell Paucity Leads to Dysfunctional Immune Surveillance in Pancreatic Cancer. *Cancer cell* 37, 289-307.e289, doi:10.1016/j.ccell.2020.02.008 (2020).
- 30 Salmon, H. et al. Expansion and Activation of CD103(+) Dendritic Cell Progenitors at the Tumor Site Enhances Tumor Responses to Therapeutic PD-L1 and BRAF Inhibition. *Immunity* 44, 924-938, doi:10.1016/j.immuni.2016.03.012 (2016).
- 31 Spranger, S. et al. Density of immunogenic antigens does not explain the presence or absence of the T-cell-inflamed tumor microenvironment in melanoma. *Proceedings of the National Academy of Sciences* 113, E7759, doi:10.1073/pnas.1609376113 (2016).
- 32 Spranger, S., Dai, D., Horton, B. & Gajewski, T. F. Tumor-Residing Batf3 Dendritic Cells Are Required for Effector T Cell Trafficking and Adoptive T Cell Therapy. *Cancer cell* 31, 711-723.e714, doi:10.1016/j.ccell.2017.04.003 (2017).
- 33 Spranger, S., Bao, R. & Gajewski, T. F. Melanoma-intrinsic beta-catenin signalling prevents anti-tumour immunity. *Nature* 523, 231-235, doi:10.1038/nature14404 (2015).
- 34 Hoare, M. et al. NOTCH1 mediates a switch between two distinct secretomes during senescence. *Nature cell biology* 18, 979-992, doi:10.1038/ncb3397 (2016).
- 35 Kortlever, R. M. et al. Myc Cooperates with Ras by Programming Inflammation and Immune Suppression. *Cell* 171, 1301-1315.e1314, doi:10.1016/j.cell.2017.11.013 (2017).
- 36 Luke, J. J., Bao, R. & Sweis, R. F. WNT/beta-catenin Pathway Activation Correlates with Immune Exclusion across Human Cancers. 25, 3074-3083, doi:10.1158/1078-0432.ccr-18-1942 (2019).
- 37 Peng, W. et al. Loss of PTEN Promotes Resistance to T Cell-Mediated Immunotherapy. *Cancer Discov* 6, 202-216, doi:10.1158/2159-8290.cd-15-0283 (2016).
- 38 Wang, Q. et al. Tumor Evolution of Glioma-Intrinsic Gene Expression Subtypes Associates with Immunological Changes in the Microenvironment. *Cancer cell* 32, 42-56.e46, doi:10.1016/j.ccell.2017.06.003 (2017).
- 39 Di Mitri, D. et al. Tumour-infiltrating Gr-1+ myeloid cells antagonize senescence in cancer. *Nature* 515, 134-137, doi:10.1038/nature13638 (2014).
- 40 Shabaneh, T. B. et al. Oncogenic BRAF(V600E) Governs Regulatory T-cell Recruitment during Melanoma Tumorigenesis. 78, 5038-5049, doi:10.1158/0008-5472.can-18-0365 (2018).
- 41 Noy, R. & Pollard, J. W. Tumor-associated macrophages: from mechanisms to therapy. *Immunity* 41, 49-61, doi:10.1016/j.immuni.2014.06.010 (2014).
- 42 Colegio, O. R. et al. Functional polarization of tumour-associated macrophages by tumour-derived lactic acid. *Nature* 513, 559-563, doi:10.1038/nature13490 (2014).
- 43 Kaneda, M. M. et al. PI3Kgamma is a molecular switch that controls immune suppression. *Nature* 539, 437-442, doi:10.1038/nature19834 (2016).
- 44 Linde, N. et al. Macrophages orchestrate breast cancer early dissemination and metastasis. *Nature communications* 9, 21, doi:10.1038/s41467-017-02481-5 (2018).
- 45 Kitamura, T., Qian, B. Z. & Pollard, J. W. Immune cell promotion of metastasis. *Nature reviews. Immunology* 15, 73-86, doi:10.1038/nri3789 (2015).
- 46 Qian, B. Z. et al. CCL2 recruits inflammatory monocytes to facilitate breast-tumour metastasis. *Nature* 475, 222-225, doi:10.1038/nature10138 (2011).
- 47 Coffelt, S. B. et al. IL-17-producing gammadelta T cells and neutrophils conspire to promote breast cancer metastasis. *Nature* 522, 345-348, doi:10.1038/nature14282 (2015).
- 48 Wellenstein, M. D. et al. Loss of p53 triggers WNT-dependent systemic inflammation to drive breast cancer metastasis. *Nature* 572, 538-542, doi:10.1038/s41586-019-1450-6 (2019).
- 49 Szczerba, B. M. et al. Neutrophils escort circulating tumour cells to enable cell cycle progression. *Nature* 566, 553-557, doi:10.1038/s41586-019-0915-y (2019).
- 50 Wherry, E. J. T cell exhaustion. *Nature immunology* 12, 492-499 (2011).
- 51 McLane, L. M., Abdel-Hakeem, M. S. & Wherry, E. J. CD8 T Cell Exhaustion During Chronic Viral Infection and Cancer. *Annual review of immunology* 37, 457-495, doi:10.1146/annurev-immunol-041015-055318 (2019).
- 52 Schietinger, A. et al. Tumor-Specific T Cell Dysfunction Is a Dynamic Antigen-Driven Differentiation Program Initiated Early during Tumorigenesis. *Immunity* 45, 389-401, doi:10.1016/j.immuni.2016.07.011 (2016).
- 53 Martinez, G. J. et al. The transcription factor NFAT promotes exhaustion of activated CD8(+) T cells. *Immunity* 42, 265-278, doi:10.1016/j.immuni.2015.01.006 (2015).
- 54 Ahrends, T. et al. CD4(+) T Cell Help Confers a Cytotoxic T Cell Effector Program Including Coinhibitory Receptor Downregulation and Increased Tissue Invasiveness. *Immunity* 47, 848-861.e845, doi:10.1016/j.immuni.2017.10.009 (2017).
- 55 Liu, Y. et al. IL-2 regulates tumor-reactive CD8+ T cell exhaustion by activating the aryl hydrocarbon receptor. *Nature immunology*, doi:10.1038/s41590-020-00850-9 (2021).
- 56 Mann, T. H. & Kaech, S. M. Tick-TOX, it's time for T cell exhaustion. *Nature immunology* 20, 1092-1094, doi:10.1038/s41590-019-0478-y (2019).
- 57 Scott, A. C. et al. TOX is a critical regulator of tumour-specific T cell differentiation. *Nature* 571, 270-274, doi:10.1038/s41586-019-1324-y (2019).
- 58 Jin, X. et al. Dramatic rise in plasma viremia after CD8(+) T cell depletion in simian immunodeficiency virus-infected macaques. *The Journal of experimental medicine* 189, 991-998, doi:10.1084/jem.189.6.991 (1999).
- 59 Im, S. J. et al. Defining CD8+ T cells that provide the proliferative burst after PD-1 therapy. *Nature* 537, 417-421, doi:10.1038/nature19330 (2016).
- 60 Chen, Z. et al. TCF-1-Centered Transcriptional Network Drives an Effector versus Exhausted CD8 T Cell-Fate Decision. *Immunity* 51, 840-855.e845, doi:10.1016/j.immuni.2019.09.013 (2019).
- 61 Sade-Feldman, M. et al. Defining T Cell States Associated with Response to Checkpoint Immunotherapy in Melanoma. *Cell* 175, 998-1013.e1020, doi:https://doi.org/10.1016/j.cell.2018.10.038 (2018).
- 62 Kurtulus, S. et al. Checkpoint Blockade Immunotherapy Induces Dynamic Changes in PD-1(-)CD8(+) Tumor-Infiltrating T Cells. *Immunity* 50, 181-194.e186 (2019).
- 63 Jansen, C. S. et al. An intra-tumoral niche maintains and differentiates stem-like CD8 T cells. *Nature* 576, 465-470, doi:10.1038/s41586-019-1836-5 (2019).
- 64 Ledford, H., Else, H. & Warren, M. Cancer immunologists scoop medicine Nobel prize. *Nature* 562, 20-21, doi:10.1038/d41586-018-06751-0 (2018).
- 65 Galon, J. & Bruni, D. Tumor Immunology and Tumor Evolution: Intertwined Histories. *Immunity* 52, 55-81, doi:10.1016/j.immuni.2019.12.018 (2020).
- 66 Forde, P. M. et al. Neoadjuvant PD-1 Blockade in Resectable Lung Cancer. 378, 1976-1986, doi:10.1056/NEJMoa1716078 (2018).
- 67 Amaria, R. N. et al. Neoadjuvant immune checkpoint blockade in high-risk resectable melanoma. *Nature medicine* 24, 1649-1654, doi:10.1038/s41591-018-0197-1 (2018).
- 68 Nishino, M., Ramaiya, N. H., Hatabu, H. & Hodi, F. S. Monitoring immune-checkpoint blockade: response evaluation and biomarker development. *Nature reviews. Clinical oncology* 14, 655-668, doi:10.1038/nrclinonc.2017.88 (2017).
- 69 Rizvi, N. A. et al. Cancer immunology. Mutational landscape determines sensitivity to PD-1 blockade in non-small cell lung cancer. *Science* 348, 124-128, doi:10.1126/science.aaa1348 (2015).
- 70 Cristescu, R. et al. Pan-tumor genomic biomarkers for PD-1 checkpoint blockade-based immunotherapy. 362, doi:10.1126/science.aar3593 (2018).
- 71 Zaretsky, J. M. et al. Mutations Associated with Acquired Resistance to PD-1 Blockade in Melanoma. *New England Journal of Medicine* 375, 819-829, doi:10.1056/NEJMoa1604958 (2016).
- 72 Kalbasi, A. et al. Uncoupling interferon signaling and antigen presentation to overcome immunotherapy resistance due to JAK1 loss in melanoma. *Science translational medicine* 12, eabb0152, doi:10.1126/scitranslmed.abb0152 (2020).
- 73 Benci, J. L. et al. Tumor Interferon Signaling Regulates a Multigenic Resistance Program to Immune Checkpoint Blockade. *Cell* 167, 1540-1554.e1512, doi:10.1016/j.cell.2016.11.022 (2016).
- 74 Koyama, S. et al. Adaptive resistance to therapeutic PD-1 blockade is associated with upregulation of alternative immune checkpoints. *Nature communications* 7, 10501, doi:10.1038/ncomms10501 (2016).
- 75 Pai, C. S. et al. Clonal Deletion of Tumor-Specific T Cells by Interferon-gamma Confers Therapeutic Resistance to Combination Immune Checkpoint Blockade. *Immunity* 50, 477-492.e478, doi:10.1016/j.immuni.2019.01.006 (2019).
- 76 Binnewies, M. et al. Understanding the tumor immune microenvironment (TIME) for effective therapy. *Nature medicine* 24, 541-550, doi:10.1038/s41591-018-0014-x (2018).
- 77 Motzer, R. J. et al. Nivolumab plus Ipilimumab versus Sunitinib in Advanced Renal-Cell Carcinoma. *New England Journal of Medicine* 378, 1277-1290, doi:10.1056/NEJMoa1712126 (2018).
- 78 Hellmann, M. D. et al. Nivolumab plus Ipilimumab in Advanced Non-Small-Cell Lung Cancer. *New England Journal of Medicine* 381, 2020-2031, doi:10.1056/NEJMoa1910231 (2019).



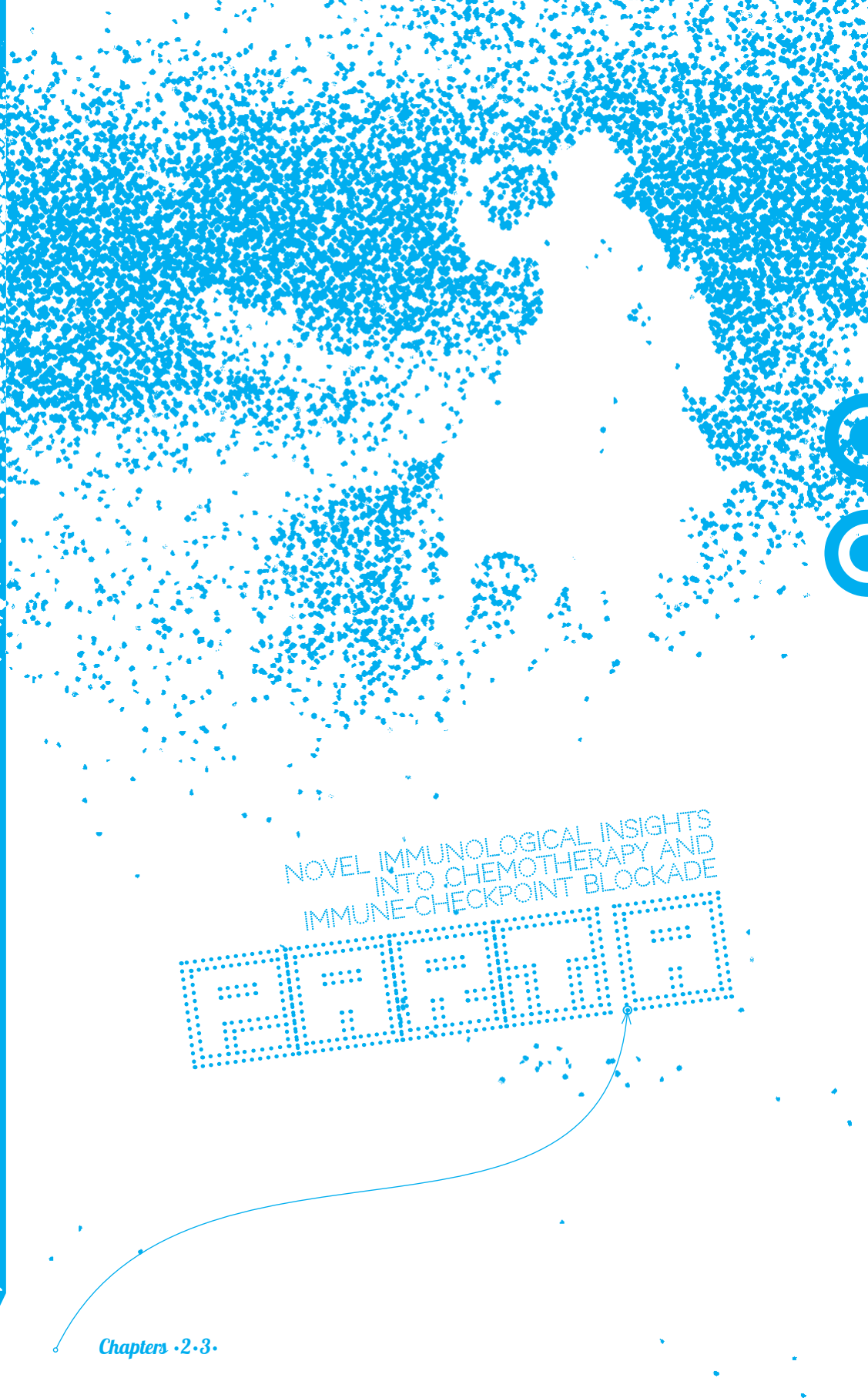
INTRODUCTION

- 79 Sharma, P. et al. Initial results from a phase II study of nivolumab (NIVO) plus ipilimumab (IPI) for the treatment of metastatic castration-resistant prostate cancer (mCRPC; CheckMate 650). *Journal of Clinical Oncology* 37 (2019).
- 80 Long, G. V. et al. Epacadostat plus pembrolizumab versus placebo plus pembrolizumab in patients with unresectable or metastatic melanoma (ECHO-301/KEYNOTE-252): a phase 3, randomised, double-blind study. *The Lancet. Oncology* 20, 1083-1097, doi:10.1016/S1470-2045(19)30274-8 (2019).
- 81 Huang, A. C. et al. T-cell invigoration to tumour burden ratio associated with anti-PD-1 response. *Nature* 545, 60-65, doi:10.1038/nature22079 (2017).
- 82 Anagnostou, V. et al. Multimodal genomic features predict outcome of immune checkpoint blockade in non-small-cell lung cancer. *Nature Cancer* 1, 99-111, doi:10.1038/s43018-019-0008-8 (2020).
- 83 Spitzer, M. H. et al. Systemic Immunity Is Required for Effective Cancer Immunotherapy. *Cell* 168, 487-502. e415, doi:10.1016/j.cell.2016.12.022 (2017).
- 84 Talmadge, J. E. & Gabrilovich, D. I. History of myeloid-derived suppressor cells. *Nature reviews. Cancer* 13, 739-752, doi:10.1038/nrc3581 (2013).
- 85 Gabrilovich, D. I., Ostrand-Rosenberg, S. & Bronte, V. Coordinated regulation of myeloid cells by tumours. *Nature Reviews Immunology* 12, 253-268, doi:10.1038/nri3175 (2012).
- 86 Gabrilovich, D. I., Ostrand-Rosenberg, S. & Bronte, V. Coordinated regulation of myeloid cells by tumours. *Nature reviews. Immunology* 12, 253-268, doi:10.1038/nri3175 (2012).
- 87 Stromnes, I. M., Greenberg, P. D. & Hingorani, S. R. Molecular pathways: myeloid complicity in cancer. *Clinical cancer research : an official journal of the American Association for Cancer Research* 20, 5157-5170, doi:10.1158/1078-0432.ccr-13-0866 (2014).
- 88 Wu, W.-C. et al. Circulating hematopoietic stem and progenitor cells are myeloid-biased in cancer patients. *Proceedings of the National Academy of Sciences* 111, 4221, doi:10.1073/pnas.1320753111 (2014).
- 89 Marigo, I. et al. Tumor-induced tolerance and immune suppression depend on the C/EBPbeta transcription factor. *Immunity* 32, 790-802, doi:10.1016/j.immuni.2010.05.010 (2010).
- 90 Strauss, L. et al. RORC1 Regulates Tumor-Promoting "Emergency" Granulo-Monocytopenia. *Cancer cell* 28, 253-269, doi:10.1016/j.ccell.2015.07.006 (2015).
- 91 Cortez-Retamozo, V. et al. Origins of tumor-associated macrophages and neutrophils. *Proceedings of the National Academy of Sciences of the United States of America* 109, 2491-2496, doi:10.1073/pnas.1113744109 (2012).
- 92 Wu, C. et al. Spleen mediates a distinct hematopoietic progenitor response supporting tumor-promoting myelopoiesis. *The Journal of clinical investigation* 128, 3425-3438, doi:10.1172/JCI97973 (2018).
- 93 Cortez-Retamozo, V. et al. Angiotensin II drives the production of tumor-promoting macrophages. *Immunity* 38, 296-308, doi:10.1016/j.immuni.2012.10.015 (2013).
- 94 Chongsathidkiet, P. et al. Sequestration of T cells in bone marrow in the setting of glioblastoma and other intracranial tumors. *Nature medicine* 24, 1459-1468, doi:10.1038/s41591-018-0135-2 (2018).
- 95 Chen, D. S. & Mellman, I. Oncology meets immunology: the cancer-immunity cycle. *Immunity* 39, 1-10, doi:10.1016/j.immuni.2013.07.012 (2013).
- 96 Hildner, K. et al. Batf3 deficiency reveals a critical role for CD8alpha+ dendritic cells in cytotoxic T cell immunity. *Science* 322, 1097-1100, doi:10.1126/science.1164206 (2008).
- 97 Sharma, M. D. et al. Activation of p53 in Immature Myeloid Precursor Cells Controls Differentiation into Ly6c(+)CD103(+) Monocytic Antigen-Presenting Cells in Tumors. *Immunity* 48, 91-106. e106, doi:10.1016/j.immuni.2017.12.014 (2018).
- 98 McDonnell, A. M., Prosser, A. C., van Bruggen, I., Robinson, B. W. & Currie, A. J. CD8alpha+ DC are not the sole subset cross-presenting cell-associated tumor antigens from a solid tumor. *European journal of immunology* 40, 1617-1627, doi:10.1002/eji.200940153 (2010).
- 99 Ruhland, M. K. et al. Visualizing Synaptic Transfer of Tumor Antigens among Dendritic Cells. *Cancer cell* 37, 786-799. e785 (2020).
- 100 Roberts, E. W. et al. Critical Role for CD103(+)/CD141(+) Dendritic Cells Bearing CCR7 for Tumor Antigen Trafficking and Priming of T Cell Immunity in Melanoma. *Cancer cell* 30, 324-336, doi:10.1016/j.ccell.2016.06.003 (2016).
- 101 Salmon, H. et al. Expansion and Activation of CD103⁺ Dendritic Cell Progenitors at the Tumor Site Enhances Tumor Responses to Therapeutic PD-L1 and BRAF Inhibition. *Immunity* 44, 924-938, doi:10.1016/j.immuni.2016.03.012 (2016).
- 102 Binnewies, M. et al. Unleashing Type-2 Dendritic Cells to Drive Protective Antitumor CD4+ T Cell Immunity. *Cell* 177, 556-571. e516, doi:https://doi.org/10.1016/j.cell.2019.02.005 (2019).
- 103 Borst, J., Ahrends, T., Bąbala, N., Melief, C. J. M. & Kastenmüller, W. CD4(+) T cell help in cancer immunology and immunotherapy. *Nature reviews. Immunology* 18, 635-647, doi:10.1038/s41577-018-0044-0 (2018).
- 104 Zander, R. et al. CD4(+) T Cell Help Is Required for the Formation of a Cytolytic CD8(+) T Cell Subset that Protects against Chronic Infection and Cancer. *Immunity* 51, 1028-1042. e1024, doi:10.1016/j.immuni.2019.10.009 (2019).
- 105 Schuurhuis, D. H. et al. Immature Dendritic Cells Acquire Cd8+ Cytotoxic T Lymphocyte Priming Capacity upon Activation by T Helper Cell-Independent or-Dependent Stimuli. *Journal of Experimental Medicine* 192, 145-150, doi:10.1084/jem.192.1.145 (2000).
- 106 Gerner, M. Y., Torabi-Parizi, P. & Germain, R. N. Strategically localized dendritic cells promote rapid T cell responses to lymph-borne particulate antigens. *Immunity* 42, 172-185, doi:10.1016/j.immuni.2014.12.024 (2015).
- 107 Glodde, N. et al. Reactive Neutrophil Responses Dependent on the Receptor Tyrosine Kinase c-MET Limit Cancer Immunotherapy. *Immunity* 47, 789-802 (2017).
- 108 Gray, E. E. & Cyster, J. G. Lymph node macrophages. *Journal of innate immunity* 4, 424-436, doi:10.1159/000337007 (2012).
- 109 Moran, I., Grootveld, A. K., Nguyen, A. & Phan, T. G. Subcapsular Sinus Macrophages: The Seat of Innate and Adaptive Memory in Murine Lymph Nodes. *Trends in immunology* 40, 35-48, doi:10.1016/j.it.2018.11.004 (2019).
- 110 Martinez-Pomares, L. & Gordon, S. CD169+ macrophages at the crossroads of antigen presentation. *Trends in immunology* 33, 66-70, doi:10.1016/j.it.2011.11.001 (2012).
- 111 Junt, T. et al. Subcapsular sinus macrophages in lymph nodes clear lymph-borne viruses and present them to antiviral B cells. *Nature* 450, 110-114, doi:10.1038/nature06287 (2007).
- 112 Asano, K. et al. CD169-positive macrophages dominate antitumor immunity by crosspresenting dead cell-associated antigens. *Immunity* 34, 85-95, doi:10.1016/j.immuni.2010.12.011 (2011).
- 113 Pucci, F. et al. SCS macrophages suppress melanoma by restricting tumor-derived vesicle-B cell interactions. *Science* 352, 242-246, doi:10.1126/science.aaf1328 (2016).
- 114 Zhao, F. et al. Paracrine Wnt5a- and -3b2-Catenin Signaling Triggers a Metabolic Program that Drives Dendritic Cell Tolerization. *Immunity* 48, 147-160. e147, doi:10.1016/j.immuni.2017.12.004 (2018).
- 115 Ogawa, F. et al. Prostanoid induces premetastatic niche in regional lymph nodes. *The Journal of clinical investigation* 124, 4882-4894, doi:10.1172/jci73530 (2014).
- 116 DeVito, N. C., Plebanek, M. P., Theivanthiran, B. & Hanks, B. A. Role of Tumor-Mediated Dendritic Cell Tolerization in Immune Evasion. *Frontiers in immunology* 10, doi:10.3389/fimmu.2019.02876 (2019).
- 117 Alonso, R. et al. Induction of anergic or regulatory tumor-specific CD4(+) T cells in the tumor-draining lymph node. 9, 2113, doi:10.1038/s41467-018-04524-x (2018).
- 118 Huber, A., Dammeijer, F., Aerts, J. & Vroman, H. Current State of Dendritic Cell-Based Immunotherapy: Opportunities for in vitro Antigen Loading of Different DC Subsets? *Frontiers in immunology* 9, 2804, doi:10.3389/fimmu.2018.02804 (2018).
- 119 van Gulijk, M., Dammeijer, F., Aerts, J. & Vroman, H. Combination Strategies to Optimize Efficacy of Dendritic Cell-Based Immunotherapy. *Frontiers in immunology* 9, 2759, doi:10.3389/fimmu.2018.02759 (2018).
- 120 Hegmans, J. P. et al. Consolidative dendritic cell-based immunotherapy elicits cytotoxicity against malignant mesothelioma. *American journal of respiratory and critical care medicine* 181, 1383-1390, doi:10.1164/rccm.200909-1465OC (2010).
- 121 Aerts, J. et al. Autologous Dendritic Cells Pulsed with Allogeneic Tumor Cell Lysate in Mesothelioma: From Mouse to Human. *Clinical cancer research : an official journal of the American Association for Cancer Research* 24, 766-776, doi:10.1158/1078-0432.ccr-17-2522 (2018).
- 122 Mitchell, D. A. et al. Tetanus toxoid and CCL3 improve dendritic cell vaccines in mice and glioblastoma patients. *Nature* 519, 366-369, doi:10.1038/nature14320 (2015).
- 123 Gross, S. et al. Twelve-year survival and immune correlates in dendritic cell-vaccinated melanoma patients. *JCI insight* 2, doi:10.1172/jci.insight.91438 (2017).
- 124 Wculek, S. K., Cueto, F. J., Mujal, A. M., Melero, I. & Krummel, M. F. Dendritic cells in cancer immunology and immunotherapy. 20, 7-24, doi:10.1038/s41577-019-0210-z (2020).
- 125 Cornelissen, R. et al. Extended Tumor Control After Dendritic Cell Vaccination With Low Dose Cyclophosphamide as Adjuvant Treatment in Patients With Malignant Pleural Mesothelioma. *American journal of respiratory and critical care medicine* (2015).



INTRODUCTION

- 126 van der Burg, S. H., Arens, R., Ossendorp, F., van Hall, T. & Melief, C. J. Vaccines for established cancer: overcoming the challenges posed by immune evasion. *Nature reviews. Cancer* 16, 219-233, doi:10.1038/nrc.2016.16 (2016).
- 127 Saxena, M., van der Burg, S. H., Melief, C. J. M. & Bhardwaj, N. Therapeutic cancer vaccines. *Nature reviews. Cancer*, doi:10.1038/s41568-021-00346-0 (2021).
- 128 Sahin, U. & Tureci, O. Personalized vaccines for cancer immunotherapy. *Science* 359, 1355-1360, doi:10.1126/science.aar7112 (2018).
- 129 Sahin, U. et al. Personalized RNA mutanome vaccines mobilize poly-specific therapeutic immunity against cancer. *Nature* 547, 222-226, doi:10.1038/nature23003 (2017).
- 130 Kenter, G. G. et al. Vaccination against HPV-16 oncoproteins for vulvar intraepithelial neoplasia. *The New England journal of medicine* 361, 1838-1847, doi:10.1056/NEJMoa0810097 (2009).
- 131 Hu, Z. et al. Personal neoantigen vaccines induce persistent memory T cell responses and epitope spreading in patients with melanoma. *Nature medicine*, doi:10.1038/s41591-020-01206-4 (2021).
- 132 Melief, C. J. M. & Welters, M. J. P. Strong vaccine responses during chemotherapy are associated with prolonged cancer survival. 12, doi:10.1126/scitranslmed.aaz8235 (2020).
- 133 Massarelli, E. et al. Combining Immune Checkpoint Blockade and Tumor-Specific Vaccine for Patients With Incurable Human Papillomavirus 16-Related Cancer: A Phase 2 Clinical Trial. *JAMA oncology* 5, 67-73, doi:10.1001/jamaoncol.2018.4051 (2019).
- 134 Beyranvand Nejad, E. et al. Tumor Eradication by Cisplatin Is Sustained by CD80/86-Mediated Costimulation of CD8+ T Cells. *Cancer research* 76, 6017-6029, doi:10.1158/0008-5472.can-16-0881 (2016).
- 135 Suzuki, E., Sun, J., Kapoor, V., Jassar, A. S. & Albelda, S. M. Gemcitabine has significant immunomodulatory activity in murine tumor models independent of its cytotoxic effects. *Cancer biology & therapy* 6, 880-885 (2007).
- 136 Casares, N. et al. Caspase-dependent immunogenicity of doxorubicin-induced tumor cell death. *The Journal of experimental medicine* 202, 1691-1701, doi:10.1084/jem.20050915 (2005).
- 137 Vanneman, M. & Dranoff, G. Combining immunotherapy and targeted therapies in cancer treatment. *Nature reviews. Cancer* 12, 237-251, doi:10.1038/nrc3237 (2012).
- 138 Tzeng, A. et al. Temporally Programmed CD8 α + DC Activation Enhances Combination Cancer Immunotherapy. *Cell reports* 17, 2503-2511, doi:https://doi.org/10.1016/j.celrep.2016.11.020 (2016).
- 139 Wada, S. et al. Cyclophosphamide Augments Antitumor Immunity: Studies in an Autochthonous Prostate Cancer Model. *Cancer research* 69, 4309, doi:10.1158/0008-5472.CAN-08-4102 (2009).
- 140 Laheru, D. et al. Allogeneic granulocyte macrophage colony-stimulating factor-secreting tumor immunotherapy alone or in sequence with cyclophosphamide for metastatic pancreatic cancer: a pilot study of safety, feasibility, and immune activation. *Clinical cancer research : an official journal of the American Association for Cancer Research* 14, 1455-1463, doi:10.1158/1078-0432.ccr-07-0371 (2008).
- 141 Klaeger, S. et al. The target landscape of clinical kinase drugs. *Science* 358, eaan4368, doi:10.1126/science.aan4368 (2017).
- 142 Demetri, G. D. et al. Efficacy and Safety of Imatinib Mesylate in Advanced Gastrointestinal Stromal Tumors. *New England Journal of Medicine* 347, 472-480, doi:10.1056/NEJMoa020461 (2002).
- 143 Medina, B. D. & Liu, M. Oncogenic kinase inhibition limits Batf3-dependent dendritic cell development and antitumor immunity. 216, 1359-1376, doi:10.1084/jem.20180660 (2019).
- 144 Dammeijer, F., Lau, S. P., van Eijck, C. H. J., van der Burg, S. H. & Aerts, J. Rationally combining immunotherapies to improve efficacy of immune checkpoint blockade in solid tumors. *Cytokine & growth factor reviews* 36, 5-15, doi:10.1016/j.cytogfr.2017.06.011 (2017).
- 145 Pai, C. S. et al. Clonal Deletion of Tumor-Specific T Cells by Interferon- γ Confers Therapeutic Resistance to Combination Immune Checkpoint Blockade. *Immunity* 50, 477-492.e478, doi:10.1016/j.immuni.2019.01.006 (2019).
- 146 Ebert, P. J. R. et al. MAP Kinase Inhibition Promotes T Cell and Anti-tumor Activity in Combination with PD-L1 Checkpoint Blockade. *Immunity* 44, 609-621, doi:10.1016/j.immuni.2016.01.024 (2016).
- 147 Drost, J. & Clevers, H. Organoids in cancer research. *Nature Reviews Cancer* 18, 407-418, doi:10.1038/s41568-018-0007-6 (2018).
- 148 Zitvogel, L., Pitt, J. M., Daillère, R., Smyth, M. J. & Kroemer, G. Mouse models in oncoimmunology. *Nature Reviews Cancer* 16, 759-773, doi:10.1038/nrc.2016.91 (2016).
- 149 Guerin, M. V., Finisguerra, V., Van den Eynde, B. J., Bercovici, N. & Trautmann, A. Preclinical murine tumor models: A structural and functional perspective. *eLife* 9, e50740, doi:10.7554/eLife.50740 (2020).
- 150 Willimsky, G. & Blankenstein, T. Sporadic immunogenic tumours avoid destruction by inducing T-cell tolerance. *Nature* 437, 141-146, doi:10.1038/nature03954 (2005).
- 151 DuPage, M., Mazumdar, C., Schmidt, L. M., Cheung, A. F. & Jacks, T. Expression of tumour-specific antigens underlies cancer immunoediting. *Nature* 482, 405-409, doi:10.1038/nature10803 (2012).
- 152 Devaud, C. et al. Tissues in different anatomical sites can sculpt and vary the tumor microenvironment to affect responses to therapy. *Molecular therapy : the journal of the American Society of Gene Therapy* 22, 18-27, doi:10.1038/mt.2013.219 (2014).
- 153 Beatty, G. L. et al. Exclusion of T Cells From Pancreatic Carcinomas in Mice Is Regulated by Ly6C(low) F4/80(+) Extratumoral Macrophages. *Gastroenterology* 149, 201-210, doi:10.1053/j.gastro.2015.04.010 (2015).
- 154 Lee, J. W., Komar, C. A., Bengsch, F., Graham, K. & Beatty, G. L. Genetically Engineered Mouse Models of Pancreatic Cancer: The KPC Model (LSL-Kras(G12D/+);LSL-Trp53(R172H/+);Pdx-1-Cre), Its Variants, and Their Application in Immuno-oncology Drug Discovery. *Curr Protoc Pharmacol* 73, 14.39.11-14.39.20 (2016). <http://europepmc.org/abstract/MED/27248578
- 155 Rozeman, E. A. et al. Survival and biomarker analyses from the OpACIN-neo and OpACIN neoadjuvant immunotherapy trials in stage III melanoma. *Nature medicine* 27, 256-263, doi:10.1038/s41591-020-01211-7 (2021).
- 156 Topalian, S. L., Taube, J. M. & Pardoll, D. M. Neoadjuvant checkpoint blockade for cancer immunotherapy. *Science* 367, eaax0182, doi:10.1126/science.aax0182 (2020).
- 157 Yost, K. E. et al. Clonal replacement of tumor-specific T cells following PD-1 blockade. *Nature medicine* 25, 1251-1259 (2019).
- 158 Roh, W. et al. Integrated molecular analysis of tumor biopsies on sequential CTLA-4 and PD-1 blockade reveals markers of response and resistance. *Science translational medicine* 9, eaah3560, doi:10.1126/scitranslmed.aah3560 (2017).
- 159 Galluzzi, L., Humeau, J., Buqué, A., Zitvogel, L. & Kroemer, G. Immunostimulation with chemotherapy in the era of immune checkpoint inhibitors. *Nature Reviews Clinical Oncology*, doi:10.1038/s41571-020-0413-z (2020).
- 160 de Gooijer, C. J. et al. Switch-maintenance gemcitabine after first-line chemotherapy in patients with malignant mesothelioma (NVALT19): an investigator-initiated, randomised, open-label, phase 2 trial. *Lancet Respir Med*, doi:10.1016/s2213-2600(20)30362-3 (2021).
- 161 Mantovani, A., Marchesi, F., Malesci, A., Laghi, L. & Allavena, P. Tumour-associated macrophages as treatment targets in oncology. *Nature reviews. Clinical oncology* 14, 399-416, doi:10.1038/nrclinonc.2016.217 (2017).
- 162 Spolski, R., Li, P. & Leonard, W. J. Biology and regulation of IL-2: from molecular mechanisms to human therapy. *Nature Reviews Immunology* 18, 648-659, doi:10.1038/s41577-018-0046-y (2018).
- 163 Kalia, V. et al. Prolonged Interleukin-2R α Expression on Virus-Specific CD8+ T Cells Favors Terminal-Effector Differentiation In Vivo. *Immunity* 32, 91-103, doi:https://doi.org/10.1016/j.immuni.2009.11.010 (2010).
- 164 Beltra, J.-C. et al. IL2R β -dependent signals drive terminal exhaustion and suppress memory development during chronic viral infection. *Proceedings of the National Academy of Sciences* 113, E5444-E5453, doi:10.1073/pnas.1604256113 (2016).



NOVEL IMMUNOLOGICAL INSIGHTS
INTO CHEMOTHERAPY AND
IMMUNE-CHECKPOINT BLOCKADE



2

Floris Dammeijer
Mandy van Gulijk
Evalyn E Mulder
Melanie Lukkes
Larissa Klaase
Thierry van den Bosch
Menno van Nimwegen
Sai Ping Lau
Kitty Latupeirissa
Sjoerd Schetters
Yvette van Kooyk
Louis Boon
Antien Moyaart
Yvonne M. Mueller
Peter D Katsikis
Alexendar M. Eggermont
Heleen Vroman
Ralph Stadhouders
Rudi Hendriks
Jan von der Thüsen
Dirk J. Grünhagen
Kees Verhoef
Thorald van Hall
Joachim G Aerts

Cancer Cell. 2020 Nov 9;38(5):685-700.e8.

PART A
*Novel immunological insights
into chemotherapy and
immune-checkpoint blockade*

THE PD-1/PD-L1-CHECKPOINT
RESTRAINS T-CELL IMMUNITY IN TUMOR-DRAINING
LYMPH NODES

PART A
Novel immunological insights
into chemotherapy and
immune-checkpoint blockade

THE PD-1/PD-L1-CHECKPOINT
RESTRAINS T-CELL IMMUNITY IN TUMOR-DRAINING
LYMPH NODES

SUMMARY

PD-1/PD-L1-checkpoint blockade therapy is generally thought to relieve tumor-cell mediated suppression in the tumor microenvironment but PD-L1 is also expressed on non-tumor macrophages and conventional dendritic cells (cDCs). Here we show in mouse tumor models that tumor-draining lymph nodes (TDLNs) are enriched for tumor-specific PD-1+ T cells which closely associate with PD-L1+ cDCs. TDLN-targeted PD-L1-blockade induces enhanced anti-tumor T-cell immunity by seeding the tumor site with progenitor-exhausted T cells, resulting in improved tumor control. Moreover, we show that abundant PD-1/PD-L1-interactions in TDLNs of non-metastatic melanoma patients, but not those in corresponding tumors, associate with early distant disease recurrence. These findings point at a critical role for PD-L1 expression in TDLNs in governing systemic anti-tumor immunity, identifying high-risk patient groups amendable to adjuvant PD-1/PD-L1-blockade therapy.

Significance.

The majority of cancer patients do not or only temporarily respond to anti-PD-1/PD-L1 blocking antibodies with mechanisms of resistance being incompletely known. Tumor-draining lymph nodes (TDLNs) have been found to be crucial for anti-tumor T-cell priming. We identify PD-1/PD-L1 interactions to occur frequently in TDLNs of solid-tumor bearing mice and with specific inhibition of PD-1/PD-L1 signaling in TDLNs induces effective anti-tumor immune responses capable of reducing distant tumor growth in several tumor models. In non-metastatic melanoma patients high frequency PD-1/PD-L1 interactions in the TDLN associated with early distant disease recurrence independent of known prognostic markers. These findings identify TDLNs as important sites mediating-PD-L1 immunotherapy efficacy, challenging the current dogma that the PD-1-checkpoint restricts T-cell immunity primarily at the effector site.

INTRODUCTION

Drugs targeting the PD-1/PD-L1 pathway have revolutionized the treatment of multiple cancer types including non-small cell lung cancer, renal cancer and melanoma with a subset of patients experiencing durable responses. However, still a majority of patients and cancer types do not, or only temporarily respond to these immune checkpoint blocking (ICB) drugs^{1,2}. PD-1/PD-L1 blocking antibodies are believed to act primarily in the tumor microenvironment (TME), by re-invigorating exhausted T cells and thereby reviving pre-existing anti-tumor immunity². Based on this hypothesis, several theories have been proposed to explain the lack of ICB-efficacy in patients, such as a lack of PD-L1 expression or T-cell infiltration in the TME and upregulation of other co-inhibitory receptors or suppressive molecules following ICB-therapy^{3,4}. However, the predictive value of these proposed biomarkers remains poor in the majority of tumors, while the relevance of PD-L1-expression at other sites remains unknown. Furthermore, results from recent trials evaluating combination therapy with anti-PD-(L)1 and other co-inhibitory pathways in the TME have been disappointing⁵⁻⁸. Therefore, a more comprehensive interrogation of the molecular and spatial mechanisms of anti-PD-1/PD-L1 therapy is needed to further boost immunotherapy efficacy.

Several recent insights exploring the biology of the PD-1 receptor and its corresponding ligand PD-L1 offer clues into what drives ICB-efficacy. Besides tumor cells, myeloid cells expressing PD-L1 have been revealed to be essential for ICB-efficacy as anti-PD-L1 antibodies remained effective in transplanted tumor cells lacking PD-L1 in a variety of models⁹⁻¹². Furthermore, these seminal discoveries offer an explanation for the rather unexpected finding that PD-1 primarily acts by inhibiting signaling downstream of the CD28 costimulatory receptor following B7-ligation, proposedly by myeloid cells^{13,14}. Where this interaction and therapeutic disruption in case of anti-PD-1/PD-L1 antibodies takes place, however, is still unknown as current genetic and pharmacologic interventions (e.g. with the S1PR-blocking agent FTY720) limit proper spatiotemporal analysis of ICB-induced anti-tumor immune responses^{9,11,15}. Additional insights into these dynamics may improve ICB-response prediction and future immunotherapy development.

Recent investigations analyzing T-cell receptor (TCR) clonotypes in mouse and patient tumors before and after anti-PD-1 therapy suggest the appearance of novel, previously non-existing clonotypes in ICB-treated tumors, and a limited expansion capacity of tumor-resident T cells following treatment^{16,17}. In contrast to terminally differentiated tumor-resident T cells, T-cell factor 1 (TCF-1)-expressing progenitor-exhausted T cells have recently been described to generate effector T-cell progeny, however their exact origins remain unknown¹⁸. These findings, together with an abundance of B7-expressing antigen-presenting cells being exposed to draining tumor-antigens prompted us to investigate the

PART A
Novel immunological insights
into chemotherapy and
immune-checkpoint blockade

THE PD-1/PD-L1-CHECKPOINT
RESTRAINS T-CELL IMMUNITY IN TUMOR-DRAINING
LYMPH NODES

role of tumor-draining lymph nodes (TDLNs) in efficacy of anti-PD-L1-therapy in multiple pre-clinical tumor mouse models. We find that TDLNs harbor significant proportions of tumor-specific PD-1⁺ T cells co-localizing with PD-L1 expressing myeloid cells including conventional dendritic cells (cDCs). Selective targeting of PD-L1 only in the TDLN, reveals that TDLN-localized T-cells are capable of mounting effective anti-tumor immune responses thereby demonstrating that TDLN-resident T cells are able to generate ICB-mediated immunity. Finally, we show the role of this PD-1/PD-L1 interaction in the TDLN of stage II melanoma patients, independent of known prognostic parameters. TDLNs in patients with early disease recurrence are enriched for PD-1/PD-L1 interactions which seem to primarily occur between T cells and CD11c⁺ DCs. In patients without disease recurrence there are fewer PD-1/PD-L1 interactions in the TDLN. These results offer unexplored insights in the role of TDLNs in generating effective anti-tumor immunity and challenge the current dogma that PD-1/PD-L1-blockade occurs primarily at the tumor site.

METHODS

Mouse models.

Female 8-12-week-old CBA/J mice and C57BL/6 mice were purchased from Janvier and Envigo, respectively, and housed under specific pathogen-free conditions in individually ventilated cages at the animal care facility of the Erasmus MC, Rotterdam. All mouse experiments were controlled by the animal welfare committee (IvD) of the Erasmus MC and approved by the national central committee of animal experiments (CCD) under the permit number AVD101002017867, in accordance with the Dutch Act on Animal Experimentation and EU Directive 2010/63/EU.

Mouse tumor cell lines.

The AC29 mesothelioma cell line was derived from tumors induced by crocidolite asbestos into CBA/J mice and was kindly provided by Prof. Bruce W.S. Robinson (Queen Elizabeth II Medical Centre, Nedlands, Australia). The OVA-transfected AE17 cell line was kindly provided by Prof. Delia J. Nelson (Curtin University, Perth, Australia). All mesothelioma cell lines were cultured in RPMI1640 medium containing 25 mmol/L HEPES, Glutamax, 50mg/mL gentamicin (all obtained from Gibco) and 5% fetal bovine serum (FBS) (Capricorn Scientific) in a humidified atmosphere and at 5% CO₂, in air. For culturing AE17-OVA cells, the culture medium was supplemented with 50 mg/mL geneticin (Gibco). The MC38, B16F10, KPC3 and lentivirally transduced KPC3-OVA tumor cell lines were cultured in IMDM medium (Gibco) containing L-Glutamine, 25 mmol/L HEPES, 50mg/mL gentamicin and 8% FBS. Authentication of the cell lines was performed by short tandem microsatellite

repeat analysis or by antigen-specific T cell recognition. For culture, either culture flasks or CellSTACKs (Corning Life Sciences) were used to reach the appropriate tumor cell frequencies for injection.

Melanoma patient cohort.

For this study, cutaneous melanoma patients who underwent a sentinel lymph node biopsy (SLNB) at the Erasmus Medical Center (MC) Cancer Institute between 2005 and 2016 and had a *negative* SLN (i.e. no metastasis to the TDLN) were identified. From this cohort, two extreme populations of patients were identified: 1) patients with a negative SLN with early (< 48 months) distant recurrence (with or without prior locoregional/regional lymph node recurrence); 2) patients with a negative SLN without recurrence (> 96 months). In an attempt to avoid confounding influences of prior malignant disease on TDLNs, patients who developed (prior) metastatic disease within the regional lymph nodes (similar to the SLN basin) within 9 months were excluded.

Histopathological information of the primary melanoma and SLN were retrieved from the pathology reports. Patient characteristics and follow-up data were obtained from the medical records. This study was approved by the Erasmus MC Ethics Committee (ref. no. MEC-2017-375). Human tissues and patient data were used according to “The Code for Proper Secondary Use of Human Tissue” and “The Code of Conduct for the Use of Data in Health Research” as stated by the Federation of Dutch Medical Scientific Societies.

According to aforementioned criteria, 40 patients were eligible. A pathologist from the Erasmus MC Cancer Institute a) assessed the presence of sufficient formalin-fixed paraffin-embedded (FFPE) SLN specimen, b) revised a hematoxylin and eosin (H&E) slide for each SLN confirming the absence of (micro)metastasis according to previously published protocols (*Van der Ploeg et al. European Journal of Cancer 2010¹⁹*), c) selected one (of the) SLN(s) per patient. Eventually, sufficient and representative SLN material could be retrieved from 15 patients in group 1. Consequently, 15 cases from group 2 were randomly identified as well.

The median patient age was 50 years (interquartile range [IQR] 41 – 59), with a male predominance of 67% (20 males). Median duration to distant metastasis was 21.0 months (9.0 – 36.0). Further clinicopathological features and follow-up of all patients, and per subgroup, are summarized in table S1.

In vivo experiments in mouse tumor models.

For tumor inoculation, mice were i.p. injected with AC29 (10⁷), AE17-OVA (10⁶) or MC38: (2.5x10⁵) tumor cells in 300 µL PBS. KPC3 (10⁴), KPC3-OVA (10⁴) or B16F10 (10⁴) tumor cells were injected s.c. in 200 µL PBS in the flanks of mice that were briefly anesthetized using isoflurane. In case of non-TDLN and TDLN characterization, mice with established

PART A
Novel immunological insights
into chemotherapy and
immune-checkpoint blockade

THE PD-1/PD-L1-CHECKPOINT
RESTRAINS T-CELL IMMUNITY IN TUMOR-DRAINING
LYMPH NODES

i.p. tumors (AC29, AE17-OVA and MC38) were killed when profoundly ill according to the body condition score, which was around day 20. Mice with established s.c. tumors (B16F10, KPC3 and KPC3-OVA) were euthanized when tumor size reached 1000-2000 mm³ (measured by 0.52 x length x width x height). For B16F10 and KPC3 tumor models, this tumor size was reached around day 20 whereas this size was reached at ~ day 45 for the KPC3-OVA model. Mice were randomly assigned to experimental groups.

anti-PD-L1 treatment.

Dependent on treatment arm, mice with established peritoneal mesothelioma (AC29 or AE17-OVA) or peritoneal carcinomatosis (colon-carcinoma derived; MC38) were treated with either 200 µg isotype (clone 2A3, BioXCell), 2.5 µg anti-PD-L1 antibody (clone MIH5, provided by L. Boon Bioceros) or 200 µg anti-PD-L1 antibody in 50 µL PBS when injected intravenously or, in case of intrapleural injection, in 200 µL PBS via injection in the pleural cavity of mice that were under short-term anesthesia.

FTY720 administration.

To block lymphocyte trafficking, AC29 tumor-bearing mice received either vehicle or FTY720 (Sigma-Aldrich) from day 9 onwards via drinking water (2.5 µg/mL) and via daily oral gavage (2 µg/g body weight). Retention of lymphocytes in lymphoid organs was assessed on day 14 in peripheral blood by flow cytometry.

CEL treatment. In LN-macrophage depletion experiments, mice bearing AC29 mesothelioma tumors received 10 µL CEL (Clodrosome) dissolved in 190 µL PBS (5%) or 200 µL PBS i.p., serving as a negative control.

Dendritic-cell therapy. For BMDC-transfer AC29 tumor lysate was produced and DCs were cultured as previously described (Dammeijer et al. Cancer Immunology Research 2017). Briefly, tumor lysate was produced by disrupting frozen tumor cells by four cycles of freeze-thaw cycles with liquid nitrogen followed by sonication. BMDCs were generated as reported previously (Dammeijer et al. Cancer Immunology Research 2017), using recombinant murine GM-CSF (provided by B. Lambrecht VIB, Ghent) in DC-culture medium followed by loading with tumor lysate and activation with CpG (Invitrogen) on day 9 and injection at day 10 following CFSE-labeling according to manufacturer's instructions (Thermo Fisher). Cells were checked for surface expression of CD11c and MHC-II to confirm the DC-phenotype prior to administration (data not shown).

Adoptive-cell transfer of OT-I and OT-II cells.

For adoptive cell transfer of OT-I and OT-II cells, OT-I and OT-II CD45.1 (Ly5.1) were generated as reported previously (Hope, Front Immunol, 2019). LNs and spleens were harvested from 9-11 week-old female OT-I and OT-II CD45.1 transgenic mice after which OT-I and OT-II

cells were isolated by negative selection, using EasySep magnetic nanoparticles (StemCell Technologies), according to manufacturer's protocol. Subsequently, CD45.1 OT-I and OT-II cells were labeled with Far Red Proliferation Dye (Thermo Fisher) according to the manufacturer's instructions, and injected i.v. (2.5×10^5 - 3.0×10^5 cells/mouse) into recipient mice.

Blood was collected at defined time points by tail vein incision to evaluate immune responses in peripheral blood. Mice were examined every 1-2 days for evidence of illness caused by overt tumor growth and euthanized at predefined endpoints or when mice were profoundly ill in case of survival analysis.

Preparation of single cell suspensions.

Single-cell suspensions were generated from isolated interim blood, non-TDLN, TDLN and tumor tissue of mice from each group as previously reported 20. Briefly, blood was collected in EDTA tubes (Microvette CB300, Sarstedt) after which the volume was determined. Subsequently, collected blood was lysed by erythrocyte lysis using osmotic lysis buffer (8.3% NH₄Cl, 1% KHCO₃, and 0.04% Na₂EDTA in Milli-Q). Single-cell suspensions of non-TDLNs, TDLNs and spleens were generated by mechanically dispersing the lymph nodes through a 100-µm nylon mesh cell strainer (BD Biosciences) followed by osmotic lysis of erythrocytes in case of spleens. Tumors were collected, weighed in a microbalance and dissociated using a validated tumor dissociation system (Miltenyi Biotec) according to protocol. After dissociation, cell suspensions were filtered through a 100-µm nylon mesh cell strainer.

Flow cytometry.

In order to measure cytokine production in lymphoid cells by flow cytometry, cells were restimulated for 4 hours at 37 °C using PMA and ionomycin (Sigma-Aldrich) supplemented with GolgiPlug (BD Biosciences). For cell surface staining, single cells were stained with antibodies together with anti-mouse 2.4G2 (anti-CD16/CD32) antibody (Provided by L. Boon, Bioceros; 1:300) for 30 minutes at 4°C. After this incubation period, cells were washed with FACS buffer (0.05% NaN₃, 2% BSA in PBS), followed by a PBS wash and stained for viability using fixable LIVE/DEAD aqua cell stain (Thermo Fisher, 1:200) at 4°C for 15 minutes. After two washing steps with FACS buffer, cells were either directly measured or, in case of intracellular staining, fixed and permeabilized with Foxp3 / Transcription Factor Staining Buffer Set (Thermo Fisher) to stain nuclear factors. Intranuclear antibodies were incubated for 60 minutes at 4°C. A fixed number of counting beads (Polysciences Inc.) was added to the samples derived from blood prior to acquisition of the data to determine the absolute amount of cells.

In order to detect OVA₍₂₅₇₋₂₆₄₎ specific CD8⁺ T cells in the AE17-OVA and KPC3-OVA models, PE-labeled tetramers of H-2K^b major histocompatibility complex class I loaded

PART A
Novel immunological insights
into chemotherapy and
immune-checkpoint blockade

THE PD-1/PD-L1-CHECKPOINT
RESTRAINS T-CELL IMMUNITY IN TUMOR-DRAINING
LYMPH NODES

with OVA₍₂₅₇₋₂₆₄₎ peptide were obtained²¹. Tetramer-binding to CD4⁺ T cells was used to determine the level of background signal and to set cutoff limits. To assess the binding of *in vivo* administered anti-PD-L1, single cell suspensions of processed tissues were washed with FACS buffer and incubated with 5% normal donkey serum for 30 minutes on 4°C. After washing with FACS buffer, cells were counterstained using a donkey anti-rat IgG2A antibody labeled with either a Cy5-fluorochrome or a Alexa Fluor 488 fluorochrome (Jackson ImmunoResearch) for 30 minutes on 4°C. Subsequently, cells were incubated for 10 minutes at 4°C with 5% rat serum in FACS buffer after washing with FACS buffer. Data were acquired using a LSR II flow cytometer equipped with three lasers and FACSDiva software (v.8.0.2) after compensation with UltraComp Compensation beads (Thermo Fisher). Acquired data were analyzed by using a licensed version of Flowjo (v.10.4.2).

Immune cell subsets were characterized using the following set of markers following single cell, alive and CD45⁺ cell selection: CD8⁺ T cells (CD3⁺/CD4⁺/CD8⁺), CD4⁺ T-helper cells (CD3⁺/CD8⁺/CD4⁺/FoxP3⁻), Tregs (CD3⁺/CD8⁺/CD4⁺/FoxP3⁺/CD25^{high}). In the myeloid-cell panels, a lineage mix (CD3/CD19/CD335) was included. Subsets were characterized as: subcapsular sinus macrophages (Lineage⁻/Ly6C^{low}/Ly6G⁻/CD169⁺/F480⁺), medullary sinus macrophages (Lineage⁻/CD11b⁺/Ly6C^{low}/Ly6G⁻/CD169⁺/F480⁺), granulocytes (Lineage⁻/CD11b⁺/Ly6G⁺), conventional type 1 dendritic cells (cDC1: lineage⁻/CD11c⁺/MHC-II⁺/CD11b⁻), cDC2 (lineage⁻/CD11c⁺/MHC-II⁺/CD11b⁻). In the experiments performed in figure S3, CD172a and XCR1 were additionally included to characterize cDC2 and cDC1, respectively.

Multicolor confocal microscopy.

TDLNs were embed in Tissue-TEK II optimum cutting temperature medium (Sakura), snap-frozen, and stored at -80°C. Tissue sections were cut at 16µm on a cryostat (Cryostar NX70, Thermo Fisher Scientific) and rehydrated in in 0.1 M Tris buffer for 30 minutes and blocked with blocking buffer (0.1 M Tris buffer, 0.02% Triton X-100, 1% normal mouse serum, 1%BSA and 5% normal donkey serum) for 1 hour. After washing with 0,1 M Tris buffer, sections were stained with a donkey anti-rat antibody that would bind to the therapeutic antibody in blocking buffer for 6 hours at 4°C followed by an incubation with 5% normal rat serum in blocking buffer for 10 minutes. Subsequently, sections were stained with directly labeled primary antibodies in Tris blocking buffer for 16 hours at 4°C and subsequently stained with streptavidin for 2 hours. After extensive washing with Tris buffer, nuclei were counterstained with JOJO-1 Iodide (Thermo Fisher) and tissue sections were mounted in Fluoromount-G (Thermo Fischer). Acquisition of whole cross-sections was performed on a Leica TCS SP8 confocal microscope with tunable white-light laser, 405 nm violet laser, and Leica PMT and HyD hybrid detectors. Acquisition was performed in 3 individual sequential acquisition steps, optimized tunable excitation and emission settings were

defined experimentally using single stains, timed gating with the pulsed white light laser in combination with the HyD detector was applied with AF488, AF555, AF555, AF594 and AF647 dyes. Following acquisition, the tiled images were merged and compensated using the LAS X Merge and Channel Dye Separation module (using single stains under identical acquisition settings), respectively, after which the images were further analyzed using Imaris 9.2 (Bitplane). Following the histocytometry work flow as previously described, cellular identities were created to investigate co-localization. The channel for CD8⁺ and CD4⁺ cells was obtained by first creating a mask channel by selecting for CD8⁺ CD11c⁻ and CD4⁺ CD11c⁻ voxels, respectively. Next, a CD8 “T cell” and CD4 “T cell” expression channel was created by combining the CD8⁺ or CD4⁺ voxels on the CD8⁺ CD11c⁻ mask and CD4⁺ CD11c⁻ mask, respectively, to exclude CD8⁺ CD11c⁺ DCs and CD4⁺ CD11c⁺ DCs from this channel. In addition, channels for CD169⁺ macrophages and CD11c⁺ DCs that were bound by anti-PD-L1 were created by selecting CD169⁺ anti-PD-L1⁺ voxels or CD11c⁺ anti-PD-L1⁺ voxels, respectively. These channels, together with the CD8⁺ CD11c⁻ channel, were used to create surfaces with Imaris Surface Module (Bitplane) for figure representation. For publication and clarity purposes, we applied a gamma correction of 0.7 to the images, except for the surfaces.

TIL re-stimulation culture.

Frozen single-cell suspensions generated from end-stage AE17-OVA tumors were thawed and stained with the CellTrace Far Red Cell Proliferation dye according to manufacturer's protocol. After labeling with the proliferation dye, cells were counted in trypan blue with a hemocytometer using the Bürker-Türk method. Subsequently, cells were resuspended in 2.0x10⁶ cells/mL culture medium consisting of IMDM containing L-Glutamine, Glutamax, 25 mmol/L HEPES, 50 mg/mL gentamicin, 50 mmol/L mercaptoethanol (Sigma-Aldrich), 10% FBS, 4ng/mL IL-2, 4 ng/mL IL-7 4 ng/ml, 4 ng/mL IL-15 that was supplemented either with either 10 µg/mL isotype, 1 µg/mL OVA₍₂₅₇₋₂₆₄₎ peptide (provided by Anaspec) and 10 µg/mL isotype or with 1 µg/mL OVA₍₂₅₇₋₂₆₄₎ peptide and 10 µg/mL anti-PD-L1. Cells were incubated for three days in a humidified atmosphere and at 5% CO₂, in air, after which the cells were harvested and stained for extracellular and intracellular markers.

PLA and multiplex staining (cmIHC).

PLA and cmIHC was performed with an automated, validated and accredited staining system (Ventana Benchmark Discovery ULTRA, Ventana Medical Systems, Tucson, AZ, USA). PLA was performed on 43 (34 TDLNs and 9 matched tumor samples) samples, in brief following deparaffinization and heat-induced antigen retrieval with CC1 (#950-500, Ventana Medical Systems) at 95°C for 64 minutes the tissue samples were co-incubated with anti-PD-L1 SP263 (#790-4905, Ventana Medical Systems) and anti-PD-1 NT105

PART A
Novel immunological insights
into chemotherapy and
immune-checkpoint blockade

THE PD-1/PD-L1-CHECKPOINT
RESTRAINS T-CELL IMMUNITY IN TUMOR-DRAINING
LYMPH NODES

(#760-4895, Cell Marque) at 37°C for 1 hour. Next, AP proximity detection (#253-5080 and #253-6037, Ventana Medical Systems) was performed for 16 minutes followed by pH buffer (#253-5083, Ventana Medical Systems) and proximity activator (#253-5082, Ventana Medical Systems) at 47°C for 12 minutes. Conjugating enzyme NP-HRP (#760-6038, Ventana Medical Systems) was added for 12 minutes followed by a DISC, amplified using TSA-HQ (#760-4519, Ventana Medical Systems) for 12 minutes and detected by using anti-HQ-HRP (#760-4820, Ventana Medical Systems) for 12 minutes. Visualization was performed using DAB (#760-159, Ventana Medical Systems) followed by hematoxylin II counter stain for 12 minutes and then a blue coloring reagent for 8 minutes according to the manufactures instructions (Ventana Medical Systems, Tucson, AZ, USA).

PLA with cmlHC was performed on 6 additional slides, followed after PLA staining (see above) a CC2 (#950-123, Ventana Medical Systems) 100°C for 8 minutes stripping step was performed. CD68 KP1 (#790-2931, #253-5083, Ventana Medical Systems) was incubated at 37°C for 32 minutes followed by secondary antibody, mouse omnimap HRP (#760-4310, Ventana Medical Systems) at 37°C for 24 minutes and visualized with purple (#760-229, Ventana Medical Systems) for 32 minutes. CC2 100°C for 8 minutes stripping step was performed and anti-CD8 (#790-4460, Ventana Medical Systems) was incubated at 37°C for 32 minutes followed by secondary antibody, rabbit omnimap HRP (#760-4311, Ventana Medical Systems) at 37°C for 24 minutes and visualized with Teal (#760-247, Ventana Medical Systems) for 32 minutes. CC2 100°C for 8 minutes stripping step was performed and anti-CD11c 5D11 (#111M-17, Cell Marque) was incubated at 37°C for 32 minutes followed by secondary antibody mouse-NP (#760-4816, Ventana Medical Systems) at 37°C for 32 minutes, enzyme conjugation was needed with NP-AP (#760-4827, Ventana Medical Systems) enzyme 37°C for 32 minutes visualized with Disc Yellow (#760-239, Ventana Medical Systems) for 44 minutes. Hematoxylin II counter stain for 8 minutes and then a blue coloring reagent for 4 minutes according to the manufactures instructions (Ventana Medical Systems).

Quantification of PLA and multiplex stainings.

Scanned slides were viewed using NDP-viewing software (Hamamatsu) at 40x magnification and regions of interest were randomly selected from cortical regions, excluding germinal centers and captured and imported into ImageJ software (NIH). For enumeration of contacts, the number of contacts were manually counted per 40x high-power field (hpf) and the average of a total of 8 hpfs was included into analysis. A similar approach was taken to identify cells of origin in the multiplex staining assay where PD-1/PD-L1-positivity was assessed on CD8⁺/CD8⁻ and CD11c⁺/CD68⁺/CD11c⁺CD68⁺/CD11c⁺CD68⁻-expressing cells, respectively. As a more objective and representative measure of total contacts, acquired 40x images were automatically quantified using a developed macro

which includes 2 basic steps; the first step assessing total cell-surface area per hpf with the final step determining the percentage of PLA-positivity following color-dissection and thresholding (*supplementary data S1*). The percentage of PLA-assay positivity was then taken as a percentage of total cell-surface area and the average of 15 hpfs was included for analysis.

Statistical analysis.

Data are expressed as means with the standard error of the mean (SEM). Comparisons between groups with independent samples were performed using the Mann-Whitney *U* test or independent t-test whereas the Wilcoxon-signed rank test or paired t-test were used to compare paired samples (see figure legends). In case of correlations, the Pearson correlation was used to test statistical significance. Survival data were plotted as Kaplan-Meier survival curves, using the log-rank test to determine statistical significance. P-value of 0.05 and below was considered significant

(*), $p < 0.01$ (**) and $p < 0.001$ (***) as highly significant. Data were analyzed using GraphPad Prism software (Graphpad, V5.01 and V8.0).

RESULTS

TDLNs are enriched for PD-1⁺ tumor-specific T cells.

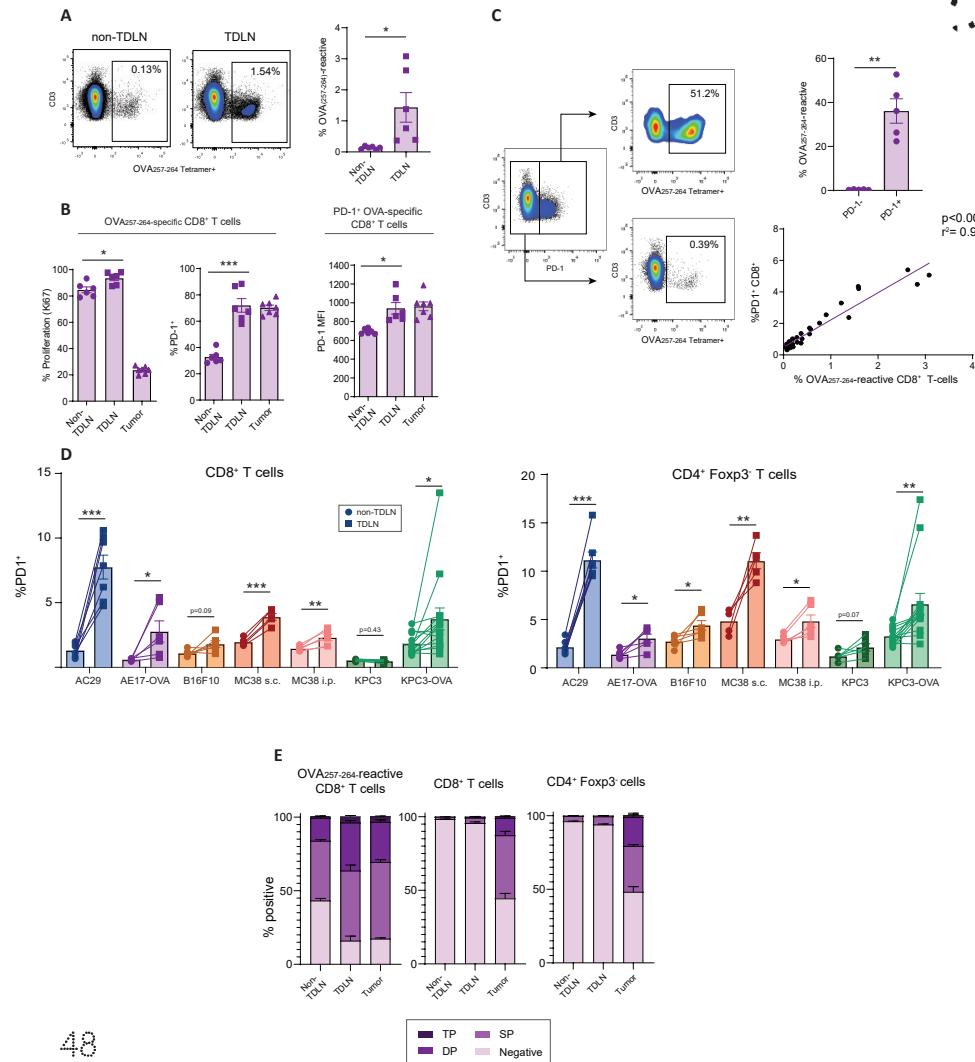
To gain insight into the activity of the PD-1/PD-L1-axis in LNs, we analyzed the frequencies and phenotype of tumor antigen-specific CD8⁺ T cells in LNs of ovalbumin (OVA)-expressing AE17 mesothelioma tumors. AE17-OVA tumor cells were injected intraperitoneally and at late stage disease mediastinal LNs that drain tumors in the peritoneal cavity (TDLNs) and inguinal control LNs (non-TDLNs) were analyzed. We found higher frequencies of OVA₂₅₇₋₂₆₄-specific CD8⁺ T cells in the TDLN, compared with a near absence of these cells in a non-TDLN (Fig. 1A, S1A). Tumor-specific CD8⁺ T cells in the TDLN were highly proliferative, expressed PD-1 with higher frequencies and to higher levels than those in non-TDLNs (Fig. 1B). In the TDLN, the proportions of PD-1-expressing CD8⁺ T cells strongly correlated with the frequency of tumor-specific CD8⁺ T cells and could therefore serve as a marker for tumor-specificity (Fig. 1C, S1A). Therefore, we enumerated PD-1⁺ CD4⁺ and CD8⁺ T cells in several solid tumor models and consistently found higher frequencies of PD-1⁺ T cells in TDLNs compared to non-TDLNs, irrespective of cancer type, mouse genetic background, tumor localization or T-cell subset, except for the KPC3 pancreatic cancer model (Fig. 1D). This difference in PD-1 expression did not appear to result from tumor metastasis to the TDLN, as the frequency of CD45⁺ cells was equally low in both TDLNs and non-TDLNs (Fig. S1B). The poorly immunogenic KPC3 pancreatic cancer cell line did not induce PD-

PART A
Novel immunological insights
into chemotherapy and
immune-checkpoint blockade

THE PD-1/PD-L1-CHECKPOINT
RESTRAINS T-CELL IMMUNITY IN TUMOR-DRAINING
LYMPH NODES

1⁺ T cells in the TDLN, suggesting that PD-1 expression is related to immunogenicity of the tumor. In line with this hypothesis, introduction of the immunogenic OVA-antigen in KPC3 recapitulated the results of the other tumor models (Fig. 1D). In addition to high PD-1 display, tumor antigen-specific CD8⁺ T cells in TDLNs expressed other co-inhibitory receptors like TIM-3 and TIGIT, resembling T cells from the tumor site (Fig. 1E). In contrast to PD-1 expression, other parameters of lymphocyte activation such as proliferation were not consistently increased across different models (Fig. S1C), but absolute T cell numbers were enhanced (Fig. S1D).

Figure 1. Tumor-draining lymph node harbor PD-1⁺ tumor-specific T cells. (A) Dot plots and quantification of CD8⁺ T cells in non-TDLNs and TDLNs showing percentages of OVA(257-264)-tetramer⁺ T cells. (B) Proliferation (Ki-67) and PD-1-positivity were determined on ovalbumin (OVA)(257-264)-tetramer⁺ CD8⁺ T-cells in non-TDLNs, TDLNs and tumor. Furthermore, PD-1-expression (MFI) was assessed on (PD-1⁺) OVA(257-264)-tetramer⁺ CD8⁺ T-cells. (C) Tetramer-positivity of PD1⁺ and PD1⁻ CD8⁺ T cells in the TDLN. In addition, proportions of PD-1⁺ CD8⁺ T cells were plotted against proportions of OVA(257-264)-tetramer⁺ CD8⁺ T cells in the TDLN and a Pearson correlation coefficient was calculated (r^2). (D) Comparison of frequencies of PD-1⁺ CD8⁺ (left panel) and CD4⁺ Foxp3⁺ T-helper (Th) cells (right panel) between TDLNs (circles) and non-TDLNs (squares) in different solid tumor models (different colors) transfected with/without OVA, or injected orthotopically (i.p.) or subcutaneously (s.c.) in CBA/J (AC29) or C57BL/6 mice (n = 6-7 mice/group, n = 14 in case of KPC3-OVA). (E) TIM-3, TIGIT and PD-1-single-positivity and co-expression was assessed on T cells in different tissues (SP = single positive, DP = double positive, TP = triple positive). Means and standard error of the mean (SEMs) are shown, paired t-tests were performed to determine statistical significance.



To more comprehensively characterize both CD4⁺ and CD8⁺ PD-1⁺ tumor-specific T cells in TDLNs and their dynamics, we infused naïve CD45.1⁺ OT-I and OT-II cells in AE17-OVA-bearing CD45.2⁺ mice and assessed their frequency and phenotype across tissues over time (Fig. 2A). As expected, CD45.1⁺ cells initially accumulated in secondary lymphoid organs including the TDLN, followed by egress and migration in blood to finally infiltrate tumor tissue 6 days post-injection (Fig. 2B). Upon homing to TDLNs, CD45.1⁺ T cells upregulated PD-1 and proliferated, suggesting PD-1 to be associated with activation rather than T-cell exhaustion (Fig. 2C). Globally, PD-1⁺ T cells further preferentially accumulated in TDLNs over time, where a subgroup of cells expressed effector molecules including IL-2, IFN γ and granzyme-B (Fig. 2D). In addition to increased expression of effector molecules, PD-1⁺ CD4⁺ and CD8⁺ T cells expressed more CD28, CD44, CD69 and SLAMF6 (Ly108) compared to their PD-1⁻ counterparts (Fig. S2)²². These results show initial activation of early-effector T cells in TDLNs, but not in non-TDLN, prior to PD-1 expression and migration to the tumor.

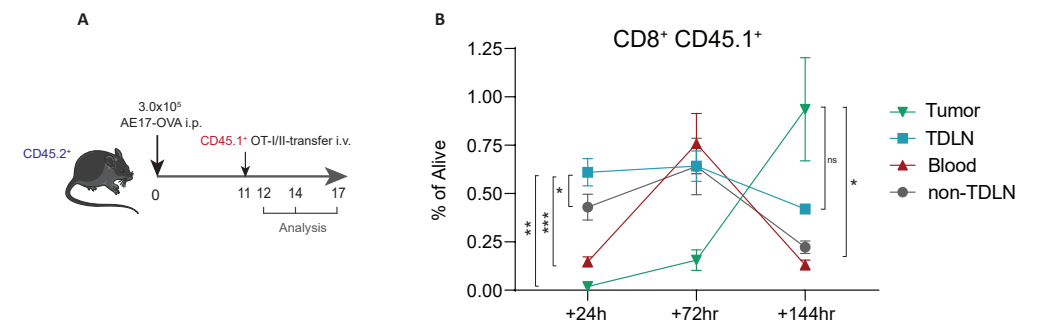
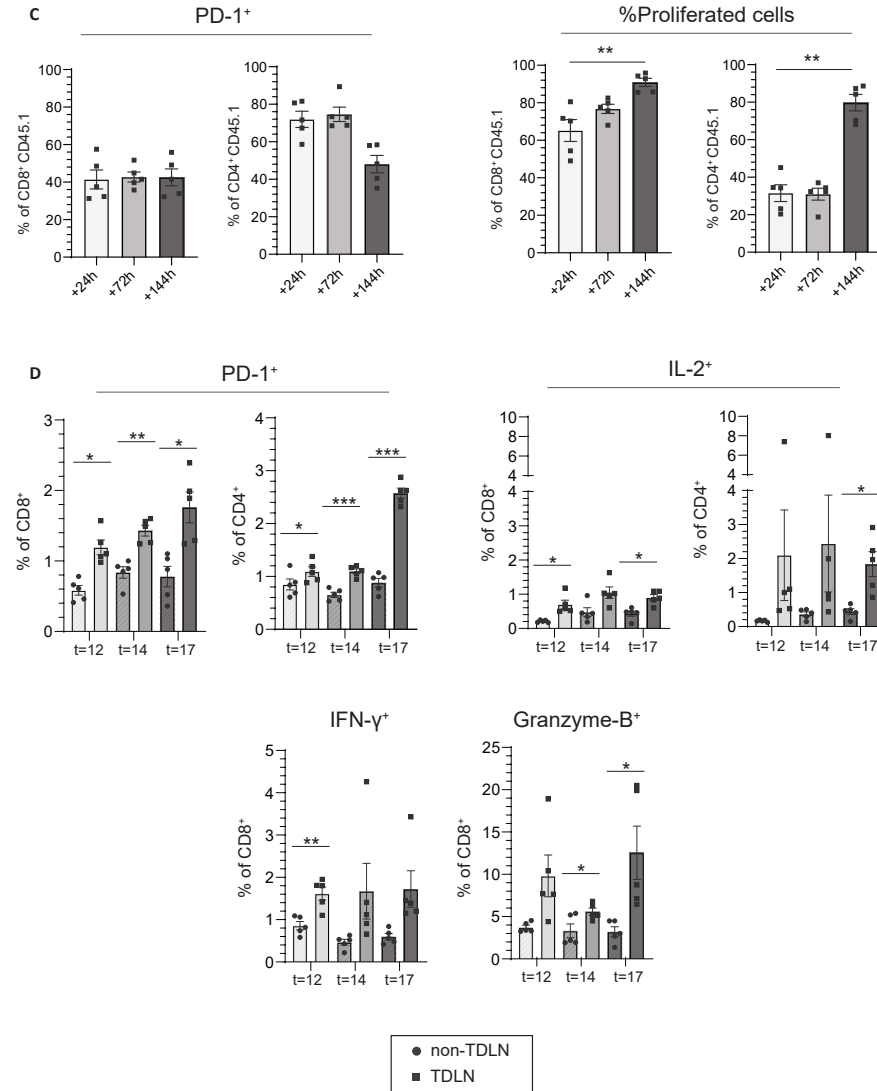


Figure 2. T-cells are activated in TDLNs prior to migration and activation in the tumor. (A) Experimental design (n=5-6 mice per group per time point). (B) Frequencies of CD45.1⁺ cells were determined in tumor, TDLN, blood and non-TDLN. (C) PD-1 positivity as well as the percentage of cells undergoing proliferation of CD8⁺CD45.1⁺ cells in

PART A
Novel immunological insights
into chemotherapy and
immune-checkpoint blockade

THE PD-1/PD-L1-CHECKPOINT
RESTRAINS T-CELL IMMUNITY IN TUMOR-DRAINING
LYMPH NODES

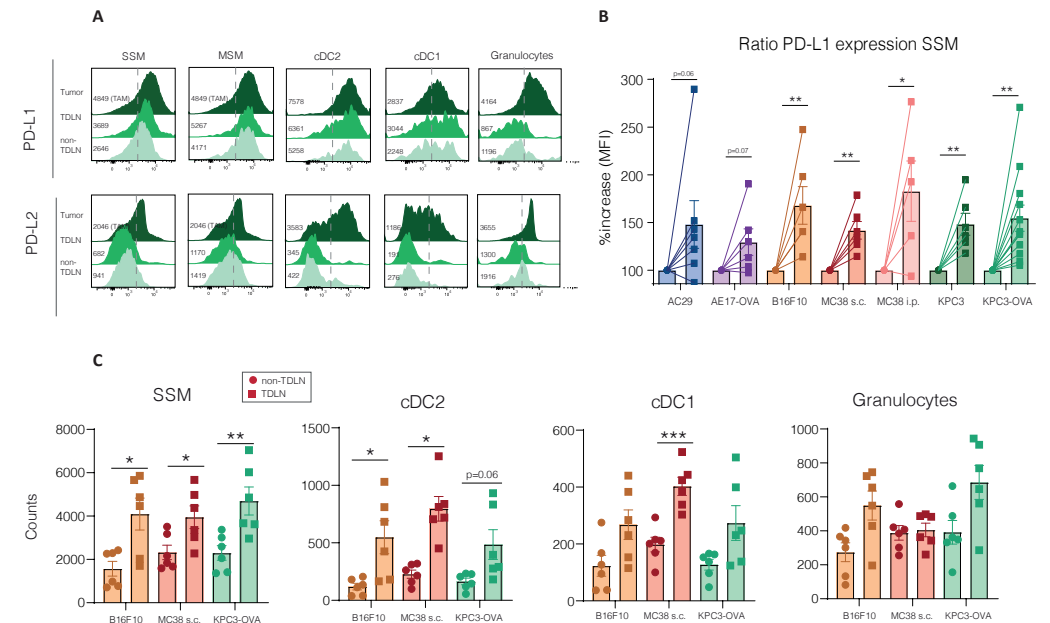
>>



the TDLN. (D) Percentages of PD-1⁺, IL-2⁺, IFN-γ⁺ and granzyme-B⁺ were compared for CD8⁺ T cells and CD4⁺ T cells in TDLN (circles) and non-TDLN (squares). Means and SEMs are shown, paired t-tests were used to calculate statistical significance. * = p < 0.05, ** p < 0.01, *** p < 0.001. TDLN = tumor-draining lymph node, i.v. = intravenous, SEM = standard error of the mean, IL-2 = interleukin 2, IFN-γ = interferon-gamma.

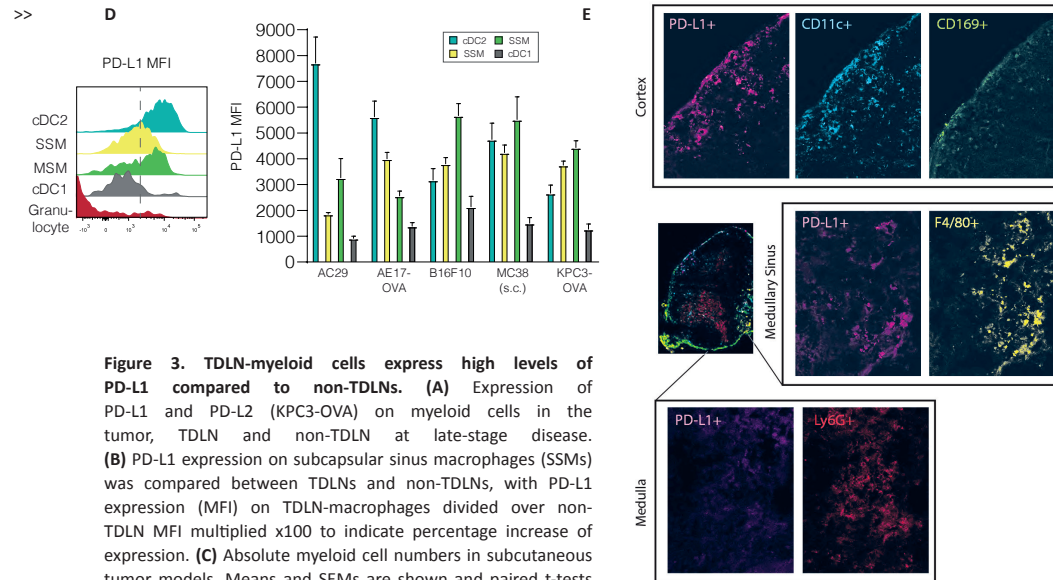
TDLNs contain abundant PD-L1^{high}-expressing myeloid cells including migratory cDC2s.

Next, we set out to quantify and characterize the ligands of PD-1 on LN myeloid cells. LNs harbor a complex architecture of myeloid cells including CD11b⁺ dendritic cells (DCs) and macrophages lining the subcapsular (CD169⁺ SSM) and medullary sinuses (F4/80⁺ MSM), type 1 and 2 conventional DCs (cDC1 and cDC2) and granulocytes interspersed between T cells in the paracortex²³⁻²⁵. TDLN-residing myeloid cells including SSMs and cDCs but not granulocytes expressed high levels of PD-L1, approaching levels found on their intratumoral counterparts (Fig. 3A). Interestingly, TDLN myeloid cells lacked or displayed low surface expression of PD-L2, whereas PD-L2 was strongly present on all investigated cells in the TME. PD-L1 expression and myeloid cell numbers were consistently higher in TDLNs compared to non-TDLNs in the investigated solid tumor models, paralleling PD-1 positivity on T cells (Fig. 3B-C). To evaluate which myeloid cells particularly expressed PD-L1 and therefore could be involved in suppressing PD-1⁺ expressing T cells, we quantified PD-L1 on the aforementioned cell types and found especially high levels on cDC2s and both types of macrophages (SSM and MSM) in all tested tumor models (Fig. 3D). These findings were corroborated by multicolor confocal microscopy of TDLN tissue, where F4/80⁺ MSMs in the medulla and CD11c⁺ DCs in the LN cortex expressed the highest levels of PD-L1, whereas expression levels were negligible in granulocytes (Fig. 3E).



PART A
Novel immunological insights
into chemotherapy and
immune-checkpoint blockade

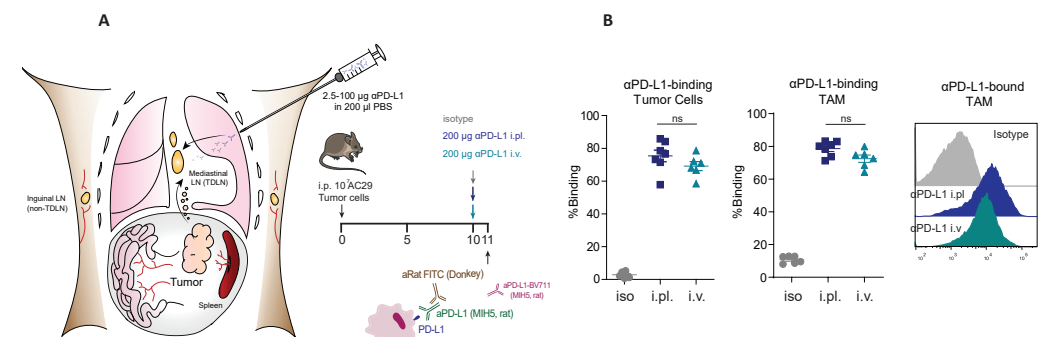
THE PD-1/PD-L1-CHECKPOINT
RESTRAINS T-CELL IMMUNITY IN TUMOR-DRAINING
LYMPH NODES



DCs can be subdivided into migratory and resident subsets based on differential expression of CD11c and MHC-II (Fig. S3A)²⁶. Based on this distinction, we detected a particularly strong increase in migratory cDC2s, especially in TDLNs (Fig. S3B). These cells expressed high levels of PD-L1 in addition to CD80 compared to cDC1s (Fig. S3C-D), which is in line with recent findings identifying migratory PD-L1⁺ DCs to predominantly present tumor-derived antigens in the TDLN²⁷. These data indicate increased frequencies of PD-L1⁺ cells in TDLNs compared to non-TDLNs, especially for macrophages and cDC2s.

Low-dose intrapleural PD-L1 antibody administration selectively targets TDLNs.

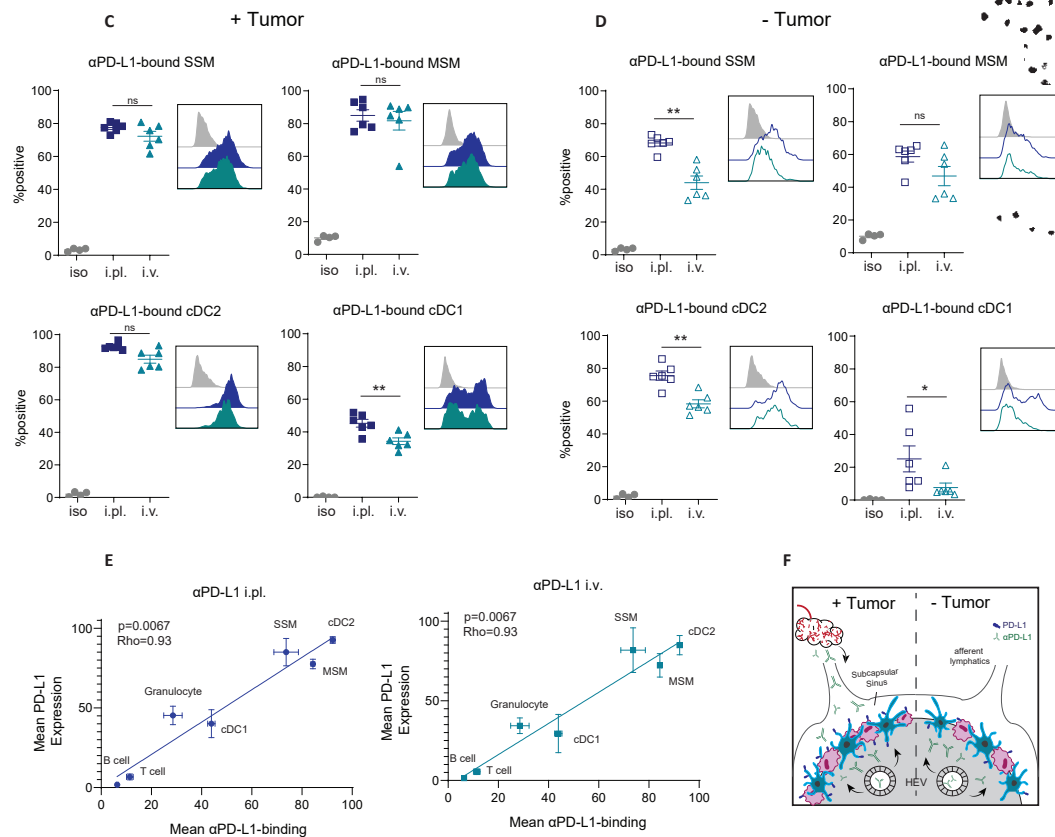
In order to study the effect of selectively targeting the PD-1/PD-L1 axis in the TDLN on tumor progression we set up a system by which we selectively target TDLNs with therapeutic PD-L1 antibodies prohibited antibody availability in the tumor environment itself. We examined the option to administer ICB antibody via the intrapleural route. This location drains directly to mediastinal LNs which are the TDLNs of intraperitoneal



PART A
Novel immunological insights
into chemotherapy and
immune-checkpoint blockade

THE PD-1/PD-L1-CHECKPOINT
RESTRAINS T-CELL IMMUNITY IN TUMOR-DRAINING
LYMPH NODES

>>



quantified on intratumoral cell types, and **(C)** on cells in the TDLN. Histograms showing PD-L1 expression patterns are displayed. **(D)** Quantification of antibody-binding on cells in mediastinal LNs in the absence of tumor (open squares and circles). **(E)** Mean PD-L1 expression on TDLN cells subsets derived from isotype treated animals (stained with the BV711-antibody) was correlated to anti-PD-L1 antibody binding (detected using the secondary anti-rat FITC-labeled antibody) for both i.p. (left) and i.v. (right) injection routes. A Pearson correlation coefficient (Rho) was determined. **(F)** A graphical depiction of the proposed model showing that anti-PD-L1 antibodies reach TDLNs via intravascular and afferent lymphatics in the presence of tumor. Means and SEMs are shown and Mann-Whitney tests were performed indicating statistical significance. ns = not significant ($p \geq 0.05$), * = $p < 0.05$, ** $p < 0.01$. i.p. = intraperitoneal, i.v. = intravenous, TDLN = tumor-draining lymph node, Ab = antibody, SSM = subcapsular sinus macrophages, MSM = medullary sinus macrophages, cDC = conventional dendritic cell, SEM = standard error of the mean.

As we could now successfully target TDLNs via i.p.l. injections we next examined the extent to which the efficacy of ICB depends on TDLNs and therefore titrated the i.p.l.-administered anti-PD-L1-antibody dose to a level that allowed selective blockade in the mediastinal TDLN, with no antibody drainage to the intraperitoneal tumor nor the circulation (Fig. S4B-C). At a near 100-fold lower anti-PD-L1-dosage of 2.5 μg , macrophages and cDCs in the TDLN still bound the antibody, albeit not completely, whereas the antibody did not reach non-TDLN nor tumor cells, TAMs or circulating monocytes and DCs (Fig. S4B-C).

TDLN-specific PD-L1 antibody elicits anti-tumor T-cell immunity and tumor control.

Using these established doses for local (2.5 μg i.p.l.) TDLN targeting and for systemic (200 μg i.p.l.) overall targeting of PD-L1, we examined the therapeutic effect of this ICB in two syngeneic tumor models, AC29 mesothelioma and MC38 colon carcinoma (Fig. 5A, S5A). Systemic targeting of PD-L1 as well as local TDLN targeting resulted in decreased tumor burden and increased survival (Fig. 5B, S5B). These therapeutic effects were quite strong, considering that not all PD-L1 molecules were blocked in TDLN at these low doses (Fig. S4B). CD8⁺ tumor-infiltrating T cells (TILs) simultaneously expressing multiple co-inhibitory receptors were increased in MC38 tumor tissue, indicating a more exhausted phenotype which is in line with recent findings in the same tumor model²⁹. Systemically administered anti-PD-L1 increased T-cell proliferation in blood, whereas both TDLN targeted and systemic treatment caused elevated frequencies of CD69⁺ cells (Fig. 5C). Whereas increased tumor infiltration of T cells was markedly induced by systemic anti-PD-L1 treatment, TDLN-targeted anti-PD-L1 specifically induced KLRG-1⁺ effector T-cell infiltration in the AC29 tumor model (Fig. 5C). In addition, while nearly all TILs were TOX-positive, TOX-MFI was significantly decreased in both treatment groups. Recent research has shown that tumors may harbor TCF1⁺ CD8⁺ T cells with a stem-like phenotype, giving rise to distinct populations, including terminally-differentiated exhausted T cells¹⁸. Similarly, we could identify a subset of TILs with a stem-like phenotype termed T_{Ex}prog, characterized by the surface marker SLAMF6⁺ (Ly108), being a surrogate marker for TCF-1, displaying low Ki-67, TIM-3 and CD39. (Fig. 5D-E, Fig. S5D-F)³⁰. Intratumoral CD8⁺ and CD4⁺ T_{Ex}prog cells were increased by TDLN-targeted and systemic PD-L1 blockade with decreased levels of proliferation indicating preserved stemness following treatment (Fig. 5F).

PART A
Novel immunological insights
into chemotherapy and
immune-checkpoint blockade

THE PD-1/PD-L1-CHECKPOINT
RESTRAINS T-CELL IMMUNITY IN TUMOR-DRAINING
LYMPH NODES

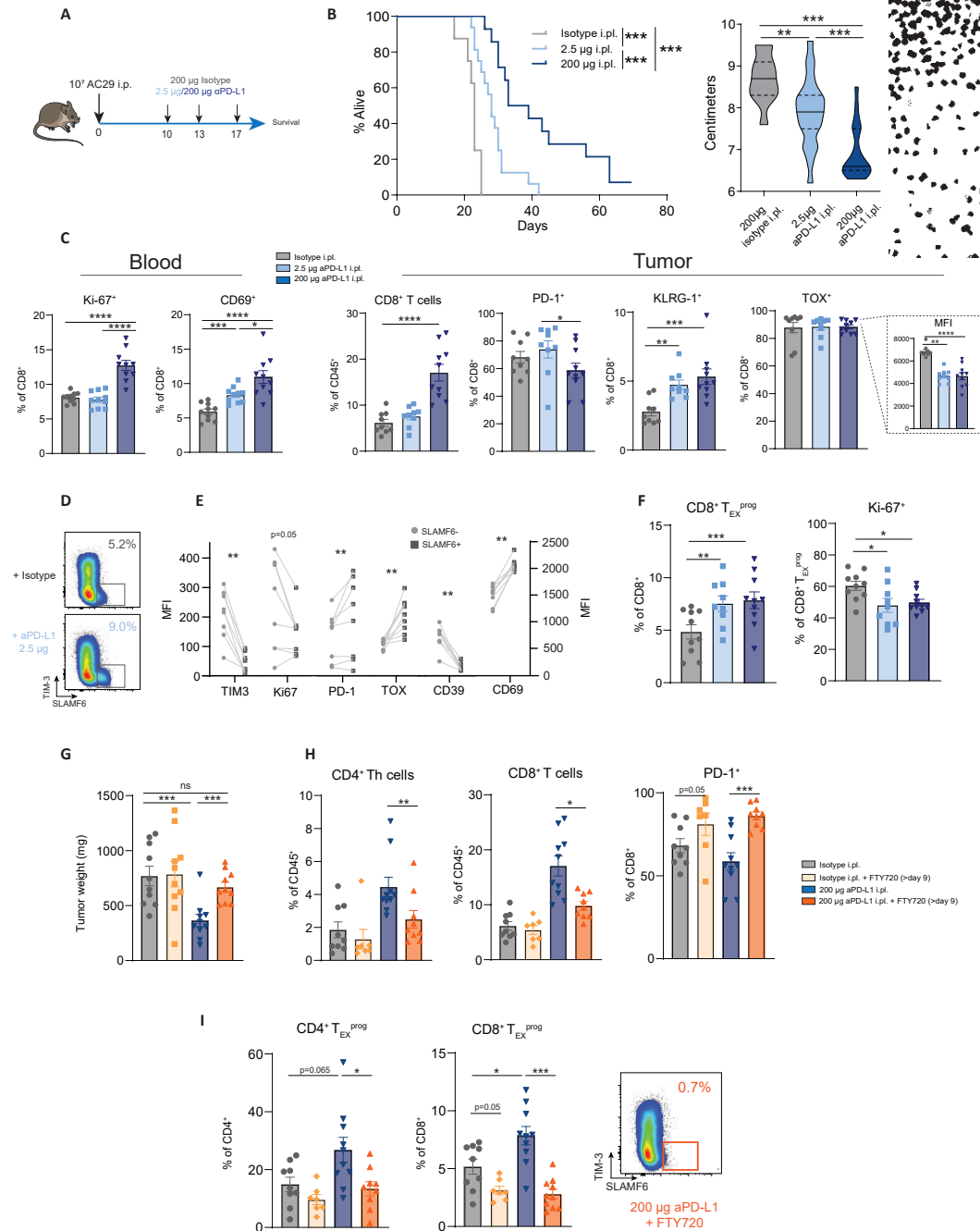


Figure 5. Specific targeting of PD-L1 in the TDLN by low-dose intrapleural injection of anti-PD-L1 enhances clinical responses in the AC29 tumor model and is abrogated by FTY720 treatment. (A) Experimental setup (n = 8-15/group) with mice being treated with either LN-local (2.5 µg) or systemic anti-PD-L1 antibodies (200 µg) i.p. and survival was monitored. (B) Kaplan-Meier curve of the experiment in A showing tumor survival. Log-rank tests were used to determine statistical significance. In addition, abdominal circumferences (being a measure of ascites volume) were measured on t = 21 post tumor-cell injection and displayed as violin-plots. (C) Blood was isolated +4 days after first injection with anti-PD-L1 treatment and characterized by multicolor flow cytometry. Tumor infiltrating lymphocytes (TILs) were characterized by multicolor flow cytometry for frequencies as well as for positivity for PD-1, KLRG1 and TOX. (D) CD8⁺ T_{EX}^{prog} cells in tumor tissue were characterized by positivity for SLAMF6 and further identified in (E) for expression of TIM3, Ki67, PD-1, TOX, CD39 and CD69. (F) Frequencies of tumor-infiltrating CD8⁺ T_{EX}^{prog} cells and their level of proliferation (Ki67⁺) (G) S1P receptor agonist FTY720 administration via drinking water and oral gavage at day 9-20 and isotype or anti-PD-L1 treatment (200 µg) i.p. at day 10, 13 and 17 (9-10 mice per group). (H) Frequencies of CD4⁺ Th cells and CD8⁺ T cells of CD45⁺ T cells and PD-1 positivity on CD8⁺ T cells were determined of TILs. (I) Frequency of CD4⁺ and CD8⁺ T_{EX}^{prog} cells was determined for total CD4⁺ and CD8⁺ TILs, respectively. Means and SEMs are shown and Mann-Whitney tests were performed indicating statistical significance. ns = not significant (p ≥ 0.05), * = p < 0.05, ** p < 0.01. i.p. = intraperitoneal, i.pl. = intrapleural, T_{EX}^{prog} = progenitor-exhausted T cells, SEM = standard error of the mean.

FTY720 abrogates systemic and TDLN-specific anti-PD-L1 immunotherapy efficacy.

In order to confirm the role of the T cells activated in TDLN following PD-L1 treatment, we administered the S1P receptor agonist FTY720, which abrogates T-cell egress from lymphoid organs³¹ during anti-PD-L1 treatment. Retention of T cells in lymphoid organs was confirmed by decreased frequencies of T cells but not NK cells in peripheral blood (Figure S6A). FTY720-administration abrogated anti-PD-L1 treatment efficacy and prevented influx of CD4⁺ Th- and CD8⁺ TILs but retained T cells exhibiting increased PD-1 expression (Figure 5G-H). In addition, FTY720 administration neutralized both spontaneous and additional anti-PD-L1 mediated induction of tumor CD4⁺ and CD8⁺ T_{EX}^{prog} cells following local- and systemically administered anti-PD-L1 treatment (Fig. 5I, S6B). These results indicate that PD-L1 blockade not solely relies on re-invigoration of TME-localized T cells but in fact amplifies priming and activation of T cells, including T_{EX}^{prog}, from the TDLN.

PD-L1 antibody blockade amplifies T_{EX}^{prog} induction in TDLNs.

To investigate the functional consequences of blocking the PD-1/PD-L1 axis in TDLNs on tumor-infiltrating T cells, we repeated the aforementioned experiment in the aggressive AE17 mesothelioma expressing the OVA model antigen allowing interrogation of tumor-specific T cells (Fig. S7A). CD45.1⁺ T-cell proliferation was enhanced in TDLNs compared to non-TDLN following anti-PD-L1 treatment (Fig. S7B). CD45.1⁺ T cells were proliferating more and were more frequently present in TDLN compared to tumor early following systemic anti-PD-L1 while no significant differences between isotype-treated animals were found (Fig. S7C). Anti-PD-L1 treatment markedly increased endogenous CD45.1⁺ T_{EX}^{prog} cells, starting in the TDLN after 24hrs, followed by blood and tumor on 72 and 144hrs, respectively (Fig. S7D). In an efficacy experiment, repeated dosing of anti-PD-L1

PART A
Novel immunological insights
into chemotherapy and
immune-checkpoint blockade

THE PD-1/PD-L1-CHECKPOINT
RESTRAINS T-CELL IMMUNITY IN TUMOR-DRAINING
LYMPH NODES

locally in the TDLN and systemically resulted in decreased AE17-OVA-tumor burden (Fig. 6A-B), without overt increase in (tumor-specific) TILs (Fig. 6C). To assess the replicative potential and phenotype of TILs following anti-PD-L1 therapy, we developed an *ex vivo* T-cell stimulation assay in which CD8⁺ TILs were stimulated with cognate antigen in the presence of their original TME with or without blocking PD-L1 antibodies (Fig. 6D). Stimulation with SIINFELK-peptide led to increased CD8⁺ T-cell activation in this assay, with profound upregulation of PD-1 following the addition of anti-PD-L1 *in vitro* (Fig. 6D). This induced activation system selectively triggered CD8⁺ TILs and not CD4⁺ TILs due to the lack of MHC-II binding OVA peptide. PD-L1 blockade in tumor cell cultures of mice treated with LN-targeted therapeutic ICB induced TIL activity to much higher extent than non-treated mice, as measured by increased cell frequencies, proliferation and decrease in PD-1 levels (Fig. 6E). These findings demonstrate that PD-L1 blockade in the TDLN alleviates the suppressive impact on intranodal tumor-specific T cells, resulting in trafficking to the tumor site where they display a much improved responsiveness to OVA tumor antigen.

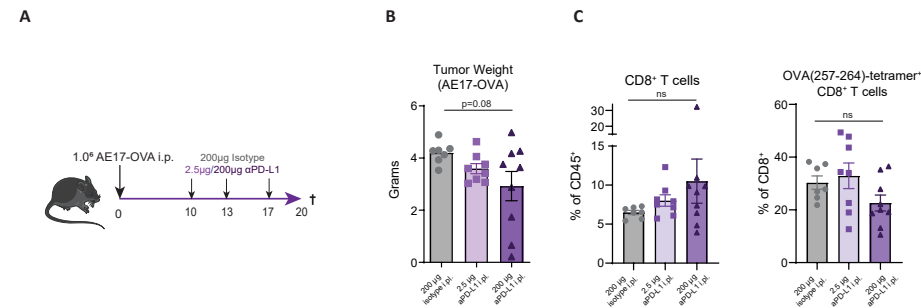
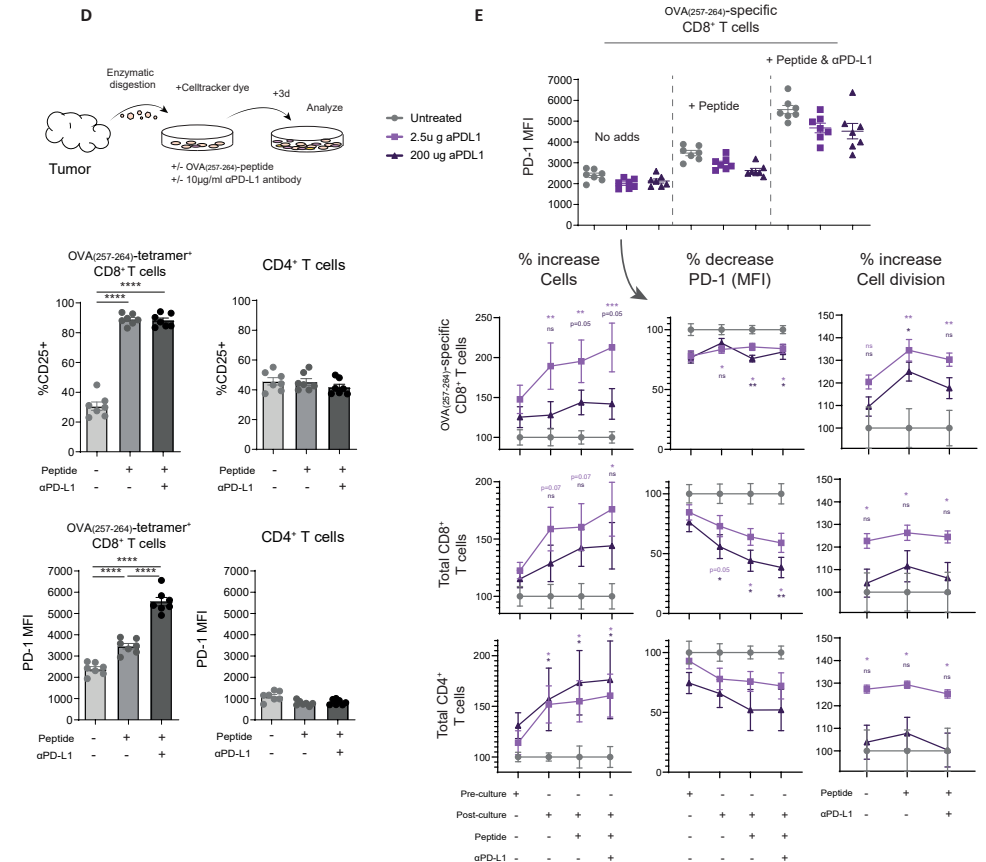


Figure 6. Specific targeting of PD-L1 in the TDLN elicits durable anti-tumor immune responses capable of reinvigoration *in vitro*. (A) Experimental design (n=7-9 mice per group). (B) Tumor weights of the different treatment groups. (C) Frequencies of total CD8⁺ T cells and OVA(257-264)-specific CD8⁺ T cells in tumors as percentages of total alive CD45⁺ leukocytes or CD8⁺ T cells, respectively. (D) Design and validation of the *in vitro* culture system mimicking the tumor-microenvironment. Means and SEMs are depicted with paired t-tests used for statistical analysis. (E) Tumor single cell suspensions from isotype (gray), anti-PD-L1 LN-specifically (pink) and anti-PD-L1 systemically (purple) treated mice were cultured as described in D. Means and SEMs are shown, Mann-Whitney tests were used to evaluate statistical significance. For E, treatment arms were normalized to isotype treated animals and baseline and post-3 day culture values for the several conditions are shown.



Response to PD-L1-blockade occurs independent from TDLN macrophages.

In order to investigate which PD-L1-expressing cells in the TDLN were most likely responsible for inhibiting T-cell responses we made use of low dose i.p. administrated clodronate encapsulated liposomes (CEL), which specifically deplete LN macrophages upon phagocytosis³². SSMs and MSMs, but not cDC2, were effectively depleted from the TDLN within 48 hours at a dose of 5% CEL, whereas macrophages in non-TDLNs and in the intraperitoneal tumor remained essentially unaltered (Fig. 7A-B). Importantly, repeated TDLN-localized CEL administration failed to abrogate anti-PD-L1 efficacy (Fig. 7C-D), demonstrating a negligible contribution of macrophages to anti-PD-L1 therapy in this model, which is in line with recently published data in genetically-modified models²⁹. We then examined TDLNs using multicolor confocal microscopy to visualize co-localization of

PART A
Novel immunological insights
into chemotherapy and
immune-checkpoint blockade

THE PD-1/PD-L1-CHECKPOINT
RESTRAINS T-CELL IMMUNITY IN TUMOR-DRAINING
LYMPH NODES

anti-PD-L1-expressed cDC2s with CD8⁺ T cells. CD8⁺ T cells did not co-localize with SSMs and MSMs in TDLNs, but we frequently found clusters of PD-L1 positive DCs and CD8⁺ T cells (Fig. 7E). Together our data indicate an active role for TDLN in reinvigoration of tumor-specific T cells by ICB, most likely via PD-L1 expressing cDC(2)s, but not macrophages.

PD-1/PD-L1 interactions in TDLN but not in tumor TME correlate with prognosis in melanoma patients.

As all the aforementioned data were derived from pre-clinical solid tumor models, it remained unclear whether PD-1/PD-L1 interaction takes place in patient TDLNs. Melanoma is a disease with a highly variable prognosis depending on the presence of distant and LN metastasis (stage III-IV), and in case of absence of distant metastasis (stage I-II); tumor characteristics including thickness (Breslow's-depth), tumor histology and presence of ulceration^{33,34}. The melanoma setting is particularly suited for TDLN-characterization as these tissues are generally extracted for staging purposes with the aim of identifying patients that may benefit from adjuvant systemic (immuno-)therapy³⁵. To identify whether melanoma TDLNs feature PD-1/PD-L1-axis activity in the absence of LN-metastasis, we stained for PD-1/PD-L1-interactions in TDLNs of systemic treatment-naive stage II melanoma using a proximity ligation assay (PLA, Fig 8A). We studied PD-1/PD-L1-positivity in TDLNs of stage II patients remaining disease free following surgery (n = 19) and patients with early distant disease recurrence (n = 15) (Table S1). As expected, known prognostic factors from the primary tumor such as Breslow's-depth, presence of ulceration and nodular histology were overrepresented in the short-RFS cohort compared to patients remaining long-term free of disease^{33,36}. We detected a significantly higher PD-1/PD-L1-interaction density in patients with a short recurrence-free survival (RFS; < 48 months) compared to patients remaining disease free for more than 96 months (Fig. 8B), reflecting possible ineffective anti-tumor immune surveillance. Similar results were obtained when contacts were numerically quantified or alternatively calculated as percentage of total cell-surface area using automated software analysis (Methods S1). Interestingly, short RFS was associated with increased PD-1/PD-L1-contact density irrespective of the aforementioned prognostic factors, indicating that this process of PD-L1-mediated immune suppression arises independently of these primary tumor characteristics (Fig 8C). To gain insight into which cells were involved in PD-1/PD-L1-interaction, we combined the PLA with multicolor immunofluorescence staining for CD8, CD11c and CD68. Using this method, we observed high PD-1/PD-L1-signalling in germinal centers largely devoid of CD8⁺ T cells which is in line with previous data (containing primarily B cells and follicular T helper cells, *excluded from analysis in 8A-C*³⁷). Also numerous interactions elsewhere in the LN-cortex were present (Fig. 8D). Similar to the murine data, these contacts were particularly established by CD8⁺ (and to a lesser degree CD8⁻) T cells and CD11c⁺ DCs whereas CD68⁺ macrophages barely associated with T cells (Fig. 8E). To investigate whether PD-1/PD-L1-interactions occur in melanoma tumors to a similar extend as in TDLNs, we performed PLA on matched primary tumor tissue of a subset of patients from whom material was available. Intriguingly, PD-1/PD-L1 interactions in tumor tissue of melanoma patients (n=9) were scarce compared to the TDLN with the extent of the remainder of interactions not correlating with RFS (Fig.

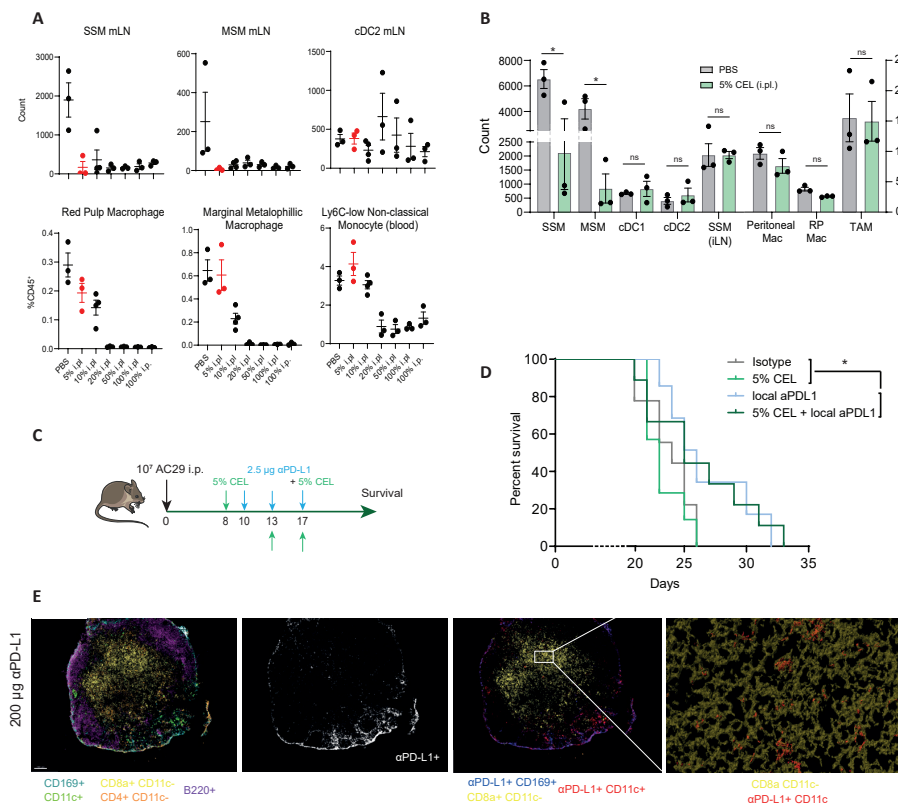


Figure 7. TDLN-local anti-PD-L1 treatment efficacy occurs independent of macrophages. (A-B) CBA/J (non-tumor bearing; A, and tumor-bearing; B) mice were treated with a range of clodronate-encapsulated liposomes (CEL) concentrations in PBS and myeloid cell subsets were analyzed 48 hours later. In red is the dose established for subsequent experiments (n=3-4 mice per group). (C) Experimental setup (n = 7-8 per group). (D) KM-curve of the survival of the experiment described in C. As isotype/5%CEL and anti-PD-L1/combo treatment showed significant overlap, these groups were pooled and Log-rank tests were performed. (E) TDLN tissue 24 hours following systemic (200 μg) anti-PD-L1 antibody treatment allowing for visualizing of antibody binding to different myeloid cell subsets in the TDLN was assessed using 6-color confocal microscopy. i.p. = intraperitoneal, anti-PD-L1 = anti-PD-L1 antibody. Ns = not significant (p ≥ 0.05), * = p < 0.05, ** p < 0.01. i.p. = intraperitoneal, i.pl. = intrapleural, i.v. = intravenous, SSM = subcapsular sinus macrophages, MSM = medullary sinus macrophage, cDC = conventional dendritic cell, Mac = macrophage, TAM = tumor-associated macrophage, TDLN = tumor-draining lymph node, CEL = clodronate encapsulated liposome, SEM = standard error of the mean.

PART A
Novel immunological insights
into chemotherapy and
immune-checkpoint blockade

THE PD-1/PD-L1-CHECKPOINT
RESTRAINS T-CELL IMMUNITY IN TUMOR-DRAINING
LYMPH NODES

8F). PD-L1 alone, however, was expressed in tumor tissue showing that the lack of PLA-positivity did not result from absence of PD-L1-expression (Fig. 8G). These findings support our initial findings in mice and highlight a previously unidentified role for PD-1/PD-L1-interactions in human TDLNs, possibly identifying high risk patient groups for adjuvant immunotherapy.

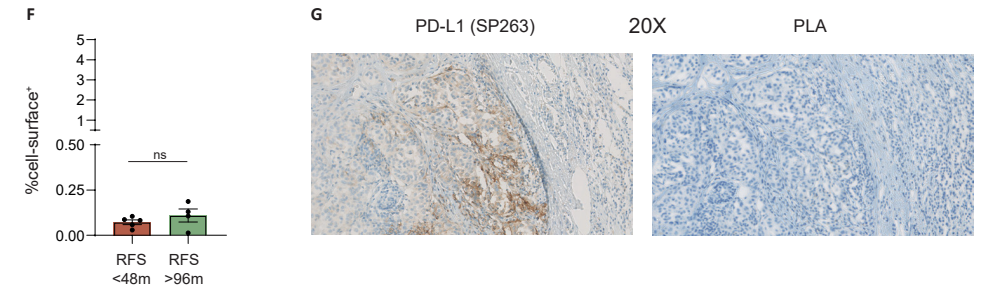
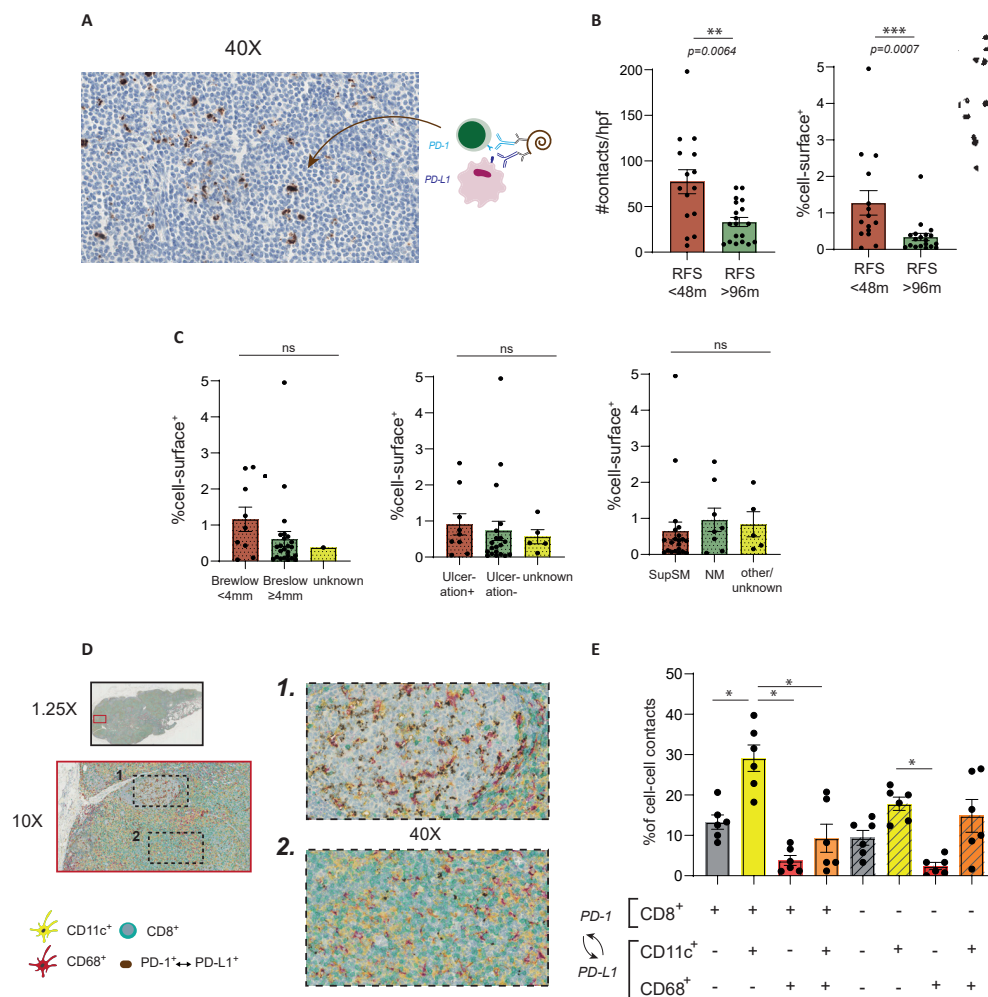


Figure 8. Stage II melanoma TDLNs harbor frequent PD-1/PD-L1 interactions which associates with early distant recurrence following surgery, and not in primary tumor tissue. (A) 40X magnified exemplary image of a stage II melanoma TDLN (sentinel node) displaying several PD-1/PD-L1-contacts stained using PLA. (B) Quantification of the average number of contacts, in patients with an early (< 48 months) recurrence of disease following surgery (n = 15) and no recurrence after 96 months (n = 19) either via manual (left) and automated (right) quantification analysis. Statistical significance was determined using Mann-Whitney tests and means plus SEMs were depicted. (C) Using the outcome measure project in right panel B, patient tumors were divided according to Breslow's-depth (tumor-thickness), presence of tumor ulceration and histological subtype. (D-E) Multiplexed images from 6 patient TDLNs high in PD-1/PD-L1 contacts (5 short, 1 long RFS) were constructed combining the PLA with CD8 (green), CD11c (yellow) and CD68 (red), followed by counterstaining with hematoxylin (blue). 40X magnification images were acquired from cortical LN-regions showing germinal centers (1.) and surrounding area (2.) rich in PD-1/PD-L1-positivity. The latter images were used to identify the cells of origin establishing the contacts in E. (F) PD-1/PD-L1 interactions in primary tissue of stage II melanoma patients were stained using PLA (n = 9). The average number of contacts was enumerated from patients with an early recurrence (n = 5) and no recurrence after 96 months (n = 4). (G) A 20X magnified exemplary image of primary tumor tissue of stage II melanoma patients displaying PD-L1 expression (clone SP263; left) and PD-1/PD-L1 interactions using PLA (right). Means and SEMs are shown, Mann-Whitney tests were used to calculate statistical significance. TDLN = tumor-draining lymph node, RFS = recurrence-free survival, PLA = Proximity Ligation Assay, SupSM = Superficial spreading melanoma, NM = nodular melanoma, SEM = standard error of the mean.

DISCUSSION

Our data formally establish a role for TDLNs in generating primary anti-tumor immune responses following anti-PD-L1 ICBs, a checkpoint that is generally regarded to act primarily at the TME². These data could offer an explanation for the apparent clinical incongruences in which tumor PD-L1 negative tumors may still respond to anti-PD-1 blockade which has resulted in (chemo-)immunotherapy being first-line treatment in several metastatic cancers irrespective of PD-L1-positivity^{35,38,39}. Although multiple mechanisms will likely define response to ICB-therapy, alleviating immune suppression in the TDLN could propel systemic anti-tumor T-cell immunity to effectively control distant tumor sites. Our data reveal a critical role of PD-L1 on cDCs in the TDLN, without negating the involvement of this inhibitory ligand in the TME.

PART A
Novel immunological insights
into chemotherapy and
immune-checkpoint blockade

THE PD-1/PD-L1-CHECKPOINT
RESTRAINS T-CELL IMMUNITY IN TUMOR-DRAINING
LYMPH NODES

Our data show that PD-1 expression on T cells in the TDLN seems to correlate with antigenicity of the tumor, which might explain the conflicting results from others showing a minor dependency on T cells from the TDLN⁴⁰. Tumor-mutational burden has been identified as a predictive marker for ICB-efficacy in patients and our data strengthen the role of TDLNs as possible mediators of ICB-responses as these potentially immunogenic tumor-antigens are likely to drain or be transported to TDLNs for further T-cell induction⁴¹. Others have previously hinted towards a role for LNs in generating anti-tumor immunity following PD-1/PD-L1 ICB in patients by describing several dysfunctional T-cell subsets arising following treatment^{17,42}. Our data formally establish these notions and directly complement recent findings on TIL-clonality in patients treated with anti-PD-1 therapy, in which an extratumoral source of immunotherapy-elicited T cells was suggested¹⁶.

TDLNs could therefore be pivotal in generating effective anti-tumor T-cell responses following liberation by anti-PD-1/PD-L1 antibodies, as has been previously shown to be the case for other cancer immunotherapies⁴³. Surgical removal of the TDLN in mouse tumor models revealed a contribution of TDLNs to ICB efficacy but as LNs are known to amplify direct anti-tumor effects of immunotherapy, formal assessment of their role in ICB therapy is lacking^{15,43,44}. The role of TDLNs as main hubs in providing anti-tumor T-cell immunity following ICB furthermore fits with recent insights into PD-1/PD-L1 biology showing that PD-1 inhibits CD28-B7 mediated T-cell co-stimulation, a process that takes place in a B7-rich environment such as LNs, and is less likely in the immune-suppressive tumor-microenvironment^{13,14}. Furthermore, anti-tumor T cells in TDLN are less exhausted compared to TIL and thus may have a proliferative advantage with ICB⁴⁵.

Our tumor models evaluate the role of TDLN in a relatively early stage, at a time that T cell priming following tumor cell inoculation might still be occurring. The aggressiveness of the model prohibits treatment in later phases. TILs were not significantly decreased following FTY720-treatment on day 9, which suggests that initial priming has largely occurred in the preceding time window (Fig. 5H). Importantly, we do not exclude a role for PD-L1 blockade in the TME, but have technically not been able to selectively administer antibody to the i.p.l. or s.c. located tumors in order to directly compare the importance of TDLN and TME to PD-L1 treatment efficacy. The exact contribution of TDLN versus TME during PD-1/PD-L1 checkpoint blockade therapy remains to be elucidated, however our data clearly unraveled the involvement of lymph nodes.

We identify PD-L1⁺ cDCs, most likely cDC2s, as main targets of anti-PD-L1 antibodies in the TDLN, and not macrophages. Recently, Oh et al. showed that DC-specific genetic PD-L1-ablation phenocopied the effects of complete PD-L1-knock-out mice in bearing MC38 tumors, whereas macrophage-direct PD-L1-elimination did not²⁹. However, as PD-L1 was ablated systemically via the CD11c promotor, analyses into the site and preferred mechanism of PD-L1-PD-1-blockade mediated anti-tumor rejection remained elusive.

Classically, a division of labor has been proposed with cDC2s predominantly inducing CD4⁺ T-cell activation and cDC1s priming CD8⁺ T-cells⁴⁶. We show however that cDC2s are significantly more PD-L1-positive and frequent in TDLNs compared to cDC1s and co-localize with CD8⁺ T cells in the TDLN cortex, challenging the current dogma. In agreement with our findings are recent publications by different groups showing cDC2s to be efficient CD8⁺ T-cell stimulators in the context of solid cancer and viral infection, in addition to their well-described role in activating CD4⁺ T cells^{47,48}. Moreover, comprehensive analysis of tumor- and TDLN-DCs by Maier et al. shows that both cDC1s and cDC2s adopt a regulatory phenotype upon apoptotic tumor-cell ingestion and upregulate PD-L1 thereby preventing proper T-cell induction²⁷. These combined findings provide a rationale for manipulating cDC2s for the benefit of cancer immunotherapy.

Our analysis of PD-1/PD-L1-axis activity in non-metastatic TDLNs of melanoma patients complements our findings in murine solid tumor models by identifying a subset of patients with high PD-1/PD-L1 interaction density which was associated with early disease relapse following surgery. Although these early stage (II) patients generally have a favorable prognosis following primary resection, a minor subset eventually presents with distant recurrences bearing a poor prognosis^{36,49}. It is tentative to speculate that PD-L1-mediated suppression of anti-tumor T-cell responses in the TDLNs of these patients is involved in the development or progression of distant metastasis, and future research will likely shed more light on the validity of this hypothesis. An ancillary observation supporting this hypothesis is the fact that the two patients who received primary anti-PD-1 antibodies at disease recurrence resulting in durable complete responses were the second and third-highest expressers of PD-1/PD-L1 in the TDLN (Fig. S8). Although the TDLNs bearing these high-density contacts were excised at primary disease presentation, it is likely that distant micrometastases bearing a similar genetic and TME-makeup would be susceptible to later anti-PD1 ICB therapy.

Perhaps unexpectedly, we found PD-1/PD-L1-interactions to occur sporadically in primary melanoma tumors compared to corresponding TDLNs. Moreover, PD-L1 expression in melanoma tumors has been variably linked to favorable prognosis while its predictive value is limited⁵⁰⁻⁵². Our data suggest that PD-1/PD-L1-axis activity in TDLNs rather than the tumor itself could be a primary target for PD-1/PD-L1 checkpoint blocking antibodies, thereby amplifying anti-tumor T-cell induction. As PD-1 ICB is currently being administered adjuvant to surgery in stage IIIB-C disease, it will be of interest to assess the validity of PD-1/PD-L1 expression in the TDLN of these patients. A different approach currently being investigated is the neo-adjuvant administration of anti-PD-1 which shows early encouraging results^{53,54}. This is in line with our hypothesis claiming that targeting the PD-1/PD-L1 checkpoint when the TDLN is still *in situ* could harness effective anti-tumor immunity. Further evidence supporting this notion comes from neo-adjuvant and

PART A
Novel immunological insights
into chemotherapy and
immune-checkpoint blockade

THE PD-1/PD-L1-CHECKPOINT
RESTRAINS T-CELL IMMUNITY IN TUMOR-DRAINING
LYMPH NODES

metastatic PD-1-blockade studies showing increased proliferation of activated CD8⁺ PD-1⁺/HLA-DR⁺ T cells in peripheral blood early after start of ICB treatment, followed by increased T-cell infiltrates in the tumor^{53,55}.

In summary, our findings implicate TDLNs as key orchestrators of anti-tumor T-cell immune responses which can be induced following blockade of PD-L1 in the TDLN. These data challenge the current dogma that PD-1/PD-L1-checkpoint act primarily at the effector (tumor) site and offers additional avenues for biomarker and combination-immunotherapy discovery.

REFERENCES

- 1 Dammeijer, F., Lau, S. P., van Eijck, C. H. J., van der Burg, S. H. & Aerts, J. Rationally combining immunotherapies to improve efficacy of immune checkpoint blockade in solid tumors. *Cytokine & growth factor reviews*, doi:10.1016/j.cytogfr.2017.06.011 (2017).
- 2 Ribas, A. & Wolchok, J. D. Cancer immunotherapy using checkpoint blockade. *Science* 359, 1350-1355 (2018).
- 3 Nishino, M., Ramaiya, N. H., Hatabu, H. & Hodi, F. S. Monitoring immune-checkpoint blockade: response evaluation and biomarker development. *Nature reviews. Clinical oncology* 14, 655-668, doi:10.1038/nrclinonc.2017.88 (2017).
- 4 Koyama, S. et al. Adaptive resistance to therapeutic PD-1 blockade is associated with upregulation of alternative immune checkpoints. *Nature communications* 7, 10501, doi:10.1038/ncomms10501 (2016).
- 5 Havel, J. J., Chowell, D. & Chan, T. A. The evolving landscape of biomarkers for checkpoint inhibitor immunotherapy. *Nature reviews. Cancer* 19, 133-150, doi:10.1038/s41568-019-0116-x (2019).
- 6 Ready, N. et al. First-Line Nivolumab Plus Ipilimumab in Advanced Non-Small-Cell Lung Cancer (CheckMate 568): Outcomes by Programmed Death Ligand 1 and Tumor Mutational Burden as Biomarkers. *Journal of clinical oncology : official journal of the American Society of Clinical Oncology* 37, 992-1000, doi:10.1200/JCO.18.01042 (2019).
- 7 Long, G. V. et al. Efficacy of pembrolizumab versus placebo plus pembrolizumab in patients with unresectable or metastatic melanoma (ECHO-301/KEYNOTE-252): a phase 3, randomised, double-blind study. *The Lancet. Oncology* 20, 1083-1097, doi:10.1016/S1470-2045(19)30274-8 (2019).
- 8 Hellmann, M. D. et al. Nivolumab plus ipilimumab in Advanced Non-Small-Cell Lung Cancer. *The New England journal of medicine*, doi:10.1056/NEJMoa1910231 (2019).
- 9 Lau, J. et al. Tumour and host cell PD-L1 is required to mediate suppression of anti-tumour immunity in mice. *Nature communications* 8, 14572, doi:10.1038/ncomms14572 (2017).
- 10 Tang, H. et al. PD-L1 on host cells is essential for PD-L1 blockade-mediated tumor regression. *The Journal of clinical investigation* 128, 580-588 (2018).
- 11 Lin, H. et al. Host expression of PD-L1 determines efficacy of PD-L1 pathway blockade-mediated tumor regression. *The Journal of clinical investigation* 128, 1708 (2018).
- 12 Kleinovink, J. W. et al. PD-L1 expression on malignant cells is no prerequisite for checkpoint therapy. *Oncoimmunology* 6, e1294299, doi:10.1080/2162402x.2017.1294299 (2017).
- 13 Hui, E. et al. T cell costimulatory receptor CD28 is a primary target for PD-1-mediated inhibition. *Science* 355, 1428-1433 (2017).
- 14 Kamphorst, A. O. et al. Rescue of exhausted CD8 T cells by PD-1-targeted therapies is CD28-dependent. *Science* 355, 1423-1427 (2017).
- 15 Chamoto, K. et al. Mitochondrial activation chemicals synergize with surface receptor PD-1 blockade for T cell-dependent antitumor activity. *Proceedings of the National Academy of Sciences of the United States of America* 114, E761-E770 (2017).
- 16 Yost, K. E. et al. Clonal replacement of tumor-specific T cells following PD-1 blockade. *Nature medicine* 25, 1251-1259, doi:10.1038/s41591-019-0522-3 (2019).
- 17 Sade-Feldman, M. et al. Defining T Cell States Associated with Response to Checkpoint Immunotherapy in Melanoma. *Cell* 175, 998-1013.e1020, doi:https://doi.org/10.1016/j.cell.2018.10.038 (2018).
- 18 Jansen, C. S. et al. An intra-tumoral niche maintains and differentiates stem-like CD8 T cells. *Nature* 576, 465-470 (2019).
- 19 van der Ploeg, A. P. et al. EORTC Melanoma Group sentinel node protocol identifies high rate of submicrometastases according to Rotterdam Criteria. *European journal of cancer* 46, 2414-2421, doi:10.1016/j.ejca.2010.06.003 (2010).
- 20 Dammeijer, F. et al. Depletion of Tumor-Associated Macrophages with a CSF-1R Kinase Inhibitor Enhances Antitumor Immunity and Survival Induced by DC Immunotherapy. *Cancer immunology research* 5, 535-546, doi:10.1158/2326-6066.CIR-16-0309 [pii] 10.1158/2326-6066.CIR-16-0309 (2017).
- 21 Zhao, M. et al. Rapid in vitro generation of bona fide exhausted CD8⁺ T cells is accompanied by Tcf7 promoter methylation. *PLOS Pathogens* 16, e1008555 (2020).
- 22 Kurtulus, S. et al. Checkpoint Blockade Immunotherapy Induces Dynamic Changes in PD-1(-)CD8(+) Tumor-Infiltrating T Cells. *Immunity* 50, 181-194 e186 (2019).

PART A
Novel immunological insights
into chemotherapy and
immune-checkpoint blockade

THE PD-1/PD-L1-CHECKPOINT
RESTRAINS T-CELL IMMUNITY IN TUMOR-DRAINING
LYMPH NODES

- 23 Gray, E. E. & Cyster, J. G. Lymph node macrophages. *Journal of innate immunity* 4, 424-436, doi:10.1159/000337007 (2012).
- 24 Eisenbarth, S. C. Dendritic cell subsets in T cell programming: location dictates function. *Nature reviews. Immunology* 19, 89-103, doi:10.1038/s41577-018-0088-1 (2019).
- 25 Glodde, N. et al. Reactive Neutrophil Responses Dependent on the Receptor Tyrosine Kinase c-MET Limit Cancer Immunotherapy. *Immunity* 47, 789-802.e789, doi:10.1016/j.immuni.2017.09.012 (2017).
- 26 Ohl, L. et al. CCR7 governs skin dendritic cell migration under inflammatory and steady-state conditions. *Immunity* 21, 279-288 (2004).
- 27 Maier, B. et al. A conserved dendritic-cell regulatory program limits antitumour immunity. *Nature* 580, 257-262, doi:10.1038/s41586-020-2134-y (2020).
- 28 Kool, M. et al. Alum adjuvant boosts adaptive immunity by inducing uric acid and activating inflammatory dendritic cells. *The Journal of experimental medicine* 205, 869-882, doi:10.1084/jem.20071087 (2008).
- 29 Oh, W., Cheung, Navarro, Xiong, Cubas, Totpal, Chiu, Wu, Comps-Agrar, Leader, Merad, Roose-Germa, Warming, Yan, Kim, Rutz, Mellman PD-L1 expression by dendritic cells is a key regulator of T-cell immunity in cancer. *Nature Cancer* (2020).
- 30 Beltra, J. C. et al. Developmental Relationships of Four Exhausted CD8(+) T Cell Subsets Reveals Underlying Transcriptional and Epigenetic Landscape Control Mechanisms. *Immunity* 52, 825-841 e828 (2020).
- 31 Yanagawa, Y. et al. FTY720, a novel immunosuppressant, induces sequestration of circulating mature lymphocytes by acceleration of lymphocyte homing in rats. II. FTY720 prolongs skin allograft survival by decreasing T cell infiltration into grafts but not cytokine production in vivo. *Journal of immunology* (Baltimore, Md. : 1950) 160, 5493-5499 (1998).
- 32 van Rooijen, N. & Hendriks, E. Liposomes for specific depletion of macrophages from organs and tissues. *Methods Mol Biol* 605, 189-203 (2010).
- 33 Schadendorf, D. et al. Melanoma. *Nature reviews. Disease primers* 1, 15003, doi:10.1038/nrdp.2015.3 (2015).
- 34 Verver, D. et al. Risk stratification of sentinel node-positive melanoma patients defines surgical management and adjuvant therapy treatment considerations. *European journal of cancer* 96, 25-33, doi:10.1016/j.ejca.2018.02.022 (2018).
- 35 Eggermont, A. M. M., Robert, C. & Ribas, A. The new era of adjuvant therapies for melanoma. *Nature reviews. Clinical oncology* 15, 535-536, doi:10.1038/s41571-018-0048-5 (2018).
- 36 Verver, D. et al. Development and validation of a nomogram to predict recurrence and melanoma-specific mortality in patients with negative sentinel lymph nodes. *The British journal of surgery* 106, 217-225, doi:10.1002/bjs.10995 (2019).
- 37 Shi, J. et al. PD-1 Controls Follicular T Helper Cell Positioning and Function. *Immunity* 49, 264-274.e264, doi:10.1016/j.immuni.2018.06.012 (2018).
- 38 Gandhi, L. et al. Pembrolizumab plus Chemotherapy in Metastatic Non-Small-Cell Lung Cancer. *The New England journal of medicine* 378, 2078-2092, doi:10.1056/NEJMoa1801005 (2018).
- 39 Paz-Ares, L. et al. Pembrolizumab plus Chemotherapy for Squamous Non-Small-Cell Lung Cancer. *The New England journal of medicine* 379, 2040-2051, doi:10.1056/NEJMoa1810865 (2018).
- 40 Siddiqui, I. et al. Intratumoral Tcf1(+)PD-1(+)CD8(+) T Cells with Stem-like Properties Promote Tumor Control in Response to Vaccination and Checkpoint Blockade Immunotherapy. *Immunity* 50, 195-211 e110 (2019).
- 41 Samstein, R. M. et al. Tumor mutational load predicts survival after immunotherapy across multiple cancer types. *Nature Genetics* 51, 202-206, doi:10.1038/s41588-018-0312-8 (2019).
- 42 Li, H. et al. Dysfunctional CD8 T Cells Form a Proliferative, Dynamically Regulated Compartment within Human Melanoma. *Cell* 176, 775-789 e718 (2019).
- 43 Spitzer, M. H. et al. Systemic Immunity Is Required for Effective Cancer Immunotherapy. *Cell* 168, 487-502. e415, doi:10.1016/j.cell.2016.12.022 (2017).
- 44 Fransen, M. F. et al. Tumor-draining lymph nodes are pivotal in PD-1/PD-L1 checkpoint therapy. *JCI insight* 3 (2018).
- 45 Hope, J. L. et al. Microenvironment-Dependent Gradient of CTL Exhaustion in the AE17sOVA Murine Mesothelioma Tumor Model. *Frontiers in immunology* 10, 3074 (2019).
- 46 Wculek, S. K. et al. Dendritic cells in cancer immunology and immunotherapy. *Nature reviews. Immunology* 20, 7-24 (2020).
- 47 Ruhland, M. K. et al. Visualizing Synaptic Transfer of Tumor Antigens among Dendritic Cells. *Cancer cell* 37, 786-799 e785 (2020).

- 48 Bosteels, C. et al. Inflammatory Type 2 cDCs Acquire Features of cDC1s and Macrophages to Orchestrate Immunity to Respiratory Virus Infection. *Immunity* 52, 1039-1056 e1039 (2020).
- 49 von Schuckmann, L. A. et al. Risk of Melanoma Recurrence After Diagnosis of a High-Risk Primary Tumor. *JAMA dermatology* 155, 688-693, doi:10.1001/jamadermatol.2019.0440 (2019).
- 50 Morrison, C. et al. Predicting response to checkpoint inhibitors in melanoma beyond PD-L1 and mutational burden. *Journal for immunotherapy of cancer* 6, 32, doi:10.1186/s40425-018-0344-8 (2018).
- 51 Hodi, F. S. et al. Nivolumab plus ipilimumab or nivolumab alone versus ipilimumab alone in advanced melanoma (CheckMate 067): 4-year outcomes of a multicentre, randomised, phase 3 trial. *The Lancet. Oncology* 19, 1480-1492, doi:10.1016/s1470-2045(18)30700-9 (2018).
- 52 Daud, A. I. et al. Programmed Death-Ligand 1 Expression and Response to the Anti-Programmed Death 1 Antibody Pembrolizumab in Melanoma. *Journal of clinical oncology : official journal of the American Society of Clinical Oncology* 34, 4102-4109, doi:10.1200/jco.2016.67.2477 (2016).
- 53 Huang, A. C. et al. A single dose of neoadjuvant PD-1 blockade predicts clinical outcomes in resectable melanoma. 25, 454-461, doi:10.1038/s41591-019-0357-y (2019).
- 54 Ross, M. I. et al.
- 55 Herbst, R. S. et al. Predictive correlates of response to the anti-PD-L1 antibody MPDL3280A in cancer patients. *Nature* 515, 563-567, doi:10.1038/nature14011 (2014).

PART A
Novel immunological insights
into chemotherapy and
immune-checkpoint blockade

THE PD-1/PD-L1-CHECKPOINT
RESTRAINS T-CELL IMMUNITY IN TUMOR-DRAINING
LYMPH NODES

SUPPLEMENTARY DATA

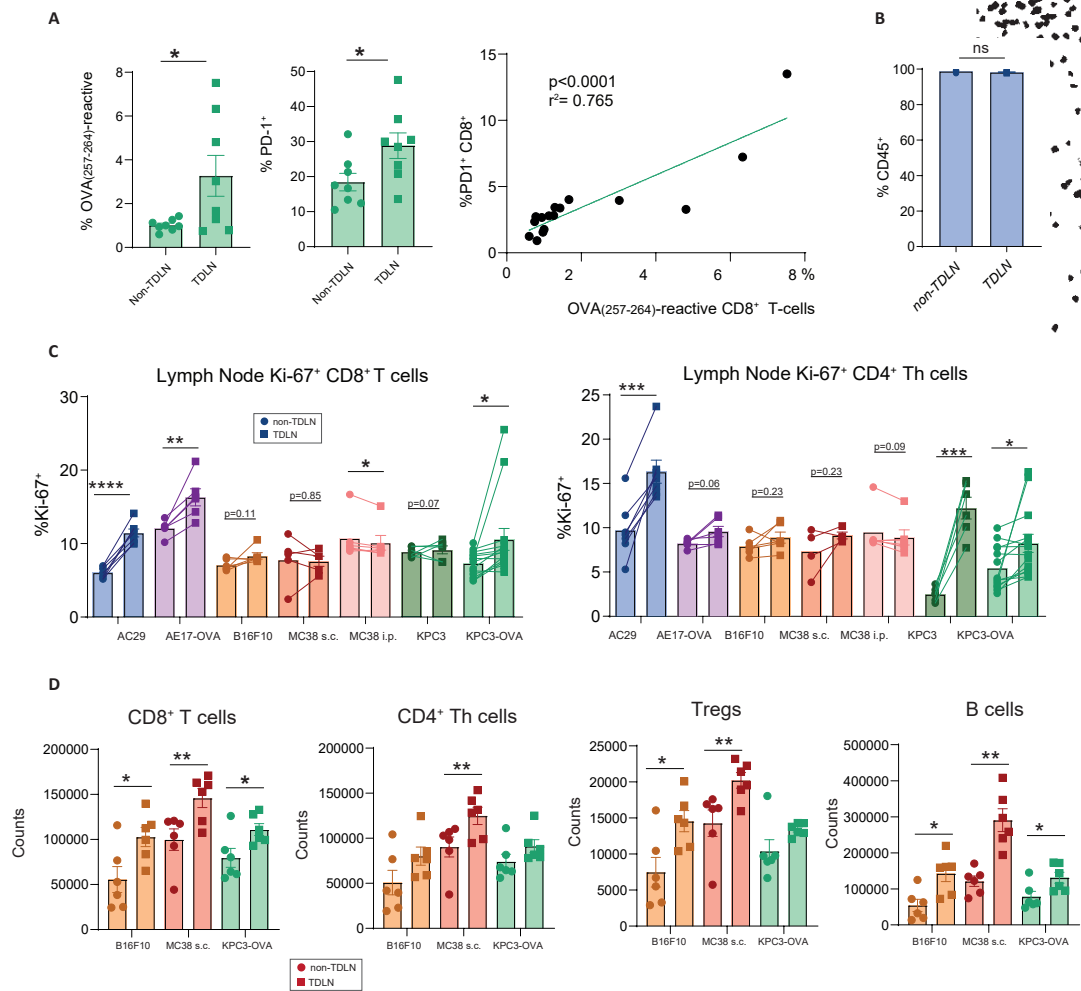


Figure S1. (A) Similar to Fig.1A, TDLNs and non-TDLNs from end-stage disease KPC3-OVA-bearing mice were harvested and stained for PD-1-positivity and OVA(257-264)-reactive CD8⁺ T cells using tetramers. Medians and SEM are shown and a Wilcoxon matched-pairs signed rank test was used to calculate statistical significance. In addition, total PD-1⁺ CD8⁺ T cells were plotted against OVA(257-264)-tetramer⁺ CD8⁺ T cells in the TDLN and a correlation was made and a Pearson correlation coefficient was calculated (r^2). (B) Graphs showing CD45⁺ cell frequencies in TDLN and non-TDLN. (C) CD8⁺ and CD4⁺ Th-cell proliferation was assessed in TDLNs (squares) versus non-TDLNs (circles) by intra-nuclear Ki-67-staining using flow cytometry. (D) Absolute lymphocyte cell numbers were quantified in subcutaneous tumor models allowing for ipsi- (tumor draining) and contralateral (non-tumor draining) LN extraction and evaluation. Means and SEMs are shown and paired t-tests were performed. Means and SEMs are shown, including p-values determined by ratio paired t-tests. * = $p < 0.05$, ** $p < 0.01$, *** $p < 0.001$. SSM = subcapsular sinus macrophages, Treg = Regulatory T cell, SEM = standard error of the mean

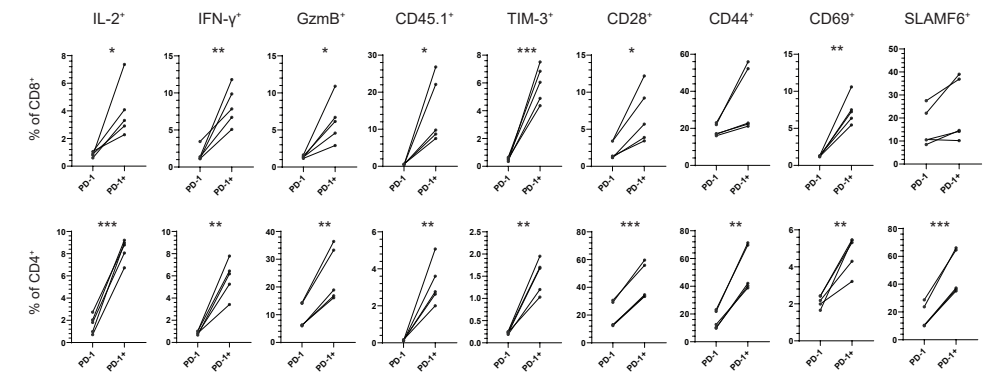


Figure S2. Levels of IL-2, IFN γ , granzyme B, CD45.1, TIM-3, CD28, CD44, CD69 and SLAMF6 were determined for PD-1- and PD-1⁺ CD4⁺ and CD8⁺ T cells isolated from TDLN 17 days after AE17-OVA tumor inoculation. Means and SEMs are shown, paired T-tests were used to calculate statistical significance. * = $p < 0.05$, ** $p < 0.01$, *** $p < 0.001$.

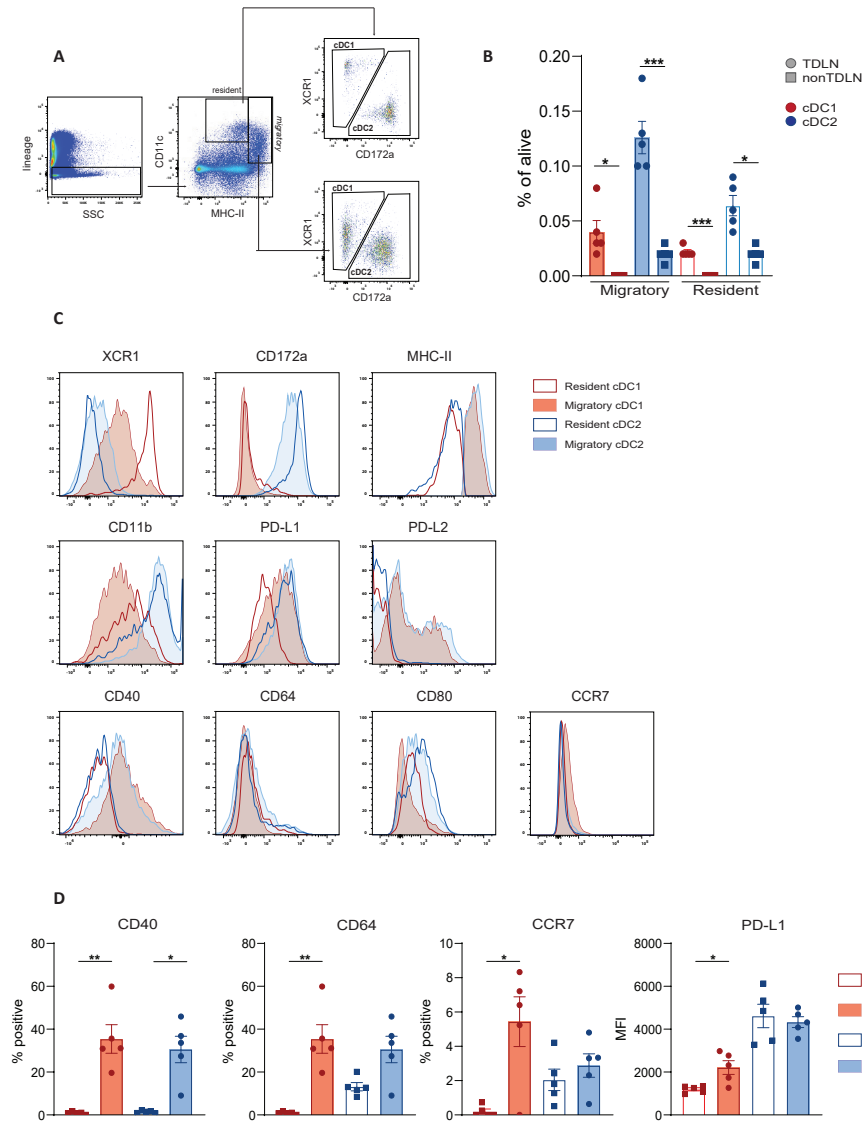
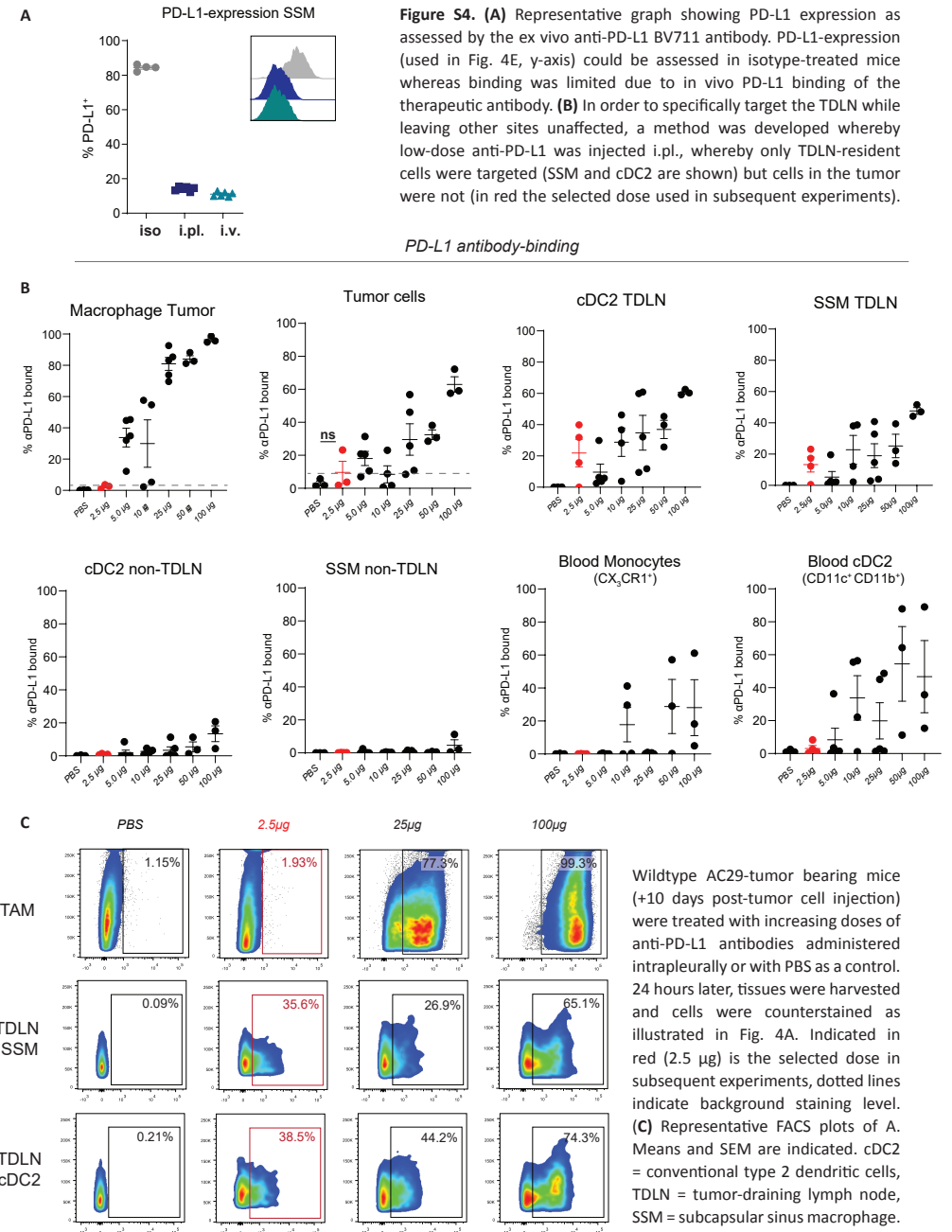


Figure S3. (A) Gating strategy of resident and migratory conventional dendritic cell type 1 and 2 (cDC1s and cDC2s) in TDLNs and non-TDLNs isolated from AE17-OVA tumor-bearing mice 12 days after tumor inoculation. (B) Frequencies of migratory and resident cDC1s (red) and cDC2s (blue) of alive were determined in TDLN (circles) and non-TDLNs (squares). (C) Histograms showing level of expression of XCR1, CD172a, MHC class II, CD11b, PD-L1, PD-L2, CD40, CD62, CD80 and CCR7 on resident (open) and migratory (closed) cDC1s (red) and cDCs (blue) in the TDLN. (D) Histograms demonstrating frequencies of CD40, CD64, CCR7 and MFI for PD-L1 for resident (open) and migratory (closed) cDC1s (red) and cDC2s (blue). Means and SEMs are shown, paired t-tests were used to calculate statistical significance. * = $p < 0.05$, ** $p < 0.01$, *** $p < 0.001$. TDLN = tumor-draining lymph node.

PART A
Novel immunological insights
into chemotherapy and
immune-checkpoint blockade

THE PD-1/PD-L1-CHECKPOINT
RESTRAINS T-CELL IMMUNITY IN TUMOR-DRAINING
LYMPH NODES



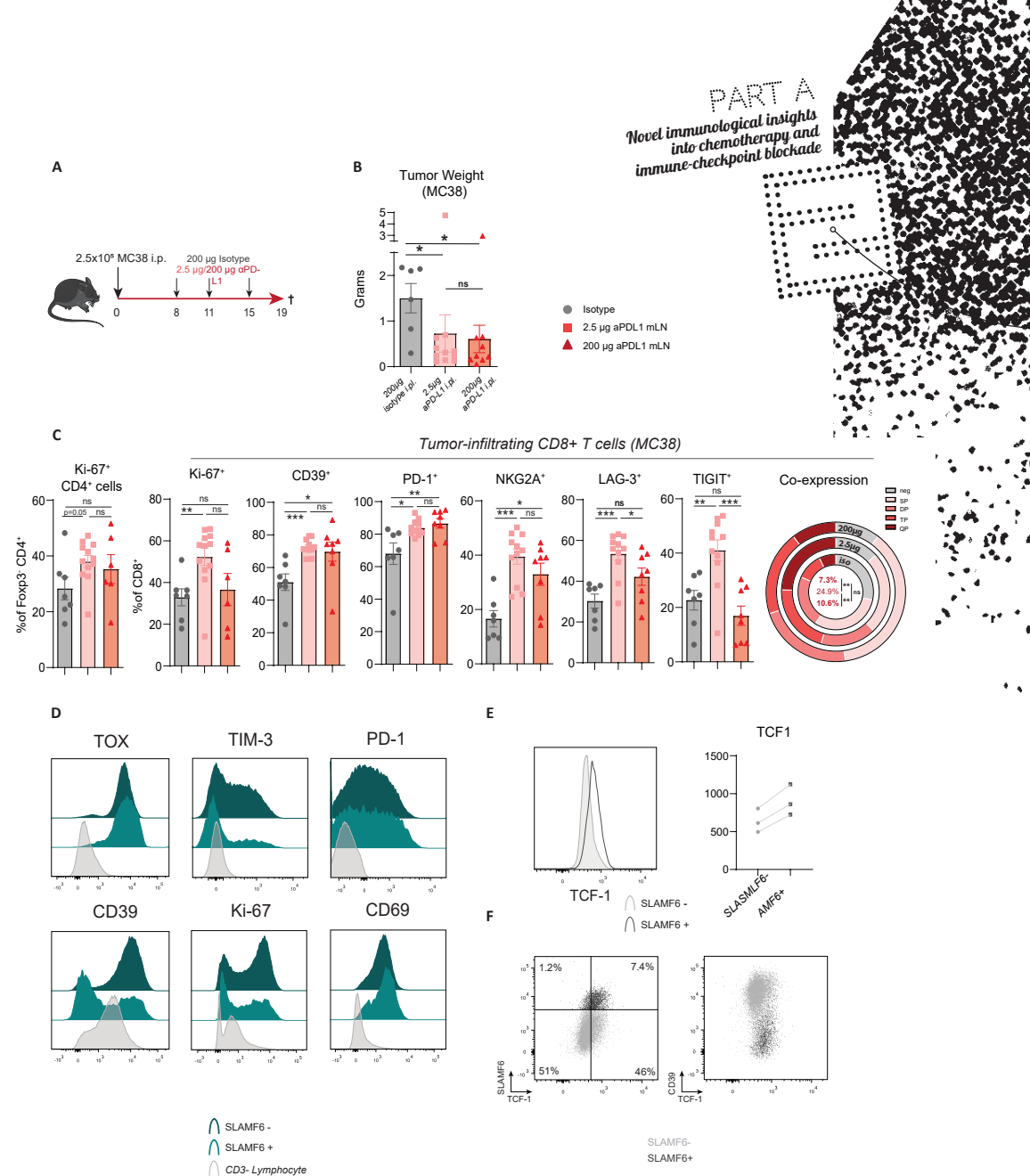


Figure S5. (A) C57/Bl6 mice were inoculated with 2.5×10^6 MC38 tumor cells i.p. and treated with either isotype, 2.5 μ g of anti-PD-L1 (local) or 200 μ g of anti-PD-L1 (systemic) i.p. at day 8, 11 and 15. Mice were euthanized 19 days following tumor injection (4 days after the last treatment) and **(B)** tumors weights were quantified. **(C)** Tumors were enzymatically digested and stained for flow cytometry to assess CD4+ and CD8+ TIL-phenotype. In addition to sole expression of individual co-inhibitory checkpoints on CD8+ T cells, mean co-expression of receptors was evaluated with SP indicating receptor single positivity. DP = double positive, TP = triple positive and QP = quadruple positive for the investigated checkpoints. Inside the circle, statistical significance is indicated for QP-cells between the different treatment groups. **(D)** Phenotype of SLAMF6+CD8+ T cells was compared to SLAMF6-CD8+T cells and CD3-lymphocytes in tumor tissue of AC29 tumor-bearing mice isolated 20 days after tumor inoculation. **(E)** Expression level of TCF-1 was determined in SLAMF6+CD8+ T cells versus SLAMF6-CD8+T cells. **(F)** Representative dotplots showing expression of TCF1 and SLAMF6 (left plot) and TCF1 and CD39 (right plot) in CD8+ TILs. Means and SEMs are shown and Mann-Whitney tests were performed in case of tumor analysis, whereas unpaired t-tests were used for interim blood analyses. ns = not significant ($p \geq 0.05$), * = $p < 0.05$, ** $p < 0.01$. *** $p < 0.001$. **** $p < 0.0001$. anti-PD-L1 = anti-PD-L1 antibody, i.p. = intraperitoneal, i.pl. = intrapleural, i.v. = intravenous, TDLN = tumor-draining lymph node, Th cells = T-helper cells.

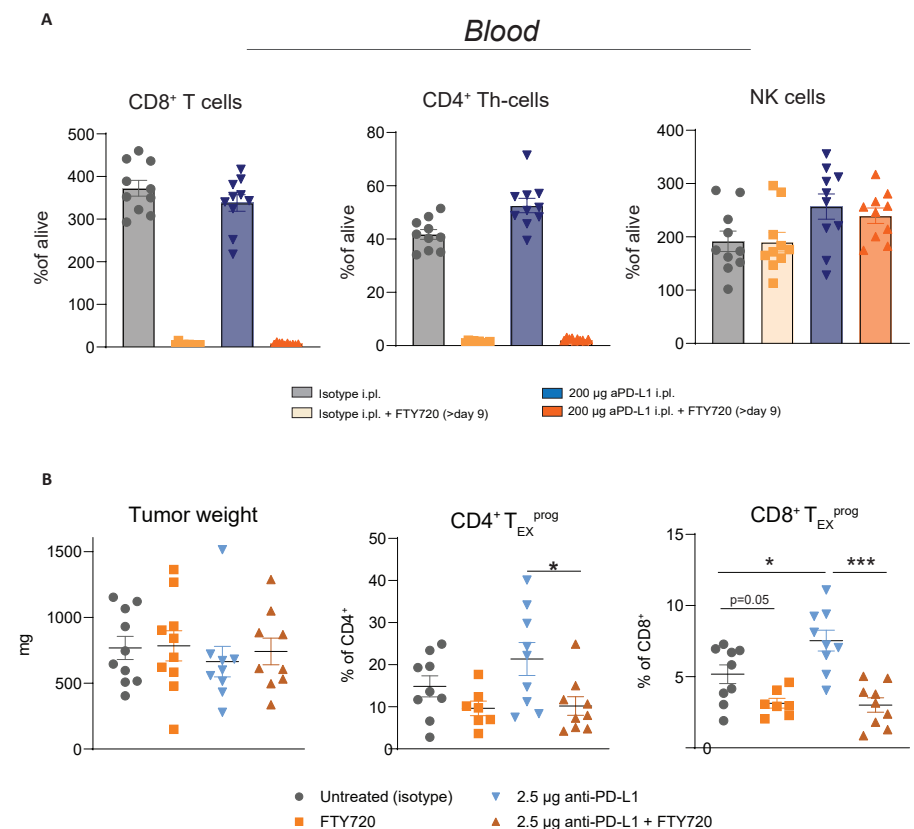


Figure S6. (A) Comparison of frequencies of CD8+ T cells, CD4+ Th- cells and NK cells in peripheral blood of AC29 tumor-bearing mice isolated at day 14 (4 days after first anti-PD-L1 treatment (200 μ g i.p.) and 5 days after start FTY720). **(B)** AC29 tumor-bearing mice received S1P receptor agonist FTY720 via drinking water and oral gavage at day 9-20 and isotype or TDLN-local anti-PD-L1 treatment (2.5 μ g) i.p. at day 10, 13 and 17. Mice were sacrificed at day 20 followed by tumor isolation, enzymatic digestion and staining of tumor tissue for flow cytometry. Tumor weight was determined after isolation. Frequency of CD4+ and CD8+ T_{EX} cells was determined for total CD4/8+ TILs. Means and SEMs are shown. Mann-Whitney tests were performed. ns = not significant ($p \geq 0.05$), * = $p < 0.05$, ** $p < 0.01$, *** $p < 0.001$, i.pl. = intrapleural, SEM = standard error of the mean

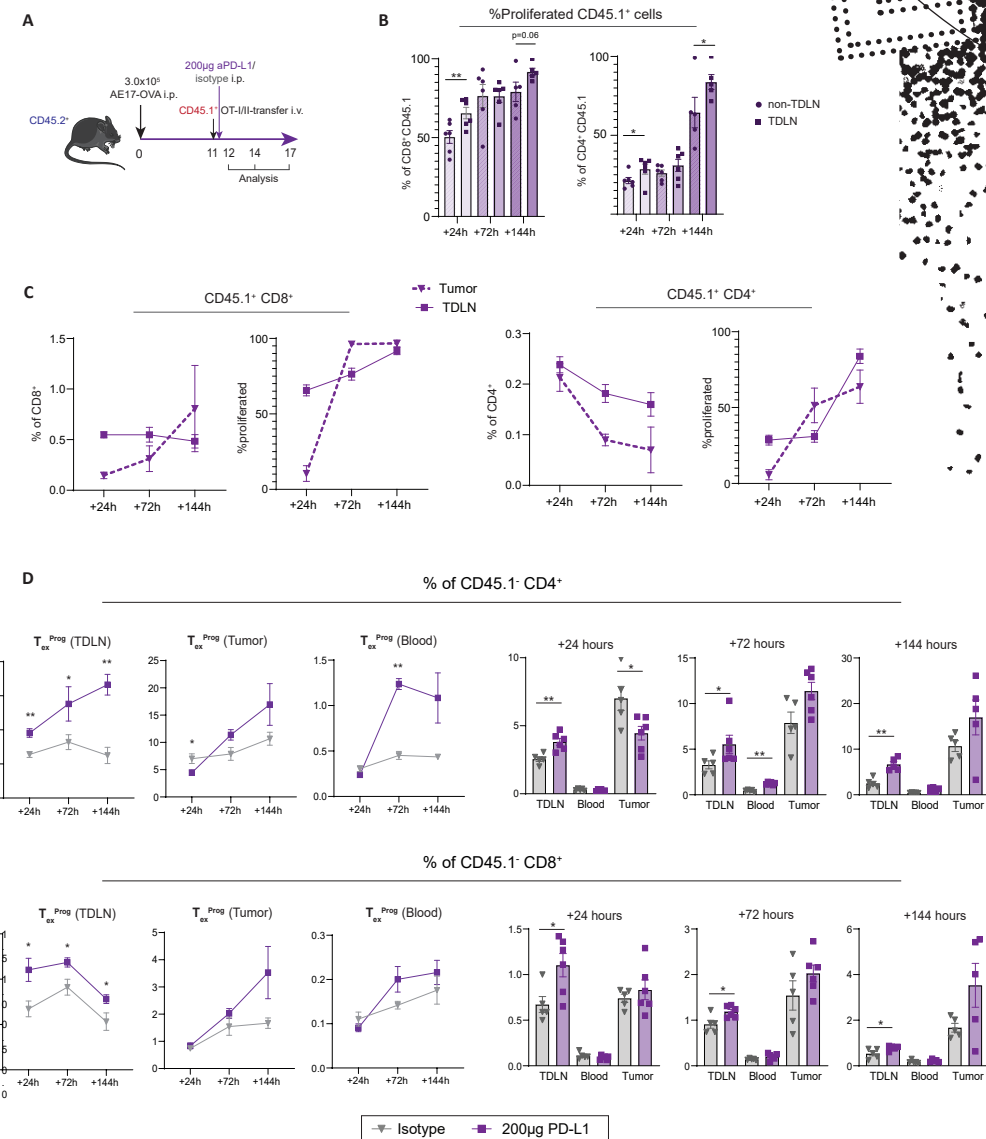


Figure S7. (A) Wildtype CD45.2+ congenic mice injected i.p. with AE17-OVA tumor cells received cell-trace labeled CD45.1+ OT-I and OT-II cells i.v. at day 11 followed by i.p. injection of isotype or anti-PD-L1 therapy (200 µg) at day 11 and mice were sacrificed (n=5-6/group/time point) at day 12, 14 and 17. (B) Percentage of proliferated CD45.1+ cells of the CD45.1+ CD8+ T-cell population in and CD45.1+ CD4+ T-cell population in TDLN and non-TDLN. (C) Graphs showing frequencies of CD45.1+ cells of CD8+ and CD4+ T cells and percentage of proliferated CD45.1+ CD4/8+ T cells isolated from TDLN and tumor (dotted line) at indicated time points in anti-PD-L1 treated animals. (D) Endogenous (CD45.1-) TEXprog CD4+ (above) and CD8+ (below) cells in TDLN, blood and tumor 24, 72 and 144 hours post a one-time systemically administered dose of anti-PD-L1 (200 µg) visualized through time (left) or per tissue (right). * = p < 0.05, ** p < 0.01, TEXprog = progenitor-exhausted T cells. i.v. = intravenous, i.p. = intraperitoneal. TDLN = tumor-draining lymph node.

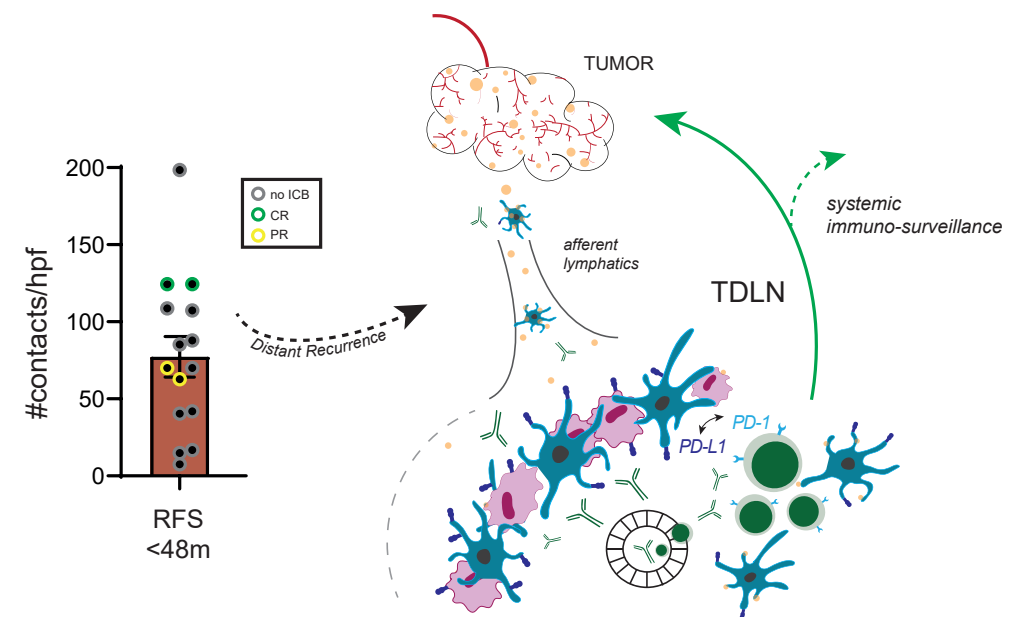


Figure S8. Graphical abstract including patients not receiving immunotherapy at distant disease recurrence (gray) and those experiencing complete response (CR, green) or partial response (PR, yellow) following PD-1 (-containing) immunotherapy are highlighted from the graph in Fig. 8A.

PART A
Novel immunological insights
into chemotherapy and
immune-checkpoint blockade

THE PD-1/PD-L1-CHECKPOINT
RESTRAINS T-CELL IMMUNITY IN TUMOR-DRAINING
LYMPH NODES

Table S1. Clinicopathological descriptives of all samples, and per subgroup (recurrence < 48 months vs. no recurrence > 96 months), n (%) or median (IQR).

Characteristics	All patients (n=30)	Recurrence <48mo (n=15)	No recurrence >96mo (n=15)	P-value
Patient characteristics				
Age	50 (41 – 59)	55 (49 – 63)	43 (35 – 52)	0.006
Sex				0.005
Male	20 (67)	14 (93)	6 (40)	
Female	10 (33)	1 (7)	9 (60)	
Tumor characteristics				
Breslow, mm	2.4 (1.8 – 4.9)	3.7 (2.3 – 6.0)	2.0 (1.3 – 2.6)	0.002
Ulceration				0.003
Absent	17 (68)	6 (43)	11 (100)	
Present	8 (32)	8 (57)	0	
Unknown	5	1	4	
Histology				0.001
SSM	18 (67)	6 (40)	12 (100)	
NM	8 (30)	8 (53)	0	
Other	1 (4)	1 (7)	0	
Unknown	3	0	3	
Location				0.324
Arm	6 (20)	3 (20)	3 (20)	
Leg	7 (23)	2 (13)	5 (33)	
Trunk	16 (53)	10 (67)	6 (40)	
Head & Neck	1 (3)	0	1 (7)	
SLN surgical removal				
No. of SNs	1.0 (1.0 – 2. 0)	1.0 (1.0 – 2.0)	1.0 (1.0 – 2.0)	0.233
SN Region				0.245
Axillar	20 (67)	12 (80)	8 (53)	
Inguinal-iliac	9 (30)	3 (20)	6 (40)	
Cervical	1 (3)	0	1 (7)	

Outcome				
Time to distant metastasis, months		21 (9-36)	N/A	-
Status*				-
[median time to status, months] NED		N/A	15 (100)	
CR		2 (13)	[108.0] N/A	
		[21.0]		
AWD		2 (13)	N/A	
		[57.5]		
DOD		11 (73)	N/A	
		[25.0]		
Site(s) of first distant recurrence			N/A	-
One metastatic organ Lung only		4 (27)		
Brain only		2 (13)		
Other		1 (7)		
Multiple metastatic organs		8 (53)		

* No evidence of disease (NED), Complete response (CR), Alive with disease (AWD), Dead of disease (DOD)

Methods S1. Automatic quantification of PLA on melanoma sentinel lymph nodes using ImageJ software and corresponding macros. PLA = proximity ligation assay.

Methods

The following macro scripts were designed and used to quantify PD-1/PD-L1 interaction density at TDLN slides of at 40X magnification. A total of 15 images per TDLN were randomly selected from the LN cortex, excluding images containing germinal centers. These images were then loaded into ImageJ software (ImageJ, V1.52, Fuji platform) and the macros below were run, with the results from 2, being taken as a percentage of 1, establishing the percentage of cell surface area positive for PD-1/PD-L1.

Macro 1

```
run("Color Threshold...");
// Color Thresholder 2.0.0-rc-69/1.52s
// Autogenerated macro, single images only!
min=newArray(3);
max=newArray(3);
filter=newArray(3);
a=getTitle();
run("HSB Stack");
run("Convert Stack to Images");
selectWindow("Hue");
rename("0");
selectWindow("Saturation");
rename("1");
selectWindow("Brightness");
rename("2");
min[0]=0;
max[0]=255;
filter[0]="pass";
min[1]=0;
max[1]=255;
filter[1]="pass";
min[2]=205;
max[2]=255;
filter[2]="stop";
for (i=0;i<3;i++){
selectWindow(""+i);
setThreshold(min[i], max[i]);
run("Convert to Mask");
if (filter[i]=="stop") run("Invert");
}
imageCalculator("AND create", "0","1");
imageCalculator("AND create", "Result of 0","2");
for (i=0;i<3;i++){
selectWindow(""+i);
close();
}
selectWindow("Result of 0");
close();
selectWindow("Result of Result of 0");
rename(a);
// Colour Thresholding-----
run("Measure");
```

Macro 2

```
rename("test.jpg");
run("Split Channels");
selectWindow("test.jpg (blue)");
setAutoThreshold("Default");
//run("Threshold...");
setThreshold(0, 195);
setThreshold(0, 108);
run("Measure");
```

3

Floris Dammeijer
Cornedine J. De Gooijer
Mandy van Gulijk
Melanie Lukkes
Larissa Klaase
Lysanne A. Lieveense
Cynthia Waasdorp
Merel Jebbink
Gerben P. Bootsma
Jos A. Stigt
Bonne Biesma
Margaretha E.H. Kaijen-Lambers
Joanne Mankor
Heleen Vroman
Robin Cornelissen
Paul Baas
Vincent Van der Noort
Jacobus A. Burgers
Joachim G. Aerts

EBioMedicine. 2020 Dec 22:103160.

PART A
*Novel immunological insights
into chemotherapy and
immune-checkpoint blockade*

IMMUNE MONITORING IN MESOTHELIOMA
PATIENTS IDENTIFIES NOVEL IMMUNE-MODULATORY
FUNCTIONS OF GEMCITABINE
ASSOCIATING WITH CLINICAL RESPONSE

SUMMARY

Gemcitabine is a frequently used chemotherapeutic agent but its effects on the immune system are incompletely understood. Recently, the randomized NVALT19-trial revealed that maintenance gemcitabine after first-line chemotherapy significantly prolonged progression-free survival (PFS) compared to best supportive care (BSC) in malignant mesothelioma. Whether these effects are paralleled by changes in circulating immune cell subsets is currently unknown. These analyses could offer improved mechanistic insights into the effects of gemcitabine on the host and guide development of effective combination therapies in mesothelioma. We stained peripheral blood mononuclear cells (PBMCs) and myeloid-derived suppressor cells (MDSCs) at baseline and 3 weeks following start of gemcitabine or BSC treatment in a subgroup of mesothelioma patients included in the NVALT19-trial. In total, 24 paired samples including both MDSCs and PBMCs were included. We performed multicolour flow-cytometry to assess co-inhibitory and stimulatory receptor- and cytokine expression and matched these parameters with PFS and OS. Gemcitabine treatment was significantly associated with an increased NK-cell- and decreased T-regulatory cell proliferation whereas the opposite occurred in control patients. Furthermore, myeloid-derived suppressor cells (MDSCs) frequencies were lower in gemcitabine-treated patients and this correlated with increased T-cell proliferation following treatment. Whereas gemcitabine variably altered co-inhibitory receptor expression, co-stimulatory molecules including ICOS, CD28 and HLA-DR were uniformly increased across CD4⁺ T-helper, CD8⁺ T- and NK-cells. Although preliminary in nature, the increase in NK-cell proliferation and PD-1 expression in T cells following gemcitabine treatment was associated with improved PFS and OS. Gemcitabine treatment was associated with widespread effects on circulating immune cells of mesothelioma patients with responding patients displaying increased NK-cell and PD-1⁺ T-cell proliferation. These exploratory data provide a platform for future on treatment-biomarker development and novel combination treatment strategies.

INTRODUCTION

Advances in the field of mesothelioma treatment have been limited with recent trials involving anti-PD-1 or anti-CTLA-4 monotherapy yielding no significant improvements in clinical outcomes^{1,2}. Therefore, the mainstay of treatment for mesothelioma remains platinum-pemetrexed doublet chemotherapy with a median overall survival ranging from 13-16 months with a persisting demand for novel effective treatments³. Recently, we reported results from the NVALT19-study, a randomized phase II open-label trial investigating the benefit of maintenance gemcitabine in mesothelioma patients who did not progress following first-line chemotherapy⁴. Gemcitabine significantly improved progression-free survival (PFS) compared to best-supportive care (BSC)-treated mesothelioma patients and was associated with a manageable toxicity. Overall survival, however, was only improved in a small group of patients warranting mechanistic analysis of why some benefitted and others did not.

The last decade has witnessed a surge in studies reporting immune-modifying functions of chemotherapy relying partially, or completely on elicited immune-mediated tumour destruction⁵. Chemotherapy-induced immune activation can be successively monitored in peripheral blood, with clinically responding patients exhibiting marked increases in immune-effector cell frequencies and phenotype depending on the type of agent investigated⁶⁻⁷. Gemcitabine has previously been reported to decrease the frequencies of myeloid-derived suppressor cells (MDSCs) and T-regulatory (Treg) cells in humans and preclinical tumour models⁸⁻¹⁰. Furthermore, Albelda and colleagues found that the anti-tumour efficacy of gemcitabine was lost in nude mice lacking T cells underscoring their role in dictating tumour outcome¹¹. The effects of gemcitabine on T- and NK-cell phenotype and proliferation in patients are currently unknown and could yield novel insights into the immunological mechanisms underlying the efficacy of gemcitabine.

We hypothesised that gemcitabine could improve antitumor immune responses by positively modulating cytotoxic T cells, regulatory T cells, and myeloid-derived suppressor cells and that these immunomodulatory effects could be detected in peripheral blood during treatment. This exploratory study paves the way for further in depth investigations of the mechanism of action of gemcitabine and its association with clinical response in mesothelioma, and potentially in other solid cancer types.

METHODS

Trial design and study population.

Blood samples obtained during the NVALT19-study were used to assess the effect of

gemcitabine on PBMCs. The NVALT19-study was a multicentre, investigator-initiated, open-label, randomized, phase 2 trial, conducted in The Netherlands between 2014 and 2019, investigating the efficacy of switch maintenance gemcitabine in 130 malignant mesothelioma patients. Patients without progressive disease were included 21-42 days after having obtained 4-6 cycles of first-line platinum-pemetrexed chemotherapy. Gemcitabine was administered at day one and eight of every 21-day cycle at a dose of 1250mg/m² until disease progression (according to modified RECIST-criteria in pleural malignant mesothelioma¹², unacceptable toxicity or death.

The NVALT19 study was conducted in agreement with the Declaration of Helsinki and according to the ICH Harmonized Tripartite Guideline on Good Clinical Practice. The NVALT19 study-protocol was approved by the central ethical committee and local institutional review boards (Reference number: METC19.0668, e-supplement). All patients provided written informed consent (Netherlands Trial Registry: NTR4132/NL3847) for the NVALT19 study and the current subgroup analyses. Further trial details have been published elsewhere⁴.

The current study is a predefined exploratory analysis of a subgroup of patients included in the NVALT19 trial (see supplemental study protocol). Paired baseline and week three blood samples were collected from 46 malignant pleural mesothelioma patients of which 27 received gemcitabine and 19 BSC. For 12 patients, only PBMC data were available and in 10 patients only MDSCs were measured for varying reasons including insufficient sample quality and acquisition of samples beyond the predefined time range. Both PBMCs and MDSCs were available for 24 cases. A flowchart of how samples were selected for analysis is shown in figure S8. Patient groups had similar characteristics at baseline (Table S1).

To assess the T- and NK-cell phenotype, we constructed several comprehensive immune cell flow-cytometry panels including markers of proliferation, memory differentiation, co-stimulatory/-inhibitory receptors and cytokine production capacity (Table S2A). Also, myeloid cell subsets were investigated focusing on MDSCs with monocyte and dendritic cell (DC-)subsets being characterized in a subgroup of patients (Table S2B).

Peripheral blood processing.

Peripheral blood samples were acquired at day one of cycle one (before the start of therapy; baseline) and at day one of cycle two (median 21 days in gemcitabine group (range: 19-42 days), median 22 days in the BSC group (range: 18-49 days)). Approximately 20 millilitres of blood were collected in EDTA tubes and transported to the laboratory facility within 4 hours for immediate processing in order to preserve the MDSC-phenotype. PBMCs were isolated by density-gradient centrifugation using Ficoll-hypaque (GE Healthcare). A total of 1×10^6 cells were used for fresh flow cytometry staining of myeloid-derived suppressor

cells (MDSC). The remaining cells were cryopreserved in 10% dimethylsulfoxide (Sigma-Aldrich), 40% FCS (Gibco) and RPMI (Invitrogen, Molecular Probes) for later reconstitution and analysis.

Flow cytometry.

T- and NK-cell lymphocyte characterization was performed on PBMCs stored in liquid nitrogen following thawing and reconstitution in medium with FCS and FACS-staining buffer. For cytokine analysis, cells were first stimulated for 4 hours *in vitro* at 37°C using phorbol 12-myristate 13-acetate (PMA) and ionomycin (Sigma-Aldrich), supplemented with GolgiStop (BD Biosciences). In both instances, cells were first stained for membrane markers (Figure S2) allowing for immune-cell subset identification, for 30 minutes at 4°C, followed by fixation and permeabilization using the FoxP3 transcription factor-kit according to the manufacturer's instructions (Thermofisher Scientific). Subsequently, intracellular proteins were stained for 60 minutes at 4°C after which cells were suspended in staining buffer and acquired on a LSR II flow cytometer (BD Biosciences). Flow cytometric analysis were performed using FlowJo software (v10, Tree Star Inc.).

Statistical Analysis.

All statistical analyses other than Kaplan-Meier curves (produced in R, statistical significance determined using a Log-Rank test and Cox proportional hazard regression analyses to estimate hazard ratios) were executed using Graphpad Prism software (version 8). For survival analyses within each subgroup, the unadjusted 95% CIs were reported¹³. Using the same software, heatmaps were constructed depicting mean changes in cell parameters, which were derived from the ratio of individual patient data from day 21 post start of treatment divided by baseline values. Paired non-parametric (Wilcoxon matched-pairs signed rank) tests were performed in order to calculate statistical significance of changes compared to baseline values. When continuous variables (e.g. magnitude of increase/decrease in MDSCs during therapy) were compared, non-parametric Spearman correlations were established yielding a Spearman Rho and corresponding p-value. In case of a Gaussian distribution of the data, a Pearson correlation coefficient was computed generating an r-squared (r²)- and p-value indicating statistical significance. Only, in case a paired sample was available, the samples were included in the analyses. Sensitivity analyses were performed demonstrating comparable clinical efficacy of gemcitabine in the immunomonitoring compared to the complete NVALT19 cohort (Hazard ratio (HR) of 0.62, 95% CI -1.487-0.137) similar to that observed in the entire NVALT19 cohort (HR 0.48; 95% CI, 0.33 to 0.71 Figure S9).

PART A
Novel immunological insights
into chemotherapy and
immune-checkpoint blockade

IMMUNE MONITORING IN MESOTHELIOMA
PATIENTS IDENTIFIES NOVEL IMMUNE-MODULATORY
FUNCTIONS OF GEMCITABINE
ASSOCIATING WITH CLINICAL RESPONSE

RESULTS

Gemcitabine differentially modulates proliferation of circulating lymphocyte subsets.

NK-cell proliferation significantly increased during gemcitabine treatment, whereas untreated patients exhibited a decrease in both CD8⁺ T-cells and natural killer (NK)-cell proliferation through time, (Figure 1). Additionally, FoxP3⁺ CD4⁺ T regulatory-cell (Treg) proliferation was strongly decreased in gemcitabine-treated patients compared to untreated patients. As FoxP3-expression marks a heterogeneous group of activated and regulatory T-cells, we further subdivided FoxP3⁺ cells based on the markers CD45RA and the magnitude of FoxP3-expression as described by Miyara *et al*¹⁴. (Figure S1A). Using this distinction, we found that the proliferation of activated FoxP3-high Tregs (aTregs), previously described to be highly immune-suppressive, was decreased following gemcitabine. Similarly, FoxP3-expressing T-helper (Th) cell-proliferation was diminished following treatment (Figure S1B). No statistically significant changes in T-cell frequencies (of total leukocytes) or T-cell memory subset distribution were noted in either patient group (Figure S2). These findings illustrate that regulatory and non-regulatory lymphocyte subsets may be differentially affected by gemcitabine chemotherapy.

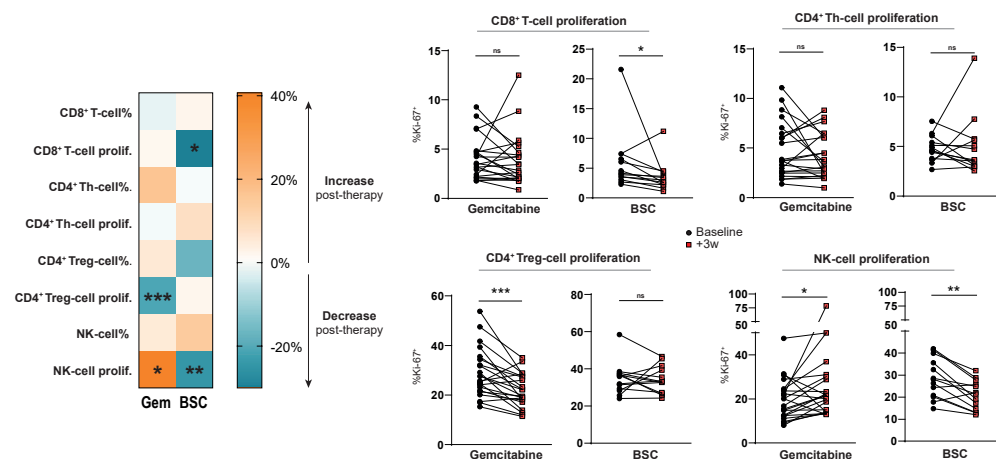


Figure 1. Gemcitabine differentially modulates proliferation in circulating lymphocyte subsets. T-cell percentages subtypes of total (CD45⁺) leukocytes and proliferation determined by intracellular Ki-67-staining in peripheral blood of mesothelioma patients treated with or without gemcitabine at baseline, and after 3 weeks. A heatmap shows the mean changes per parameter compared to baseline values in both patient groups. Wilcoxon matched-pairs signed rank tests were performed to calculate statistical significance. A total of 35 patients were included in the analysis (n=22 GEM; n=13 BSC). Th = T-helper, Treg = regulatory T cell, NK = natural killer, BSC = best supportive care, ns = not significant, * = p<0.05, ** = p<0.01, *** = p<0.001.

Gemcitabine depletes MDSCs in mesothelioma correlating with improved T-cell proliferation.

Gemcitabine has previously been reported to deplete MDSCs but whether this occurs in mesothelioma or affects T-cell proliferation *in vivo* remains largely unknown. We assessed CD11b⁺ CD33⁺ HLA-DR⁻ MDSC frequencies by direct *ex vivo* measurement following ficoll-density gradient centrifugation and could confirm significant MDSC-reduction by gemcitabine in patients (Figure 2A). The magnitude of MDSC-reduction significantly correlated with CD4⁺ T-helper and CD8⁺ T-cell but not NK-cell proliferation, strengthening results by others showing T-cell suppressive capacities of MDSCs *in vitro* (Figure 2B)¹⁵. Other myeloid cell subsets available in a subset of patients showed less interference of gemcitabine, with only plasmacytoid dendritic cells (pDC) being significantly increased following treatment, which is in line with earlier data in pancreatic cancer patients (Figure S3)¹⁶. These data show that the decreased MDSCs in peripheral blood of mesothelioma patients during gemcitabine therapy were paralleled by an increased T-cell proliferation.

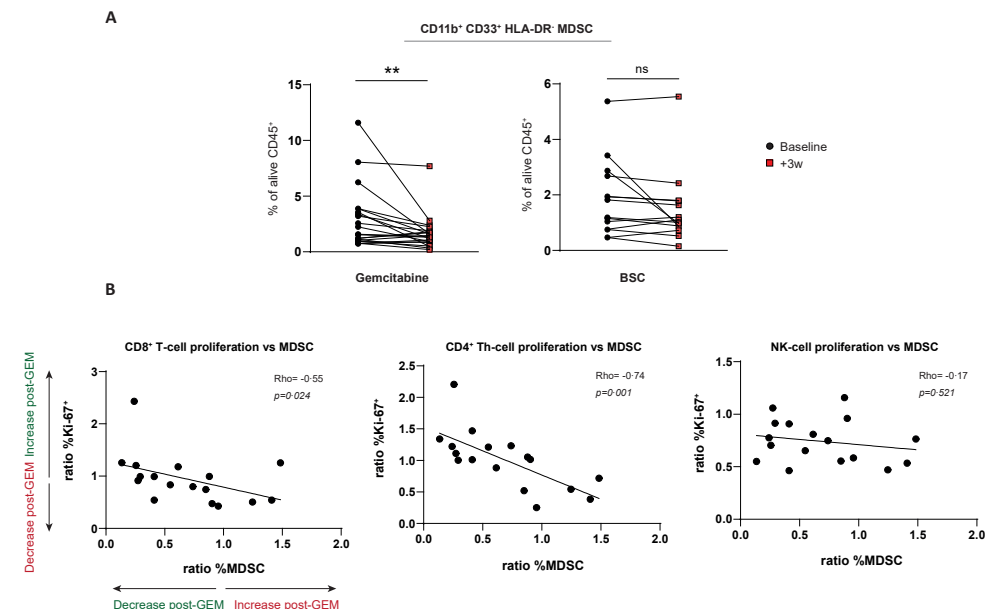


Figure 2. The gemcitabine-associated decrease in MDSCs correlates with increased T-cell proliferation. (A) changes in percentages of myeloid derived suppressor cells (MDSCs) following gemcitabine or best-supportive care (BSC). (B) correlations of CD8⁺, CD4⁺ FoxP3 (Th)- and NK-lymphocyte proliferation (Ki67⁺) dynamics with changes in MDSC-frequencies in peripheral blood following gemcitabine (GEM) treatment. Wilcoxon matched-pairs signed rank tests were performed to calculate statistical significance. MDSCs were available for 35 patients (n=21 GEM; n=14 BSC). Spearman correlation coefficients were calculated and a Rho was generated for 17 gemcitabine-treated patients of whom matched T-cells and MDSCs were available. NK = natural killer, ns = not significant, ** = p<0.01.

Gemcitabine promotes an activated T-cell and NK-cell phenotype.

In order to complement our understanding of how gemcitabine alters T-cell phenotype and aid rational combination therapy selection, we analysed the expression of a variety of co-inhibitory and –stimulatory receptors on peripheral blood lymphocytes in our patient cohort (Figure 3A). Percentages of receptor-positive cells mirrored median fluorescent intensity (MFI) values enabling MFI for further analysis (Figure S4). Besides PD-1, which was significantly increased on CD8⁺ T cells in gemcitabine-treated patients only, the majority of inhibitory receptors changed with similar dynamics in both patients groups, albeit more markedly following gemcitabine (Figure 3B). In patients with a malignancy, NK cells have been reported to express several co-inhibitory receptors including TIM-3 which has been associated with increased NK-cell maturation but diminished functionality upon TIM-3-ligation¹⁷. NK cells expressed CTLA-4, LAG-3, TIM-3 and CD39, of which the latter two were significantly increased in the gemcitabine group but not in the control group (Figure 3B). As the upregulation of co-inhibitory receptors is associated with both exhaustion and activation of lymphocytes, we assessed co-stimulatory receptor expression on T- and NK-cells to attempt to differentiate between these cellular states. As opposed to co-inhibitory receptors whose expression was heterogeneously altered following gemcitabine, co-stimulatory markers including ICOS, CD28 and HLA-DR were uniformly increased on both T- and NK cells in treated patients (Figure 3C). Interestingly, these changes did not correlate with decreasing MDSC-frequencies nor were they related to the magnitude of Treg-proliferation which we found to be decreased following gemcitabine treatment earlier (Figure S5).

These findings suggest that, whereas T-cell proliferation relates to MDSCs, the activation phenotype does not. T-cell activation in turn may result from direct gemcitabine-mediated modulation or indirectly via effects on tumour cells⁵. T-cell activation due to increased (tumour-derived) antigen recognition was deemed unlikely as gemcitabine did not affect or induce activation of effector-memory T cells specifically. Gemcitabine treatment rather increased activation marker expression across all memory subsets investigated, including naïve T-cells (Figure 4).

Gemcitabine does not alter cytokine expression by T cells.

In addition to co-inhibitory and –stimulatory receptor expression on circulating T cells, we assessed cytokine- and granzyme-production capacity by stimulating PBMCs *in vitro* with PMA/ionomycin followed by intracellular staining. In contrast to aforementioned surface-markers, cytokine production did not statistically differ in treated and untreated patients although a trend towards increased expression was appreciated in gemcitabine-treated patients (Figure S6A). Cytokine and granzyme-expression was found to be strongly coupled

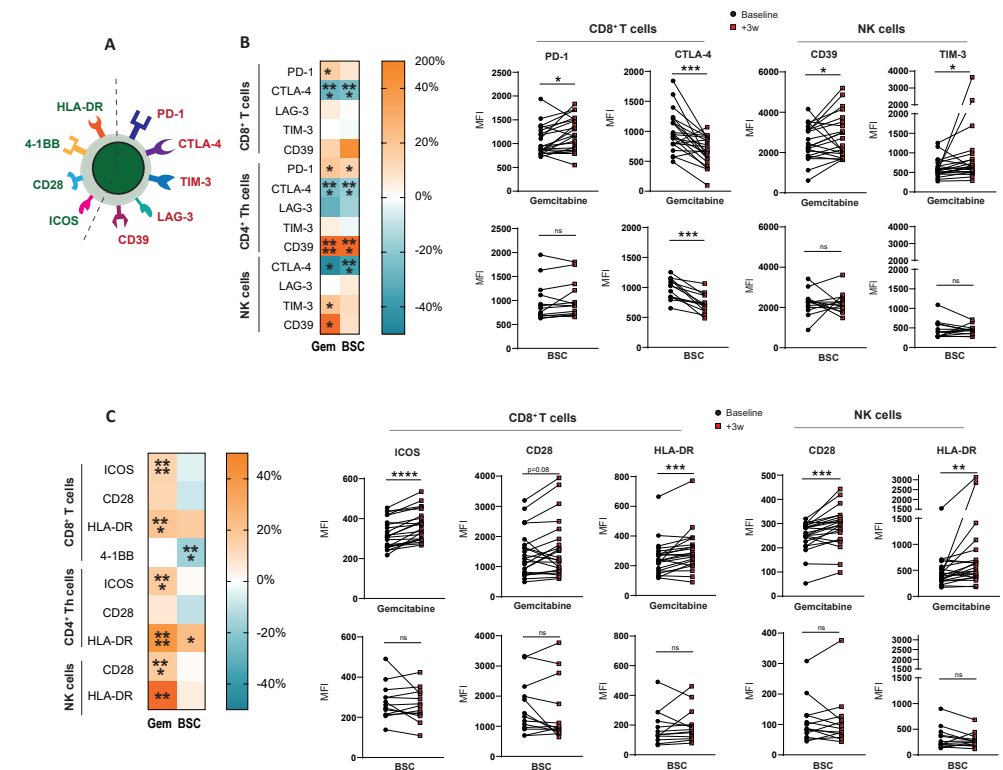


Figure 3. Gemcitabine-treated patients display an activated lymphocyte phenotype in peripheral blood. (A) co-stimulatory (green) and co-inhibitory (red) receptors assessed on lymphocyte surface in peripheral blood. **(B)** heatmaps displaying mean percentage of change and paired analyses of co-inhibitory receptors **(C)** and co-stimulatory receptor expression in response to gemcitabine or best-supportive care (BSC). Wilcoxon matched-pairs signed rank tests were performed to calculate statistical significance. A total of 35 patients were included in the analysis (n=22 GEM; n=13 BSC). Th = T-helper, Treg = regulatory T cell, NK = natural killer, BSC = best supportive care, PD-1 = programmed cell death protein 1, CTLA-4 = cytotoxic T-lymphocyte-associated protein 4, TIM-3 = T-cell immunoglobulin and mucin-domain containing-3, ICOS = inducible co-stimulatory molecule, HLA-DR = human-leukocyte antigen DR, MFI = mean fluorescent intensity, ns = not significant, * = p<0.05, ** = p<0.01, *** = p<0.001, **** = p<0.0001.

to specific memory T-cell subsets (Figure S6B). Specifying cytokine expression (e.g. IFN γ) to memory subsets yielded increased expression for high cytokine-producing subsets after gemcitabine although this did not reach statistical significance (Figure S6C, *data not shown*).

PART A
Novel immunological insights
into chemotherapy and
immune-checkpoint blockade

IMMUNE MONITORING IN MESOTHELIOMA
PATIENTS IDENTIFIES NOVEL IMMUNE-MODULATORY
FUNCTIONS OF GEMCITABINE
ASSOCIATING WITH CLINICAL RESPONSE

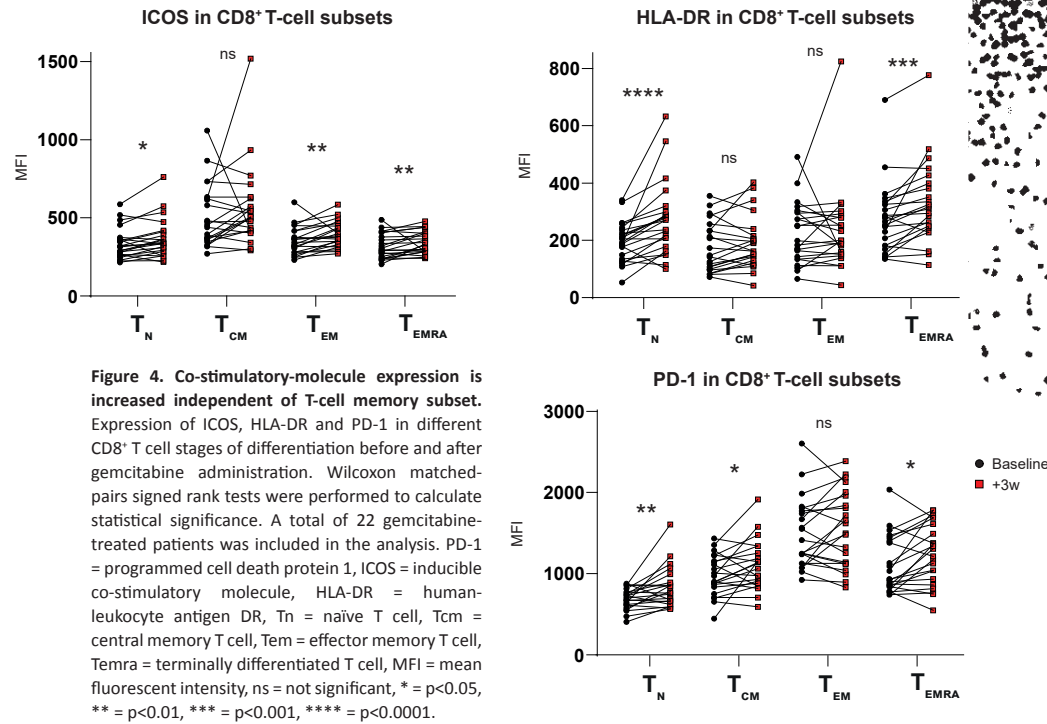


Figure 4. Co-stimulatory-molecule expression is increased independent of T-cell memory subset. Expression of ICOS, HLA-DR and PD-1 in different CD8⁺ T cell stages of differentiation before and after gemcitabine administration. Wilcoxon matched-pairs signed rank tests were performed to calculate statistical significance. A total of 22 gemcitabine-treated patients was included in the analysis. PD-1 = programmed cell death protein 1, ICOS = inducible co-stimulatory molecule, HLA-DR = human-leukocyte antigen DR, Tn = naïve T cell, Tcm = central memory T cell, Tem = effector memory T cell, Temra = terminally differentiated T cell, MFI = mean fluorescent intensity, ns = not significant, * = $p < 0.05$, ** = $p < 0.01$, *** = $p < 0.001$, **** = $p < 0.0001$.

Immune monitoring identifies lymphocyte parameters associated with response to gemcitabine.

Although we detected increased markers of T- and NK-cell activation in gemcitabine-treated patients, the biological and clinical relevance of these findings remains unknown. Relating the investigated parameters to patient outcomes may also further define whether gemcitabine-mediated immune effects could potentially drive disease outcome. Furthermore, as OS was not significantly improved by gemcitabine in the intention to treat-population, biomarkers for patient stratification are warranted. We correlated the expression of key parameters, which were significantly altered by gemcitabine, to patient OS and PFS in both the gemcitabine-treated patients and the BSC-cohort, to detect which parameters indicated potential clinical benefit. We found that patients, showing an increase in NK-cell proliferation following gemcitabine, had a significantly better PFS and OS (HR for OS: 0.45, $p = 0.01$, HR PFS: 0.48, $p = 0.01$, Figure 5). In addition, an increase in PD-1-expression on proliferating (but not total) CD8⁺ T cells was associated with improved clinical outcome (HR OS: 0.43, $p < 0.01$, HR PFS: 0.56, $p = 0.04$). These parameters did not correlate with improved clinical outcome in BSC-treated patients, suggesting a gemcitabine-specific

response (Figure S7A). ICOS-expression in CD8⁺ T cells was near uniformly increased following gemcitabine except in one patient who coincidentally experienced progressive disease and death soon after treatment with gemcitabine (HR for increased vs. decreased ICOS-expression OS: 0.22, $p = 0.03$, HR PFS: 0.22, $p = 0.03$, Figure S7B). The magnitude of ICOS-induction by gemcitabine further correlated with improved response to therapy albeit not significantly (Figure S7C). These findings derived from a small exploratory cohort analysis suggest that key gemcitabine-induced immune effects might be associated with a survival benefit. This might help to better understand the interaction between and predict the efficacy of chemotherapy and immunotherapy.

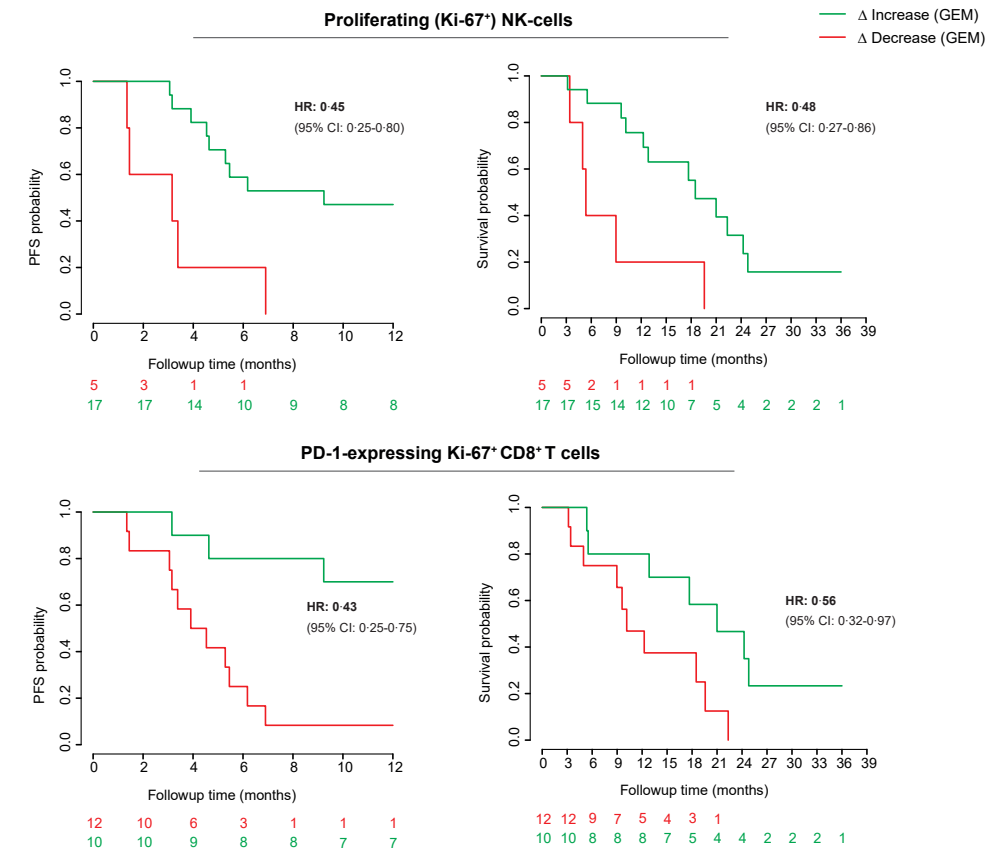


Figure 5. Increases in NK- and PD-1⁺T-cell proliferation following gemcitabine correlate with clinical outcome. Kaplan-Meier (KM-) curves showing differences in progression free- (PFS) and overall survival (OS) between patients exhibiting an increase (green) or decrease (red) of selected immune parameters following gemcitabine (GEM). 22 gemcitabine-treated patients were included in the analysis. Log-rank tests were applied. NK = natural killer, PD-1 = programmed cell death protein 1, HR = hazard ratio, CI = confidence interval.

DISCUSSION

Using comprehensive immune monitoring of peripheral blood in mesothelioma patients treated with gemcitabine, we uncovered widespread myeloid and lymphoid immune modulation that might associate with treatment response. The alterations in T- and NK-cell proliferation and activation that were detected have not been previously reported for this kind of chemotherapy and tumour type. The increased PD-1 and ICOS-expression on lymphocytes following gemcitabine furthermore suggests that the combination of gemcitabine with immunotherapy using antagonistic and agonistic antibodies to PD-1 and ICOS, respectively, might be efficacious. These findings are of particular importance, as anti-PD-1 monotherapy was recently found to be ineffective in the majority of mesothelioma patients, emphasizing the demand for novel drug combinations to sensitize mesothelioma to immune-checkpoint inhibitors¹. In line with our suggestions are recent data by De Lara *et al.*, showing increased efficacy of gemcitabine-anti-PD-1 treatment in a preclinical mesothelioma model and radiographic responses in two mesothelioma patients following combination therapy¹⁸. Further randomized studies are needed to confirm whether these combinations are effective in larger patient cohorts. As gemcitabine is widely used for a variety of cancer including pancreatic cancer, breast cancer and non-small cell lung cancer (NSCLC), these findings could potentially be extrapolated to other tumour types as well.

The pleiotropic functions of gemcitabine on a wide variety of immune cells *in vivo* without functional *in vitro* data, preclude us from pinpointing which cellular mechanisms are mainly responsible for therapeutic benefit. Furthermore, we documented a significantly increased proliferation of NK-cells and decreased Treg-proliferation in gemcitabine-treated patients, while cell frequencies remained largely unaltered in peripheral blood. Although our method of cell isolation precludes proper enumeration of cells, several explanations could account for this discrepancy. First, as we assessed cellular states following the first cycle of chemotherapy, a change in proliferation would likely precede consequent changes in cell frequencies, which may become apparent at later time points. Secondly, whereas cellular state characterized by markers such as Ki-67, PD-1 and ICOS may offer a snapshot of underlying T-cell biology, circulating cell frequencies may not adequately reflect what happens in tumours. Although we did not have pre- and post-treatment tumour tissues, pre-clinical findings by others confirm increased NK-cell infiltration and decreased MDSC-frequencies into gemcitabine-treated tumours¹⁹. The fact that the investigated patients were only recently pre-treated with first-line chemotherapy could further influence circulating leukocyte frequencies. Whether this also accounts for the observed decrease in CD8⁺ T-cell proliferation in BSC-patients, or whether this is due to differences in time to disease progression, remains unknown. Furthermore, factors like concurrent infection or other comorbidities could have influenced the effects observed in our analysis. However,

clinical and laboratory assessments were captured at baseline and after three weeks (at start of the second treatment cycle) and these did not reveal clear confounding factors. Moreover, by including a non-gemcitabine (BSC)-treated patient cohort first-line treatment induced alterations and confounding factors independent of treatment should have been comparable between both patients groups, increasing the likelihood that a real difference between the two groups was detected. Further investigations e.g. in pre-clinical disease models and functional *in vitro* studies in larger patients cohorts will be needed to formally establish causality of the observed immunological alteration in gemcitabine-treated mesothelioma patients.

As opposed to T-cell proliferation, which was tightly correlated to MDSC-frequencies, NK-cell proliferation and increased lymphocyte activation were not, suggesting that other mechanisms could be responsible for these shifts in phenotypes. Gemcitabine has recently been reported to increase tumour NKG2D-ligand expression *in vitro*²⁰, which could explain the increases in NK-cell proliferation and activation. In addition, gemcitabine has been found to increase tumour-antigenicity in mesothelioma mouse models by increasing antigen-presenting cell (APC) MHC-expression and promoting cross-presentation of tumour-antigens leading to increased tumour control²¹⁻²³. Although we did not assess tumour-specific immune responses, we observed increased expression of activation markers in both naïve- and memory T-cell subsets, unlikely reflecting novel effector-T-cell clone induction. Whether this global change in T- and NK-cell activation resulted from direct effects of gemcitabine on lymphocytes, or from increased tumour adjuvanticity (e.g. by release of inflammatory mediators from dying tumour cells, as has been reported for gemcitabine) remains to be investigated²³.

Although gemcitabine did not uniformly or significantly increase circulating PD-1⁺/Ki-67⁺ CD8⁺ T cells (data not shown), an increase was associated with improved clinical outcome (Fig. 5) similar to recent reports identifying a similar population to associate with anti-PD-1 therapy response in NSCLC and melanoma²⁴⁻²⁵. Although the exact nature of this phenotype remains to be identified, these cells showed significant overlap with tumour-infiltrating T cells in previous analyses, which, irrespective of the type of treatment, inferred durable tumour control²⁵.

Our exploratory study design bears some important limitations. Although our sample size was limited with regard to the total NVALT19 population, we could show that our cohort was representative of the total study population with comparable clinical outcomes and patients characteristics (Table S1, Fig. S9). It is tempting to speculate whether the observed outliers also correlate with alternative clinical outcomes, as is shown for ICOS-expression which increased in all but one patient in response to gemcitabine, with that patient performing poorest (Fig. S7). The limited cohort size and absence of a validation group precludes formal conclusions to be made on the effects of gemcitabine on circulating

PART A
Novel immunological insights
into chemotherapy and
immune-checkpoint blockade

IMMUNE MONITORING IN MESOTHELIOMA
PATIENTS IDENTIFIES NOVEL IMMUNE-MODULATORY
FUNCTIONS OF GEMCITABINE
ASSOCIATING WITH CLINICAL RESPONSE

immunity and therefore should be considered exploratory. Nonetheless, the results from this pilot study indicate immune-mediated anti-cancer efficacy of gemcitabine, warranting further research into these phenomenon in larger cohorts.

We report novel observations on circulating T- and NK-cells in gemcitabine-treated mesothelioma patients in a subset of patients from the NVALT-19 trial. These findings suggest preferential activation of anti-tumour immune cell populations and inhibition of Tregs and MDSCs. These pilot data, if validated in larger prospective cohorts, may provide a platform for future development of on-treatment biomarkers that predict improved patient outcome.

REFERENCES

- 1 Popat S, Curioni-Fontecedro A, Polydoropoulou V, Shah R, O'Brien M, Pope A, et al. A multicentre randomized phase III trial comparing pembrolizumab (P) vs single agent chemotherapy (CT) for advanced pre-treated malignant pleural mesothelioma (MPM): results from the European Thoracic Oncology Platform (ETOP 9- 15) PROMISE-meso trial. *Annals of Oncology* 2019;30
- 2 Maio M, Scherpereel A, Calabro L, Aerts J, Perez SC, Bearz A, et al. Tremelimumab as second-line or third-line treatment in relapsed malignant mesothelioma (DETERMINE): a multicentre, international, randomised, double-blind, placebo controlled phase 2b trial. *Lancet Oncology* 2017;19:e161–e72.
- 3 Scherpereel A, Wallyn F, Albelda SM, Munck C. Novel therapies for malignant pleural mesothelioma. *Lancet Oncology* 2018;19(3):e161–72.
- 4 de Gooijer CJ, van der Noort V, Stigt JA, Baas P, Biesma B, Cornelissen R, et al. Switch maintenance gemcitabine after first line chemotherapy in patients with malignant mesothelioma (NVALT19): an investigator-initiated randomised open label phase 2 trial. *Lancet Respiratory Medicine* 2021; doi: 10.1016/S2213-2600(20)30362-3.
- 5 Galluzzi L, Buque A, Kepp O, Zitvogel L, Kroemer G. Immunological effects of conventional chemotherapy and targeted anticancer agents. *Cancer Cell* 2015;28 (6):690–714.
- 6 Aerts J, de Goeje PL, Cornelissen R, Kaijen-Lambers MEH, Bezemer K, van der Leest CH, et al. Autologous dendritic cells pulsed with allogeneic tumor cell lysate in mesothelioma: from mouse to human. *Clinical Cancer Research* 2018;24 (4):766–76.
- 7 Zitvogel L, Kepp O, Kroemer G. Immune parameters affecting the efficacy of chemotherapeutic regimens. *Nature Reviews Clinical Oncology* 2011;8(3):151–60.
- 8 Suzuki E, Kapoor V, Jassar AS, Kaiser LR, Albelda SM. Gemcitabine selectively eliminates splenic Gr-1+/CD11b+ myeloid suppressor cells in tumor-bearing animals and enhances antitumor immune activity. *Clinical Cancer Research* 2005;11(18):6713–21.
- 9 Eriksson E, Wenthe J, Irenaeus S, Loskog A, Ullenhag G. Gemcitabine reduces MDSCs, tregs and TGFbeta-1 while restoring the teff/treg ratio in patients with pancreatic cancer. *Journal of Translational Medicine* 2016;14(1):282.
- 10 Homma Y, Taniguchi K, Nakazawa M, Matsuyama R, Mori R, Takeda K, et al. Changes in the immune cell population and cell proliferation in peripheral blood after gemcitabine-based chemotherapy for pancreatic cancer. *Clinical Translational Oncology* 2014;16(3):330–5.
- 11 Suzuki E, Sun J, Kapoor V, Jassar AS, Albelda SM. Gemcitabine has significant immunomodulatory activity in murine tumor models independent of its cytotoxic effects. *Cancer Biology & Therapy* 2007;6(6):880–5.
- 12 Byrne MJ, Nowak AK. Modified RECIST criteria for assessment of response in malignant pleural mesothelioma. *Annals of Oncology* 2004;15(2):257–60.
- 13 Rothman KJ. No adjustments are needed for multiple comparisons. *Epidemiology* 1990;1(1):43–6.
- 14 Miyara M, Yoshioka Y, Kitoh A, Shima T, Wing K, Niwa A, et al. Functional delineation and differentiation dynamics of human CD4+ T cells expressing the FoxP3 transcription factor. *Immunity* 2009;30(6):899–911.
- 15 Condamine T, Dominguez GA, Youn JI, Kossenkova AV, Mony S, Alicea-Torres K, et al. Lectin-type oxidized LDL receptor-1 distinguishes population of human polymorphonuclear myeloid-derived suppressor cells in cancer patients. *Science Immunology* 2016;1(2).
- 16 Soeda A, Morita-Hoshi Y, Makiyama H, Morizane C, Ueno H, Ikeda M, et al. Regular dose of gemcitabine induces an increase in CD14+ monocytes and CD11c+ dendritic cells in patients with advanced pancreatic cancer. *Japanese Journal of Clinical Oncology* 2009;39 (12):797–806.
- 17 Ndhlovu LC, Lopez-Verges S, Barbour JD, Jones RB, Jha AR, Long BR, et al. Tim-3 marks human natural killer cell maturation and suppresses cell-mediated cytotoxicity. *Blood* 2012;119(16):3734–43.
- 18 Tallon de Lara P, Cecconi V, Hiltbrunner S, Yagita H, Friess M, Bode B, et al. Gemcitabine synergizes with immune checkpoint inhibitors and overcomes resistance in a preclinical model and mesothelioma patients. *Clinical Cancer Research* 2018;24 (24):6345–54.
- 19 Gurlevik E, Fleischmann-Mundt B, Brooks J, Demir IE, Steiger K, Ribback S, et al. Administration of gemcitabine after pancreatic tumor resection in mice induces an antitumor immune response mediated by natural killer cells. *Gastroenterology* 2016;151(2):338–50 e7.
- 20 Gravett AM, Dalgleish AG, Copier J. In vitro culture with gemcitabine augments death receptor and NKG2D ligand expression on tumour cells. *Scientific Reports* 2019;9 (1):1544.

PART A
Novel immunological insights
into chemotherapy and
immune-checkpoint blockade

IMMUNE MONITORING IN MESOTHELIOMA
PATIENTS IDENTIFIES NOVEL IMMUNE-MODULATORY
FUNCTIONS OF GEMCITABINE
ASSOCIATING WITH CLINICAL RESPONSE

- 21 McDonnell AM, Lesterhuis WJ, Khong A, Nowak AK, Lake RA, Currie AJ, et al. Tumor-infiltrating dendritic cells exhibit defective cross-presentation of tumor antigens, but is reversed by chemotherapy. *European Journal of Immunology* 2015;45 (1):49–59.
- 22 Nowak AK, Lake RA, Marzo AL, Scott B, Heath WR, Collins EJ, et al. Induction of tumor cell apoptosis in vivo increases tumor antigen cross-presentation, crosspriming rather than cross-tolerizing host tumor-specific CD8 T cells. *Journal of Immunology* 2003;170(10):4905–13.
- 23 Liu WM, Fowler DW, Smith P, Dagleish AG. Pre-treatment with chemotherapy can enhance the antigenicity and immunogenicity of tumours by promoting adaptive immune responses. *British Journal of Cancer* 2010;102(1):115–23.
- 24 Kamphorst AO, Pillai RN, Yang S, Nasti TH, Akondy RS, Wieland A, et al. Proliferation of PD-1+ CD8 T cells in peripheral blood after PD-1 targeted therapy in lung cancer patients. *Proceedings of the National Academy of Sciences* 2017;114(19):4993.
- 25 Huang AC, Postow MA, Orlowski RJ, Mick R, Bengsch B, Manne S, et al. T-cell invigoration to tumour burden ratio associated with anti-PD-1 response. *Nature* 2017;545(7652):60–5.

SUPPLEMENTARY DATA

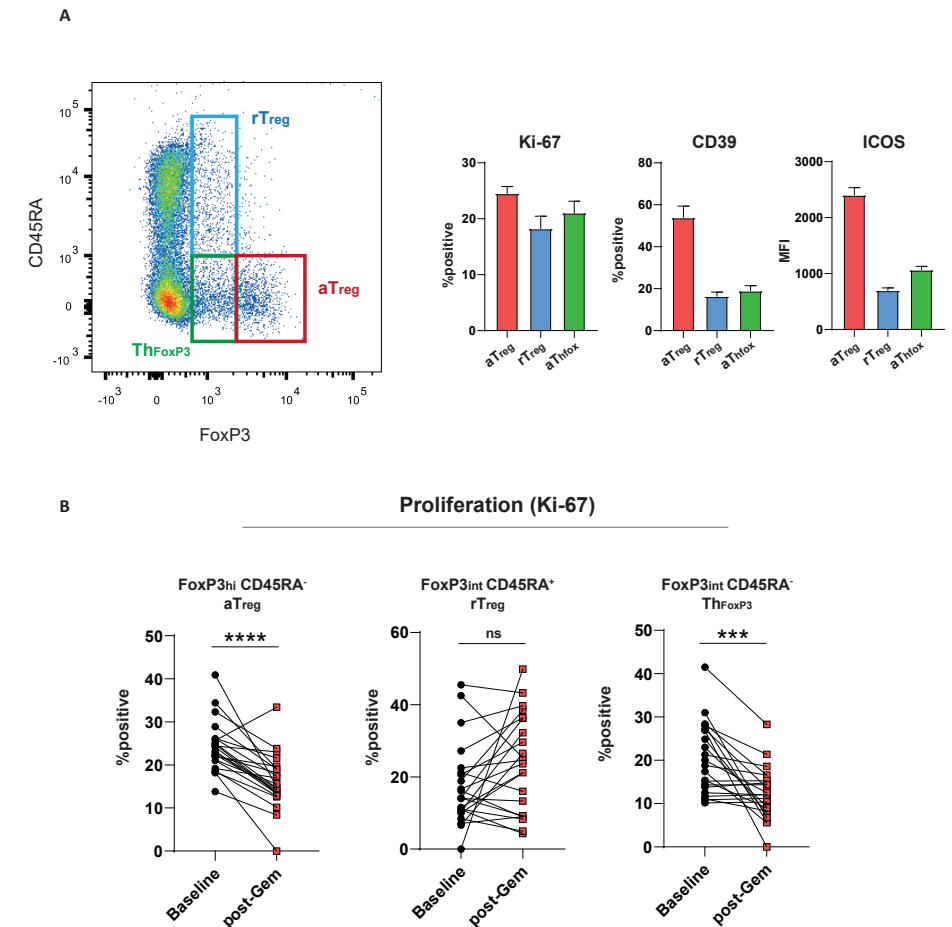
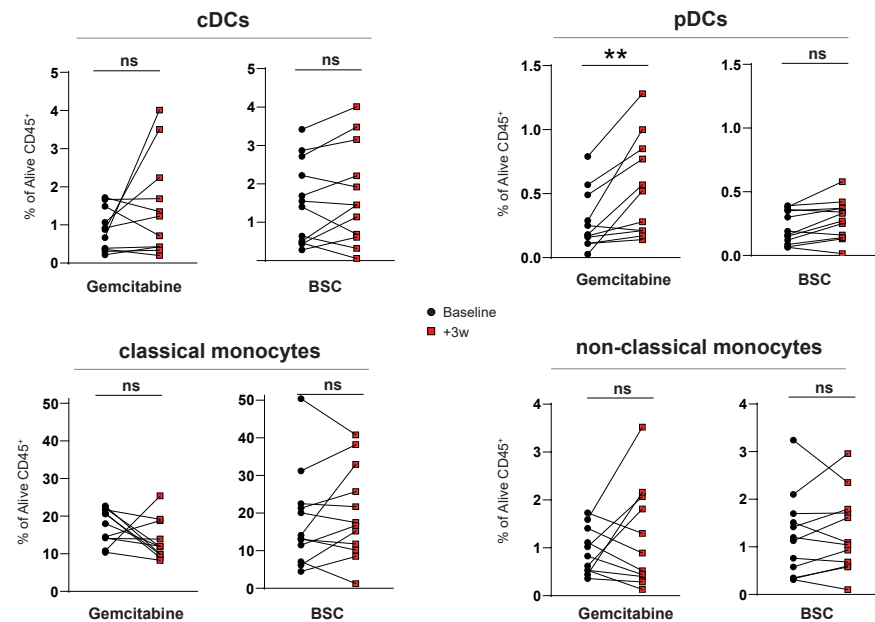
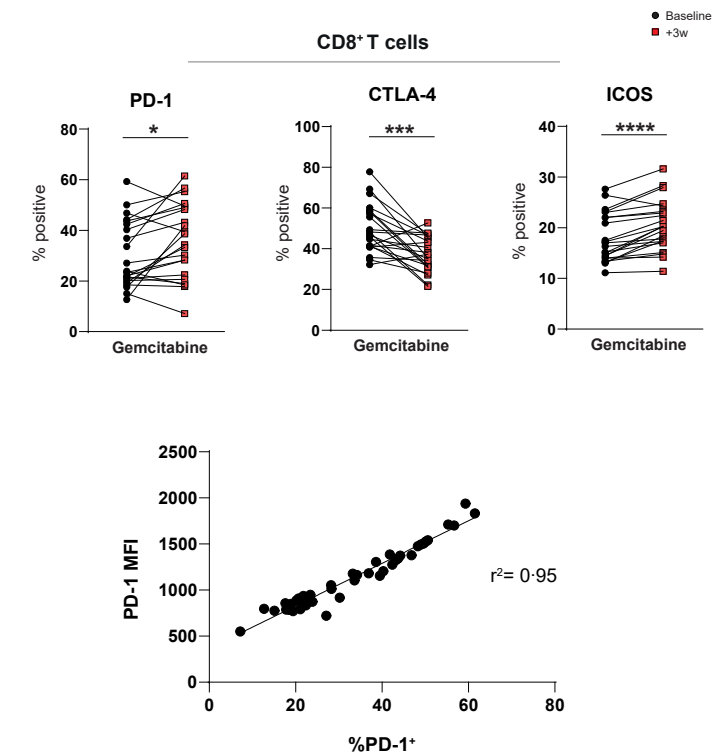
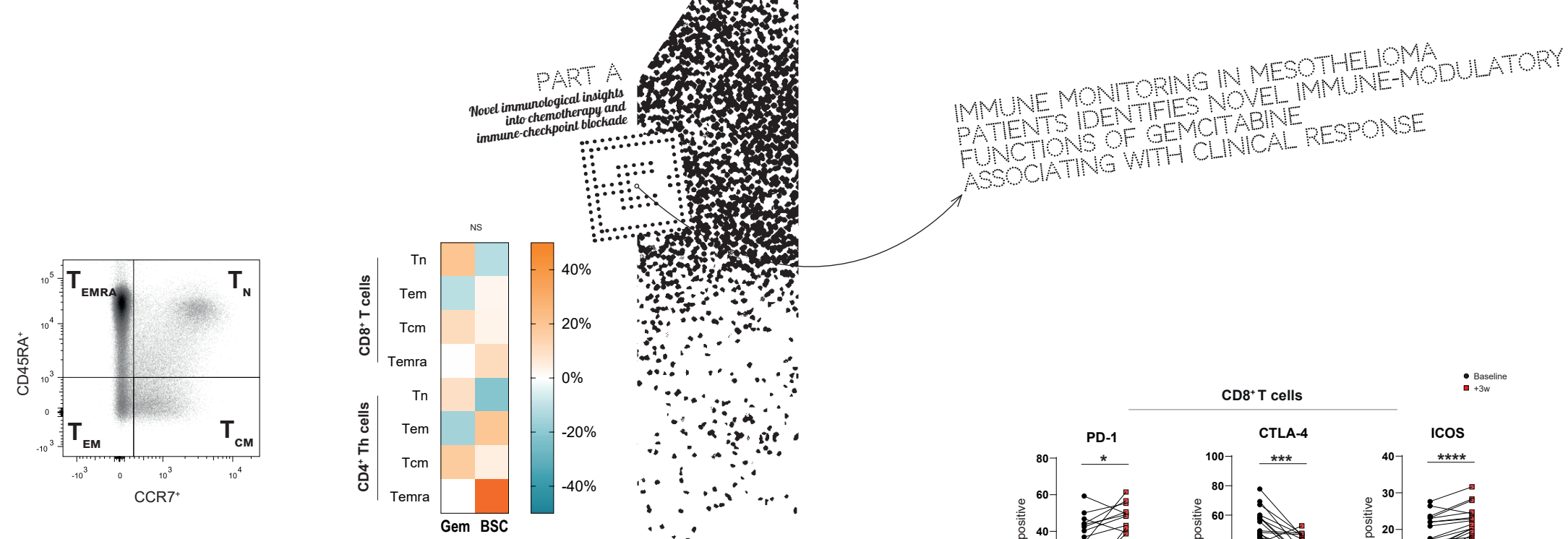


Figure S1. Proliferation is decreased in activated Treg and Foxp3-expressing Th-cells following gemcitabine treatment. (A) Representative flow cytometry plot of regulatory T cells (Tregs) gated according to Miyara et al. using CD45RA and FoxP3. Activated Tregs (aTregs) are the highest expressers of Ki-67, CD39 and ICOS on baseline as compared to resting Tregs (rTregs) or FoxP3-positive T-helper cells (bar graphs showing means with SEM). Wilcoxon matched-pairs signed rank tests were performed to calculate statistical significance. A total of 22 gemcitabine-treated patients was included in the analysis. (B) Proliferation as determined by Ki-67 expression between the different FoxP3-expressing CD4⁺ T-cell subsets. hi = high, int = intermediate, MFI = mean fluorescent intensity, ns = not significant, *** = $p < 0.001$, **** = $p < 0.0001$.



PART A
Novel immunological insights
into chemotherapy and
immune-checkpoint blockade

IMMUNE MONITORING IN MESOTHELIOMA
PATIENTS IDENTIFIES NOVEL IMMUNE-MODULATORY
FUNCTIONS OF GEMCITABINE
ASSOCIATING WITH CLINICAL RESPONSE

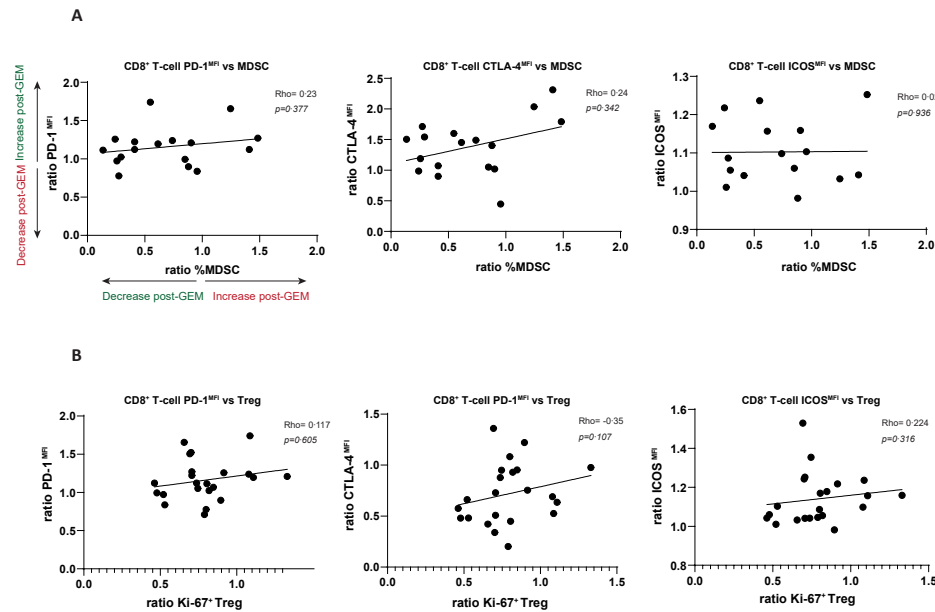


Figure S5. No correlations between lymphocyte receptor expression and Treg proliferation or MDSCs. (A) Correlations between the changes in PD-1/CTLA-4/ICOS MFI with changes in MDSCs and (B) Treg-proliferation in peripheral blood following gemcitabine (GEM) treatment. Spearman correlation coefficients were calculated and a Rho was generated for 17 gemcitabine-treated patients of whom matched T-cells and MDSCs were available. MDSC = myeloid derived suppressor cell, Treg = regulatory T cell, PD-1 = programmed cell death protein 1, CTLA-4 = cytotoxic T-lymphocyte-associated protein 4, ICOS = inducible co-stimulatory molecule, MFI = mean fluorescent intensity

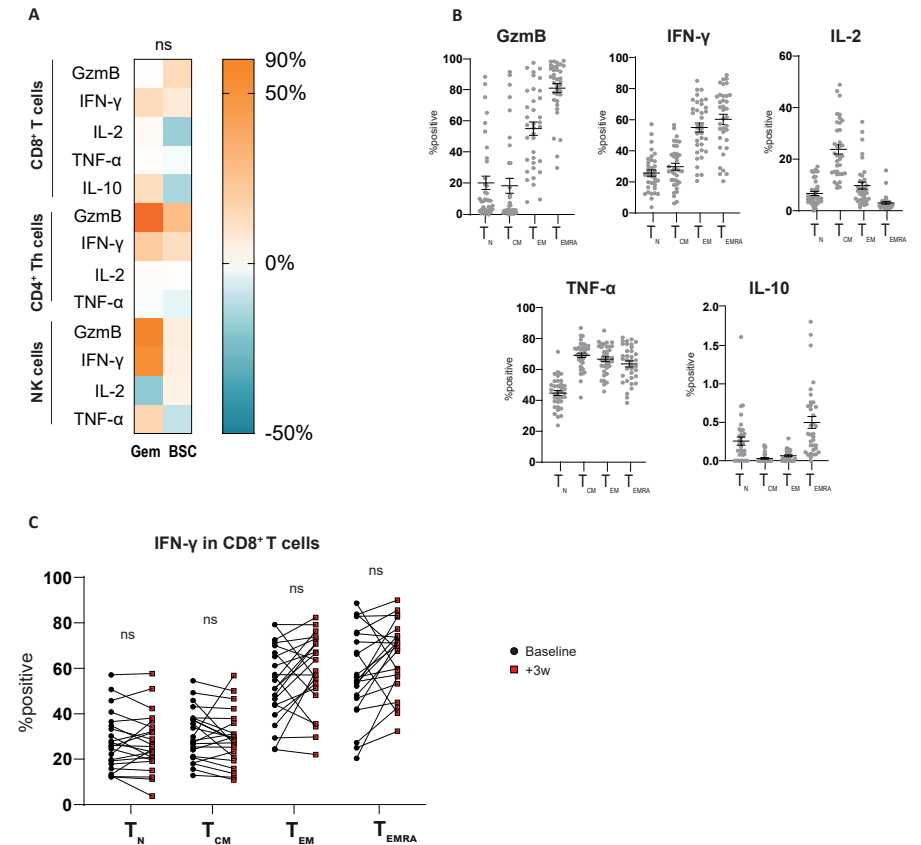


Figure S6. Gemcitabine is not associated with increased cytokine or granzyme expression in lymphocytes. (A) heatmap showing mean changes in cytokine/granzyme-B expression before and after gemcitabine (GEM) or best-supportive care (BSC) in different lymphocyte subsets. (B) expression of intracellular effector molecules in different CD8⁺ T-cell memory subsets on baseline. (C) expression of IFNγ by different CD8⁺ T-cell memory subsets following gemcitabine. Wilcoxon matched-pairs signed rank tests were performed to calculate statistical significance. All included patients were used to compute b, whereas 22 gemcitabine-treated patients were included in c. GzmB = granzyme B, IFNγ = interferon-gamma, IL-2 = interleukin 2, TNF-α = tumour-necrosis factor alpha, IL-10 = interleukin 10, NK = natural killer, Th = T-helper, T_N = naïve T cell, T_{CM} = central memory T cell, T_{EM} = effector memory T cell, T_{EMRA} = terminally differentiated T cell, ns = not significant.

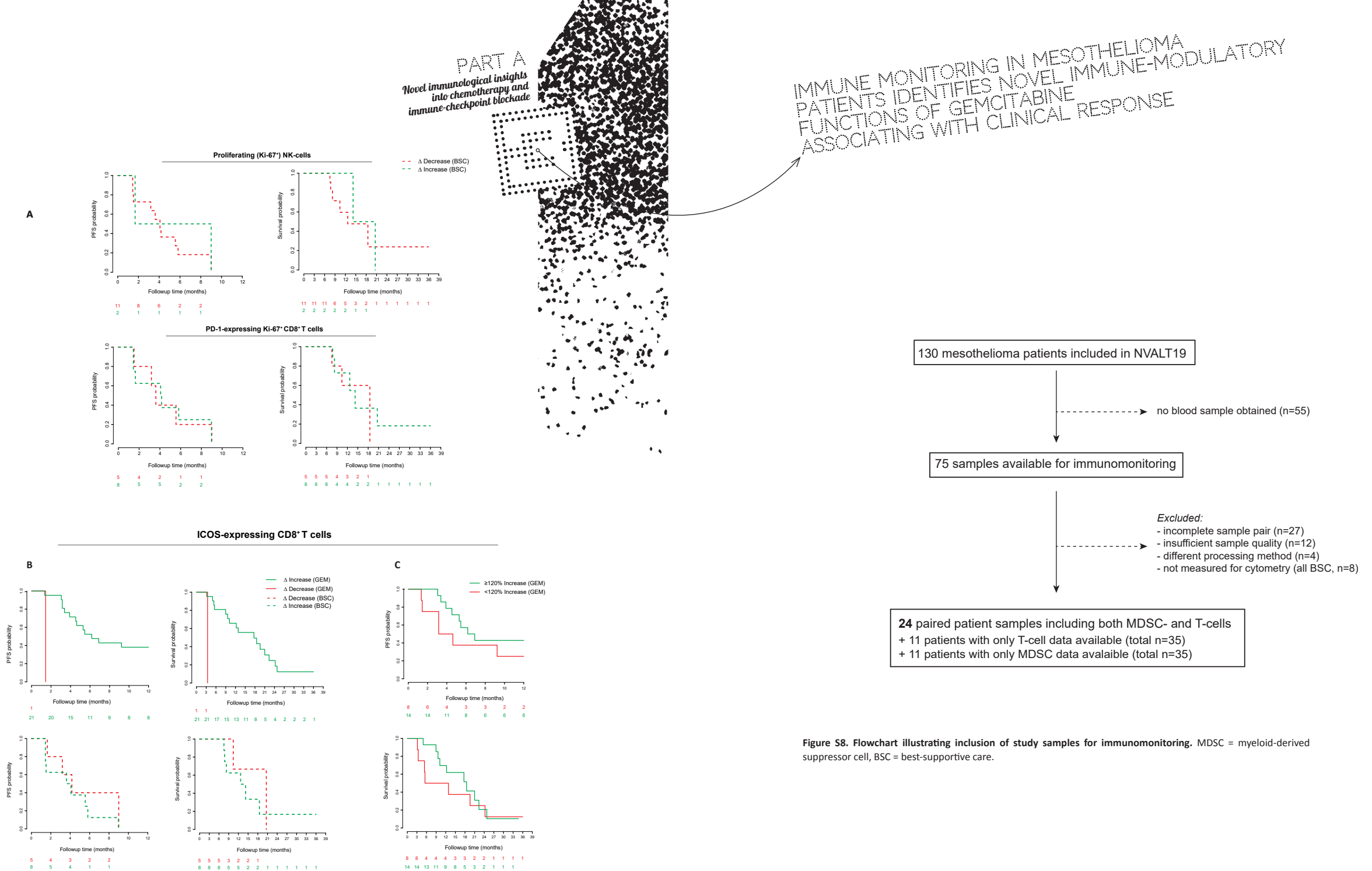


Figure S7. Parameters associated with clinical outcome in gemcitabine-treated patients are not detected in control patients. (A-B) Kaplan-Meier (KM-) curves showing differences in progression free- (PFS) and overall survival (OS) between patients exhibiting an increase (green) or decrease (red) of selected immune parameters compared to baseline. Log-rank tests were used to determine statistical significance. **(C)** the median change in ICOS-expression in the total group (GEM + BSC) compared to baseline (+20%) is shown. NK = natural killer, PD-1 = programmed cell death protein 1, ICOS = inducible co-stimulatory molecule, HR = hazard ratio, CI = confidence interval.

PART A
Novel immunological insights
into chemotherapy and
immune-checkpoint blockade

IMMUNE MONITORING IN MESOTHELIOMA
PATIENTS IDENTIFIES NOVEL IMMUNE-MODULATORY
FUNCTIONS OF GEMCITABINE
ASSOCIATING WITH CLINICAL RESPONSE

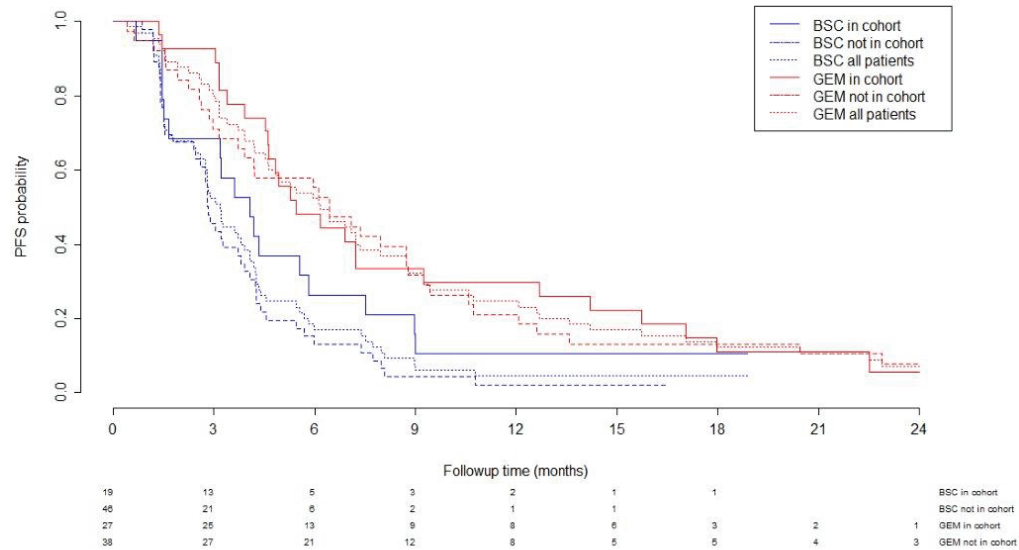
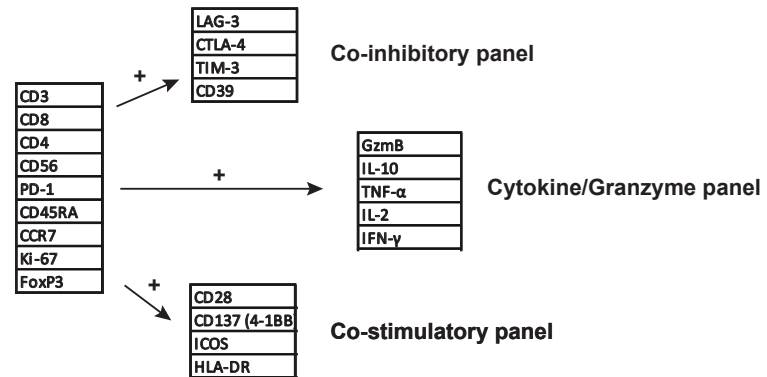


Figure S9. No differences in progression-free survival between immunomonitoring patients and the complete NVALT19 cohort. Individual progression-free survival (PFS) KM-curves of all BSC- (blue) and gemcitabine (red) treated patients in the NVALT19-study (dotted line) those included in the immunomonitoring cohort (closed line) and not included (dashed line). The hazard ratio (HR) of the subgroup (0.62, 95% CI -1.487-0.137) is similar to that observed in the entire NVALT19 cohort (HR 0.48; 95% CI, 0.33 to 0.71; p = 0.0002).

Table S1. Patient and tumour characteristics of the included, and total NVALT19 cohort.

	Immune monitoring subgroup			Total cohort NVALT19 study	
	Gemcitabine (n=27) Number, %	BSC (n=19) Number, %	Total (n=46) Number, %	Gemcitabine (n=65) Number, %	BSC (n=65) Number, %
Sex					
Female	3 (11)	4 (21)	39	7 (11)	11 (17)
Male	24 (89)	15 (79)	7	58 (89)	54 (83)
Age					
Median (years)	68	70	68	69	69
Range	43-79	57-80	43-80	43-84	35-82
WHO performance score					
0	16 (59)	10 (53)	26 (57)	37 (57)	38 (58)
1	11 (41)	8 (42)	19 (41)	27 (42)	25 (38)
2	0	1 (5)	1	0	2 (3)
Histological subtype					
Epithelial	24 (89)	17 (89)	41 (89)	57 (88)	57 (88)*
Biphasic	3 (11)	2 (11)	5 (11)	5 (8)	6 (9)
Sarcomatoid	0	0	0	3 (4)	2 (3)
Best response to first-line treatment					
Complete response	2 (7)	0	2 (4)	2 (3)	1 (2)
Partial response	6 (22)	7 (37)	13 (28)	25 (38)	26 (40)
Stable disease	19 (70)	12 (63)	31 (67)	38 (58)	38 (58)
Tumor stage					
Stages I-II	14 (52)	11 (58)	25 (54)	31 (48)	30 (46)
Stages III-IV	9 (33)	27 (42%)	12 (26)	25 (39)	27 (42)
Unknown	4 (15)	5 (26)	9 (20)	9 (14)	8 (12)

WHO; World Health Organization. *While on study, the diagnosis of one patient was changed into another malignancy.



Myeloid panel

Lineage*
CD14
CD15
CD16
CD11b
CD33
CD11c
CD123
PD-L1
HLA-DR

*

CD3
CD19
CD56

Table S2. Flow-cytometry panels used for the immune characterization studies. In case of a; a backbone was constructed using the markers in the left column with additional co-inhibitory, -stimulatory and cytokine/granzyme markers being added in the individual panels. b, lymphocytes were excluded from myeloid cell analyses by selecting lineage (CD3, CD19 or CD56) negative cells.

IMPROVING THE EFFICACY
OF CANCER VACCINES FOR SOLID TUMORS
BY COMBINATION IMMUNOTHERAPY



Chapters •4•5•6•7•

4

Floris Dammeijer
Lysanne A. Lieverse
Marijn D.M. Veerman
Henk C. Hoogsteden
Joost P. Hegmans
Lidia R. Arends
Joachim G. Aerts

J Clin Oncol. 2016 Sep 10;34(26):3204-12.

PART B
Improving the efficacy of
cancer vaccines for solid tumors
by combination immunotherapy

THE EFFICACY OF TUMOR VACCINES
AND CELLULAR IMMUNOTHERAPIES IN
NON-SMALL CELL LUNG CANCER:
A SYSTEMATIC REVIEW AND META-ANALYSIS

SUMMARY

PD-1 checkpoint-blockers have recently been approved as second-line treatment for advanced non-small cell lung cancer (NSCLC). Unfortunately, only a subgroup of patients responds and shows long term survival to these therapies. Tumor vaccines and cellular immunotherapies could synergize with checkpoint blockade, but which of these treatments is most efficacious is unknown. In this meta-analysis we assessed the efficacy of tumor vaccination and cellular immunotherapy in NSCLC. We searched for randomized controlled trials investigating cellular immunotherapy or vaccines in NSCLC. We used random effects models to analyze overall survival (OS) and progression free survival (PFS) expressed as hazard ratios (HR) and differences in months. The effect of immunotherapy type, disease stage, tumor histology, and concurrent chemotherapy was assessed using subgroup analysis and meta-regression. All procedures were performed according to the PRISMA guidelines.

We identified 18 RCTs that matched our selection criteria, including 6756 patients. Immunotherapy extended NSCLC survival and PFS, expressed as HR (OS: HR=0.81, 95%CI=0.70-0.94, $p=0.01$, PFS: HR=0.83, 95%CI=0.72-0.95, $p=0.006$) and month difference (OS: difference=5.43 months, 95%CI=3.20-7.65, $p<0.005$, PFS: difference=3.24 months, 95%CI=1.61-4.88, $p<0.005$). Cellular therapies outperformed tumor vaccines (OS as HR: $p=0.005$, month difference: $p<0.001$, PFS as HR: $p=0.001$, month difference: $p=0.004$). There was a benefit of immunotherapy in low stage over high stage NSCLC and concurrent administration of chemotherapy only in one of four outcome measures evaluated (PFS in months: $p=0.01$ and PFS as HR: $p=0.031$, respectively) There was no significant effect of tumor histology on survival nor PFS. Tumor vaccines and cellular immunotherapies enhance overall survival and PFS in NSCLC. Cellular immunotherapy was found to be more effective than tumor vaccination. These findings have implications for future studies investigating combination immunotherapy in NSCLC.

INTRODUCTION

Lung cancer is the leading cause of cancer related mortality worldwide¹. Non-small cell lung cancer (NSCLC) comprises 85% of all lung cancers and has a 5-year survival rate of 4% in case of metastatic disease². Current treatment options for advanced NSCLC include chemotherapy and radiotherapy, but these treatments only modestly improve survival. Recent advances made include the targeting of several driver-mutations responsible for tumor progression. Targeting the mutant EGF-receptor and the EML4-ALK fusion protein has been found effective, however, resistance to these therapies inevitably ensues³⁻⁵. Therefore, novel treatment strategies to improve NSCLC survival are warranted.

Immunotherapy aims to establish or enhance an effective immune response towards the tumor. This can be accomplished via different strategies including tumor vaccination, adoptive transfer of immune cells and modification of the immune system to boost an established immune response⁶. The latter category of drugs includes the checkpoint inhibitors anti-PD-(L)1 and anti-CTLA-4 that have recently been tested for efficacy in NSCLC⁷⁻⁹. The beneficial role for blocking CTLA-4 in NSCLC remains inconclusive^{9,10}, but PD-1 blockade has proven to be effective in treating NSCLC^{7,11}. Nevertheless, the majority of patients does not respond to checkpoint inhibition therapy^{7,12,13}.

There are several ways in which an immune response towards a tumor can be induced as has been described in some recent reviews on this topic^{6,14,15}. Tumor vaccines elicit an *in vivo* immune response specifically towards a tumor associated antigen formulated in the vaccine. This form of therapy has proven to be safe and effective in eliciting tumor-specific immune responses in different cancers including NSCLC¹⁶⁻¹⁸. It is also possible to circumvent endogenous antigen presentation by directly administering antigen stimulated T cells or dendritic cells (DCs)^{19,20}. Tumor vaccines and cellular therapies are aimed specifically towards tumor antigens and therefore have a limited toxicity profile as opposed to established chemotherapy and checkpoint blockade²¹⁻²³.

Eliciting potent T-cell response via vaccines or cellular therapies and simultaneously 'releasing the brakes' on these T cells with checkpoint inhibitors may unleash the full potential of immunotherapy and improve the proportion of patients responding to therapy. Synergies between checkpoint inhibitor therapy and tumor or cellular vaccines are currently being investigated in several clinical trials²⁴. Which form of immunotherapy; vaccine or cellular therapy, is most promising to combine with checkpoint inhibitors such as PD-1 blockers is currently unknown. In this meta-analysis we show that vaccination and cellular immunotherapies improved the overall survival (OS) and progression free survival (PFS) in NSCLC patients. Cellular therapies outperformed tumor vaccines for all the outcomes assessed. Other factors such as tumor histology or the preconditioning of patients with low dose cyclophosphamide had no effect on survival or PFS.

METHODS

Database search.

On the 17th of June 2015, we searched for relevant studies in the following databases: Embase, Medline (Ovid SP), Web of Science, Cochrane Central Register for Controlled Trials, Pubmed Publisher and Google Scholar. There were no limitations on the year of publication for all the databases interrogated. Search entries were constructed for each individual database (Supplementary data). The search initially involved other thoracic malignancies including SCLC and mesothelioma. No language restrictions were applied. We also searched manually through conference abstracts and checked references from relevant publications and review articles. All procedures were performed according to the PRISMA guidelines²⁵.

Eligibility.

Articles were included based on title and abstract if they concerned clinical evaluation of a tumor vaccine or cellular immunotherapy in NSCLC. Articles were excluded when they involved less than 5 NSCLC patients, or did not report well-defined clinical endpoints for survival or time to progression of disease. All articles on checkpoint blockade therapy or biological response modifiers (e.g. interferons, interleukins) were excluded. When we obtained all records on vaccine and cellular therapies in NSCLC, we selected the randomized controlled trials to study the efficacy of treatment. Studies that were not randomized or lacked complete outcome data were excluded for this particular research question. If multiple articles covered the same study population, the study with the most recent and complete survival data was used. Remaining studies that investigated the predictive value of immune factors in blood were later used for systematic review. Authors of the individual studies were contacted in case of missing data. Two investigators (F.D. and L.L.) independently screened abstracts and reviewed full texts for eligibility. Data extraction was performed (F.D. and G.V.) according to a predefined data extraction form. Any discrepancies were resolved by consensus with a third reviewer (J.A.).

Data collection and outcomes.

Treatment characteristics (type and timing of treatment, dose) patient demographics, tumor histology, disease stage (low stage disease ranging from stage I-II/IIIA and high stage disease being III(B)-IV), and relevant outcome measures were collected according to a predefined data extraction form. The outcome measures overall OS and progression free survival PFS were assessed, and when PFS was not available, time to progression (TTP) and relapse free survival (RFS) were included to increase the comparability and power of our analysis. These outcome measures were inconsistently reported as either hazard ratios

(HR) or as median months survival or time to disease progression or both, and all were included for further analysis. Tumor response rates were not evaluated because they were inconsistently reported and have been found to correlate poorly with immunotherapy efficacy²⁶. The risk of bias was determined using the Cochrane Collaboration Risk of Bias Assessment Tool²⁷.

Statistical Methods.

Random effects models were used to compute summary effect sizes for all the outcome measures investigated, thereby taking heterogeneity across studies into account^{28,29}. When available, HR from different studies were pooled to calculate the overall survival benefit of vaccine and cellular immunotherapy in NSCLC. Additionally, median differences were generated and combined when median survival times or median months PFS were reported. We addressed several possible sources of heterogeneity (expressed as I^2) including type of immunotherapy (tumor vaccine vs. cellular therapy), limited or advanced disease (I-II/IIIA vs. III(B)-IV), histology (% adenocarcinoma), preconditioning therapy with low dose cyclophosphamide (in case of vaccines) and concurrent administration of chemotherapy, using subgroup analysis and meta-regression (in case of the proportion adenocarcinoma). Funnel plots were generated to assess the presence of publication bias. In order to define the extent of publication bias, Duval and Tweedie's trim and fill test and the classic fail-safe N test were used³⁰. The Begg and Mazumdar rank correlation test and the Egger test were applied in case of suspected publication bias to quantify the level of bias^{31,32}. All analyses were performed by a biostatistician (L.A.), using a registered copy of Comprehensive Meta-Analysis statistical software (version 2.2.064; Biostat, Englewood, NJ).

RESULTS

Search strategy result and study characteristics of included trials

Our database and manual searches yielded a total of 7832 records of which 5992 records remained following removal of duplicate articles (Figure 1). 4 additional records were manually selected from conference abstracts and reference lists. All records were screened based on title and abstract to identify trials investigating the benefit of tumor vaccination or cellular immunotherapy in the context of NSCLC. After screening, a total of 114 potential records remained that were eligible for full-text assessment. Of these, 18 individual randomized controlled trials (RCT) were eligible for subsequent meta-analysis.

The 18 RCTs included in our analysis comprised a total of 6756 patients treated with immunotherapy for NSCLC distributed over different outcome measures. A summary of the

main study characteristics is listed in table 1. Most studies focused on late stage disease (15/18 trials stage III(B)-IV). The type of treatment was evenly distributed, with 10 studies investigating tumor vaccines and the other 8 treating patients with either DC-therapy, a form of T-cell therapy (AKT; autologous activated killer T cells or CIK; cytokine induced killer cells) or a combination of the two. The proportion of adenocarcinoma histology varied extensively between studies ranging from 28-88% of total cancers. Immunotherapy was administered as monotherapy with or without low dose cyclophosphamide preconditioning or concurrently with chemotherapy. The control treatment arm was heterogeneously composed of control groups receiving only the placebo or best supportive care (BSC) and others receiving chemotherapy (when immunotherapy was combined with chemotherapy in the experimental arm). There were no studies that investigated the efficacy of tumor vaccines or cellular therapies alone versus chemotherapy treatment.

Immunotherapy significantly prolongs NSCLC survival and delays tumor progression.

Studies reported different outcome measures with some reporting hazard ratios of disease progression or survival while others reported only median overall survival and/or time to disease progression in months. We therefore analyzed HR and the differences in medians for survival and PFS separately. Cancer immunotherapy was found to be effective in extending NSCLC overall survival and PFS, both expressed as HR (cumulative OS: HR=0.81, 95%CI=0.70-0.94, $p=0.01$, PFS: HR=0.83, 95%CI=0.72-0.95, $p=0.006$, Figure 2) and median month difference (cumulative OS: difference=5.43 months, 95%CI=3.20-7.65, $p<0.005$, PFS: difference=3.24 months, 95%CI=1.61-4.88, $p<0.005$, Figure 3).

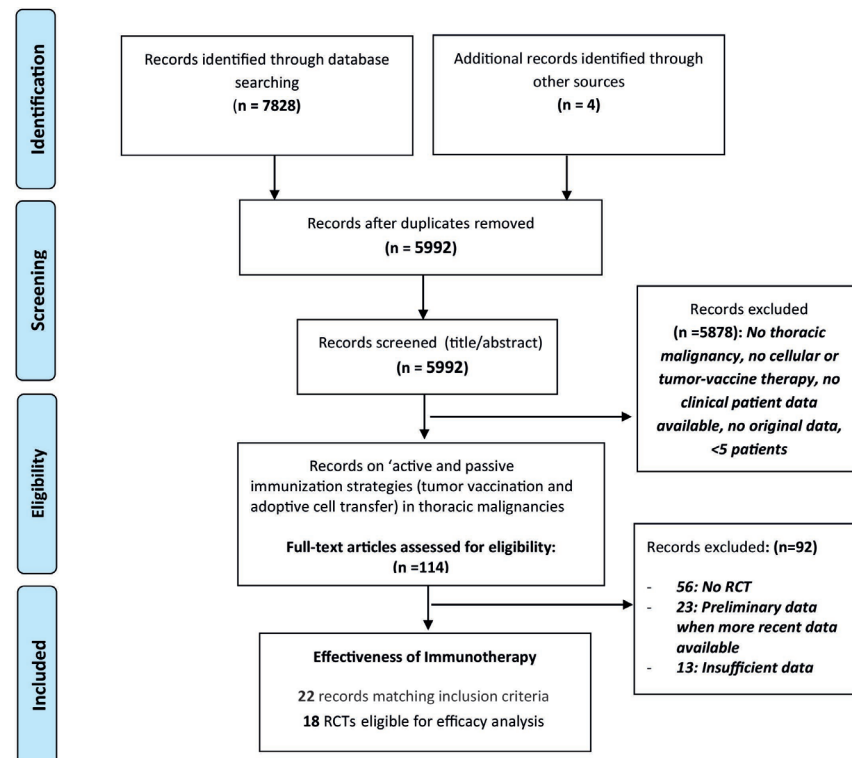


Figure 1. Prisma Flow Chart displaying the search and selection process performed.

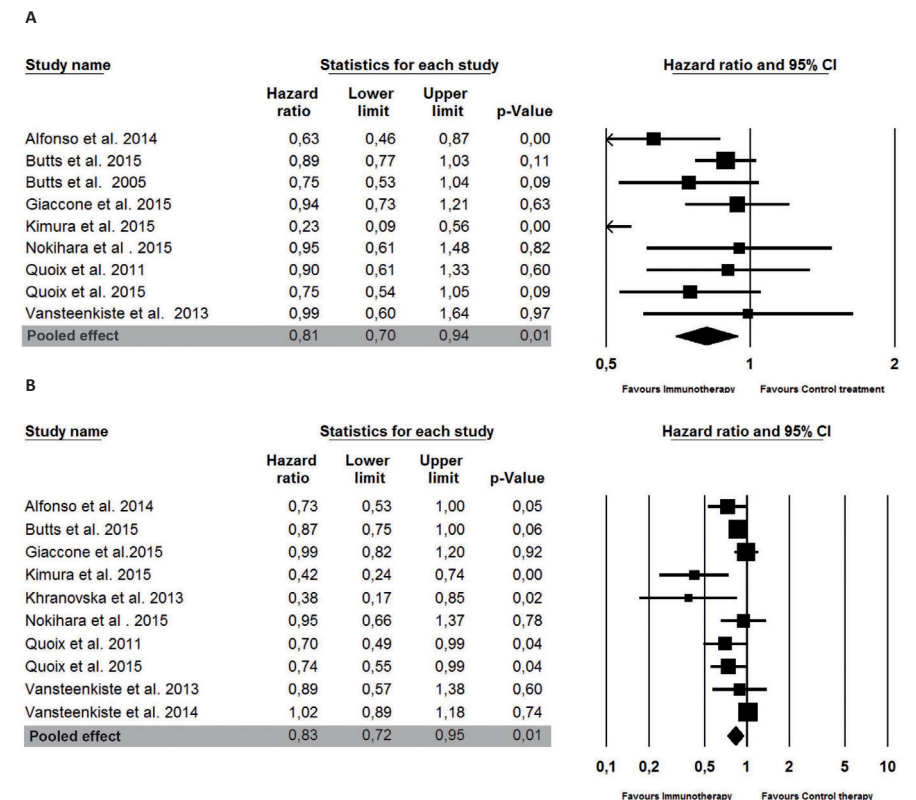
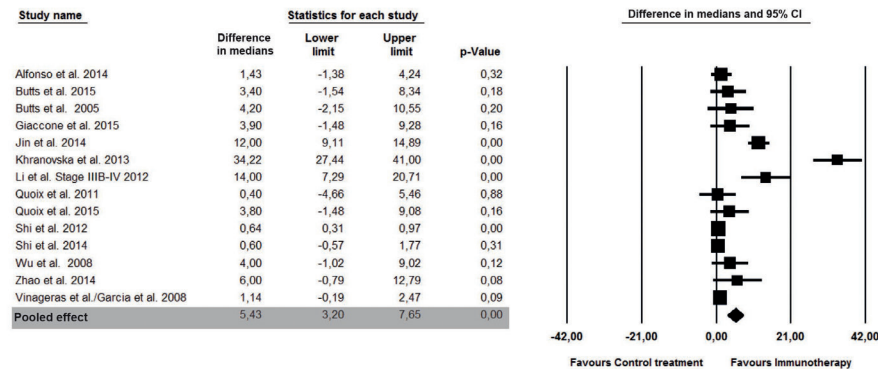


Figure 2. (A) Overall survival and (B) progression free survival when hazard ratios (HR) were reported.

PART B
Improving the efficacy of
cancer vaccines for solid tumors
by combination immunotherapy

THE EFFICACY OF TUMOR VACCINES
AND CELLULAR IMMUNOTHERAPIES IN
NON-SMALL CELL LUNG CANCER:
A SYSTEMATIC REVIEW AND META-ANALYSIS

A



B

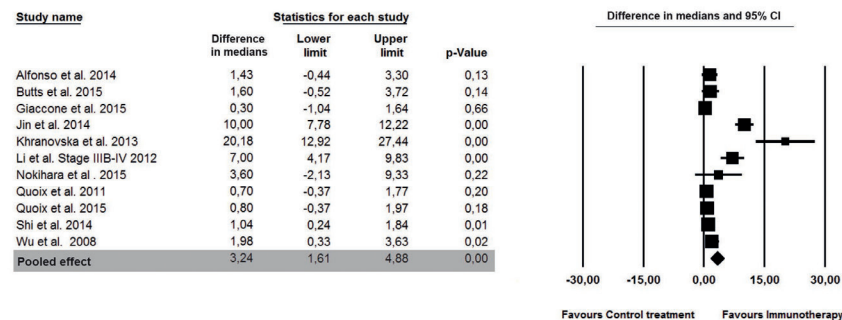


Figure 3. (A) Overall survival and (B) progression free survival expressed as mean differences in months when median overall survival data were reported.

Cellular immunotherapeutic strategies perform significantly better than tumor vaccination therapies.

There was a moderate level of heterogeneity between sample estimates for both overall survival and PFS expressed as HR (OS: $I^2=43.9\%$, PFS: $I^2=57.7\%$) and significant heterogeneity for outcome measures expressed in months (OS: $I^2=86.5\%$, PFS: $I^2=85.8\%$). To test whether this heterogeneity could be attributed to differences in type of immunotherapy (vaccine or cellular therapies), disease stage (low vs. high), concurrent chemotherapy, NSCLC histology (% adenocarcinoma) or preconditioning with low dose cyclophosphamide, subgroup analysis and meta-regression were performed. Significant heterogeneity existed between studies evaluating tumor vaccination and cellular immunotherapy treatments, with

cellular therapies being more effective than tumor vaccines for all outcome parameters evaluated (OS as HR: $p=0.005$ and median month difference: $p=0.001$, PFS as HR: $p=0.001$ and as median month difference: $p=0.004$, Table 2). There were no significant differences in survival or disease progression between studies investigating immunotherapy in high versus low stage NSCLC disease, except for the difference in median months progression free survival, being more favorable for studies involving low stage NSCLC compared to high stage disease ($p=0.010$). Studies that evaluated immunotherapy with concurrent chemotherapy performed better than studies investigating immunotherapy alone, only for time to disease progression as HR ($p=0.030$) There was no correlation between the proportion of patients with adenocarcinoma histology and the standardized mean difference for survival ($p=0.448$) or PFS ($p=0.426$, Supplementary figure 1) nor could we detect a benefit of pre-conditioning with cyclophosphamide in case of the tumor vaccines (HR OS: $p=0.577$, HR PFS: $p=0.928$).

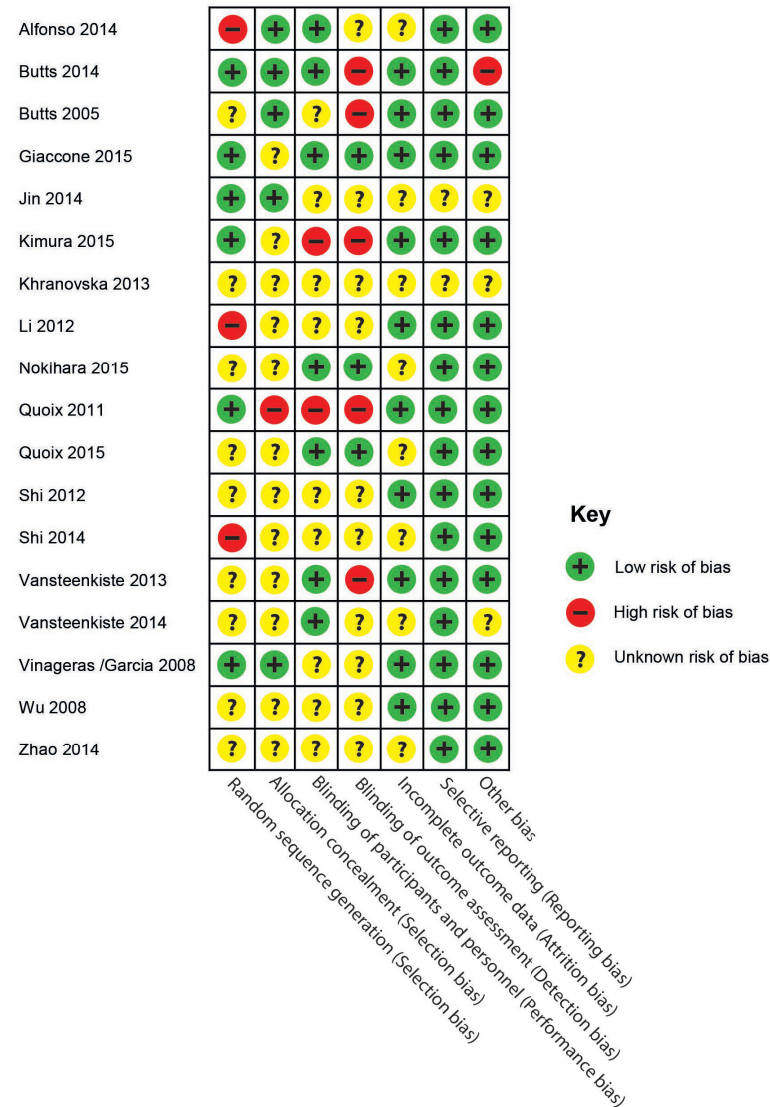
Bias assessment.

The level of bias per study was assessed using the Cochrane Collaboration Risk of Bias assessment tool²⁷. The level of bias varied extensively between studies, with several studies being deficient in thorough methodological reporting, which was in most cases due to an abstract that was available³³⁻³⁶. The studies that properly reported randomization procedures, blinding and all outcome measures were generally low in bias^{21,37,38}, but selection bias and detection bias could be detected in some trials, or were not reported³⁹⁻⁴¹ (Figure 4). With the exception of 3 studies with an unclear risk of bias^{33,35,36}, all studies lacked reporting bias, attrition bias and other sources of bias not specifically addressed by the Cochrane Collaboration risk of bias tool.

Funnel plots were constructed to investigate the presence of publication bias. There was no or minimal publication bias for overall survival expressed as HR and median months difference (Supplementary figure 2A and 2C). Adjusted values after Duval and Tweedie's trim and fill test revealed no significant alteration of the observed point estimate (data not shown). There was no publication bias for the outcome PFS expressed as median month difference (Supplementary figure 2D). There was, however, possible publication bias for PFS expressed as HR (Supplementary figure 2B), as indicated by a potential loss of significance from the Duval and Tweedie's trim and fill test (data not shown). Additional tests to quantify publication bias were inconclusive (the Egger test being significant for publication bias but two tailed Begg and Mazumdar's test not). Also, the classic fail-safe N indicated that 40 additional studies would be required to reach a p-value greater than alpha ($p=0.05$, data not shown). Therefore, the presence of publication bias for PFS expressed as HR remains uncertain.

PART B
Improving the efficacy of
cancer vaccines for solid tumors
by combination immunotherapy

THE EFFICACY OF TUMOR VACCINES
AND CELLULAR IMMUNOTHERAPIES IN
NON-SMALL CELL LUNG CANCER:
A SYSTEMATIC REVIEW AND META-ANALYSIS



DISCUSSION

Targeting the immune system to combat cancer is an effective way to enhance survival and prolong time until progression in NSCLC. In contrast to disease modifying drugs such as cytokines (IL-2, interferons) and the recently investigated checkpoint inhibitors, tumor vaccines and cellular therapies induce formation of specific tumor directed cytotoxic T cells capable of destroying cancer cells. Because of their high specificity, based on the selection of only tumor associated antigens, tumor vaccines and cellular immunotherapies are associated with limited side effects, but the efficacy of these therapies, with tumor vaccines in particular, has been controversial^{42,43}. In this meta-analysis, combining the data from all published tumor vaccine trials resulted in a significantly improved survival and prolonged time to disease progression. These results were even more pronounced for the cellular therapies. The distinction between these two immunotherapeutic strategies was the only factor that was consistently different for all outcome measures analyzed. Other factors such as disease stage and combination chemotherapy also significantly differed regarding clinical efficacy albeit not for all outcome measures. Tumor histology was not significantly associated with changes in survival or time to disease progression.

Large phase III studies such as the MAGRIT trial and the Belagenpumatucl-L phase III trial were initiated following promising phase II results but were prematurely terminated due to lack of clinical efficacy⁴². Discordant results of phase II and III studies in NSCLC research have been reported by others in the past and are thought to arise from differences in phase II and III study population characteristics, size and the (intermediate) outcome measures and the target effect size aimed for⁴⁴. Most of the phase III studies included in our analysis concerned tumor vaccination trials, and these studies attributed the majority of patients to our analysis. Given the disappointing results of these trials it is remarkable that in our meta-analysis tumor vaccination therapies significantly enhanced survival and time to disease progression, suggesting insufficient power in previous phase III trials.

Even though there was no or limited publication bias for the majority of parameters investigated, overrepresentation of phase II studies in the cellular therapies included could have attributed to the differences in efficacy compared to tumor vaccination therapy. On the other hand, it may be ascribed to the activation of the immune system with cellular therapies such as DC- and T-cell therapy. First, cellular therapies partially or totally circumvent potential immune suppression induced by vaccination and therefore directly activate anti-tumor T cells capable of targeting the tumor^{19,45}. Secondly, whereas vaccines target one predominant tumor antigen, DC (and to a lesser extent T cells) activated *in vitro* could potentially induce a polyclonal antitumor response^{46,47}. This might prevent immune escape by the tumor and induce immune responses to a multitude of tumor antigens.

Figure 4. The assessment of bias of included studies using the Cochrane Collaboration Risk of Bias Assessment Tool.

Screening patients before vaccination for expression of the targeted tumor antigen and designing personalized tumor vaccines could increase response rates to tumor vaccines^{48,49}. Several studies have correlated a specific immune response to the vaccine with increased survival and tumor responses following therapy^{37,50-57}. Identifying these patients before or after the first vaccination as a way of personalized therapy could specifically benefit those that are most likely to respond and favor the use of combination treatment in non-responding patients.

We found a statistically significant effect of chemotherapy combined with immunotherapy for the hazard ratio of disease progression, but not for other outcome measures. Chemotherapy could synergize with immunotherapies by causing immunogenic cell death of cancer cells and by disrupting immune evasion pathways but timing of combination therapies is crucial⁵⁸. We found no additive effect on tumor vaccine efficacy of low dose cyclophosphamide in our analysis (table 2), but this could be due to the limited amount of studies available for analysis. Also, few studies reported antibody responses towards the vaccine making it difficult to assess the effect of prior immune modulation. Importantly, to further target immune evasion pathways in patients, enhancing anti-tumor T-cell functionality with checkpoint inhibitors acting via PD-L1/PD-1 blockade could further improve therapeutic efficacy⁵⁹. The PD-1 blocking antibodies Nivolumab and Pembrolizumab have been recently approved for NSCLC treatment following positive phase III results^{7,60}.

There are several limitations relevant to this meta-analysis. First, there was a limited amount of studies available for some outcome measures investigated with subgroup analysis (e.g. OS HR for type of therapy and disease stage). Secondly, variability in control treatments with cellular therapies (BSC) and vaccine studies (mostly placebo) could have biased our results in favor of cellular immunotherapy. Because of incomplete reporting and heterogeneity in methodology we did not further investigate potential immune markers (e.g. antibody responses following vaccination) that could be predictive for therapeutic efficacy. More studies will have to be awaited to properly address this issue. Finally, bias could not be assessed in several of the studies included. Therefore, we did not perform sensitivity analysis after exclusion of studies with a high or unspecified degree of bias. Several larger phase 3 studies on tumor vaccines and cellular therapies are still awaited and it is inevitable in meta-analysis that studies will be missed. However, this meta-analysis is the first analysis to give a comprehensive overview of specific immunotherapies in NSCLC, assessing both tumor vaccines and cellular therapies.

In conclusion, specific immunotherapies significantly prolong NSCLC survival and PFS. Cellular immunotherapies are more effective than tumor vaccines for all outcome measures evaluated. Low stage disease and the concurrent use of chemotherapy improved efficacy but only for disease progression in months, and as hazard ratio, respectively. There was no

association between treatment efficacy and adenocarcinoma histology or preconditioning low dose cyclophosphamide. These findings are useful for the design of future studies investigating immunotherapies in NSCLC and possible synergistic combination strategies that could improve patient survival.

PART B
Improving the efficacy of
cancer vaccines for solid tumors
by combination immunotherapy

THE EFFICACY OF TUMOR VACCINES
AND CELLULAR IMMUNOTHERAPIES IN
NON-SMALL CELL LUNG CANCER:
A SYSTEMATIC REVIEW AND META-ANALYSIS

REFERENCES

- 1 Ettinger, D. S. et al. Non-small cell lung cancer, version 2.2013. Journal of the National Comprehensive Cancer Network : JNCCN 11, 645-653; quiz 653 (2013).
- 2 Cetin, K., Ettinger, D. S., Hei, Y.-j. & O'Malley, C. D. Survival by histologic subtype in stage IV nonsmall cell lung cancer based on data from the Surveillance, Epidemiology and End Results Program. Clinical Epidemiology 3, 139-148, doi:10.2147/CLEP.S17191 (2011).
- 3 Kobayashi, S. et al. EGFR mutation and resistance of non-small-cell lung cancer to gefitinib. The New England journal of medicine 352, 786-792, doi:10.1056/NEJMoa044238 (2005).
- 4 Katayama, R. et al. Mechanisms of acquired crizotinib resistance in ALK-rearranged lung Cancers. Science translational medicine 4, 120ra117, doi:10.1126/scitranslmed.3003316 (2012).
- 5 Lynch, T. J. et al. Activating mutations in the epidermal growth factor receptor underlying responsiveness of non-small-cell lung cancer to gefitinib. The New England journal of medicine 350, 2129-2139, doi:10.1056/NEJMoa040938 (2004).
- 6 Aerts, L., Hoogsteden, Hegmans. Immunotherapy prospects in the treatment of lung cancer and mesothelioma. Translational Lung Cancer Research 34-45 (2013).
- 7 Brahmer, J. et al. Nivolumab versus Docetaxel in Advanced Squamous-Cell Non-Small-Cell Lung Cancer. The New England journal of medicine 373, 123-135, doi:10.1056/NEJMoa1504627 (2015).
- 8 Garon, E. B. et al. Pembrolizumab for the treatment of non-small-cell lung cancer. The New England journal of medicine 372, 2018-2028, doi:10.1056/NEJMoa1501824 (2015).
- 9 Zatloukal P, H. D., Park K, Kang J, Butts C, Bradford S, et al. Randomized phase II clinical trial comparing tremelimumab (CP-675,206) with best supportive care following first line platinum-based therapy in patients with advanced non-small cell lung cancer. J Clin Oncol 27:15s, 2009 (suppl;abstr 8071) (2009).
- 10 Lynch, T. J. et al. Ipilimumab in combination with paclitaxel and carboplatin as first-line treatment in stage IIIB/IV non-small-cell lung cancer: results from a randomized, double-blind, multicenter phase II study. Journal of clinical oncology : official journal of the American Society of Clinical Oncology 30, 2046-2054, doi:10.1200/jco.2011.38.4032 (2012).
- 11 Borghaei, H. et al. Nivolumab versus Docetaxel in Advanced Nonsquamous Non-Small-Cell Lung Cancer. The New England journal of medicine 373, 1627-1639 (2015).
- 12 Garon, E. B. et al. Pembrolizumab for the Treatment of Non-Small-Cell Lung Cancer. The New England journal of medicine, doi:10.1056/NEJMoa1501824 (2015).
- 13 Rizvi, N. A. et al. Activity and safety of nivolumab, an anti-PD-1 immune checkpoint inhibitor, for patients with advanced, refractory squamous non-small-cell lung cancer (CheckMate 063): a phase 2, single-arm trial. The Lancet. Oncology 16, 257-265, doi:10.1016/s1470-2045(15)70054-9 (2015).
- 14 Tartour, E. & Zitvogel, L. Lung cancer: potential targets for immunotherapy. Lancet Respir Med 1, 551-563 (2013).
- 15 Anagnostou, V. K. & Brahmer, J. R. Cancer immunotherapy: a future paradigm shift in the treatment of non-small cell lung cancer. Clinical cancer research : an official journal of the American Association for Cancer Research 21, 976-984 (2015).
- 16 Kenter, G. G. et al. Vaccination against HPV-16 oncoproteins for vulvar intraepithelial neoplasia. The New England journal of medicine 361, 1838-1847, doi:10.1056/NEJMoa0810097 (2009).
- 17 Slingluff, C. L., Jr. et al. A randomized phase II trial of multipitope vaccination with melanoma peptides for cytotoxic T cells and helper T cells for patients with metastatic melanoma (E1602). Clinical cancer research : an official journal of the American Association for Cancer Research 19, 4228-4238, doi:10.1158/1078-0432.ccr-13-0002 (2013).
- 18 Nemunaitis, J. et al. Phase II study of belagenpumatucel-L, a transforming growth factor beta-2 antisense gene-modified allogeneic tumor cell vaccine in non-small-cell lung cancer. J Clin Oncol 24, 4721-4730 (2006).
- 19 Palucka, K. & Banchereau, J. Cancer immunotherapy via dendritic cells. Nature reviews. Cancer 12, 265-277, doi:10.1038/nrc3258 (2012).
- 20 Hegmans, J. P. et al. Consolidative dendritic cell-based immunotherapy elicits cytotoxicity against malignant mesothelioma. American journal of respiratory and critical care medicine 181, 1383-1390, doi:10.1164/rccm.200909-1465OC (2010).
- 21 Giaccone, G. et al. A phase III study of belagenpumatucel-L, an allogeneic tumour cell vaccine, as maintenance therapy for non-small cell lung cancer. European journal of cancer, doi:10.1016/j.ejca.2015.07.035 (2015).
- 22 Butts, C. et al. Tecemotide (L-BLP25) versus placebo after chemoradiotherapy for stage III non-small-cell lung cancer (START): a randomised, double-blind, phase 3 trial. The Lancet. Oncology 15, 59-68, doi:10.1016/s1470-2045(13)70510-2 (2014).
- 23 Wang, M. et al. Evaluation of tumour vaccine immunotherapy for the treatment of advanced non-small cell lung cancer: a systematic meta-analysis. BMJ Open 5, e006321 (2015).
- 24 Mahoney, K. M., Rennert, P. D. & Freeman, G. J. Combination cancer immunotherapy and new immunomodulatory targets. Nat Rev Drug Discov 14, 561-584, doi:10.1038/nrd4591 (2015).
- 25 Moher, D., Liberati, A., Tetzlaff, J., Altman, D. G. & Group, P. Preferred reporting items for systematic reviews and meta-analyses: the PRISMA statement. BMJ 339, b2535 (2009).
- 26 Hales, R. K. et al. Assessing oncologic benefit in clinical trials of immunotherapy agents. Annals of oncology : official journal of the European Society for Medical Oncology / ESMO 21, 1944-1951, doi:10.1093/annonc/mdq048 (2010).
- 27 Higgins, J. P. et al. The Cochrane Collaboration's tool for assessing risk of bias in randomised trials. Bmj 343, d5928, doi:10.1136/bmj.d5928 (2011).
- 28 Dersimonian, R. & Laird, N. Metaanalysis in Clinical-Trials. Control Clin Trials 7, 177-188, doi:10.1016/0197-2456(86)90046-2 (1986).
- 29 van Houwelingen, H. C., Arends, L. R. & Stijnen, T. Advanced methods in meta-analysis: multivariate approach and meta-regression. Stat Med 21, 589-624 (2002).
- 30 Duval, S. & Tweedie, R. Trim and fill: A simple funnel-plot-based method of testing and adjusting for publication bias in meta-analysis. Biometrics 56, 455-463 (2000).
- 31 Begg, C. B. & Mazumdar, M. Operating characteristics of a rank correlation test for publication bias. Biometrics 50, 1088-1101 (1994).
- 32 Egger, M., Davey Smith, G., Schneider, M. & Minder, C. Bias in meta-analysis detected by a simple, graphical test. BMJ 315, 629-634 (1997).
- 33 Khranovska, N. et al. Results from phase iii trial of dendritic cell based vaccine immunotherapy in patients with-iiia stage non-small-cell lung cancer. J Thorac Oncol 8, S910 (2013).
- 34 Zhao, M., Li, H., Li, L. & Zhang, Y. Effects of a gemcitabine plus platinum regimen combined with a dendritic cell-cytokine induced killer immunotherapy on recurrence and survival rate of non-small cell lung cancer patients. Exp Ther Med 7, 1403-1407 (2014).
- 35 Jin, C. et al. Impact of Cellular Immune Function on Prognosis of Lung Cancer Patients after Cytokine-induced Killer Cell Therapy. Asian Pac J Cancer Prev 15, 6009-6014 (2014).
- 36 Vansteenkiste, J. F. et al. 1173OMAGRIT, A DOUBLE-BLIND, RANDOMIZED, PLACEBO-CONTROLLED PHASE III STUDY TO ASSESS THE EFFICACY OF THE RECMAGE-A3 + AS15 CANCER IMMUNOTHERAPEUTIC AS ADJUVANT THERAPY IN PATIENTS WITH RESECTED MAGE-A3-POSITIVE NON-SMALL CELL LUNG CANCER (NSCLC). Annals of Oncology 25, iv409, doi:10.1093/annonc/mdu347.1 (2014).
- 37 Alfonso, S. et al. A randomized, multicenter, placebo-controlled clinical trial of racotumomab-alum vaccine as switch maintenance therapy in advanced non-small cell lung cancer patients. Clinical cancer research : an official journal of the American Association for Cancer Research 20, 3660-3671, doi:10.1158/1078-0432.ccr-13-1674 (2014).
- 38 Butts, C. et al. Tecemotide (L-BLP25) versus placebo after chemoradiotherapy for stage III non-small-cell lung cancer (START): a randomised, double-blind, phase 3 trial. The Lancet Oncology 15, 59-68, doi:10.1016/s1470-2045(13)70510-2 (2014).
- 39 Wu, C., Jiang, J., Shi, L. & Xu, N. Prospective study of chemotherapy in combination with cytokine-induced killer cells in patients suffering from advanced non-small cell lung cancer. Anticancer research 28, 3997-4002 (2008).
- 40 Vansteenkiste, J. et al. Adjuvant MAGE-A3 immunotherapy in resected non-small-cell lung cancer: phase II randomized study results. J Clin Oncol 31, 2396-2403 (2013).
- 41 Shi, S. B., Ma, T. H., Li, C. H. & Tang, X. Y. Effect of maintenance therapy with dendritic cells: Cytokine-induced killer cells in patients with advanced non-small cell lung cancer. Tumori 98, 314-319 (2012).
- 42 Cuppens, K. & Vansteenkiste, J. Vaccination therapy for non-small-cell lung cancer. Current opinion in oncology 26, 165-170, doi:10.1097/Cco.000000000000052 (2014).
- 43 Rosenberg, S. A., Yang, J. C. & Restifo, N. P. Cancer immunotherapy: moving beyond current vaccines. Nature medicine 10, 909-915, doi:10.1038/nm1100 (2004).

PART B
Improving the efficacy of
cancer vaccines for solid tumors
by combination immunotherapy

**THE EFFICACY OF TUMOR VACCINES
AND CELLULAR IMMUNOTHERAPIES IN
NON-SMALL CELL LUNG CANCER:
A SYSTEMATIC REVIEW AND META-ANALYSIS**

44 Lara, P. N. & Redman, M. W. The hazards of randomized phase II trials. *Annals of oncology : official journal of the European Society for Medical Oncology / ESMO* 23, 7-9, doi:10.1093/annonc/mdr567 (2012).

45 Restifo, N. P., Dudley, M. E. & Rosenberg, S. A. Adoptive immunotherapy for cancer: harnessing the T cell response. *Nature reviews. Immunology* 12, 269-281, doi:10.1038/nri3191 (2012).

46 Godelaine, D. et al. Polyclonal CTL responses observed in melanoma patients vaccinated with dendritic cells pulsed with a MAGE-3A1 peptide. *Journal of Immunology* 171, 4893-4897 (2003).

47 Carreno, B. M. et al. Cancer immunotherapy. A dendritic cell vaccine increases the breadth and diversity of melanoma neoantigen-specific T cells. *Science* 348, 803-808, doi:10.1126/science.aaa3828 (2015).

48 Noguchi, M., Sasada, T. & Itoh, K. Personalized peptide vaccination: a new approach for advanced cancer as therapeutic cancer vaccine. *Cancer Immunol Immun* 62, 919-929, doi:10.1007/s00262-012-1379-1 (2013).

49 Pol, J. et al. Trial Watch: Peptide-based anticancer vaccines. *Oncoimmunology* 4, doi:10.4161/216240.2X.2014.974411 (2015).

50 Antonia, S. J. et al. Combination of p53 cancer vaccine with chemotherapy in patients with extensive stage small cell lung cancer. *Clinical cancer research : an official journal of the American Association for Cancer Research* 12, 878-887 (2006).

51 Barve, M. et al. Induction of immune responses and clinical efficacy in a phase II trial of IDM-2101, a 10-epitope cytotoxic T-lymphocyte vaccine, in metastatic non-small-cell lung cancer. *J Clin Oncol* 26, 4418-4425 (2008).

52 Bolonaki, I. et al. Vaccination of patients with advanced non-small-cell lung cancer with an optimized cryptic human telomerase reverse transcriptase peptide. *Journal of clinical oncology : official journal of the American Society of Clinical Oncology* 25, 2727-2734 (2007).

53 Brunsvig, P. F. et al. Telomerase peptide vaccination in NSCLC: a phase II trial in stage III patients vaccinated after chemoradiotherapy and an 8-year update on a phase I/II trial. *Clinical cancer research : an official journal of the American Association for Cancer Research* 17, 6847-6857, doi:10.1158/1078-0432.ccr-11-1385 (2011).

54 Fakhrai, H., Tong, A., Nemunaitis, J. & Shawler, D. L. Correlation of immune responses and survival in a phase II study of belagenpumatucel-L in non-small cell lung cancer. *Journal of clinical oncology : official journal of the American Society of Clinical Oncology* 27, 3013 (2009).

55 Garcia, B. et al. Effective inhibition of the epidermal growth factor/epidermal growth factor receptor binding by anti-epidermal growth factor antibodies is related to better survival in advanced non-small-cell lung cancer patients treated with the epidermal growth factor cancer vaccine. *Clinical cancer research : an official journal of the American Association for Cancer Research* 14, 840-846, doi:10.1158/1078-0432.CCR-07-1050 (2008).

56 Kotsakis, A. et al. A phase II trial evaluating the clinical and immunologic response of HLA-A2+ non-small cell lung cancer patients vaccinated with an hTERT cryptic peptide. *Lung cancer*, doi:10.1016/j.lungcan.2014.07.018 (2014).

57 Ramlau, R. et al. A phase II study of Tg4010 (Mva-Muc1-II2) in association with chemotherapy in patients with stage III/IV non-small cell lung cancer. *Journal of thoracic oncology : official publication of the International Association for the Study of Lung Cancer* 3, 735-744 (2008).

58 Emens, L. A. & Middleton, G. The interplay of immunotherapy and chemotherapy: harnessing potential synergies. *Cancer immunology research* 3, 436-443, doi:10.1158/2326-6066.cir-15-0064 (2015).

59 Postow, M. A., Callahan, M. K. & Wolchok, J. D. Immune Checkpoint Blockade in Cancer Therapy. *Journal of clinical oncology : official journal of the American Society of Clinical Oncology*, doi:10.1200/jco.2014.59.4358 (2015).

60 Garon, E. B. et al. Pembrolizumab for the Treatment of Non-Small-Cell Lung Cancer. *New England Journal of Medicine* 372, 2018-2028, doi:10.1056/NEJMoa1501824 (2015).

61 Mitchell, P. et al. Tecemotide in unresectable stage III non-small-cell lung cancer in the phase III START study: updated overall survival and biomarker analyses. *Annals of oncology : official journal of the European Society for Medical Oncology / ESMO* 26, 1134-1142 (2015).

62 Butts, C. et al. Randomized phase IIB trial of BLP25 liposome vaccine in stage IIB and IV non-small-cell lung cancer. *Journal of clinical oncology : official journal of the American Society of Clinical Oncology* 23, 6674-6681 (2005).

63 Butts, C. et al. Updated survival analysis in patients with stage IIB or IV non-small-cell lung cancer receiving BLP25 liposome vaccine (L-BLP25): Phase IIB randomized, multicenter, open-label trial. *Journal of cancer research and clinical oncology* 137, 1337-1342 (2011).

64 Kimura, H. et al. (2015 EMBASE search) Randomized controlled phase III trial of adjuvant chemo-immunotherapy with activated killer T cells and dendritic cells in patients with resected primary lung cancer. *Cancer immunology, immunotherapy : CII* 64, 51-59, doi:10.1007/s00262-014-1613-0 (2015).

65 Skachkova, O. V. et al. Immunological markers of anti-tumor dendritic cells vaccine efficiency in patients with non-small cell lung cancer. *Exp Oncol* 35, 109-113 (2013).

66 Li, R. et al. Autologous cytokine-induced killer cell immunotherapy in lung cancer: A phase II clinical study. *Cancer immunology, immunotherapy : CII* 61, 2125-2133 (2012).

67 Hiroshi Nokihara, N. K., Toyoaki Hida, Fumio Imamura, Hiroshi Sakai, Shinji Atagi, Makoto Nishio, Christoph Helwig, Hiroyuki Achiwa, Tomohide Tamura. Phase I/II study of tecemotide cancer immunotherapy for Japanese patients with unresectable stage III non-small cell lung cancer (NSCLC). *J Clin Oncol* 33, 2015 (suppl; abstr 3036) (2015).

68 Quoix, E. et al. Therapeutic vaccination with TG4010 and first-line chemotherapy in advanced non-small-cell lung cancer: A controlled phase 2B trial. *The Lancet. Oncology* 12, 1125-1133 (2011).

69 Elisabeth A. Quoix, J. J. N., Tomasz Burzykowski, Berangere Bastien, Gisele Lacoste. TIME: A phase IIb/III randomized, double-blind, placebo-controlled study comparing first-line therapy with or without TG4010 immunotherapy product in patients with stage IV non-small cell lung cancer (NSCLC). *J Clin Oncol* 30, 2012 (suppl; abstr TPS7610) (2015).

70 Shi, S. B. et al. Efficacy of erlotinib plus dendritic cells and cytokine-induced killer cells in maintenance therapy of advanced non-small cell lung cancer. *J Immunother* 37, 250-255 (2014).

71 Garcia Verdecia, B. et al. Effective inhibition of the epidermal growth factor/epidermal growth factor receptor binding by anti-epidermal growth factor antibodies is related to better survival in advanced non-small-cell lung cancer patients treated with the epidermal growth factor cancer vaccine. *Clinical cancer research : an official journal of the American Association for Cancer Research* 14, 840-846 (2008).

72 Neninger Vinageras, E. et al. Phase II randomized controlled trial of an epidermal growth factor vaccine in advanced non-small-cell lung cancer. *Journal of clinical oncology : official journal of the American Society of Clinical Oncology* 26, 1452-1458, doi:10.1200/JCO.2007.11.5980 (2008).

PART B
Improving the efficacy of
cancer vaccines for solid tumors
by combination immunotherapy

THE EFFICACY OF TUMOR VACCINES
AND CELLULAR IMMUNOTHERAPIES IN
NON-SMALL CELL LUNG CANCER:
A SYSTEMATIC REVIEW AND META-ANALYSIS

TABLES

Table 1. List of Study Characteristics.

Reference	Type Article	Stage	No.of patients	% Adeno- carcinoma	Previous Treatments
Alfonso et al. 2014 ³⁷	Peer-reviewed	IIIB-IV	176	29%	First line chemotherapy
Butts et al. 2015 ^{22,61}	Peer-reviewed	IIIA-IIIB	1239	35%	Chemo-radiotherapy
Butts et al. 2005 ^{62,63}	Peer-reviewed	IIIB-IV	171	not reported	First line chemotherapy
Giaccone et al.2015 ²¹	Peer-reviewed	IIIA-IV	532	60%	first line chemotherapy +/- radiotherapy
Jin et al. 2014 ³⁵	Peer-reviewed	I-IIIA	943	28%	Surgery
Kimura et al. 2015 ⁶⁴	Peer-reviewed	II-IV	101	76%	Surgery +/- induction chemotherapy (IIIA)
Khranovska et al. 2013 ^{33,65}	Peer-reviewed	IIB-IIIA	120	not reported	Surgery
Li et al. Stage IIIB-IV 2012 ⁶⁶	Peer-reviewed	IIIB-IV	74	62%	No previous treatment
Nokihara et al. 2015 ⁶⁷	Abstract	III	172	67%	Chemo-radiotherapy
Quoix et al. 2011 ⁶⁸	Peer-reviewed	IIIB-IV	148	64%	No previous treatment
Quoix et al. 2015 ⁶⁹	Abstract	IV	222	88%	No previous treatment
Shi et al. 2012 ⁴¹	Peer-reviewed	IIIB-IV	60	47%	First line chemotherapy
Shi et al. 2014 ⁷⁰	Peer-reviewed	IIIB-IV	54	82%	First line chemotherapy
Vansteenkiste et al. 2013 ⁴⁰	Peer-reviewed	IB-II	182	34%	Surgery
Vansteenkiste et al. 2014 ³⁶	Abstract	IB-IIIA	2272	not reported	Surgery
Vinageras et al. /Garcia et al. 2008 ^{71,72}	Peer-reviewed	IIIB-IV	74	33%	First line chemotherapy
Wu et al. 2008 ³⁹	Peer-reviewed	IIIA- IV	59	41%	No previous treatment
Zhao et al. 2014 ³⁴	Peer-reviewed	III	157	56%	Surgery

Treatment type	Intervention Treatment	Control Treatment
Tumor Vaccine	Racotumomab (anti-idiotypic NeuGcGM3 antibody)	Placebo
Tumor Vaccine	low-dose cyclophosphamide I.V. (300mg/m ²) + Tecemotide (L-BLP25= MUC1 Ag)	Saline + Placebo
Tumor Vaccine	low-dose cyclophosphamide I.V. (300mg/m ²) + Tecemotide (L-BLP25= MUC1 Ag)	BSC
Tumor Vaccine	Belagenpumatucel-L (4 transforming growth factor (TGF)-β2 antisense gene-modified, irradiated, allogeneic NSCLC cell lines)	Placebo
Cellular Therapy	CIK-therapy	BSC
Cellular Therapy	AKT (autologous activated killer T cells) + DC-therapy + Chemotherapy	Chemotherapy
Cellular Therapy	DC-therapy	BSC
Cellular Therapy	CIK + Chemotherapy (Cisplatin + gemcitabine/paclitaxel/ navelbine)	Chemotherapy
Tumor Vaccine	Cyclophosphamide + Tecemotide (L-BLP25= MUC1 Ag)	Saline + Placebo
Tumor Vaccine	TG4010 (MVA coding for MUC1+IL-2) + Chemotherapy	Chemotherapy
Tumor Vaccine	Chemotherapy + TG4010	Chemotherapy + placebo
Cellular Therapy	DC-therapy + CIK-therapy	BSC
Cellular Therapy	Erlotinib + CIK-therapy + DC-therapy	Erlotinib
Tumor Vaccine	MAGE-A3-vaccine	Placebo
Tumor Vaccine	MAGE-A3-vaccine	Placebo
Tumor Vaccine	Cyclophosphamide + EGF-Vaccine	BSC
Cellular Therapy	Chemotherapy (docetaxel + cisplatin + CIK-therapy	Chemotherapy
Cellular Therapy	Chemotherapy (Gemcitabine+Cisplatin) + DC-therapy+ CIK-therapy	Chemotherapy

Abbreviations: NSCLC=Non-Small Cell Lung Cancer, MUC1=Mucin 1, Ag= Antigen, BSC= Best Supportive Care, TGF- β2= Transforming Growth Factor - β2, CIK= Cytokine Induced Killer Cells, AKT=Autologous Killer T-cells, DC= Dendritic Cell, MVA= Modified Vaccinia Ankara, IL-2= Interleukin 2, EGF=Epithelial Growth Factor.

Table 2. Heterogeneity explained by factors associated with treatment efficacy.

	# studies	OS HR	p-value	# studies	OS Median Month Diff.	p-value	# studies	Progression HR	p-value	# studies	Progression Median Month Diff.	p-value
Cellular Therapies	1	0.229		7	9.071		2	0.410		5	6.967	
Tumor Vaccines	8	0.851	<i>p=0.005</i>	7	1.564	<i>p<0.001</i>	8	0.890	<i>p=0.001</i>	6	0.829	<i>p=0.004</i>
High stage NSCLC	7	0.846		12	1.805		6	0.854		9	1.467	
Low stage NSCLC	1	0.990	<i>p=0.548</i>	2	22.890	<i>p=0.058</i>	3	0.823	<i>p=0.863</i>	2	14.479	<i>p=0.010</i>
With Chemotx	3	0.631		6	4.119		3	0.654		5	1.761	
Without Chemotx	6	0.853	<i>p=0.282</i>	8	6.704	<i>p=0.313</i>	7	0.906	<i>p=0.031</i>	6	5.304	<i>p=0.090</i>
With Cyclophos	3	0.872		3	1.408		2	0.880		2	1.842	
Without Cyclophos.	5	0.821	<i>p=0.577</i>	5	0.935	<i>p=0.567</i>	6	0.872	<i>p=0.928</i>	5	0.847	<i>p=0.343</i>

Abbreviations: OS= Overall Survival, Diff. = Difference, HR= Hazard Ratio, NSCLC= Non-Small Cell Lung Cancer, Chemotx= Chemotherapy, Cyclophos= Cyclophosphamide.

PART B
Improving the efficacy of
cancer vaccines for solid tumors
by combination immunotherapy

THE EFFICACY OF TUMOR VACCINES
AND CELLULAR IMMUNOTHERAPIES IN
NON-SMALL CELL LUNG CANCER:
A SYSTEMATIC REVIEW AND META-ANALYSIS

SUPPLEMENTARY DATA

Search strategy:

Embase.com

('lung cancer'/de OR 'lung tumor'/de OR 'lung carcinoma'/exp OR 'pleura cancer'/de OR 'pleura mesothelioma'/de OR mesothelioma/de OR 'malignant mesothelioma'/de OR (((lung OR pulmonar* OR thora* OR pleura* OR mesothel*) NEAR/6 (cancer* OR tumor* OR neoplas* OR malign* OR carcinom* OR adenocarcinom*)) OR mesotheliom*):ab,ti) AND (((immunization/de OR immunotherapy/de OR (immun*):ab,ti) AND ('dendritic cell'/de OR 'natural killer cell'/de OR 'T lymphocyte'/exp OR 'immunological adjuvant'/de OR (dendrit* OR (killer NEAR/3 cell*) OR ((T OR thym*) NEXT/3 (lymphocyte* OR cell*)) OR (immun* NEXT/1 adjuvant*) OR immunoadjuvant*):ab,ti) OR 'active immunization'/de OR 'cancer immunization'/de OR 'lymphocyte transfer'/de OR 'adoptive transfer'/de OR 'adoptive immunotherapy'/de OR 'immune response'/exp OR 'cancer immunotherapy'/de OR 'cancer immunization'/de OR 'passive immunization'/de OR vaccination/de OR (((immun* OR vaccin*) NEAR/3 (active* OR passive* OR cancer* OR anticancer* OR 'cell based' OR respons*)) OR ((lymphocyte* OR adoptive*) NEAR/3 transfer*)):ab,ti) AND ((random* OR factorial* OR crossover* OR (cross NEXT/1 over*) OR placebo* OR ((doubl* OR singl*) NEXT/1 blind*) OR assign* OR allocat* OR volunteer* OR trial*):ab,ti OR 'crossover procedure'/de OR 'double-blind procedure'/de OR 'clinical trial'/exp OR 'single-blind procedure'/de) NOT ([animals]/lim NOT [humans]/lim)

Medline (OvidSP)

("Lung Neoplasms"/ OR "Small Cell Lung Carcinoma"/ OR "Carcinoma, Non-Small-Cell Lung"/ OR "Pleural Neoplasms"/ OR mesothelioma/ OR (((lung OR pulmonar* OR thora* OR pleura* OR mesothel*) ADJ6 (cancer* OR tumor* OR neoplas* OR malign* OR carcinom* OR adenocarcinom*)) OR mesotheliom*).ab,ti.) AND (((immunization/ OR immunotherapy/ OR (immun*):ab,ti.) AND ("dendritic cells"/ OR exp "Killer Cells, Natural"/ OR exp "T-Lymphocytes"/ OR "Adjuvants, Immunologic"/ OR (dendrit* OR (killer ADJ3 cell*) OR ((T OR thym*) ADJ3 (lymphocyte* OR cell*)) OR (immun* ADJ adjuvant*) OR immunoadjuvant*):ab,ti.) OR exp "Immunotherapy, Active"/ OR exp "Immunization, Passive"/ OR (((immun* OR vaccin*) ADJ3 (active* OR passive* OR cancer* OR anticancer* OR "cell based" OR respons*)) OR ((lymphocyte* OR adoptive*) ADJ3 transfer*)):ab,ti.) AND (Clinical Trial.pt. OR randomized.ab,ti. OR placebo.ab,ti. OR dt.fs. OR randomly.ab,ti. OR trial.ab,ti. OR groups.ab,ti. NOT (Animals/ NOT Humans/))

PART B
Improving the efficacy of
cancer vaccines for solid tumors
by combination immunotherapy

THE EFFICACY OF TUMOR VACCINES
AND CELLULAR IMMUNOTHERAPIES IN
NON-SMALL CELL LUNG CANCER:
A SYSTEMATIC REVIEW AND META-ANALYSIS

Cochrane

(((((lung OR pulmonar* OR thora* OR pleura* OR mesothel*) NEAR/6 (cancer* OR tumor* OR neoplas* OR malign* OR carcinom* OR adenocarcinom*)) OR mesotheliom*):ab,ti) AND (((immun*):ab,ti) AND ((dendrit* OR (killer NEAR/3 cell*) OR ((T OR thym*) NEXT/3 (lymphocyte* OR cell*)) OR (immun* NEXT/1 adjuvant*) OR immunoadjuvant*):ab,ti)) OR (((immun* OR vaccin*) NEAR/3 (active* OR passive* OR cancer* OR anticancer* OR 'cell based' OR respons*)) OR ((lymphocyte* OR adoptive*) NEAR/3 transfer*)):ab,ti)

Web-of-science

TS=(((lung OR pulmonar* OR thora* OR pleura* OR mesothel*) NEAR/6 (cancer* OR tumor* OR neoplas* OR malign* OR carcinom* OR adenocarcinom*)) OR mesotheliom*)) AND (((immun*)) AND ((dendrit* OR (killer NEAR/3 cell*) OR ((T OR thym*) NEAR/3 (lymphocyte* OR cell*)) OR (immun* NEAR/1 adjuvant*) OR immunoadjuvant*)) OR (((immun* OR vaccin*) NEAR/3 (active* OR passive* OR cancer* OR anticancer* OR "cell based" OR respons*)) OR ((lymphocyte* OR adoptive*) NEAR/3 transfer*))) AND (randomized OR placebo OR randomly OR trial OR groups) NOT ((animal* OR mice OR mouse OR rat OR rats) NOT (human* OR patient*)))

PubMed publisher

(((((lung[tiab] OR pulmonar*[tiab] OR thora*[tiab] OR pleura*[tiab] OR mesothel*[tiab]) AND (cancer*[tiab] OR tumor*[tiab] OR neoplas*[tiab] OR malign*[tiab] OR carcinom*[tiab] OR adenocarcinom*[tiab])) OR mesotheliom*[tiab])) AND (((immune*[tiab] OR immuni*[tiab] OR immunother*[tiab])) AND ((dendrit*[tiab] OR (killer cell*[tiab]) OR T lymphocyte*[tiab] OR t cell*[tiab] OR immuno adjuvant*[tiab] OR immunoadjuvant*[tiab])))) OR (((immun*[tiab] OR vaccin*[tiab]) AND (active*[tiab] OR passive*[tiab] OR cancer*[tiab] OR anticancer*[tiab] OR "cell based"[tiab] OR respons*[tiab])) OR ((lymphocyte*[tiab] OR adoptive*[tiab]) AND transfer*[tiab])))) AND (randomized[tiab] OR placebo[tiab] OR randomly[tiab] OR trial[tiab] OR groups[tiab]) AND publisher[sb])

Google Scholar

"lung|pulmonary|pleural cancer|carcinoma"|mesothelioma "active|passive|cancer immunization|immunotherapy"|lymphocyte|adoptive transfer"|vaccination random|factorial|crossover|placebo|trial -rat -rats -mouse -mice

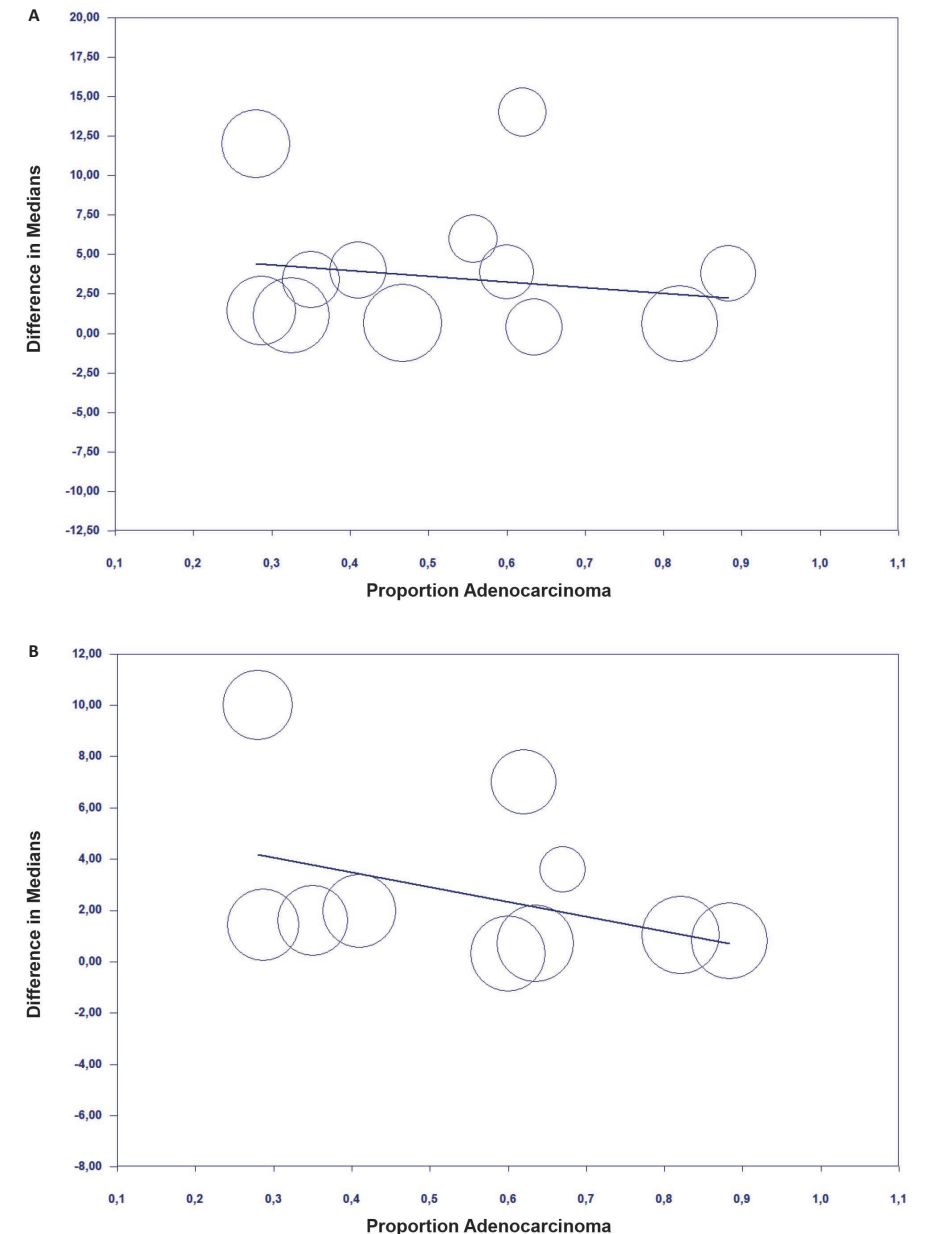


Figure S1. Meta-regression analysis showing the correlation between Non-Small Cell Lung Cancer (NSCLC) histology (% adenocarcinoma) and (A) difference in median overall survival in months, and (B) difference in median months progression free survival.

PART B
Improving the efficacy of
cancer vaccines for solid tumors
by combination immunotherapy

THE EFFICACY OF TUMOR VACCINES
AND CELLULAR IMMUNOTHERAPIES IN
NON-SMALL CELL LUNG CANCER:
A SYSTEMATIC REVIEW AND META-ANALYSIS

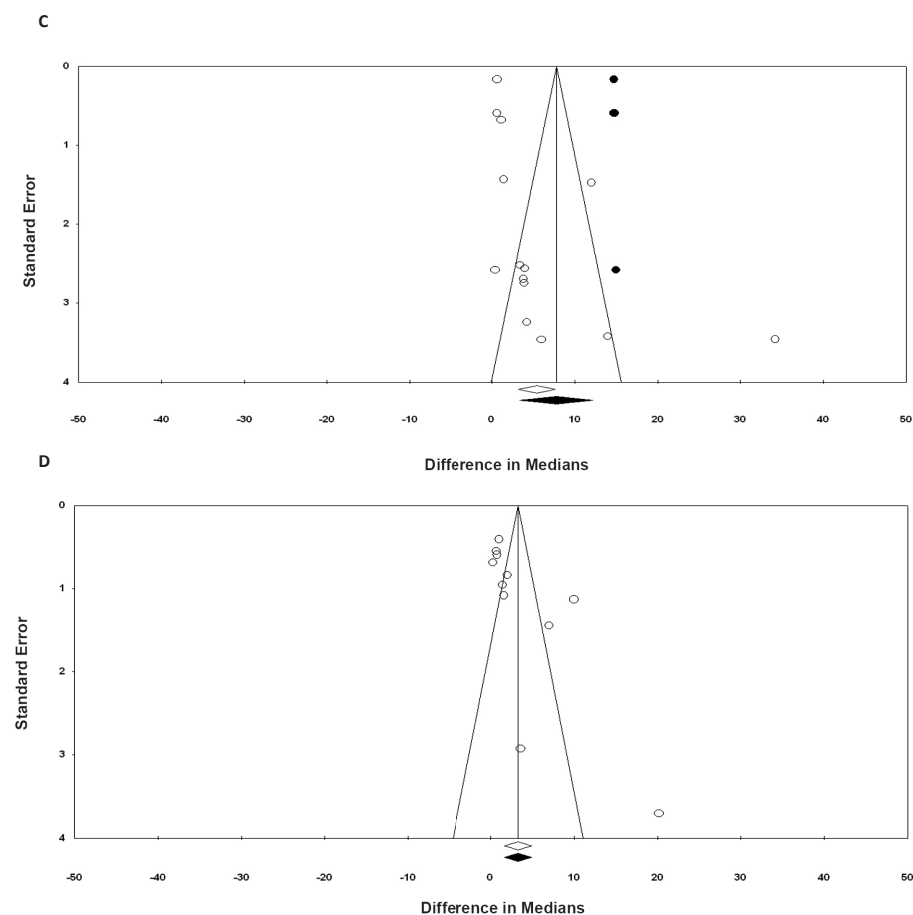
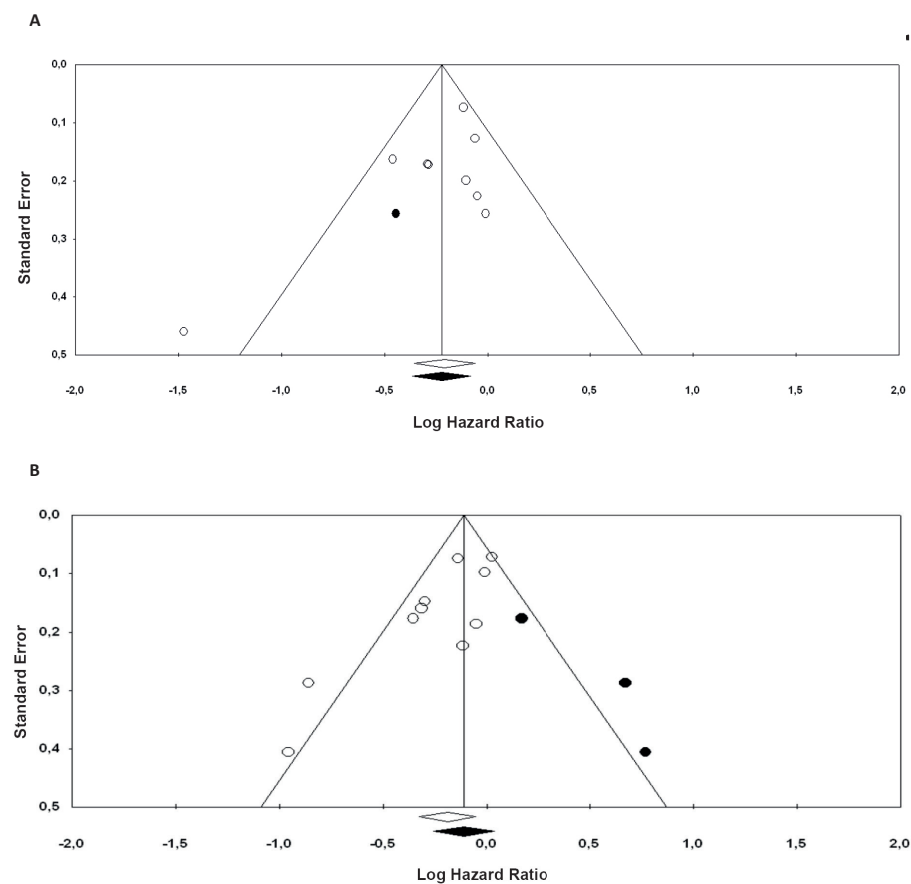


Figure S2. Duval and Tweedie's trim and fill analysis. Funnel plots depicting potential presence of publication bias when analyzing (A) survival and (B) progression free survival as hazard ratios (HR) and as (C) median month difference of survival and (D) progression free survival.

5

Floris Dammeijer
Lysanne A. Lievense
Margaretha E. Kaijen-Lambers
Menno van Nimwegen
Koen Bezemer
Joost P. Hegmans
Thorald van Hall
Rudi W. Hendriks
Joachim G. Aerts

Cancer Immunology Research. 2017 Jul;5(7):535-546.

PART B
Improving the efficacy of
cancer vaccines for solid tumors
by combination immunotherapy

DEPLETION OF TUMOR-ASSOCIATED
MACROPHAGES WITH A CSF-1R KINASE INHIBITOR
ENHANCES ANTI-TUMOR IMMUNITY AND SURVIVAL
INDUCED BY DENDRITIC CELL IMMUNOTHERAPY

SUMMARY

New immunotherapeutic strategies are needed to induce effective anti-tumor immunity in all cancer patients. Malignant mesothelioma is characterized by a poor prognosis and resistance to conventional therapies. Infiltration of tumor associated macrophages (TAM) is prominent in mesothelioma and is linked to immune suppression, angiogenesis and tumor aggressiveness. Therefore, TAM depletion could potentially reactivate anti-tumor immunity. We show that M-CSFR-inhibition using PLX3397 effectively reduced TAMs, circulating non-classical monocytes, neo-angiogenesis and ascites in mesothelioma mouse models, but did not improve survival. Importantly, when combined with dendritic cell vaccination, survival was synergistically enhanced with a concomitant decrease in TAMs and an increase in CD8⁺ T-cell numbers and functionality. Total as well as tumor antigen-specific CD8⁺ T cells in tumor tissue of combination therapy treated mice showed strongly reduced surface expression of the key inhibitory molecule PD-1, associated with exhaustion. Finally, combination therapy treated mice were protected from tumor rechallenge and displayed superior T-cell memory responses. We report that decreasing local TAM-mediated immune suppression without proper immune activation does not improve survival but when combined with dendritic cell immunotherapy generates robust and durable antitumor immunity. These findings provide new insights into the interaction between immunotherapy induced anti-tumor T cells and TAMs and offers a new therapeutic strategy for mesothelioma treatment.

INTRODUCTION

With the implementation of checkpoint inhibition therapy for several malignancies, immunotherapy has evolved to become an effective strategy in the treatment of advanced cancer¹. Although a subgroup of advanced disease stage patients benefits and shows prolonged overall survival to these therapies, the majority of patients do not respond or eventually relapse. Efforts have been made to characterize the mechanisms behind immunotherapy efficacy, leading to the distinction between inflamed, immune-sensitive tumors, and non-inflamed tumors associated with immunological exclusion or ignorance²⁻⁴. Blocking antibodies to the programmed cell death protein-1 (PD-1) appear to be most effective in patients with a pre-existing immune cell infiltrate in the tumor, which can be functionally enhanced by this form of immunotherapy⁵. The next breakthrough in cancer immunotherapy will be finding ways to sensitize non-inflamed and resistant inflamed tumors to therapy, thereby increasing response rates and survival in advanced stage cancer patients^{2,3}.

Malignant mesothelioma (MM) is a cancer with a dismal prognosis that has not improved significantly in the last decades with the broad implementation of conventional cancer treatment modalities⁶. MM is often characterized by a prominent stromal component, dominated by the presence of macrophages⁷. These tumor associated macrophages (TAMs) often display an 'alternatively activated' ('M2') immune inhibitory phenotype characterized by the production of interleukin 10 (IL-10) and surface expression of CD206 and inhibitory molecules such as PD-L1⁸. Furthermore, TAMs have been shown to be critical regulators of angiogenesis and they are closely linked to local tumor outgrowth and pleural fluid mediated immune suppression in MM patients⁹⁻¹¹. Furthermore, a high M2-TAM to CD8⁺ T-cell ratio has been shown to correlate with a poor prognosis in MM patients^{9,12}.

TAMs are known to be highly dependent on macrophage-colony stimulating factor (M-CSF) for their survival, proliferation, and recruitment towards tumors^{8,13}. In addition, M-CSF promotes an M2 phenotype¹⁴ and its levels in the tumor and circulation are correlated with poor survival in several solid tumor types¹⁵. For these reasons different approaches to inhibit the M-CSF/M-CSFR pathway have been designed in order to deplete TAMs^{16,17}. Broadly, these molecules can be subdivided into antibodies targeting M-CSF, the M-CSFR, and small molecule tyrosine kinase (TK) inhibitors with variable specificities for related kinases downstream from the receptors c-kit and FLT3¹⁵. The advantages of TK-inhibitors over antibody-mediated therapies include: (i) their capability of targeting both murine and human M-CSFR-signaling improving translatability across species, ii) inhibition of autocrine M-CSF/M-CSFR-signaling, and (iii) the absence of rebound monocytopoiesis after cessation of therapy due to intact receptor-mediated internalization of M-CSF

which is TK-independent¹³. PLX3397 (pexidartinib) is a clinically tested M-CSF-receptor (M-CSFR) and c-kit tyrosine kinase inhibitor shown to be safe and effective in reducing TAMs in several solid tumor types^{17,18}. Whether PLX3397 is effective in depleting TAMs in mesothelioma, and possibly capable of restoring anti-tumor immunity in these tumors in currently unknown.

Dendritic cell (DC)- and T-cell based therapies circumvent aberrant antigen presentation and the formation of ineffective immune responses in cancer, possibly explaining their efficacy over conventional tumor vaccines¹⁹. We have previously demonstrated that vaccination is a safe and effective way to generate functional anti-tumor immunity and clinical responses in MM patients^{20,21}. We hypothesize that TAM-mediated immune suppression could limit DC-vaccination efficacy and that depletion of TAMs would improve response rates and response durability in MM models.

Here, we show that PLX3397 is effective in depleting TAMs but that monotherapy does not improve survival in murine mesothelioma models. Combining M-CSFR-inhibition with DC vaccination (DC-therapy) to induce effective anti-tumor immune responses improved survival, whereby mice were protected from disease following tumor rechallenge. This therapeutic synergy may prove to be an alternative strategy to improve response rates and survival with immunotherapy.

METHODS

Mesothelioma Mouse Models.

Female 8-12 week old BALB/c (H-2d) mice (Envigo, Zeist, The Netherlands) and CBA/J mice (Janvier, Hannover, Germany) were housed under specific pathogen-free conditions at the animal care facility of the Erasmus MC, Rotterdam. Experiments were approved by the local Ethical Committee for Animal Welfare and complied to the Guidelines for the Welfare of Animals in Experimental Neoplasia by the United Kingdom Coordinating Committee on Cancer Research (UKCCCR) and by the Code of Practice of the Dutch Veterinarian Inspection. The AB1 cell and AC29 mesothelioma cell lines were kindly provided by Professor Bruce W.S. Robinson of the Queen Elizabeth II Medical Centre, Nedlands, Australia. These cell lines were derived from tumors induced by crocidolite asbestos injected i.p. into CBA/J and BALB/c mice²². Both cell lines were obtained in the years 2003-2005, aliquoted and stored at -190°C. Tumor cells were cultured from early passages (max. 5 passages following cell line acquisition) in RPMI 1640 medium containing 25 mM HEPES, Glutamax, 50 g/ml gentamicin, and 5% (v/v) fetal bovine serum (FBS) (all obtained from Gibco) in a humidified atmosphere and at 5% CO₂, in air. For culture, either culture flasks or CellSTACKs (Corning Life Sciences) were used to reach appropriate tumor cell frequencies for injection. AB1 and

AC29 cells were passaged once or twice a week to a new flask by treatment with 0.05% trypsin, 0.53 mM EDTA in phosphate buffered saline (PBS, all Gibco). Every 8-10 passages, cell lines were tested for mycoplasma contamination by PCR and remained negative. At the start of the experiment, CBA/J or BALB/c mice were i.p. injected with either 20x10⁶ AC29 cells or 0.5x10⁶ AB1 cells respectively, dissolved in PBS, or with PBS as control as was described previously²³. Mice were scored using the body condition score, killed if profoundly ill and scored as a death in survival analysis.

Tumor Lysate Production.

AB1 cell line-derived tumor lysate was prepared as previously described²³. Briefly, cells were suspended in PBS and frozen in liquid nitrogen and disrupted by four cycles of freeze-thawing followed by sonication for 3x 10 seconds with an amplitude of 10 microns, using a Soniprep 150 ultrasonic disintegrator equipped with a microtip (Sanyo Gallenkamp BV, Breda, The Netherlands) on ice. Cell lysate was aliquoted and stored at -80°C.

Culture Conditions of Bone Marrow-Derived DC Used for Vaccination.

DCs were generated following an adapted protocol (Lutz et al. 1999) as previously described²³. Bone-marrow derived cells seeded in 100-mm Petri dishes (day 0) and cultured in 10 ml DC Culture Medium [DC-CM]: RPMI 1640 containing glutamax-I (Gibco) supplemented with 5% (v/v) FBS, 50 µM β-mercaptoethanol (Sigma-Aldrich), 50 µg/ml gentamicin (Invitrogen), and 20 µg/mL recombinant murine granulocyte macrophage-colony-stimulating factor [GM-CSF, kindly provided by Prof. B. Lambrecht, VIB Ghent, Belgium]. Cells were cultured in a humidified atmosphere at 5% CO₂, in air. At day 3, 10 ml of fresh DC-CM was added. On day 6, 10 ml of each plate was replaced with 10 ml of fresh DC-CM. After 9 days of culture, AB1 cell lysate was added to the DC cultures, to the equivalent of three AB1 cell-equivalents per DC. After 8 hours, 10 g/ml CpG (ISS-ODN 1668, Invitrogen) was added to the culture to allow complete maturation while incubated overnight. The next day, DCs were harvested by and purified by Lympholyte-Mammal (Cedarlane) density gradient centrifugation, the interphase washed three times in PBS and resuspended at a concentration of viable cells. The quality of the DC preparation was determined by cell-counting, morphologic analysis and cell surface marker expression by flow cytometry, as previously described²³.

DC-culture with PLX3397.

Mature, lysate pulsed-DCs were generated as demonstrated above and cultured for 48 hours in GM-CSF DC-TCM and varying concentrations of PLX3397¹⁷ (provided by Plexxikon inc. as part of a material transfer agreement) or the vehicle (Dimethyl sulfoxide, DMSO, Sigma-Aldrich) in 6-well plates. PLX3397 was reconstituted in DMSO to reach a stock

concentration of 20mM, which was then diluted to a concentration range of 0.1 to 10μM in DC-TCM. After 48 hours, cells were harvested from the 6-well plates and analyzed for viability and surface expression of immune markers using multi-color flow-cytometry.

Treatment with Tumor Lysate-Pulsed DCs and/or PLX3397.

On day 0, BALB/c or CBA/J mice were inoculated intraperitoneally with AB1 or AC29 tumor cells, respectively. On day 10, mice were treated with either 2-3x10⁶ DCs dissolved in 200μl PBS, or PBS alone. This time point was determined to be most optimal in previous experiments²³. In specified cases, treatment with either DC-therapy alone or in combination with PLX3397 commenced at day 15 to allow for enough tumor to be collected several days later and prepare a window to detect possible changes between mono- and combination treated tumors. Also, depending on the treatment arm, mice were fed *ad libitum* PLX3397-containing chow or control chow of equal nutritional value and consistency until the end of the experiment or prior to rechallenge. The optimal dose to effectively deplete TAMs was determined by Plexxikon and has been further corroborated in different tumor models to be 290 mg PLX3397/kg chow (delivering daily doses of approximately 45 mg/kg)²⁴. On day 15 post-tumor cell injection, prior and after rechallenge, blood was obtained via tail vein extraction. During the remainder of the follow-up period, mice were examined daily for evidence of illness caused by overt tumor growth.

Immunohistochemistry (IHC) on Tumor Material.

Tumor biopsies were embedded in Tissue-Tek II optimum cutting temperature medium (Miles, Naperville, IL, USA), snap-frozen, and stored at at -80°C. Tissue sections (6 μm) were cut on a cryostat (Cryostar NX70, Thermo-Fisher Scientific). Frozen sections were warmed to RT, fixed with acetone for 10 minutes and rinsed in PBS. Sections were incubated in peroxidase blocking solution (0.1% H₂O₂ and 0.1% sodium azide in PBS) for 30 minutes and rinsed with PBS. Slides were placed in a semi-automatic stainer (Sequenza) and incubated in 1:10 diluted normal Goat serum (CLB, Amsterdam, Netherlands) for 10 min and subsequently for 60 min with the diluted primary Abs, followed by rinsing in PBS for 5 min and incubation for 30 min with diluted secondary Abs. Double-immunostaining was carried out using antibodies supplied in table S1. Binding of antibody was detected using alkaline phosphatase- (AP-) or peroxidase- conjugated goat anti-rat (Sigma-Aldrich) and Naphthol-AS-MX-phosphate (0.30mg·mL⁻¹; Sigma-Aldrich) + new fuchsin (160mg·mL⁻¹ in 2MHCl; Chroma-Gesellschaft, Köngen, Germany) or AEC (0.1M NaAc + 1% AEC stock [100mg AEC in 10ml DMF], Vectorlabs), respectively, were used as substrate. The specificity was checked using a protein concentration-matched non-relevant rat antibody and PBS. Finally, the sections were rinsed in distilled water and mounted in vecta mount (Vector). Slides were scanned using a Nanozoomer 2.0 HT (Hamamatsu).

Quantification of IHC Images.

Scanned IHC-slides were viewed using NDP-viewing software (Hamamatsu) at 20x and 40x magnification and regions of interest were captured and imported into ImageJ software (NIH). Colors were separated, thresholds were installed to select for positive cells and these were depicted as percentage of total area. For each sample, 5 random areas (including tumor rim and center) at 20x magnification were selected, analyzed and averaged. CD8-positive cells were well demarcated and counted (average of 5 random tumor areas per sample) to be expressed as cells/mm².

Preparation of Single Cell Suspensions from Tissues.

Single cell suspensions were generated from the spleens, blood and tumors of mice from each group. All tissues were either weighed in a microbalance in case of tumors and spleens, or volume determined for blood. Briefly, spleens were aseptically removed and mechanically dispersed over 100 μm nylon mesh cell strainer (BD Biosciences) followed by erythrocyte lysis using osmotic lysis buffer (8.3% NH₄Cl, 1% KHCO₃, and 0.04% Na₂EDTA in Milli-Q). Blood was collected in EDTA tubes (Microvette CB300, Sarstedt) and subsequently lysed. Tumors were collected, and dissociated using a validated tumor dissociation system (Miltenyi Biotec). Cells suspensions were filtered through a 100 μm nylon mesh cell strainer (BD Biosciences) and counted in trypan blue with a hemocytometer using the Burkert-Turk method.

Flow Cytometry.

For measurements of cytokine production in lymphoid cells by flow cytometry, cells were re-stimulated for 4 h at 37°C using PMA and ionomycin supplemented with GolgiStop (BD Biosciences). For assessing cytokine production by myeloid cells, cells were subjected to 4 hours incubation with Golgistop. For cell surface marker staining, cells were washed with FACS-wash (0.05% NaN₃, 2% BSA in PBS) and Fc II/III receptor blocking was performed using anti-mouse 2.4G2 antibody (1:300; kindly provided by L. Boon, Bioceros, Utrecht, The Netherlands). After the blocking procedure, antibodies (supplementary table 1) for cell surface staining were added into each sample and placed on ice for 30 minutes. Cells were washed in FACS-wash followed by a PBS wash, and then stained for viability using fixable LIVE/DEAD aqua cell stain (Thermo-Fisher Scientific, 1:200). After two additional washes with FACS-wash, cells were either measured or in case of intracellular staining; fixated, permeabilized and stained using Fix/Perm buffer (in case of nuclear protein staining, eBioscience) or 4% PFA and 0.5% saponin (in case of cytokine stainings, Sigma-Aldrich). Antibodies were stained for 30 minutes in case of the PFA/Saponin protocol and 60 minutes for the intranuclear staining protocol, on ice in the dark. A fixed number of counting beads (Polysciences Inc.) was added prior to data acquisition to determine the

absolute amount of cells. Data were acquired using an LSR II flow cytometer (BD) equipped with three lasers and FACSDiva software (BD) and analyzed by FlowJo (Tree Star Inc., USA) software V10.1. In order to detect tumor-antigen specific CD8⁺ T cells in the CBA/J model, dextramers specific for potentially dominant WT1 and Mesothelin epitopes were constructed. Peptides for WT1 and Mesothelin were selected based on freely available tools (IEDB Analysis Resource) predicting likelihood of processing, MHC-I (H2-Kk) binding affinity and immunogenicity of the chosen peptides. The peptide sequences for WT1 and Mesothelin selected were SENHTAPIL, and QEATLLHAV, respectively. Dextramers were labeled to APC or PE fluorochromes and ordered from Immudex (Copenhagen, Denmark). Dextramers were stained independently from one another following company instructions on cells pre-treated in RPMI containing 50nM Dasatinib for 30 minutes at 37°C to limit TCR internalization. FMO and dextramer binding-CD4⁺ T cells was used to determine background signal and set cut-off limits.

Microarray Analysis of AB1 and AC29.

Biotin-labeled cRNA derived from AB1 and AC29 (n=3 samples) was hybridized to the Mouse Genome 430 2.0 Array according to the manufacturer's instructions (Affymetrix); data were analyzed with BRB-ArrayTools (version3.7.0, National Cancer Institute) using Affymetrix CEL files obtained from GCOS (Affymetrix To examine the quality of the various arrays, the R package affyQCReport for generating QC reports was run starting from the CEL files. All created plots indicated a high quality of samples and an overall comparability. Raw intensity values of all samples were normalized by RMA normalization (Robust Multichip Analysis) (background correction and quantile normalization) using Partek version 6.4 (Partek Inc., St. Louis, MO). Genes involved in myeloid cell chemotaxis and survival, and expression of clinically relevant tumor antigens were manually selected and plotted for both AB1 and AC29 cell lines. The GEO accession number for this microarray is GSE97150.

Statistical Analysis.

Data are expressed as medians with interquartile range. Comparisons between groups were made using the Mann-Whitney U-test for independent samples, or the Wilcoxon signed rank test in case of paired samples. When correlations were depicted, Spearman's rank correlation test was performed to test for statistical significance. A two-tailed value of $p < 0.05$ was considered statistically significant. Survival data were plotted as Kaplan-Meier survival curves, using the log-rank test to determine statistical significance. Data was analyzed using Graphpad Prism software (Graphpad, V5.01)

RESULTS

DC-therapy synergizes with M-CSFR-inhibition in orthotopic mesothelioma mouse models.

In the past we have shown that applying DC-therapy in syngeneic and orthotopic mesothelioma mouse models is an effective and translational system for assessing anti-tumor T-cell responses and evaluating treatment efficacy^{23,25}. The AB1 and AC29 mesothelioma cell lines are injected intraperitoneally (i.p.) in BALB/c and CBA/J mice, respectively. Compared with the BALB/c model, the CBA/J model has a more pronounced TAM-dependent phenotype (Fig S1A), which may be explained by the increased expression of M-CSF and CCL-2, being key TAM-homing and survival factors as determined by microarray (accession number: GSE97150, Fig S1B). In line with this M2-TAM-dominant phenotype, CBA/J mice injected with AC29 mesothelioma cells develop ascites, paralleling disease heterogeneity also seen in mesothelioma patients^{22,26,27}.

Here we used the M-CSFR-inhibitor PLX3397 to target TAMs *in vivo*. To ensure that there was no direct effect of PLX3397 on the murine mesothelioma cell lines, expression of M-CSFR and c-kit was determined using flow cytometry and tissue microarray analysis, which showed negligible levels of both molecules (Fig. S1B). Furthermore, to exclude any direct effects of PLX3397 on matured tumor-lysate pulsed DCs to be administered in the DC-therapy protocol, these cells were cultured *in vitro* with increasing levels of PLX3397 or vehicle alone and cell viability and membrane expression of relevant surface markers was assessed by flow cytometry (Fig. S2). As previously reported, GM-CSF-cultured cells are comprised of heterogeneous populations of DCs and macrophages, which we also identified in our system (Fig. S2)²⁸. Effects of PLX3397 on DC viability or surface expression of MHC-II, CD86, PD-L1, M-CSFR, and c-kit were negligible (Fig. S2A). This resistance of DCs to PLX3397 could be explained by the rapid down-regulation of M-CSFR surface expression following maturation using unmethylated CpG (Fig. S2B-C).

Mice were left untreated or were treated at day 10, when solid tumors had established using three different regimens: (i) either PLX3397 was administered in chow and continued for the duration of the experiment, (ii) DCs were injected i.p. as monotherapy or (iii) mice were subjected to double therapy (Fig. 1A-B). PLX3397 monotherapy did not improve survival in both mesothelioma tumor models (Fig. 1C-D). DC-therapy prolonged survival only in the AC29 tumor model. Combination therapy, however, significantly enhanced survival in both tumor models, indicating therapeutic synergy (Fig. 1C-D).

PART B
Improving the efficacy of
cancer vaccines for solid tumors
by combination immunotherapy

DEPLETION OF TUMOR-ASSOCIATED
MACROPHAGES WITH A CSF-1R KINASE INHIBITOR
ENHANCES ANTI-TUMOR IMMUNITY AND SURVIVAL
INDUCED BY DENDRITIC CELL IMMUNOTHERAPY

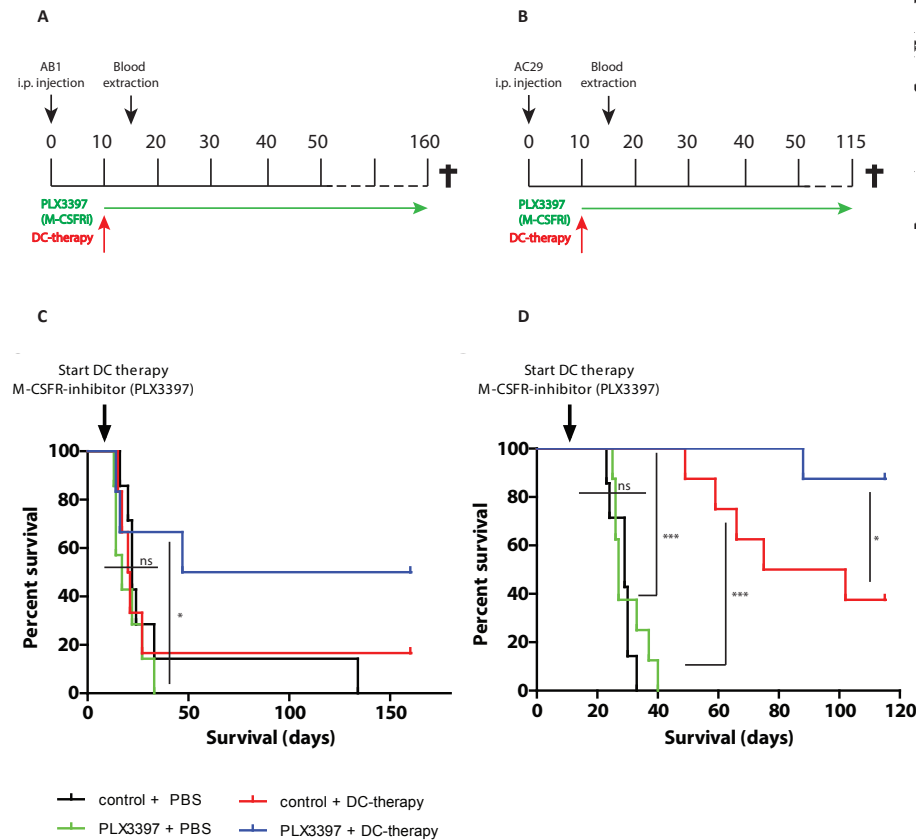


Figure 1. Efficacy of DC-therapy is synergistically enhanced by combination therapy with TAM-depletion in mesothelioma mouse models. (A-B) Wildtype, female BALB/c (n=6/arm) and CBA/J (n=8/arm) mice were i.p. injected with either 0.5×10^6 AB1 or 20×10^6 AC29 syngeneic tumor cells, respectively. Mice were then treated once on day 10 with either i.p. administration of PBS or mature, autologous tumor lysate loaded dendritic cells. Concurrently, mice were started on control or PLX3397-containing chow until the end of the experiment or until rechallenge. Blood was extracted on t=15 days and before and after rechallenge in case of CBA/J mice. Animals were monitored daily for the duration of 160 days and euthanized in case of severe illness. (C-D) Kaplan-Meier curves of the survival experiments in CBA/J (AC29) and BALB/c (AB1) mesothelioma tumor models. Statistical significance was determined using the Log-rank test with $p < 0.05$ being statistically significant. *= $p < 0.05$, **= $p < 0.01$, ***= $p < 0.001$, ns=not significant

M-CSFR inhibition causes a decrease in CD206⁺ F4/80⁺ TAM numbers, blood vessel density and ascites.

To assess whether PLX3397 was effective in depleting TAMs, we focused on the CBA/J mesothelioma model, because this is more TAM-dependent. Immunohistochemical (IHC) analysis showed an evident decrease in F4/80⁺ TAMs, CD31⁺ endothelial cells and CD206⁺ (M2) cells in PLX3397-treated mice compared with control mice (Fig. 2A-G). It has recently been shown that TAMs are crucial for tumor angiogenesis and concomitant ascites production in metastatic ovarian carcinoma²⁹. Accordingly, we found a strong correlation between CD31⁺ endothelial and TAM areas in these tumors and a decrease in ascites volume in the PLX3397-treated mice (Fig. 2D-E). Tumors of untreated mice contained a CD8⁺ T-cell infiltrate which was not further enhanced following TAM-depletion (Fig. 2H).

Taken together, these findings show that M-CSFR-inhibition effectively reduced TAMs, neo-angiogenesis and ascites in mesothelioma mouse models, but did not improve local CD8⁺ T cell infiltration.

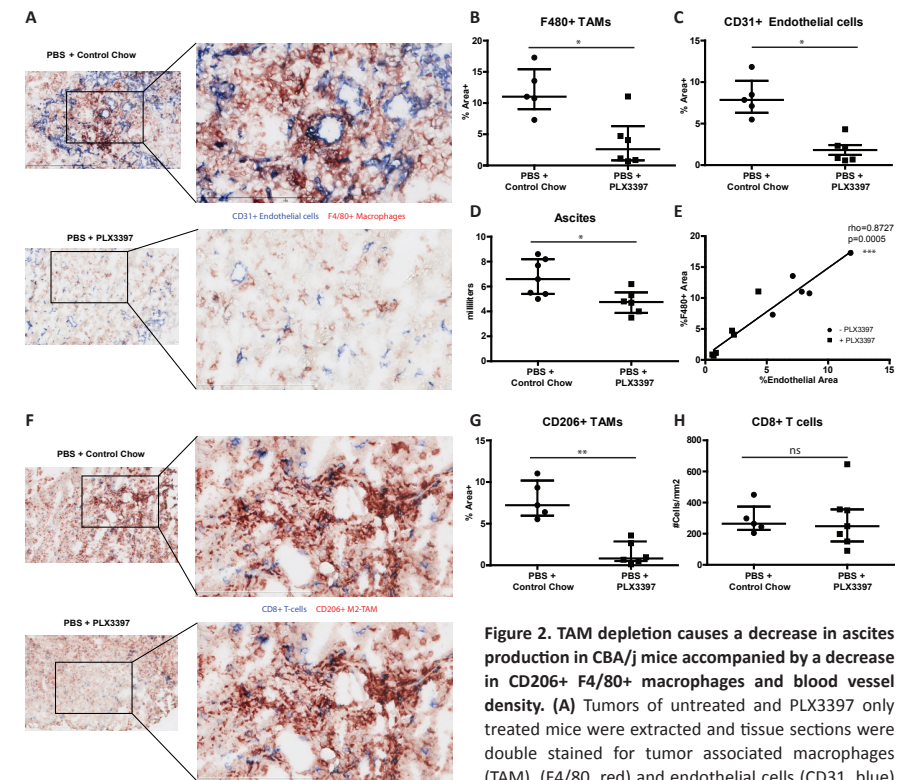


Figure 2. TAM depletion causes a decrease in ascites production in CBA/J mice accompanied by a decrease in CD206⁺ F4/80⁺ macrophages and blood vessel density. (A) Tumors of untreated and PLX3397 only treated mice were extracted and tissue sections were double stained for tumor associated macrophages (TAM), (F4/80, red) and endothelial cells (CD31, blue)

PART B
Improving the efficacy of
cancer vaccines for solid tumors
by combination immunotherapy

DEPLETION OF TUMOR-ASSOCIATED
MACROPHAGES WITH A CSF-1R KINASE INHIBITOR
ENHANCES ANTI-TUMOR IMMUNITY AND SURVIVAL
INDUCED BY DENDRITIC CELL IMMUNOTHERAPY

>>

using immunohistochemistry (IHC). Tissues are displayed at a 20X magnification (error bar length is 400µm) with a further close-up at 40X magnification (error bar length is 200µm). (B-C) F4/80+ TAMs and CD31+ endothelial cells were quantified in both groups using ImageJ software on 5 independent tumor sections (including tumor center and rim) at 20X magnification and averaged to be expressed as percentage of total area. (D) When mice were sacrificed at end stage disease, ascites was aspirated and the volume was measured and expressed as milliliters. (E) TAM- and endothelial cell density was correlated in untreated (circles) and PLX3397-treated (squares) mice. (F) Tissue sections were double stained for CD206-positivity (M2-TAM marker, red) and CD8 (cytotoxic T cells, blue) using IHC. (G) CD206+ positive cells were quantified similar to (B-C) and expressed as percentage of total area. (H) CD8+ T cells were counted (5 individual areas per tumor and averaged) and expressed as cells per cubic millimeter of tumor area (mm³).

All data is displayed as dot plots including the median and error bars indicating interquartile range. Statistical significance was determined using the Mann-Whitney U test with $p < 0.05$ being statistically significant. The Spearman's Rank Correlation coefficient (ρ) was determined in case of Fig. 2E. *= $p < 0.05$, **= $p < 0.01$, ***= $p < 0.001$, ns=not significant, DC-Tx= DC-therapy, TAM= tumor associated macrophage.

DC-therapy improves CD8⁺ T-cell phenotype whereas M-CSFR-inhibition specifically depletes non-classical monocytes in blood.

We next sought to investigate the potential mechanisms that lead to enhanced survival in DC-therapy only and combination immunotherapy arms in the CBA/J model. To this end, we extracted blood 5 days after start of treatment and analyzed the circulating immune compartment using flow cytometry (Fig. S3). DC-therapy produced a significant increase in CD8⁺ T cell numbers with CD4⁺ Foxp3⁺ T-helper cell numbers remaining unchanged, whereas proliferation, as determined by Ki-67 expression, was increased in both T-cell subsets (Fig. 3A-D, S4A). T-regulatory cells (Tregs) were decreased following DC-therapy and this was further amplified by the addition of PLX3397 treatment, resulting in an improved CD8⁺ T-cell/Treg-ratio (Fig. 3C, Fig. S4B). In addition to proliferation, CD8⁺ T cells from DC-therapy treated mice were predominantly of an effector phenotype, illustrated by the expression of Killer-cell lectin like receptor G1 (KLRG1) and CD4 co-expression (Fig. 3D-F)^{30,31}. These CD4/CD8 double positive cells were also highest in proliferation in all treatment arms as demonstrated by higher fractions Ki-67-positive cells (Fig. S4C-D).

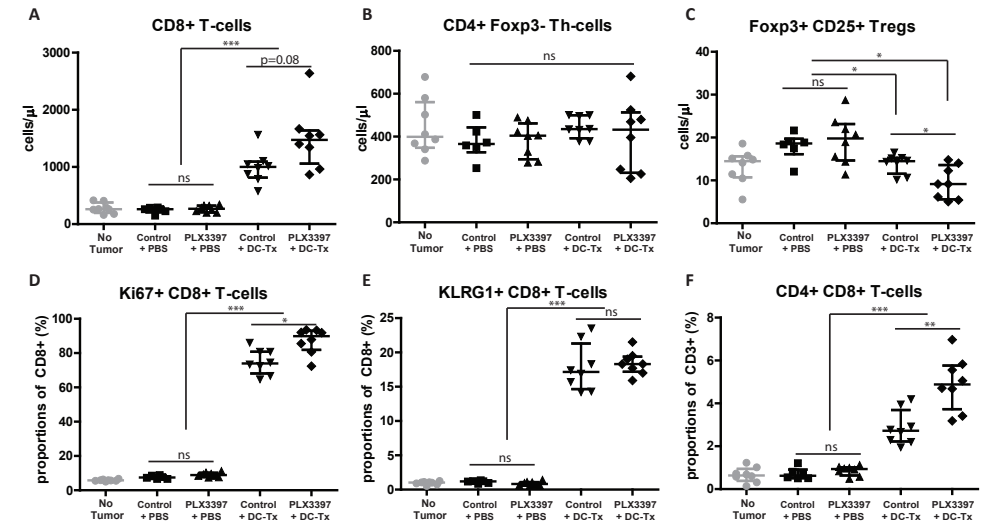


Figure 3. CD8⁺ T-cell proliferation and effector phenotype are further enhanced when combining TAM-depletion with DC-therapy whereas Tregs decrease in blood during therapy. (A-C) Blood was extracted 5 days after start of treatment (day 15 after tumor cell injection) from all CBA/J mice (n=8/group) and was analyzed by multicolor flow cytometry. Immune cell-subsets were characterized as displayed in supplementary figure S2A. (D-F) CD8⁺ T cells were further analyzed for percentage of proliferating (Ki67+, in D), and effector (KLRG1+, in E or CD4+, in F) cells. These data are indicative of two independent experiments. All data is displayed as dot plots with including the median and error bars indicating interquartile range. Statistical significance was determined using the Mann-Whitney U test with $p < 0.05$ being statistically significant. Healthy controls were measured to depict cell frequencies and phenotypes in the non-tumor bearing host, but were not included in further statistical testing. *= $p < 0.05$, **= $p < 0.01$, ***= $p < 0.001$, ns=not significant, DC-Tx= DC-therapy, Th cells= T-helper cells, Tregs= T regulatory cells.

Whereas DC-therapy primarily influenced lymphocyte dynamics and phenotype, PLX3397 therapy predominantly affected myeloid subsets (Fig. 4). Granulocyte and total monocyte numbers were increased by DC-therapy but only granulocytes were expanded by PLX3397 as mono- or combination therapy (Fig. 4A-B). Monocytes can be subdivided into classical Ly6C^{hi} and non-classical Ly6C^{low} monocytes with each subset having different functions and migration patterns in blood^{32,33}. Dissecting monocyte subsets in our model revealed nearly complete depletion of non-classical (Ly6C^{low}) monocytes in the PLX3397 treated arms, whereas classical (Ly6C^{hi}) monocytes numbers were increased (Fig. 4C-D). Interestingly, non-classical monocytes expressed high levels of PD-L1, which was significantly decreased by M-CSFR-inhibition (Fig.4F). Classical monocytes manifested low PD-L1 expression, which was similar in DC-therapy and combination therapy treated mice (Fig. 4E).

PART B
Improving the efficacy of
cancer vaccines for solid tumors
by combination immunotherapy

DEPLETION OF TUMOR-ASSOCIATED
MACROPHAGES WITH A CSF-1R KINASE INHIBITOR
ENHANCES ANTI-TUMOR IMMUNITY AND SURVIVAL
INDUCED BY DENDRITIC CELL IMMUNOTHERAPY

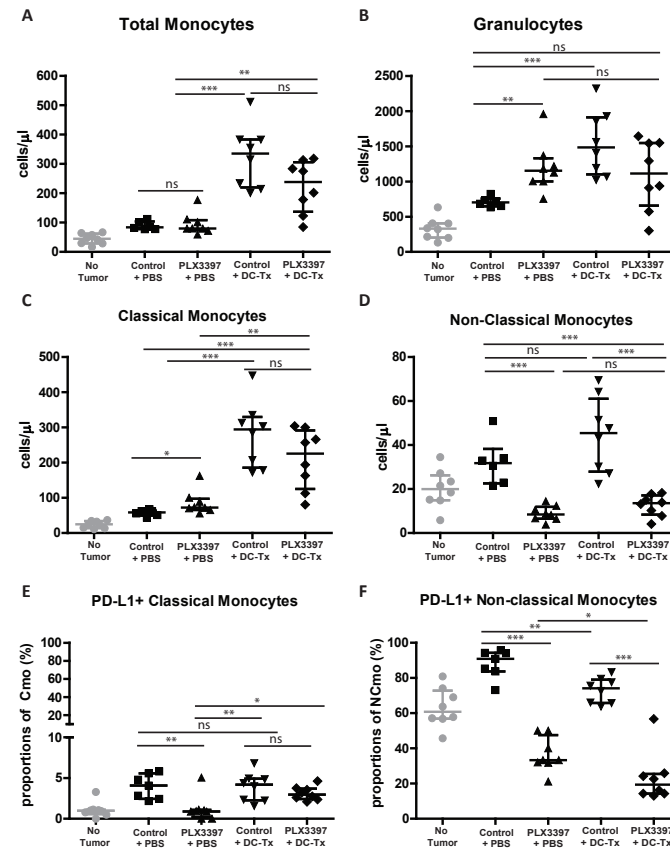


Figure 4. Non-classical monocytes are specifically depleted following M-CSFR-inhibition and these cells are highest in PD-L1 expression in blood of mice during therapy. (A-B) Total monocytes (A) and granulocytes (B) in treated tumor bearing CBA/J mice were measured in parallel with the lymphoid cell subsets depicted in Fig. 3. (C-D) Monocytes were further classified into classical (Ly6Chigh) and non-classical (Ly6Clow/-) monocytes and expressed as number of cells per μ l blood. (E-F) PD-L1 positivity was determined on both monocyte subsets and expressed as percentage of PD-L1-positive cells in each subset.

These data are indicative of two independent experiments. All data is displayed as dot plots with including the median and error bars indicating interquartile range. Statistical significance was determined using the Mann-Whitney U test with $p < 0.05$ being statistically significant. Healthy controls were measured to depict cell frequencies and phenotypes in the non-tumor bearing host, but were not included in further statistical testing.

*= $p < 0.05$, **= $p < 0.01$, ***= $p < 0.001$, ns=not significant, DC-Tx= DC-therapy, PD-L1= programmed death- ligand 1, Cmo= classical monocytes; NCmo= non-classical monocytes.

Overall, the observed synergy between therapies was illustrated in the CBA/J model by an improved CD8⁺ T-cell phenotype which was primarily DC-therapy mediated, and a decrease in PD-L1⁺ non-classical monocytes due PLX3397-treatment. Similar patterns in blood immune cell dynamics could be discerned in the AB1 tumor model, however numbers of mice were limited at day 5 after start of treatment (Fig. S5).

Tumors of combination therapy treated mice exhibit a favorable tumor microenvironment characterized by low IL-10⁺ TAMs and an increased fraction of non-exhausted CD8⁺ T-cells during therapy.

To examine the tumor microenvironment (TME) for the effects of treatment and to relate these to changes in immune cell composition observed in spleen and blood, we sacrificed mice at day 15 in our CBA/J model. Five days after commencing therapy there was already a considerable tumor burden which was at that point still comparable between the different treatment groups (Fig. 5A). TME immune composition at day 15, however, markedly differed between treatment groups in line with interim analyses in blood and findings in end stage disease tumors of diseased mice (Fig. S6A). Both IL-10⁺ (M2) and IL-10⁻ (M1) TAMs were diminished by PLX3397 as monotherapy or in combination with DC-therapy (Fig. 5B). We also further characterized peripheral blood non-classical monocytes as being higher in IL-10 and PD-L1 expression and surface MHC-II^{low}, further establishing their immune suppressive phenotype (Fig. S6B).

Confirming earlier results, the numbers of CD8⁺ tumor infiltrating lymphocytes (TILs) were not altered following PLX3397 monotherapy, and these TILs displayed an exhausted phenotype³⁴, defined as PD-1 positive, lymphocyte-activation gene 3 (LAG-3) positive, and interferon-gamma (IFN γ) negative (Fig. 5C). DC-therapy in contrast, enhanced the number of non-exhausted CD8⁺ T-cells in the tumor. This did not differ between DC-therapy only and combination therapy-treated mice (Fig. 5C) To investigate whether this was a kinetics-related phenomenon, we treated tumor-bearing mice on day 15 and analyzed the tumor 8 days later to allow for proper T-cell infiltration. In addition, we sought to identify T-cell clones specific for the clinically meaningful tumor antigens Mesothelin and Wilms Tumor 1 (WT1) to assess whether CD8⁺ T cells with these tumor-specificities were enhanced by DC-therapy and possibly enriched or improved in phenotype by co-administration of PLX3397. Both tumor antigens were highly expressed by the AC29 mesothelioma cell line (Fig. S1B) and T-cells specific for these antigens were present in tumors from mice in all treatment groups, with an increase in WT1-specific but not Mesothelin-specific CD8⁺ T cells in DC-therapy-treated mice (Fig. 5D). Importantly, there were prominent differences in CD8⁺ T-cell phenotype in combination therapy-treated mice compared to those receiving DC-therapy only, as determined by a higher proportion of PD1-negative and -intermediate expressing cells (Fig S7). These cells are known to be capable of eliciting potent anti-tumor functions³⁵⁻³⁷. In line with this less-exhausted phenotype is the lower expression of co-inhibitory molecules TIM3 and LAG3, and lower expression of CD8 indicative of enhanced activation (Fig. S7B,³⁸). Similar shifts in PD1-expression were detected in both the Mesothelin- and WT1-specific T cells (Fig. 5E, Fig. S7D).

PART B
Improving the efficacy of
cancer vaccines for solid tumors
by combination immunotherapy

DEPLETION OF TUMOR-ASSOCIATED
MACROPHAGES WITH A CSF-1R KINASE INHIBITOR
ENHANCES ANTI-TUMOR IMMUNITY AND SURVIVAL
INDUCED BY DENDRITIC CELL IMMUNOTHERAPY

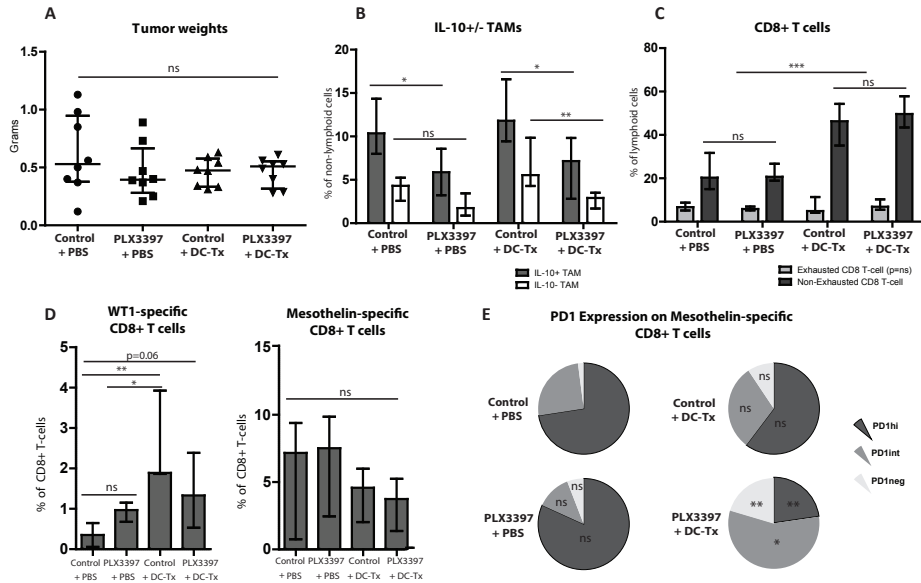


Figure 5. M-CSFR-inhibition decreases tumor associated macrophages in mesothelioma and improves the DC-therapy induced CD8+ T-cell phenotype. Identical to previous experiments, CBA/J mice were intraperitoneally inoculated with tumor cells and treated on day 10 with either DC-therapy or control PBS, and/or continuous PLX3397- or control treatment. Only now, mice were sacrificed on t=15 days to examine the tumor microenvironment, blood and spleen in the different treatment groups. For D-E, mice were treated at day 15 with either PLX3397 and/or DC-therapy and sacrificed 8 days later when tumors were harvested and analyzed. **(A)** Tumors were extracted from the peritoneal cavity and weighed. **(B)** Tumors were dissociated and single cell suspensions that were stained and analyzed by flow cytometry. TAMs were divided into IL-10 positive and negative and denoted as percentage of non-lymphoid cells, to correct for changes in lymphoid cells due to treatment. **(C)** Similar to (B), CD8+ tumor infiltrating lymphocytes (TILs) were identified. The distinction was made between 'exhausted' (Program Death 1+ [PD-1], Lymphocyte-activating-gene 3+, [LAG3+] & Interferon-gamma-[IFN γ]) and 'non-exhausted' (PD-1-, LAG3-, IFN γ +) CD8+ TILs. Cells were depicted as percentage of total lymphoid cells, to correct for changes in the myeloid compartment due to treatment. **(D)** The frequencies of WT-1 and Mesothelin-specific T cells were determined in the tumors of mice treated with or without PLX3397 and/or DC-therapy using dexamers. **(E)** Pie charts depicting the distribution of PD1-expression on Mesothelin-specific CD8+ T-cells in the tumors of mice untreated or treated with the different immunotherapies as monotherapy, or in combination.

All data is displayed as dot plots or bar graphs including the median and error bars indicating interquartile range. Pie charts are used to display distribution of PD-1 expression on CD8+ T-cells in the different treatment arms. Statistical significance was determined using the Mann-Whitney U test with $p < 0.05$ being statistically significant.

* $p < 0.05$, ** $p < 0.01$, *** $p < 0.001$, ns=not significant, DC-Tx= DC-therapy, TAM= tumor associated macrophage, IL10= Interleukin 10, WT1= Wilms Tumor 1, PD1= Programmed cell death protein 1, PD1hi= PD1-high, PD1int= PD1-intermediate, PD1neg= PD1-negative

In summary, we observed a PLX3397-dependent reduction in TAM frequency with a concurrent DC-therapy dependent increase in tumor infiltrating CD8+ T cells whose phenotype was significantly improved upon TAM-depletion as shown by a decrease in proportion of PD1-high CD8+ T cells associated with T-cell exhaustion.

Mice treated with DC-therapy are protected following tumor-rechallenge and combination therapy treated mice display superior recall responses.

To investigate whether the pro-inflammatory phenotype present at day 5 following therapy persisted in treated mice, blood was extracted 3 months later (day 107) from surviving mice (treated with DC-therapy, either as a monotherapy or in combination with PLX3397). At this time point, non-classical monocyte frequencies were low but this was less pronounced as on day 15 (Fig. 6A). The percentage of PD-L1-positive non-classical monocytes, however, was decreased and was negligible on classical monocytes (Fig. 6B). Prior to rechallenge, CD8+ T-cell numbers were increased in treated mice compared to untreated tumor naïve mice, but proliferation and effector phenotype had returned to a resting state (Fig. 6C-D).

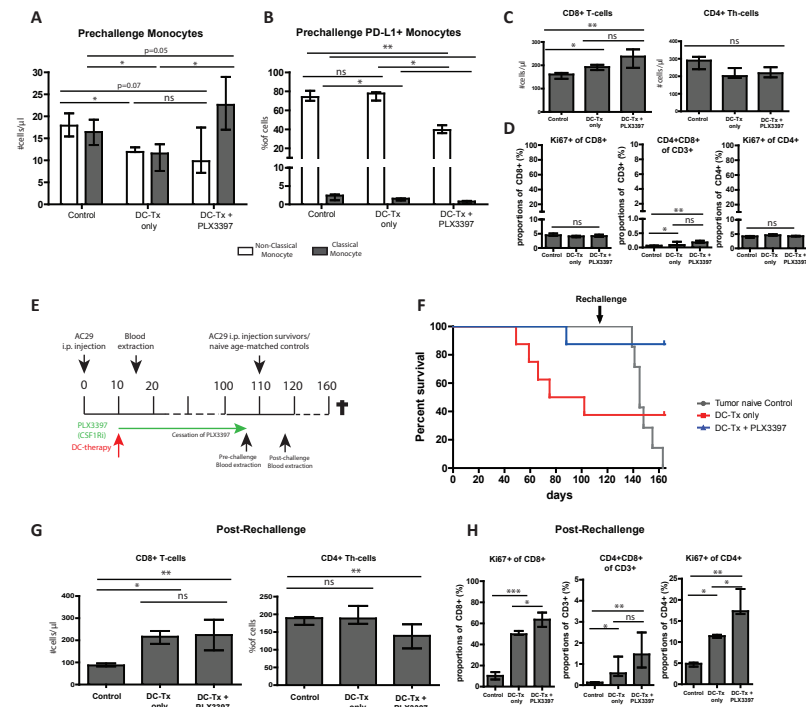


Figure 6. Mice treated with DC-therapy and/or M-CSFR-inhibition were protected from tumor-rechallenge and combination therapy treated mice displaying superior recall responses. **(A-B)** Monocyte subsets and related PD-L1 expression was assessed by flow cytometry in blood prior to rechallenge. **(C-D)** CD8+ and CD4+ T-cell frequencies and proliferation status as determined by Ki-67 were evaluated using flow cytometry. **(E)** Surviving mice from the experiment described in Figure 1 and age-matched tumor naïve mice were rechallenged and subsequently

PART B

Improving the efficacy of cancer vaccines for solid tumors by combination immunotherapy

DEPLETION OF TUMOR-ASSOCIATED MACROPHAGES WITH A CSF-1R KINASE INHIBITOR ENHANCES ANTI-TUMOR IMMUNITY AND SURVIVAL INDUCED BY DENDRITIC CELL IMMUNOTHERAPY

>> monitored for signs of illness. Three days prior to rechallenge, PLX3397-treatment in the combination therapy treated mice was terminated and mice were put on control chow for the further duration of the experiment. Also, blood was extracted at that time point, and again eight days after rechallenge. (F) Kaplan-Meier curve of survival following rechallenge. For DC-only (red) and combination therapy treated mice (blue), curves were identical to the KM-curve in figure 1 but on day t=110, mice were rechallenged. Tumor naïve littermates (grey) were injected with tumor cells in parallel to ensure tumor pathogenicity and correct for age. (G-H) T-cell features as in (C-D) were analyzed in DC-only, DC+PLX3397 combination and untreated mice before and after rechallenge. All data is displayed as bar graph or line graphs including the median and error bars indicating interquartile range. Statistical significance was determined using the Mann-Whitney U test with $p < 0.05$ being statistically significant. *= $p < 0.05$, **= $p < 0.01$, ***= $p < 0.001$, ns=not significant, DC-Tx= DC-therapy, PD-L1= programmed death-ligand 1.

To test whether surviving CBA/J mice (Fig. 1D) were free of tumor and protected against a second tumor encounter, they were re-challenged with mesothelioma in parallel with age-matched tumor-naïve mice (Fig. 6E). Three days prior to rechallenge, PLX3397 treatment was terminated and blood was again extracted eight days after rechallenge and recall responses were evaluated. After rechallenge, all tumor naïve mice reached their humane endpoint due to high tumor burden whereas DC-therapy treated and combination therapy treated mice remained disease free (Fig. 6F). CD8⁺ T-cell levels were higher in protected mice after challenge compared to control mice but similar in both treatment groups, whereas CD4⁺ T-helper cells were lower in the combination therapy treated mice (Fig. 6G). Strikingly, CD8⁺ and CD4⁺ T-cell proliferation was significantly higher in DC+PLX3397-treated mice compared to DC-only mice, indicating superior memory responses after dual immunotherapy (Fig. 6H).

Taken together, these findings demonstrate that targeting the TME and simultaneously directing the immune system to combat cancer can lead to durable responses in mesothelioma bearing mice and improved recall responses.

DISCUSSION

We have shown that combination therapy using two safe anti-cancer treatment strategies being DC-therapy and M-CSFR-inhibition through the small molecule inhibitor PLX3397, results in improved overall survival and superior anti-tumor immune reactivity in mesothelioma mouse models. Whereas TAM-depletion in itself was insufficient to increase and improve anti-tumor T-cell responses, DC-monotherapy improved survival in mice but still most mice progressed after treatment, paralleling findings in patients who develop resistance to immunotherapy^{20,21,39}. Only when PLX3397 treatment was combined with dendritic cell vaccination, we observed that the decrease in TAMs was associated with an increase in CD8⁺ T-cell numbers and functionality, both in the TME and in the circulation. In particular, our data show that CD8⁺ T cells, including WT1- and Mesothelin-specific

CD8⁺ T cells, in the TME of combination therapy-treated mice expressed lower levels of key inhibitory molecules PD-1, LAG3 and TIM3, associated with exhaustion, on their cell surface. Our findings are in line with previous reports in MM patients where a high CD8⁺ T cell to M2 TAM ratio was related to better survival^{9,12}. Combining DC-therapy with M-CSFR-blockade may be a safe and effective strategy to increase this clinically relevant ratio and improve disease prognosis.

To identify mechanisms of therapeutic resistance, we analyzed tumors in mice that received DC-monotherapy and found dense CD206⁺ F4/80⁺ TAM infiltrates similar to untreated mice (*unpublished observations*). TAMs are a major leukocyte subset in the stroma of mesothelioma and other cancers and capable of potently suppressing endogenous or treatment-induced anti-tumor T-cell responses^{8,11}. Depletion of this immune suppressive cell type may thus render previously immune resistant or escaped tumors sensitive to checkpoint inhibition⁴⁰, chemo- and radiotherapy^{41,42}, and cellular therapies such as adoptive T-cell transfer⁴³ and now also DC-therapy. Therapies such as chemo(radio) therapy and PD-1 checkpoint inhibitors, however, either come with significant side effects or appear to be most effective in boosting a pre-existing anti-tumor T cell response^{3,4}. DC-therapy effectively induces novel anti-tumor immune responses which can be further sustained and improved by targeting the generally immune suppressive TME^{23,44}.

M-CSFR-inhibition has been shown to effectively deplete TAMs in multiple tumor models but its effects on survival as monotherapy or combined with other therapies differ considerably between experimental systems^{16,18,41,45}. For example, when M-CSFR-inhibition was combined with a tumor vaccine or with certain chemotherapeutic drugs, efficacy of these therapies was abrogated, questioning the role of TAMs in tumor behavior and response to these therapies^{16,45,46}. On the other hand, Pyonteck *et al.* showed significant improvement of survival in glioblastoma (GBM) bearing mice using the M-CSFR-inhibitor BLZ945 as monotherapy¹⁶. Although resistance to monotherapy ensued in the majority of mice, tumors regressed due to skewing of M2 to M1 TAMs rather than TAM depletion. In our models, M-CSFR-inhibitor monotherapy was insufficient in prolonging survival on its own despite gross changes in stromal composition. These differences in drug efficacy may be explained by TAM-dependency of certain therapies, mechanism of M-CSFR-inhibition, timing of therapy and tumor stage and type⁴⁶. In the GBM model for example, TAM skewing was dependent on glioblastoma cell-derived factors including granulocyte-macrophage colony stimulating factor (GM-CSF)¹⁶. GM-CSF is often used to culture pro-inflammatory M1 macrophages and DCs whereas M-CSF cultured macrophages display a pronounced M2 phenotype^{14,28,47}. Other tumor types such as mesothelioma, both in patient and in mice produce considerable amounts of M-CSF, but only sparsely produce GM-CSF⁴⁸ (*unpublished observations*) providing a likely explanation for the depletion, rather than skewing of TAMs in our models.

Although CD8⁺ TILs were present in mesothelioma tumors of untreated mice, they did not increase in frequency or functionality following TAM-depletion and maintained an exhausted, dysfunctional phenotype. By inducing an immune response using DC-therapy in late stage disease, functional TIL-frequencies increased, but survival was unaltered in BALB/c mice, or prolonged in the CBA/J model with most mice showing disease progression/recurrence during follow-up. Tumor responses were only durable in the majority of mice when DC-therapy was applied in a TAM-deficient TME. We could detect this synergy between therapies in T-cell proliferation and phenotype in blood during therapy and after rechallenge, and in the tumor where T-cell phenotype was markedly improved following TAM depletion. Which immune suppressive property of TAMs is particularly involved in the induction of T-cell exhaustion in our model remains to be fully elucidated, but most likely involves multiple factors (e.g. IL-10, arginase, PD-L1)^{8,49}.

Because in MM patients, a decrease or lack of circulating DCs or loss of DC function correlates with worse survival⁵⁰, it is attractive to speculate that the PLX3397-mediated depletion of TAMs in our mouse models enhances CD8⁺ T cell functionality via DCs, paralleling reported findings in breast cancer⁵¹. However, this is not likely as we did not observe a PLX3397-mediated induction of intratumoral DCs in our mice (*unpublished observations*). This lack of functional antigen presentation in mesothelioma highlights the limited benefit of exclusively targeting the TME and advocates the use of immunotherapeutic strategies that broaden and improve novel anti-tumor immune reactions such as DC-therapy^{44,52}.

Uncertainty remains about the ontogeny of TAMs in solid tumors. While it is appreciated that classical (Ly6C^{hi}) monocytes are known to be the main precursors of inflammatory DCs and macrophages including TAMs, incongruences exist regarding the sequence of events that precede M2-TAM development^{53,54}. Seminal studies by Geissmann and Yona *et al.* have shown that classical monocytes are obligatory precursors of non-classical monocytes, and that the functions and migration patterns of both cell types differ, with non-classical monocytes being crucial for endothelial and tissue integrity^{32,33}. Others have previously described non-classical monocytes to be particularly dependent on M-CSF for their survival^{13,55}. Non-classical monocytes and TAMs share a similar immune suppressive phenotype and are most sensitive to M-CSFR-inhibition, suggesting a likely relationship between these cell types. Future research will have to further delineate the contribution of non-classical monocytes to TAMs in cancer.

In conclusion, we have demonstrated that therapeutic efficacy of M-CSFR inhibition as monotherapy is limited in mesothelioma. However, TAM-depletion combined with an effective DC-mediated anti-tumor T-cell response is capable of producing durable tumor responses and functional anti-tumor immunity.

REFERENCES

- Postow, M. A., Callahan, M. K. & Wolchok, J. D. Immune Checkpoint Blockade in Cancer Therapy. *Journal of clinical oncology : official journal of the American Society of Clinical Oncology*, doi:10.1200/jco.2014.59.4358 (2015).
- Gajewski, T. F. The Next Hurdle in Cancer Immunotherapy: Overcoming the Non-T-Cell-Inflamed Tumor Microenvironment. *Seminars in oncology* 42, 663-671, doi:10.1053/j.seminoncol.2015.05.011 (2015).
- Smyth, M. J., Ngiow, S. F., Ribas, A. & Teng, M. W. Combination cancer immunotherapies tailored to the tumour microenvironment. *Nature reviews. Clinical oncology* 13, 143-158, doi:10.1038/nrclinonc.2015.209 (2016).
- Teng, M. W., Ngiow, S. F., Ribas, A. & Smyth, M. J. Classifying Cancers Based on T-cell Infiltration and PD-L1. *Cancer research* 75, 2139-2145, doi:10.1158/0008-5472.can-15-0255 (2015).
- Tumeh, P. C. et al. PD-1 blockade induces responses by inhibiting adaptive immune resistance. *Nature* 515, 568-571, doi:10.1038/nature13954 (2014).
- Taioli, E. et al. Determinants of Survival in Malignant Pleural Mesothelioma: A Surveillance, Epidemiology, and End Results (SEER) Study of 14,228 Patients. *PLoS one* 10, e0145039, doi:10.1371/journal.pone.0145039 (2015).
- Lieverse, L. A., Bezemer, K., Aerts, J. G. & Hegmans, J. P. Tumor-associated macrophages in thoracic malignancies. *Lung cancer* 80, 256-262, doi:10.1016/j.lungcan.2013.02.017 (2013).
- Noy, R. & Pollard, J. W. Tumor-associated macrophages: from mechanisms to therapy. *Immunity* 41, 49-61, doi:10.1016/j.immuni.2014.06.010 (2014).
- Cornelissen, R. et al. Ratio of intratumoral macrophage phenotypes is a prognostic factor in epithelioid malignant pleural mesothelioma. *PLoS one* 9, e106742, doi:10.1371/journal.pone.0106742 (2014).
- Cornelissen, R. et al. Intratumoral macrophage phenotype and CD8 T lymphocytes as potential tools to predict local tumor outgrowth at the intervention site in malignant pleural mesothelioma. *Lung cancer*, doi:10.1016/j.lungcan.2015.03.013 (2015).
- Lieverse, L. A. et al. Pleural effusion of patients with malignant mesothelioma induces macrophage-mediated T cell suppression. *Journal of thoracic oncology : official publication of the International Association for the Study of Lung Cancer*, doi:10.1016/j.jtho.2016.06.021 (2016).
- Ujii, H. et al. The tumoral and stromal immune microenvironment in malignant pleural mesothelioma: A comprehensive analysis reveals prognostic immune markers. *Oncoimmunology* 4, e1009285, doi:10.1080/2162402x.2015.1009285 (2015).
- Hume, D. A. & MacDonald, K. P. Therapeutic applications of macrophage colony-stimulating factor-1 (CSF-1) and antagonists of CSF-1 receptor (CSF-1R) signaling. *Blood* 119, 1810-1820 (2012).
- Van Overmeire, E. et al. M-CSF and GM-CSF Receptor Signaling Differentially Regulate Monocyte Maturation and Macrophage Polarization in the Tumor Microenvironment. *Cancer research* 76, 35-42 (2016).
- Laoui, D., Van Overmeire, E., De Baetselier, P., Van Ginderachter, J. A. & Raes, G. Functional Relationship between Tumor-Associated Macrophages and Macrophage Colony-Stimulating Factor as Contributors to Cancer Progression. *Frontiers in immunology* 5, 489 (2014).
- Pyonteck, S. M. et al. CSF-1R inhibition alters macrophage polarization and blocks glioma progression. *Nature medicine* 19, 1264-1272, doi:10.1038/nm.3337 (2013).
- Tap, W. D. et al. Structure-Guided Blockade of CSF1R Kinase in Tenosynovial Giant-Cell Tumor. *The New England journal of medicine* 373, 428-437 (2015).
- Butowski, N. et al. Orally administered colony stimulating factor 1 receptor inhibitor PLX3397 in recurrent glioblastoma: an Ivy Foundation Early Phase Clinical Trials Consortium phase II study. *Neuro Oncol* 18, 557-564 (2016).
- Dammeijer, F. et al. The Efficacy of Tumor Vaccines and Cellular Immunotherapies in Non-Small Cell Lung Cancer: A Systematic Review and Meta-Analysis. *Journal of clinical oncology : official journal of the American Society of Clinical Oncology*, doi:10.1200/jco.2015.66.3955 (2016).
- Hegmans, J. P. et al. Consolidative dendritic cell-based immunotherapy elicits cytotoxicity against malignant mesothelioma. *American journal of respiratory and critical care medicine* 181, 1383-1390, doi:10.1164/rccm.200909-1465OC (2010).
- Cornelissen, R. et al. Extended Tumor Control After Dendritic Cell Vaccination With Low Dose Cyclophosphamide as Adjuvant Treatment in Patients With Malignant Pleural Mesothelioma. *American journal of respiratory and critical care medicine* (2015).

PART B
Improving the efficacy of
cancer vaccines for solid tumors
by combination immunotherapy

DEPLETION OF TUMOR-ASSOCIATED
MACROPHAGES WITH A CSF-1R KINASE INHIBITOR
ENHANCES ANTI-TUMOR IMMUNITY AND SURVIVAL
INDUCED BY DENDRITIC CELL IMMUNOTHERAPY

- 22 Davis, M. R., Manning, L. S., Whitaker, D., Garlepp, M. J. & Robinson, B. W. Establishment of a murine model of malignant mesothelioma. *International journal of cancer. Journal international du cancer* 52, 881-886 (1992).
- 23 Hegmans, J. P., Hemmes, A., Aerts, J. G., Hoogsteden, H. C. & Lambrecht, B. N. Immunotherapy of murine malignant mesothelioma using tumor lysate-pulsed dendritic cells. *American journal of respiratory and critical care medicine* 171, 1168-1177, doi:10.1164/rccm.200501-0570C (2005).
- 24 Sluijter, M. et al. Inhibition of CSF-1R supports T-cell mediated melanoma therapy. *PLoS one* 9, e104230, doi:10.1371/journal.pone.0104230 (2014).
- 25 Veltman, J. D. et al. Low-dose cyclophosphamide synergizes with dendritic cell-based immunotherapy in antitumor activity. *Journal of biomedicine & biotechnology* 2010, 798467, doi:10.1155/2010/798467 (2010).
- 26 Veltman, J. D. et al. Zoledronic acid impairs myeloid differentiation to tumour-associated macrophages in mesothelioma. 103, 629-641 (2010).
- 27 Robinson, B. W. & Lake, R. A. Advances in malignant mesothelioma. *The New England journal of medicine* 353, 1591-1603, doi:10.1056/NEJMra050152 (2005).
- 28 Helft, J. et al. GM-CSF Mouse Bone Marrow Cultures Comprise a Heterogeneous Population of CD11c(+) MHCII(+) Macrophages and Dendritic Cells. *Immunity* 42, 1197-1211, doi:10.1016/j.immuni.2015.05.018 (2015).
- 29 Moughon, D. L. et al. Macrophage Blockade Using CSF1R Inhibitors Reverses the Vascular Leakage Underlying Malignant Ascites in Late-Stage Epithelial Ovarian Cancer. *Cancer research* 75, 4742-4752, doi:10.1158/0008-5472.can-14-3373 (2015).
- 30 Kitchen, S. G. et al. CD4 on CD8(+) T cells directly enhances effector function and is a target for HIV infection. *Proceedings of the National Academy of Sciences of the United States of America* 101, 8727-8732 (2004).
- 31 Olson, J. A., McDonald-Hyman, C., Jameson, S. C. & Hamilton, S. E. Effector-like CD8(+) T cells in the memory population mediate potent protective immunity. *Immunity* 38, 1250-1260 (2013).
- 32 Geissmann, F., Jung, S. & Littman, D. R. Blood Monocytes Consist of Two Principal Subsets with Distinct Migratory Properties. *Immunity* 19, 71-82, doi:10.1016/S1074-7613(03)00174-2.
- 33 Yona, S. et al. Fate mapping reveals origins and dynamics of monocytes and tissue macrophages under homeostasis. *Immunity* 38, 79-91, doi:10.1016/j.immuni.2012.12.001 (2013).
- 34 Wherry, E. J. T cell exhaustion. *Nature immunology* 12, 492-499 (2011).
- 35 Ngiew, S. F. et al. A Threshold Level of Intratumor CD8+ T-cell PD1 Expression Dictates Therapeutic Response to Anti-PD1. *Cancer research* 75, 3800-3811, doi:10.1158/0008-5472.can-15-1082 (2015).
- 36 Im, S. J. et al. Defining CD8+ T cells that provide the proliferative burst after PD-1 therapy. *Nature* 537, 417-421, doi:10.1038/nature19330 (2016).
- 37 Chen, D. S. & Mellman, I. Elements of cancer immunity and the cancer-immune set point. *Nature* 541, 321-330, doi:10.1038/nature21349 (2017).
- 38 Gros, A. et al. PD-1 identifies the patient-specific CD8(+) tumor-reactive repertoire infiltrating human tumors. *The Journal of clinical investigation* 124, 2246-2259, doi:10.1172/jci73639 (2014).
- 39 Kelderman, S., Schumacher, T. N. & Haanen, J. B. Acquired and intrinsic resistance in cancer immunotherapy. *Mol Oncol* 8, 1132-1139 (2014).
- 40 Zhu, Y. et al. CSF1/CSF1R blockade reprograms tumor-infiltrating macrophages and improves response to T-cell checkpoint immunotherapy in pancreatic cancer models. *Cancer research* 74, 5057-5069, doi:10.1158/0008-5472.can-13-3723 (2014).
- 41 DeNardo, D. G. et al. Leukocyte Complexity Predicts Breast Cancer Survival and Functionally Regulates Response to Chemotherapy. *Cancer discovery* 1, 54-67, doi:10.1158/2159-8274.cd-10-0028 (2011).
- 42 Xu, J. et al. CSF1R signaling blockade stanches tumor-infiltrating myeloid cells and improves the efficacy of radiotherapy in prostate cancer. *Cancer research* 73, 2782-2794, doi:10.1158/0008-5472.can-12-3981 (2013).
- 43 Mok, S. et al. Inhibition of CSF-1 receptor improves the antitumor efficacy of adoptive cell transfer immunotherapy. *Cancer research* 74, 153-161, doi:10.1158/0008-5472.CAN-13-1816 (2014).
- 44 Carreno, B. M. et al. A dendritic cell vaccine increases the breadth and diversity of melanoma neoantigen-specific T cells. *Science* 348, 803-808, doi:10.1126/science.aaa3828 (2015).
- 45 van der Sluis, T. C. et al. Therapeutic peptide vaccine-induced CD8 T cells strongly modulate intratumoral macrophages required for tumor regression. *Cancer immunology research*, doi:10.1158/2326-6066.cir-15-0052 (2015).

- 46 De Palma, M. & Lewis, C. E. Macrophage regulation of tumor responses to anticancer therapies. *Cancer cell* 23, 277-286, doi:10.1016/j.ccr.2013.02.013 (2013).
- 47 Lacey, D. C. et al. Defining GM-CSF- and macrophage-CSF-dependent macrophage responses by in vitro models. *Journal of immunology (Baltimore, Md. : 1950)* 188, 5752-5765, doi:10.4049/jimmunol.1103426 (2012).
- 48 Chene, A. L. et al. Pleural effusions from mesothelioma patients induce recruitment of monocytes and their differentiation into M2 macrophages. *Journal of thoracic oncology : official publication of the International Association for the Study of Lung Cancer*, doi:10.1016/j.jtho.2016.06.022 (2016).
- 49 Joyce, J. A. & Fearon, D. T. T cell exclusion, immune privilege, and the tumor microenvironment. *Science* 348, 74-80, doi:10.1126/science.aaa6204 (2015).
- 50 Cornwall, S. M. et al. Human mesothelioma induces defects in dendritic cell numbers and antigen-processing function which predict survival outcomes. *Oncoimmunology* 5, e1082028 (2016).
- 51 Ruffell, B. et al. Macrophage IL-10 blocks CD8+ T cell-dependent responses to chemotherapy by suppressing IL-12 expression in intratumoral dendritic cells. *Cancer cell* 26, 623-637, doi:10.1016/j.ccell.2014.09.006 (2014).
- 52 Palucka, K. & Banchereau, J. Cancer immunotherapy via dendritic cells. *Nature reviews. Cancer* 12, 265-277, doi:10.1038/nrc3258 (2012).
- 53 Franklin, R. A. et al. The cellular and molecular origin of tumor-associated macrophages. *Science* 344, 921-925, doi:10.1126/science.1252510 (2014).
- 54 Movahedi, K. et al. Different tumor microenvironments contain functionally distinct subsets of macrophages derived from Ly6C(high) monocytes. *Cancer research* 70, 5728-5739, doi:10.1158/0008-5472.can-09-4672 (2010).
- 55 MacDonald, K. P. et al. An antibody against the colony-stimulating factor 1 receptor depletes the resident subset of monocytes and tissue- and tumor-associated macrophages but does not inhibit inflammation. *Blood* 116, 3955-3963, doi:10.1182/blood-2010-02-266296 (2010).

PART B
Improving the efficacy of
cancer vaccines for solid tumors
by combination immunotherapy

DEPLETION OF TUMOR-ASSOCIATED
MACROPHAGES WITH A CSF-1R KINASE INHIBITOR
ENHANCES ANTI-TUMOR IMMUNITY AND SURVIVAL
INDUCED BY DENDRITIC CELL IMMUNOTHERAPY

SUPPLEMENTARY DATA

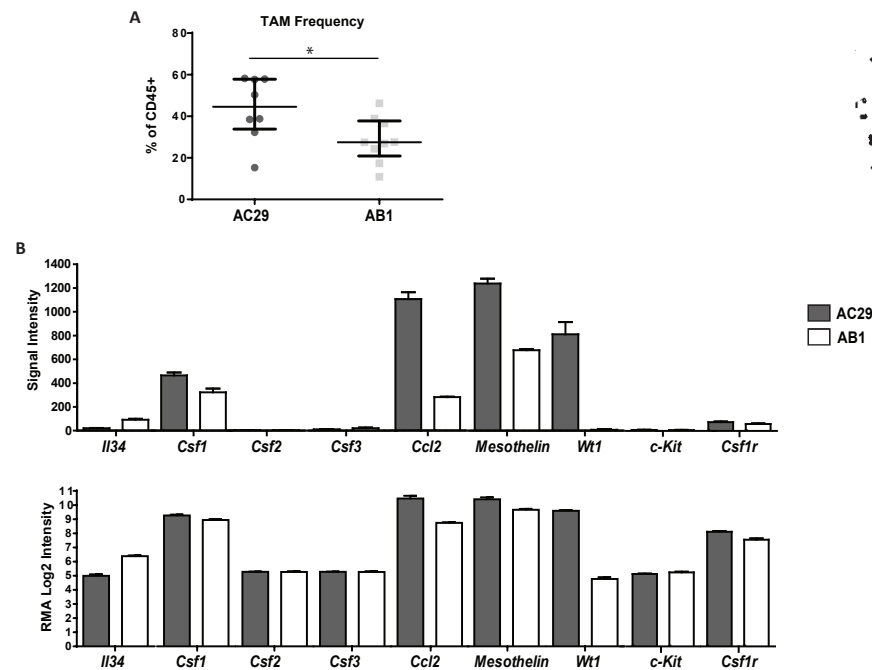


Figure S1. The AC29 mesothelioma tumor model has a more dominant TAM phenotype compared to the AB1 tumor model. (A) The proportion of CD11b, Ly6G⁺, Ly6C⁺, F4/80⁺ TAMs was determined in end-stage AB1 and AC29 mesothelioma tumors by flow cytometry and expressed as percentage of total alive CD45⁺ leukocytes. (B) The expression of key TAM-homing and survival factors was determined by microarray gene expression of AB1 and AC29 mesothelioma cell lines. IL34=interleukin 34, M-CSF= Macrophage colony stimulating factor, GM-CSF= granulocyte macrophage colony stimulating factor, G-CSF= granulocyte colony stimulating factor, CCL2= Ccl2 chemokine (C-C motif) ligand 2, WT1= Wilms Tumor 1. *= $p < 0.05$, **= $p < 0.01$, ***= $p < 0.001$, ns=not significant

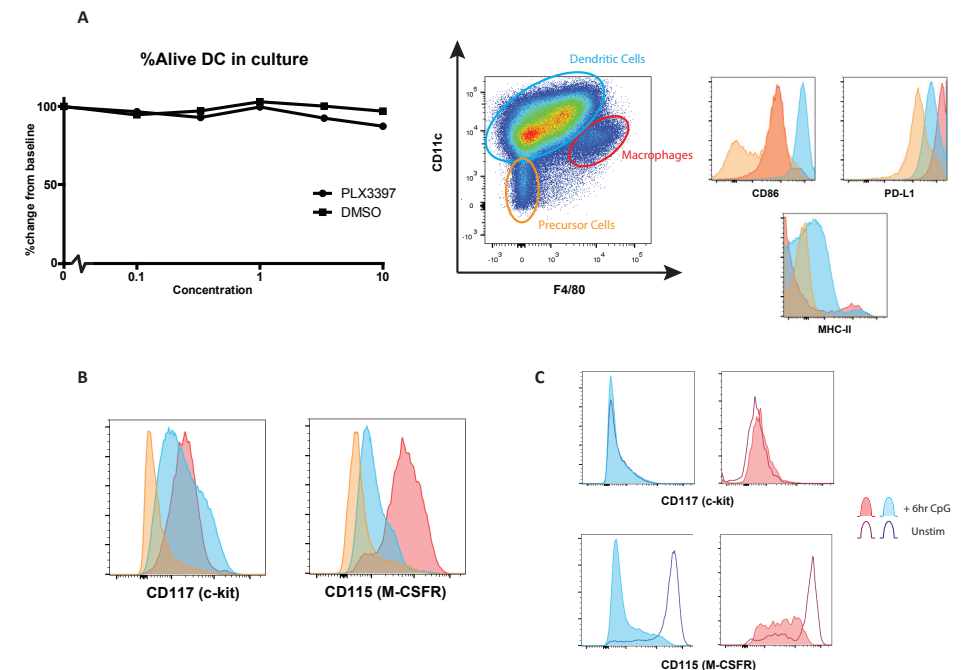


Figure S2. GM-CSF cultured dendritic cells are minimally affected by PLX3397. Mature, lysate loaded DCs were cultured for 48 hours with varying concentrations (no adds, 0.1 μ M, 0.33 μ M, 1.0 μ M, 3.33 μ M, 10.0 μ M) of PLX3397 or the vehicle DMSO to assess effects of the inhibitor on DC-survival and phenotype. (A) DC-viability was assessed using a live/dead marker and measured by flow cytometry. For all conditions, 1×10^6 cells were added to each well and viability was expressed as percentage from baseline (being DC with no adds after 48 hours). In the upper middle panel, the populations derived from the GM-CSF-based culture are depicted based on differential expression of CD11c and F4/80, with DCs being CD11c high-F4/80 low-intermediate (blue), macrophages being CD11c intermediate - F4/80 high (red), and precursor cells (orange) being double negative for both markers. In the upper right panel: differential expression of CD86, PD-L1 and MHC-II on the different cell populations after 48 hours of culture without adds. (B) expression of CD115 (M-CSF-receptor) and CD117 (c-kit) on the cell populations in (A) after 48 hours of culture without adds. (C) Dynamics in CD115 and CD117 expression in (unstimulated) DCs (blue) or macrophages (red) either unstimulated and immature (clear) or after six hours of stimulation with unmethylated CpG motifs (filled).

PART B

Improving the efficacy of cancer vaccines for solid tumors by combination immunotherapy

DEPLETION OF TUMOR-ASSOCIATED MACROPHAGES WITH A CSF-1R KINASE INHIBITOR ENHANCES ANTI-TUMOR IMMUNITY AND SURVIVAL INDUCED BY DENDRITIC CELL IMMUNOTHERAPY

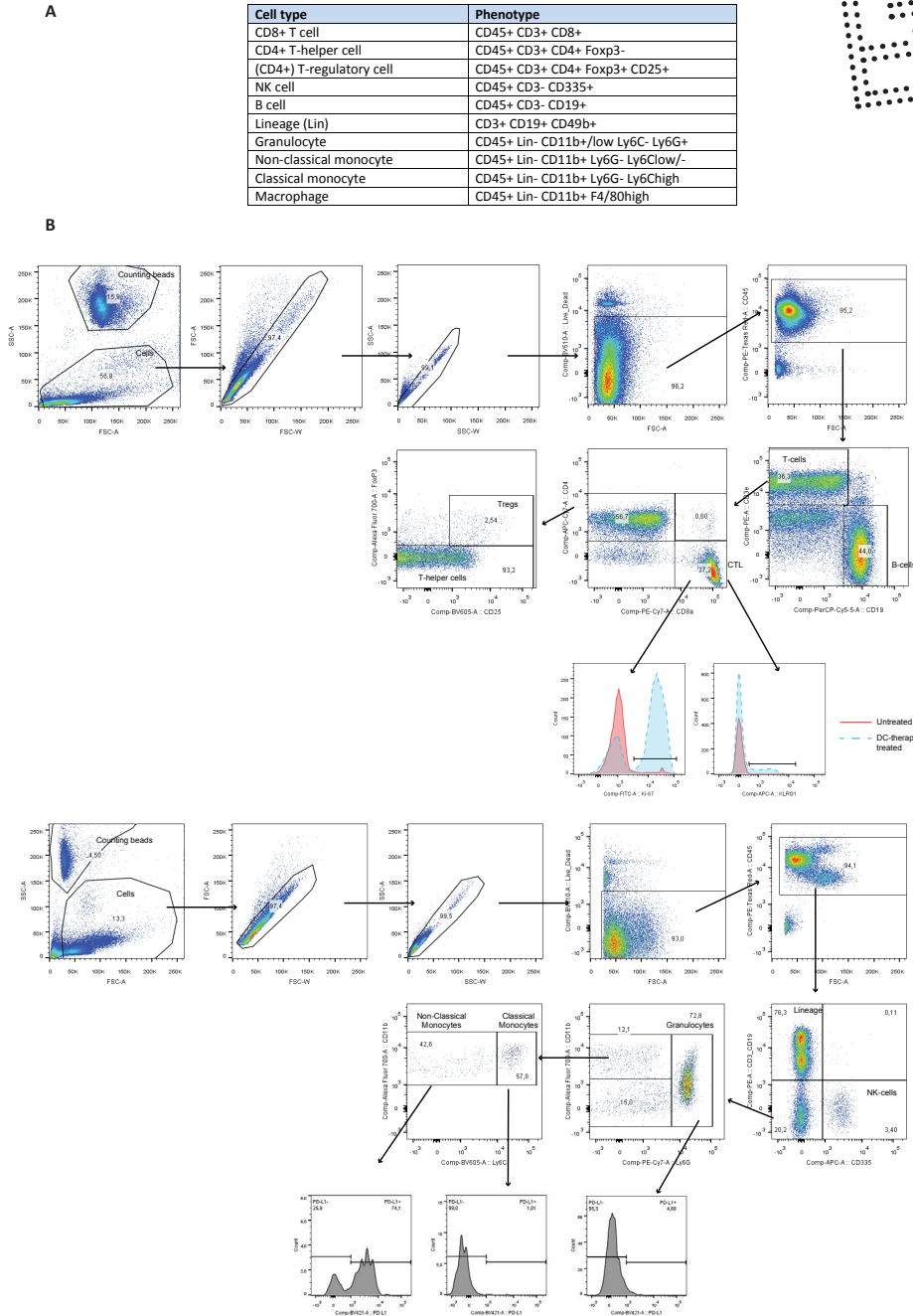


Figure S3. Gating of immune cell subsets in the blood of mice during therapy. (A) Immune cell subsets were defined based on markers derived from literature and measured by multicolor flow cytometry. (B) Cells were derived from lysed blood, tumor and spleen derived single cell suspensions. Counting beads, doublets and dead cells were gated out leaving viable single cells for subsequent immunophenotyping. For the analysis of myeloid cells, gating was preceded by removal of lymphocytes and NK-cells using a lineage mix (CD3+, CD19+ CD49b+).

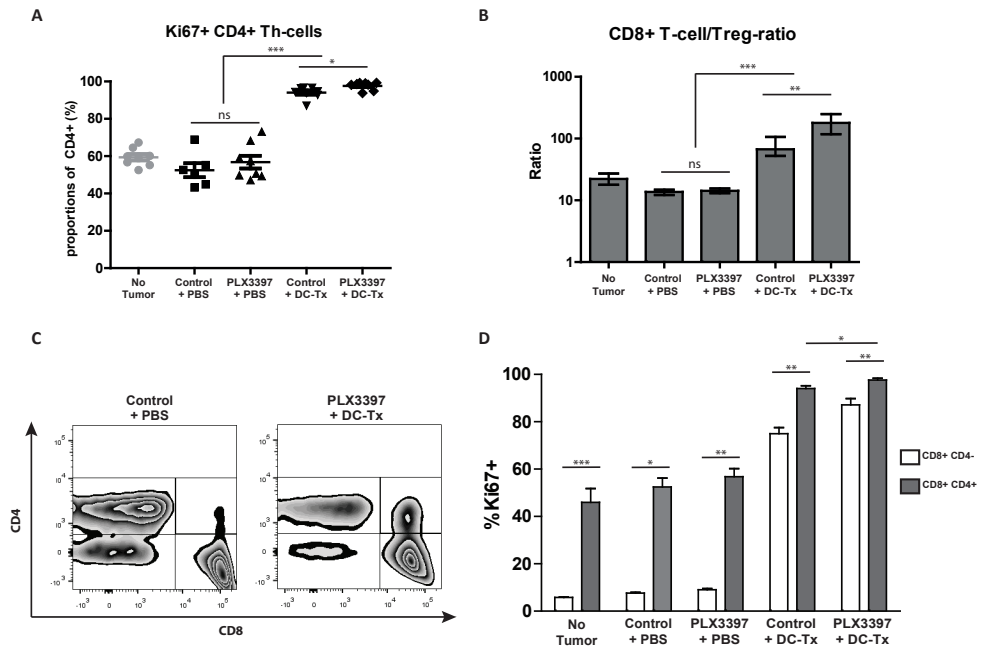


Figure S4. CD4/CD8 Double positive T cells are most abundant after DC- TAM-depletion combination therapy and highest in proliferation marker Ki-67 compared to single positive CD8+ T cells. (A) Similar to Figure 3D, proliferation was assessed in circulating CD4+ T helper cells on day 5 following treatment using the intracellular marker Ki-67. Proliferating cells are depicted as percentage of total CD4+ cells. **(B)** The ratio of absolute CD8+ T cells and T regulatory cells in blood on day 5 following start of treatment was calculated and depicted on a log axis. **(C-D)** CD4+ CD8+ double positive cells were assessed in all treatment groups but were especially evident in the combination therapy treated group. In the right panel, Ki-67-positivity in the parent population is depicted in CD4+ CD8+ double positive (grey) and CD8+ single positive cells (white). Data is displayed as dot plot or bar graph including the median and error bars indicating interquartile range. Statistical significance was determined using the Mann-Whitney U test with $p < 0.05$ being statistically significant. *= $p < 0.05$, **= $p < 0.01$, ***= $p < 0.001$, ns=not significant, DC-Tx= DC-therapy, Treg = T-regulatory cell.

PART B
Improving the efficacy of
cancer vaccines for solid tumors
by combination immunotherapy

DEPLETION OF TUMOR-ASSOCIATED
MACROPHAGES WITH A CSF-1R KINASE INHIBITOR
ENHANCES ANTI-TUMOR IMMUNITY AND SURVIVAL
INDUCED BY DENDRITIC CELL IMMUNOTHERAPY

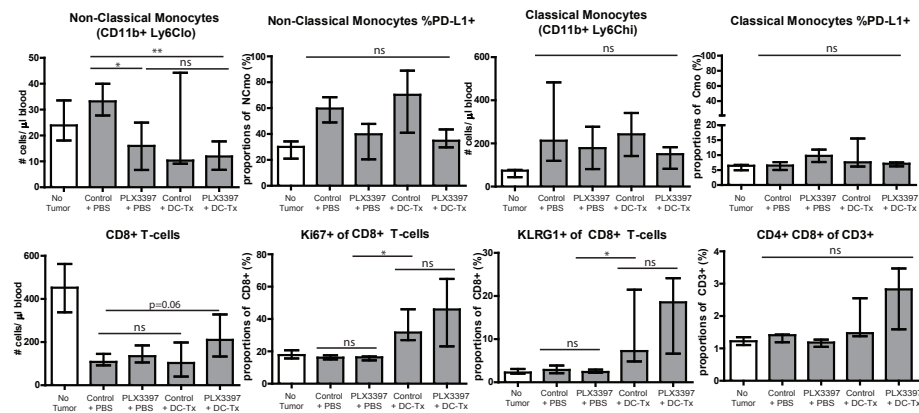


Figure S5. Similar patterns in myeloid and lymphoid cell dynamics in response to treatment were made in the BALB/c (AB1) tumor model compared to the CBA/j (AC29) model. Blood was extracted from BALB/c mice (n=4-5 at t=15, at start of experiment n=6) five days after start of therapy (t=15 post-tumor cell injection) and measured using flow cytometry. The same populations were identified and quantified as in Figure 3 and 4. All data is displayed as bar graph including the median and error bars indicating interquartile range. Statistical significance was determined using the Mann-Whitney U test with $p < 0.05$ being statistically significant. *= $p < 0.05$, **= $p < 0.01$, ***= $p < 0.001$, ns=not significant, DC-Tx= DC-therapy, PD-L1= programmed death-ligand 1, CMO= classical monocytes; NCMo= Non-classical monocytes.

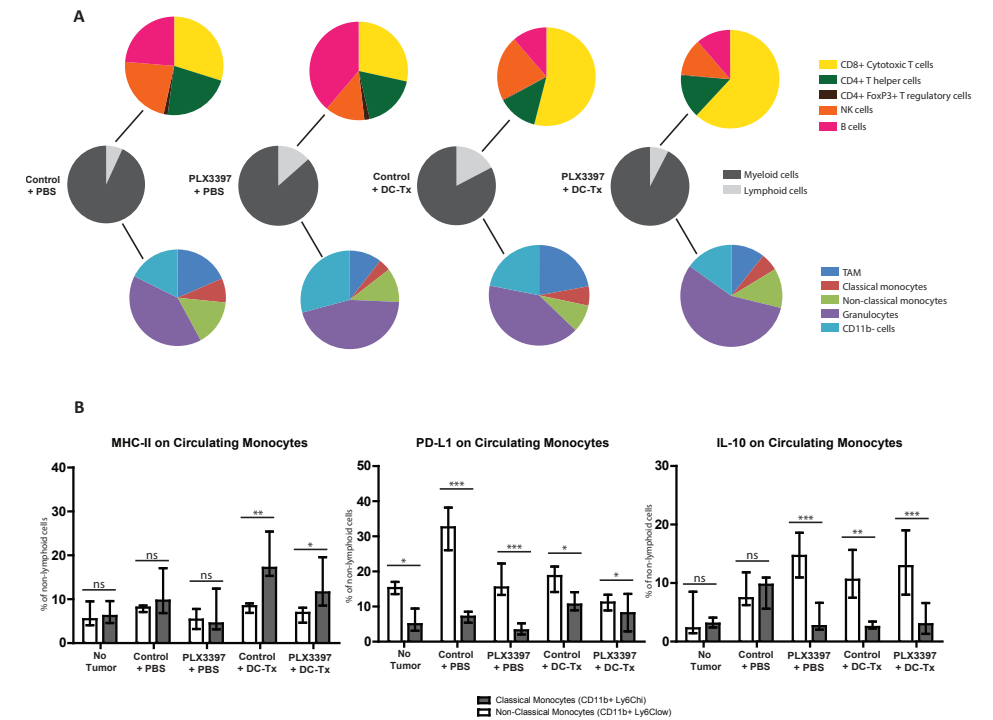


Figure S6. The TME immune contexture at day 15 post tumor injection is differentially modulated by PLX3397 and DC-therapy. (A) Tumor bearing CBA/J mice were sacrificed on t=15 days to examine the tumor microenvironment, blood and spleen in the different treatment groups. The TME of all mice in the 4 treatment groups was dissected by flow cytometry into lymphoid cells and myeloid cells, with further subset characterization per cell type. Cells are depicted as percentage of alive leukocytes (CD45+), followed by subset characterization that was depicted as percentage of lymphoid (CD3+/CD19+/CD335+) or myeloid (CD11b+) cells. (B) Circulating classical- and non-classical monocytes were further characterized by assessing surface expression of PD-L1, MHC-II and IL-10 by flow cytometry. All data is displayed as dot plots or bar graphs including the median and error bars indicating interquartile range. Statistical significance was determined using the Mann-Whitney U test, DC-Tx= DC-therapy, TAM= tumor associated macrophage, NK-cell = Natural Killer cell, MHC-II= major histocompatibility complex-II, IL-10= interleukin 10, CMO= classical monocytes; NCMo= non-classical monocytes.

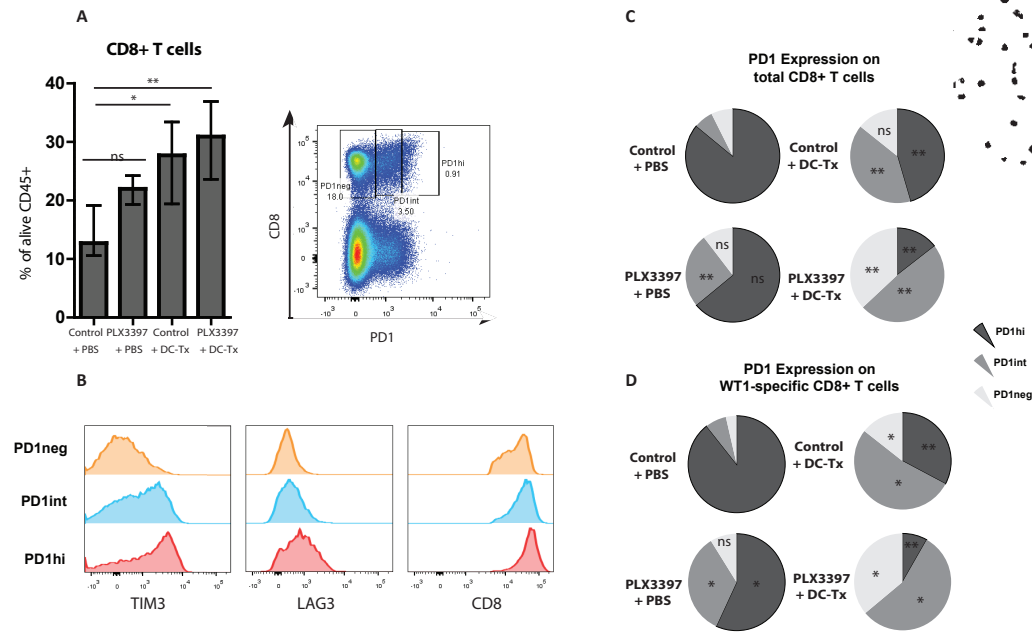


Figure S7. TAM-depletion improves CD8+ T-cell exhaustion status characterized by decreased PD1, LAG3, TIM3 and CD8 expression. (A) CD8+ T-cell frequency was determined from day 23 tumors of CBA/J mice treated on day 15 with/without PLX3397 alone or in combination with DC-therapy (left panel). Subsequently, CD8+ T cells were divided into PD1-negative, -intermediate and high cells (right panel). (B) The expression of LAG3, TIM3, and CD8 was determined on the three populations from Fig. S7A. (C-D) Proportions of PD1-high, -intermediate and negative cells were determined from total tumor CD8+ T cells (C) and WT1-specific CD8+ T cells.

*= $p < 0.05$, **= $p < 0.01$, ***= $p < 0.001$, ns=not significant, DC-Tx= DC-therapy, LAG3=Lymphocyte activation gene 3, TIM3= T-cell immunoglobulin and mucin-domain containing-3 (TIM-3).

6

Sai Ping Lau
Nadine van Montfoort
Priscilla Kinderman
Melanie Lukkes
Larissa Klaase
Menno van Nimwegen
Mandy van Gulijk
Jasper Dumas
Dana AM Mustafa
Lysanne A. Lieveense
Christianne Groeneveldt
Ralph Stadhouders
Yunlei Li
Andrew Stubbs
Koen Marijt
Heleen Vroman
Sjoerd H. van der Burg
Joachim G. Aerts
Thorald van Hall
Casper H.J. Van Eijck
Floris Dammeijer

J Immunother Cancer. 2020 Jul;8(2):e000772.

PART B
Improving the efficacy of
cancer vaccines for solid tumors
by combination immunotherapy

DENDRITIC CELL VACCINATION AND
CD40-AGONIST COMBINATION THERAPY LICENSES T
CELL-DEPENDENT ANTITUMOR IMMUNITY IN
A PANCREATIC CARCINOMA MURINE MODEL

SUMMARY

Pancreatic ductal adenocarcinoma (PDAC) is notoriously resistant to treatment including checkpoint-blockade immunotherapy. We hypothesized that a bimodal treatment approach consisting of dendritic cell (DC) vaccination to prime tumor-specific T cells, and a strategy to reprogram the desmoplastic tumor microenvironment (TME) would be needed to break tolerance to these pancreatic cancers. As a proof of concept, we investigated the efficacy of combined DC vaccination with CD40-agonistic antibodies in a poorly immunogenic murine model of PDAC. Based on the rationale that mesothelioma and pancreatic cancer share a number of tumor associated antigens, the DCs were loaded with either pancreatic or mesothelioma tumor lysates.

Immune-competent mice with subcutaneously or orthotopically growing KrasG12D/+;Trp53R172H/+;Pdx-1-Cre (KPC) PDAC tumors were vaccinated with syngeneic bone-marrow derived DCs loaded with either pancreatic cancer (KPC) or mesothelioma (AE17) lysate and consequently treated with FGK45 (CD40 agonist). Tumor progression was monitored and immune responses in TME and lymphoid organs were analyzed using multicolor flow cytometry and Nanostring analyses.

Mesothelioma-lysate loaded DCs generated cross-reactive tumor-antigen specific T-cell responses to pancreatic cancer and induced delayed tumor outgrowth when provided as prophylactic vaccine. In established disease, combination with stimulating CD40 antibody was necessary to improve survival, while anti-CD40 alone was ineffective. Extensive analysis of the TME showed that anti-CD40 monotherapy did improve CD8⁺ T-cell infiltration, but these essential effector cells displayed hallmarks of exhaustion, including PD-1, TIM-3 and NKG2A. Combination therapy induced a strong change in tumor transcriptome and mitigated the expression of inhibitory markers on CD8⁺ T cells.

These results demonstrate the potency of DC therapy in combination with CD40-stimulation for the treatment of pancreatic cancer and provide directions for near future clinical trials.

INTRODUCTION

Pancreatic adenocarcinoma is currently the fourth leading cause of cancer-related death in the United States and the third in Europe.^{1,2} The incidence is rising and it is expected that pancreatic cancer will be the second leading cause of cancer-related death by 2030.³ The current prognosis of a newly diagnosed pancreatic cancer patient is poor with a 5-year survival of 8.5%.¹ To date, surgical resection is the mainstay of curative treatment. However, this is usually not an option due to local vascular invasion or metastasis at diagnosis. Only 10-20% of all pancreatic cancer patients are eligible for surgical resection and relapse rates are high.^{4,5} Adjuvant chemotherapy following surgical resection improves median overall survival, but even with new chemotherapy regimens cure is exceedingly rare.⁶ Therefore, new treatment modalities are desperately needed in order to achieve durable disease control in pancreatic cancer patients.

Although immunotherapy yields striking results in numerous malignancies, clinical responses in pancreatic cancer have been disappointing.⁷⁻⁹ Reasons for this poor clinical response are likely multifactorial. Pancreatic cancer has been considered an immunologically 'cold' tumor with rare infiltration of cytotoxic T cells, explaining the low response rates to immune checkpoint antibodies.¹⁰⁻¹² A highly immunosuppressive tumor microenvironment (TME) consisting of a plethora of cells including myeloid-derived suppressor cells, tumor associated macrophages (TAMs) and regulatory T cells (Tregs) in conjunction with a characteristic dense desmoplastic stroma has been reported to be responsible for the observed T-cell exclusion and dysfunction in established tumors.¹³ Several therapeutic agents targeting the pancreatic TME have shown promising results.^{14,15} Seminal studies have investigated the potency of CD40-agonistic antibodies in modulating the TME and desmoplastic stroma of pancreatic cancers, thereby allowing T-cell infiltration and anti-tumor efficacy.¹⁶ This was later shown to be dependent on stromalysis by TAM-precursors which, following upregulation of matrix metallo-proteases, degrade fibrosis and support the influx and anti-tumor efficacy of T cells.^{17,18} Although some clinical responses to CD40-agonistic antibodies have been reported, durable responses are limited. A lack of successfully presented and high-quality tumor-antigens has also been proposed to be involved in the lack of immune-reactivity to pancreatic cancers.^{19,20} Akin to this, observational patient studies have shown rare long-term post-resection pancreatic cancer survivors to have increased levels of tumor-reactive T cells in their peripheral blood and tumors.^{20,21} Dendritic cells (DCs) are the most potent T-cell activators of the immune system, and DC vaccination can successfully induce immune responses and clinical responses in various less-immunogenic malignancies when loaded with the appropriate tumor antigens.²² Ideally, these antigens should be derived from the patient's own tumor. However, at this point in time, implementation of these personalized vaccines poses a

logistical hurdle. An allogeneic 'off-the-shelf' strategy for tumor lysate could circumvent this issue and standardize treatment across patients. We have previously shown that treating mesothelioma patients with autologous DCs loaded with a allogeneic tumor lysate is feasible and induces immune responses and tumor regressions in a subset of patients.²² As several tumor-associated antigens (TAAs), such as cancer-testis antigens and tumor differentiation antigens, are shared across different tumor types, this vaccine could be effective in other tumors as well, including pancreatic cancer, which co-expresses several TAAs with mesothelioma tumors (*e.g.* mesothelin, WT-1, MUC1).

Here, we investigated the efficacy of DC vaccination in a representative murine model of human PDAC. We show that vaccination with mesothelioma lysate-loaded DCs yields tumor-specific immune responses against pancreatic cancer and decreases tumor progression. In established tumors, significant prolonged survival was only achieved when DC vaccination was combined with an agonistic CD40 antibody. Extensive analysis of the TME showed that whereas CD40-agonistic antibodies as monotherapy improved intratumoral T-cell infiltration, these cells displayed hallmarks of exhaustion. In the combination treatment, an improved T-cell phenotype lacking the high expression of various inhibitory receptors was observed. Therefore, CD40-agonistic antibody treatment may sensitize pancreatic tumors to tumor-specific immune responses induced by DC vaccination. These translational studies pave the way for future clinical trials investigating DC vaccination in occult disease or as part of combination immunotherapy in inoperable pancreatic cancer patients, some of which have already been initiated (REACTiVe Trial).

METHODS

Mice.

C57BL/6 and CBA/J mice were purchased from Charles River Laboratories and Janvier respectively. All mice were housed in individually ventilated cages, maintained under specific pathogen-free conditions and used at 8-10 weeks of age. All mouse experiments were controlled by the animal welfare committee (IvD) of the Leiden University Medical Center (Leiden) or Erasmus University Medical Center (Rotterdam) and approved by the national central committee of animal experiments (CCD) under the permit numbers AVD116002015271 and AVD101002017867, in accordance with the Dutch Act on Animal Experimentation and EU Directive 2010/63/EU.

Mouse tumor cell lines.

The pancreatic cancer KPC3 cell line is derived from a primary tumor of a female KPC mouse.³¹ AE17 and AC29 cell lines are derived from mesothelioma tumors in C57BL/6

and CBA/J mice and kindly provided by Professor Bruce W.S. Robinson (Queen Elizabeth II Medical Centre, Nedlands, Australia) and Professor Peter D. Katsikis (Erasmus Medical Center, Rotterdam, The Netherlands), respectively. KPC3, AE17 and AC29 tumor cell lines were cultured in RPMI 1640 containing glutamax-I (Gibco), 50 µg/mL gentamicin (Invitrogen), and 8% fetal bovine serum (FBS) (Gibco) at 37°C in a humidified atmosphere containing 5% CO₂. Cell lines were assured to be free of rodent viruses and *Mycoplasma* by regular PCR analysis. Low passage number cultures from stock vials were used for all experiments. Transcriptomes of KPC3, AE17 and B16F10 cells from stock vials were analyzed by Macrogen NGS Services (Macrogen Inc., Seoul, Republic of Korea). Illumina platform was used with TruSeq Stranded Total RNA LT Sample Prep Kit (Human Mouse Rat) Library. MC38 transcriptome data was previously published⁴⁷ and downloaded from Sequence Read Archive (SRA) SRX6812144.

Generation of DC vaccination.

Bone-marrow derived cells seeded in 100mm Petri dishes (day 0) and cultured in 10 mL DC culture medium: RPMI 1640 containing glutamax-I (Gibco), 50 µg/mL gentamicin (Invitrogen), 5% FBS (Gibco), 50µM β-mercaptoethanol (Sigma-Aldrich) and 20 ng/mL recombinant murine granulocyte macrophage-colony-stimulating factor (GM-CSF, kindly provided by Prof. B. Lambrecht, VIB Ghent, Belgium). Cells were cultured at 37°C in a humidified atmosphere containing 5% CO₂. At day 3 and 6 fresh DC culture medium was added. Tumor cell lysate was prepared by freeze-thawing and subsequent sonication for 3x10 seconds with an amplitude of 10mm, using a Soniprep 150 ultrasonic disintegrator equipped with a microtip (Sanyo Gallenkamp). After 9 days of culture, tumor cell lysate was added to the DC cultures, to the equivalent of three tumor cells per DC. After 8 hours, 10 g/mL CpG (ISS-ODN 1668, Invitrogen) was added to the culture to allow complete maturation while incubated overnight. The next day, DCs were harvested and washed three times in PBS. The quality of the DC preparation was determined by cell counting, morphology and cell surface marker expression by flow cytometry, as previously described⁴⁸.

In vivo experiments.

Cultured tumor cells were harvested at 70% confluency. The pancreatic cancer model was generated by injecting 100,000 KPC3 cells in 100µl PBS/0.1% BSA subcutaneously in the flank of the mice or by injecting 10,000 KPC3 cells in 20µl PBS/0.1% BSA orthotopically in the pancreas. The mesothelioma model was generated by injecting 20x10⁶ AC29 cells in 200µl PBS intraperitoneally. Subcutaneous tumors were measured 3-7 times a week in three dimensions using a caliper. Mice were treated with DC immunotherapy at day -7 (seven days before tumor injection) or day 5. Repeated DC vaccination occurred at day 10, 14 and 18 in mice with subcutaneous pancreatic tumors and at day 3, 7 and 11 in mice

with orthotopic pancreatic tumors. One day after DC vaccination, FGK45 or isotype IgG2a was administered intraperitoneally (BioXCell, 70µg/dose). Mice with AC29 tumors were DC vaccinated on day 10 followed by FGK45 on day 10, 12 and 14. For CD4⁺ and CD8⁺ T-cell depletion, mice were injected i.p. two days before treatment and every 6 days onward with GK1.5 and/or 2.42 or isotype IgG2b (BioXCell, 100µg/dose). Peripheral blood samples for interim analysis were collected 4 days after DC vaccination and were immediately stained (see Flow cytometry). Mice were sacrificed at the pre-defined experimental endpoint (Fig. 1, 2 and 3h-j) or when tumors reached a volume of 1000 or 1500mm³.

Cell preparation and flow cytometry.

Whole blood or single-cell suspensions of spleen and tumor were prepared for flow cytometry. Spleens were passed through a 100µm mesh with RPMI 1640 containing glutamax-I (Gibco) and collected through centrifugation. Lymph nodes were excluded during tumor collection and tumors were dissociated using a validated tumor dissociation system (Miltenyi Biotec). To assess cytokine production, lymphoid cells were stimulated for 4 hours at 37°C using PMA and ionomycin supplemented with GolgiStop (BD Biosciences). Intracellular cytokine and transcription factor staining was performed using PFA/Saponin protocol and Foxp3 Transcription Factor Staining Buffer Kit (eBioscience) respectively. Cell surface staining was performed after blocking Fc II/III receptor using anti-mouse 2.4G2 antibody (kindly provided by L. Boon, Bioceros, Utrecht, the Netherlands) by incubating cells with fluorescently conjugated mAbs directed against murine CD3e (145-2C11), CD4 (GK1.5), CD8a (53-67), CD11b (M1/70), CD11c (N418), CD19 (1D3), CD25 (PC61), CD40 (1C10), CD44 (IM7), CD45 (30-F11), CD62L (MEL-14), CD69 (H1.2F3), CD80 (16-20A2), CD86 (GL1), CD103 (2E7), CD107a (1D4B), CD335 (29A1.4), F4/80 (BM8), FoxP3 (FJK-16s), Granzyme B (NGZB), IFNγ (XMG1.2), IL-2 (JES6-5H4), IL-10 (JES5-16E3), Ki-67 (SolA15), LAG-3 (eBioC9B7W), Ly6C (AL-21), Ly6G (RB6.8C5), MHCII (M5/114.15.2), NKG2A (16a11), PD1 (J43) PDL1 (MIH5), TIM3 (8B.2C12), TNFα (MP6-XT22), VISTA (MH5A). Cells were in addition stained for viability using fixable LIVE/DEAD aqua cell stain (Thermo Fisher Scientific). Data were acquired using an LSR-II flow cytometer (BD Biosciences) and analyzed by FlowJo v10.0.7 (Treestar).

In vitro experiments.

Tumor antigen specific T-cell detection assay: Dissected subcutaneous tumors from treated mice and lungs from wild-type C57BL/6 mice were beads homogenized in 150µl Milli-Q for four cycles of 1 minute. A Bradford assay was performed in order to assess the protein concentration. Bone-marrow derived DCs were generated as described above, and loaded with 70µg tumor lysate or 200µg lung lysate/mL DC suspension. Tumor cell line lysate loaded DCs were prepared as described above. Tumor loaded DCs were in vitro co-

cultured with paired splenocytes at a ratio of 1:10 for 4 hours at 37°C supplemented with GolgiStop (BD Biosciences). After 4 hours, intra-cellular cytokine expression was assessed by flow cytometry as described above.

IL-12p40 detection: Bone-marrow derived DCs were cultured as described above. At day 9, FGK45 (BioXCell, 30µg/mL) or isotype IgG2b (BioXCell, 30µg/mL) was added to the DC culture. After 24 hours, supernatant was collected and a sandwich ELISA assay was performed as previously described.³⁷

(Immuno)histochemistry.

Immunohistochemistry was performed with an automated, validated and accredited staining system (Ventana Benchmark Discovery ULTRA, Ventana Medical Systems, USA) using Omnimap anti-rabbit or mouse and the universal DAB detection Kit. In brief, following deparaffinization and heat-induced antigen retrieval the tissue samples were incubated according to their optimized time with CD31 (Abcam; polyclonal). Incubation was followed by hematoxylin II counter stain for 8 minutes and then a blue coloring reagent for 8 minutes according to the manufactures instructions. Tonsil tissue was used as positive control. Thrichome blue was stained using optimized protocol provided in the fully automated Ventana Benchmark Special stains system. Sirius Red was stained by hand, in brief, following deparaffinization slides were rehydrated by passage through decreasing ethanol series, 5 minutes predifferentiation step using 0,2% fosformolybdeen-acid followed by 45 minutes incubation with 0,1% Sirius Red solution. Slides were analyzed using polarization method.

mRNA expression analysis.

NanoString nCounter Technologies was applied on 120µm of Tissue-Tek(Sakura)-embedded fresh frozen tumor samples using the PanCancer IO 360™ Panel. To identify the differentially expressed genes, raw data was normalized using the values of the most stable 15 housekeeping genes selected by applying the geNorm algorithm. Unsupervised clustering of normalized gene expression values (row Z-scores) was performed using the complete linkage method with Euclidean distance measure or standard PCA/t-SNE functions in R (through RStudio v 1.1.463). For the volcano plots, Mann-Whitney U test was conducted to compare the normalized count values in two groups (i.e. monotherapy vs. combination therapy) for each of the 750 markers. The original *p*-values were adjusted for multiple testing using Benjamini-Hochberg procedure. All calculation and the volcano plots were done in program R.

Gene set enrichment analysis was performed by ranking all genes based on difference of means scaled by the standard deviation (signal-to-noise).⁴⁹ Previously reported gene sets M9480 and M5937 were used for exhausted phenotype and glycolysis

enrichment analysis⁵⁰, respectively. The false-discovery rate adjusted p -values (q -value) was considered significant when <0.05 .

Statistical analysis.

Difference between groups of interest were statistically analyzed with the non-parametric Mann-Whitney U test. Data are displayed as means with the standard error of the mean and analyzed using GraphPad Prism software (Graphpad, v7.0a). Survival data were plotted as Kaplan–Meier survival curves. The non-parametric log-rank test (Mantel-Cox test) was used to compare the survival distribution of groups of mice. In all cases a p -value of 0.05 and below was considered significant (*), $p<0.01$ (**) and $p<0.001$ (***) as highly significant.

RESULTS

DC vaccination with mesothelioma lysate induces T-cell immunity and efficacy against pancreatic cancer.

We hypothesized that vaccination with DCs loaded with mesothelioma TAAs can generate a cross-reactive immune response against pancreatic cancer. We, therefore, evaluated whether pancreatic cancer (KPC3) lysate loaded-DCs or mesothelioma (AE17) lysate loaded-DCs induced protective immunity in mice challenged with KPC3 (Fig. 1a). Comparison of RNA-seq transcriptome profiles of KPC3 and AE17, based on a predefined list of validated TAAs, revealed that 63% of the TAAs were expressed by both AE17 and KPC3 (Fig. 1b, Table S1).²³ This supports the notion of shared antigens between the two cancer types. For a more unbiased approach, we also investigated the overlap in transcriptome profiles of KPC3, AE17 and two unrelated cell lines (B16F10, MC38) (Fig. S1). Shared transcripts could be found in all four tumor cell lines. Exposure of DCs to tumor lysates and CpG led to rapid upregulation of activation markers (e.g. CD40, CD80/86) (Fig. S2). Importantly, prophylactic vaccination of mice with DCs loaded with pancreatic or mesothelioma lysate was equally effective in delaying tumor growth and both had significant smaller tumor volumes compared to untreated mice at day 20 (Fig. 1c-d).

To elucidate the mechanisms underlying DC therapy efficacy, we analyzed immune parameters in peripheral blood, spleen and tumors in both pancreatic cancer and mesothelioma lysate-loaded DC therapy treated mice. In vaccinated mice, increased frequencies of circulating CD3⁺, CD4⁺ and CD8⁺ T cells could be detected as early as four days after DC treatment (day -3 before tumor inoculation). These immune responses were durable and persisted over time until day of sacrifice (Fig. 1e). A more in-depth phenotypic analysis demonstrated that vaccinated mice had higher frequencies of activated (CD69⁺),

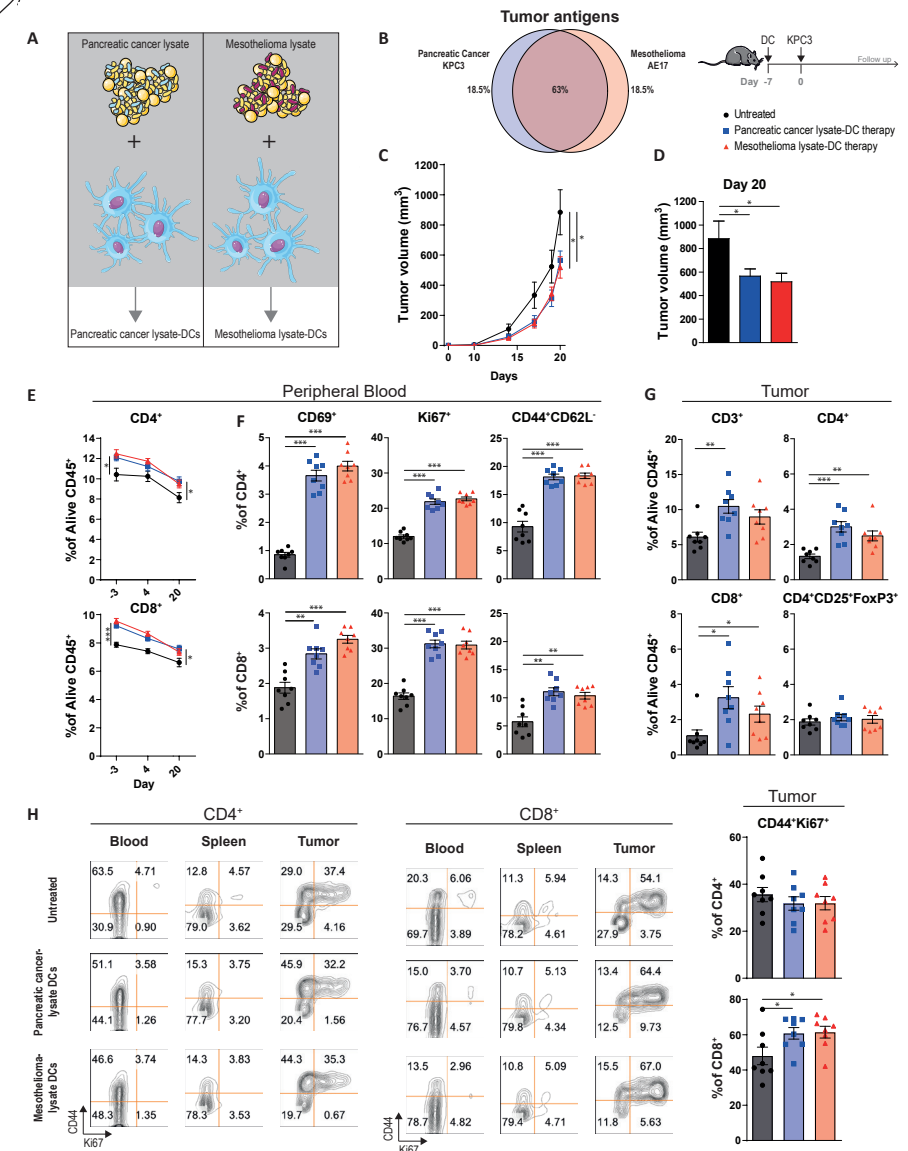


Figure 1. Mesothelioma lysate-DC vaccination is able to delay pancreatic tumor growth and induce strong T-cell immunity. (A) Dendritic cell vaccination study setup. (B) Expression of immunogenic tumor antigens as described by Cheever et al.²³ in the tumor cell line KPC3 and AE17. Percentages indicate amount of overlapping and non-overlapping genes. (C) Tumor volumes (with SEM) measured over time of untreated and treated mice. (D) Tumor size at the time of sacrifice (day 20 after tumor injection). (E) Circulating CD4⁺ and CD8⁺ T-cell frequencies at day -3, 4 and 20. (F) Percentage of CD69⁺, Ki67⁺ and CD44⁺CD62L⁺ subsets of CD4⁺ and CD8⁺ circulating T cells four days after DC vaccination. (G) CD3⁺, CD4⁺, CD8⁺ and CD4⁺CD25⁺FoxP3⁺ TILs as a percentage of alive CD45⁺ cells at day 20 after tumor injection. (H) Expression of CD44 and Ki67 on CD4⁺ and CD8⁺ T cells at day 20 in blood, spleen and tumor. N=8 per group. Significance was determined using the non-parametric Mann-Whitney U test. Data presented as the mean±s.e.m. * $P<0.05$, ** $P<0.01$, *** $P<0.001$.

proliferating (Ki-67⁺) and effector memory (CD44⁺CD62L⁻) CD4⁺ and CD8⁺ T cells in the peripheral blood compared to untreated mice. This did not differ between mesothelioma-lysate and pancreatic cancer-lysate DC-treated mice (Fig. 1f). In contrast to changes in T-cell frequencies, the expression of CD69⁺, Ki-67⁺ and CD44⁺CD62L⁻ on circulating T cells of vaccinated mice waned over time (Fig. S3). Higher frequencies of intratumoral CD4⁺ and CD8⁺ T cells were noted, paralleling the delayed tumor growth observed after vaccination (Fig. 1g). CD8⁺ tumor infiltrating lymphocytes (TILs) of treated mice more often expressed the memory marker CD44 and the proliferation marker Ki-67, which was not observed in the spleen and peripheral blood at the time of sacrifice (Fig. 1h). This was also not observed for CD4⁺ TILs. Importantly, the frequencies of regulatory CD4⁺CD25⁺FoxP3⁺ TILs remained comparable between treated and untreated mice (Fig. 1g). Therefore, DC vaccination is able to induce the infiltration of PDAC tumors with activated, proliferating CD4⁺ and CD8⁺ T cells without concomitant Treg-induction.

DC vaccination depends on tumor antigens and tumor-specific T cells.

We then assessed whether T-cell responses induced by mesothelioma lysate-loaded DCs were reactive to tumor antigens present on pancreas carcinoma cells. Mice treated with mesothelioma lysate-loaded DCs had significantly smaller tumors compared to untreated mice or those treated with non-loaded DCs, suggesting that the delay in tumor outgrowth was due to a TAA-reactive immune response (Fig. 2a). Indeed, CD8⁺ T cells isolated from vaccinated mice responded in vitro specifically to autologous pancreatic cancer lysate-loaded DCs, while T cells from untreated mice or those from non-loaded DC vaccinated mice did not (Fig. 2b). Upon stimulation, higher frequencies of CD8⁺ T cells from mesothelioma lysate-loaded DC treated mice expressed CD107a (being a marker of cytotoxic degranulation), Granzyme B, IFN γ and TNF α compared to CD8⁺ T cells from untreated mice or mice treated with non-loaded DCs. This effect was not observed when CD8⁺ T cells were stimulated with DCs loaded with a control wild type tissue lysate (Fig. 2b), demonstrating that mesothelioma lysate-loaded DCs can generate tumor-antigen specific T cells reactive to antigens also expressed by pancreatic cancer cells. In these in vitro assays, CD8⁺ T cells from vaccinated mice also responded better than those from untreated mice to DCs loaded with B16F10 melanoma lysate (Fig. S4), suggesting induction of immunity to shared tumor antigens across KPC3, AE17 and B16F10 as listed in Table S1.

CD40-agonistic antibody treatment sensitizes established pancreatic tumors to DC vaccination and improves efficacy.

As DC therapy generated systemic anti-tumor immune responses capable of stalling tumor growth when given prophylactically, we set out to test its capacity to control established KPC3 tumors. Although our pilot study demonstrated that tumor lysate-loaded DCs are

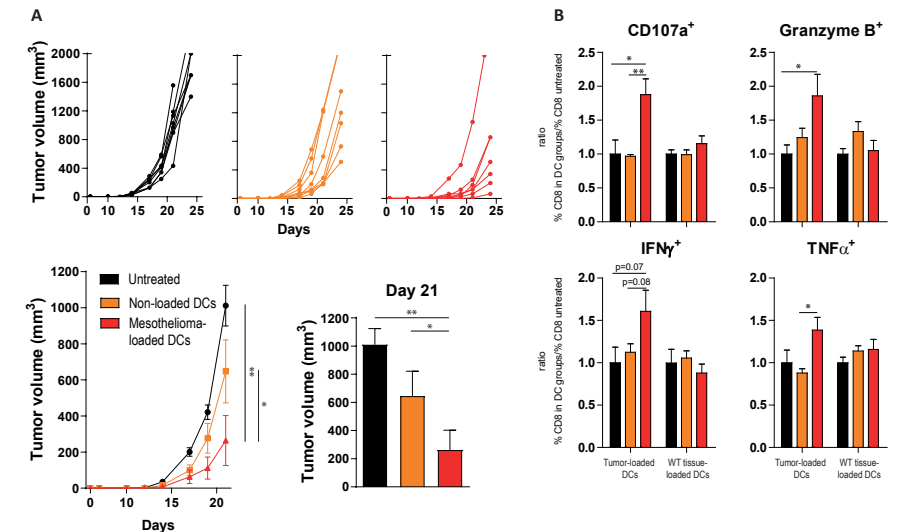


Figure 2. Tumor lysate DCs outperforms non-loaded DCs. (A) Tumor volume measured over time as individual tumor outgrowth curves and per group, and tumor size at day of sacrifice (day 21) of treated and untreated animals. **(B)** In vitro efficacy assay; Relative production of CD107a, Granzyme B, IFN γ and TNF α by CD8⁺ splenocytes of three treatment groups after stimulation with DCs loaded with autologous tumor lysate, or control lung lysate, normalized for untreated mice. N=8 per group. Significance was determined using the non-parametric Mann-Whitney U test. Data presented as the mean±s.e.m. *P<0.05, **P<0.01.

capable of inducing systemic changes in T-cell subsets, as a single therapy it was unable to increase intratumoral T cells or delay tumor growth (Fig. S5). The lack of increased T-cell infiltration found in established tumors in the presence of a systemic immune response suggested that the PDAC TME might physically obstruct T cells from infiltrating the tumor. CD40-agonistic antibodies have previously been found to allow T-cell infiltration due to TME-reorganization in pancreatic cancer, offering a treatment rationale for combination therapy with DC vaccination.¹⁶ As CD40 is also highly expressed on the tumor lysate-loaded DCs (Fig. S2), administering the antibody early following DC transfer might offer additional synergy between these treatments (Fig. S6a). Interestingly, α CD40 combined with DC vaccination resulted in significant tumor growth control when compared to untreated mice while monotherapy DC or α CD40 did not (Fig. S6b). α CD40 monotherapy was able to induce systemic and intratumoral responses (Fig. S6c-f). To show that the efficacy of this combination therapy was not limited to pancreatic cancer or the C57BL/6 mouse strain, we performed a comparable experiment in an mesothelioma tumor model (CBA/J background) yielding similar results (Fig. S7).

As treatment at day 5 after tumor cell injection still reflects minimal disease burden, we aimed at treating larger tumors (day 10) using an intensified treatment schedule (Fig. 3a).

PART B

Improving the efficacy of cancer vaccines for solid tumors by combination immunotherapy

DENDRITIC CELL VACCINATION AND CD40-AGONIST COMBINATION THERAPY LICENSES T CELL-DEPENDENT ANTITUMOR IMMUNITY IN A PANCREATIC CARCINOMA MURINE MODEL

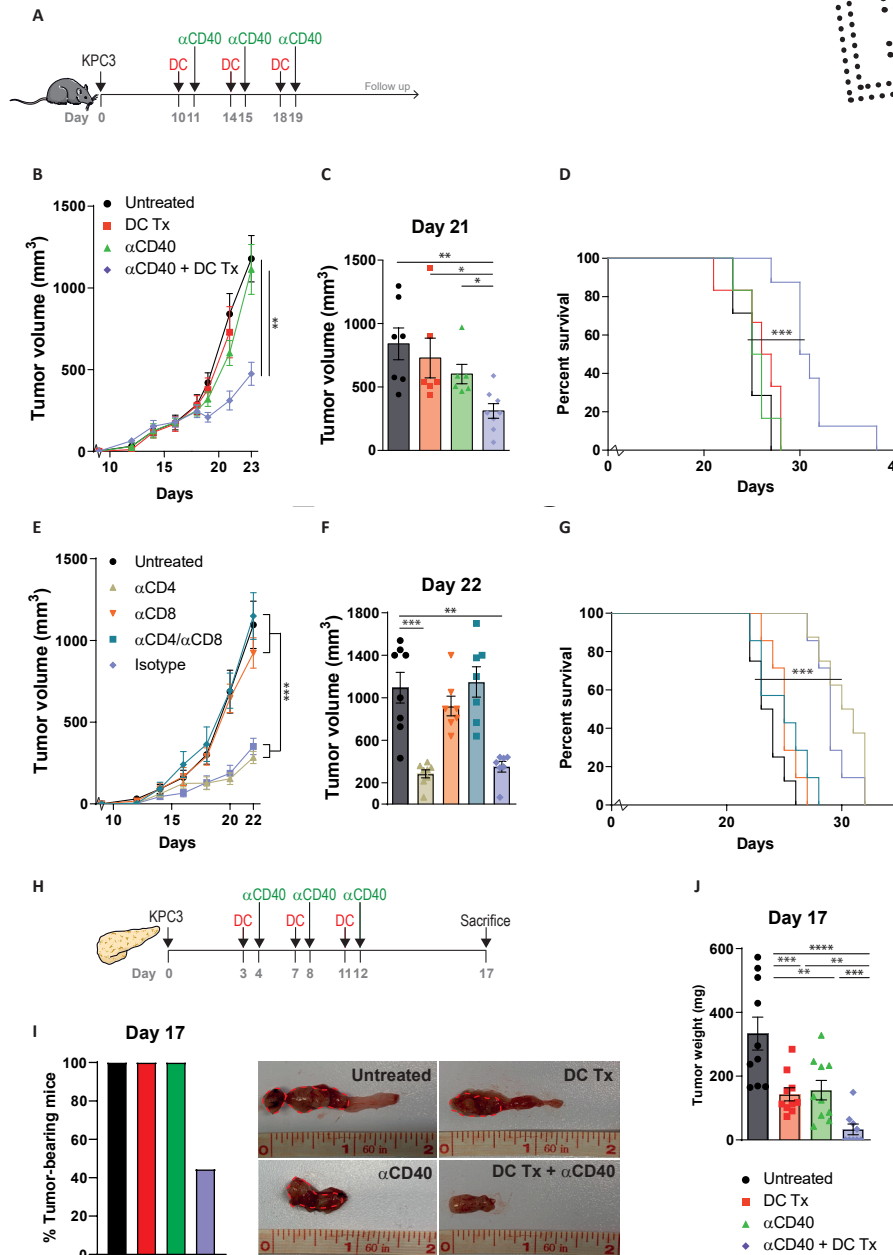


Figure 3. DC vaccination-αCD40 combination therapy improves survival of tumor-bearing mice. (A) Subcutaneous tumor model study setup. Mice were treated with AE17-lysate DCs and FGK45. (B) Tumor volumes measured over time. (C) Tumor size at day 21. (D) Kaplan-Meier analysis of treated and untreated animals. (E) Tumor volumes measured over time. (F) Tumor size at day 22. (G) Kaplan-Meier analysis of treated and untreated animals. (H) Orthotopic tumor model study setup. (I) Percentage of tumor bearing mice. (J) Tumor weight on day 17. N=8-10 per group. Significance was determined using the non-parametric Mann-Whitney U test or log-rank test. Data presented as the mean±s.e.m. *P<0.05, **P<0.01, ***P<0.001.

In this experimental setup, tumor growth and survival of mice treated with monotherapy DC vaccination or αCD40 also did not significantly differ from untreated tumor-bearing mice (Fig. 3b-d, S8). The combination therapy, however, significantly delayed tumor growth (Fig. 3b), led to significantly smaller tumor volumes and improved survival (Fig. 3c-d). In order to elucidate the immunological prerequisites of therapeutic efficacy and to demonstrate if the observed anti-tumoral response is T-cell dependent, mice were depleted of CD4⁺ and CD8⁺ T cells before receiving treatment (Fig. S9). Anti-tumoral efficacy was retained in αCD4 and isotype-treated mice receiving DC vaccination and αCD40 (Fig. 3e-g). However, therapeutic responses were mitigated in mice depleted for CD8⁺ T cells. Importantly, we assessed the efficacy of combination therapy in an orthotropic mouse model, in order to examine if our results could be replicated in a more translational model mimicking the anatomical location and phenotypic features of PDAC (Fig. 3h). Strikingly, 56% (5/9) of all combination therapy-treated mice were macroscopically free of tumor at the day of analysis (Fig. 3i, S10). In contrast, all untreated or monotherapy-treated mice bore tumors and tumor sizes were significantly larger compared to the remaining combination therapy-treated mice with tumor (Fig. 3j).

Interim peripheral blood analysis demonstrated that both monotherapy DC vaccination and αCD40 treatment induced higher frequencies of CD69⁺, Ki-67⁺ and PD-1⁺ T cells. However, this effect was more confined to CD4⁺ T cells when mice were only treated with DC vaccination, and to CD8⁺ T cells for monotherapy αCD40 (Fig. 4a). Combination therapy induced higher frequencies of CD69⁺, Ki-67⁺ and PD-1⁺ for both CD4⁺ and CD8⁺ T cells. Enrichment over time of Ki-67⁺ and PD-1⁺ T cells was detected in mice treated with either combination therapy or αCD40 monotherapy. Furthermore, CD44⁺CD62L⁺ effector memory T cells were significantly increased after both monotherapies and combination therapy (Fig. 4b). Over time, mice treated with combination therapy yielded the highest frequencies of effector memory T cells compared to mice treated with monotherapy or untreated mice. This was observed for both CD4⁺ and CD8⁺ T cells. The enrichment of effector memory T-cell frequencies was less prominent after single DC vaccination and subsequent αCD40 treatment (Fig. S6d), promoting the role of multiple vaccinations.

Combining DC vaccination and αCD40 remodels the tumor microenvironment, including T-cell exhaustion markers.

To further assess the mechanistic underpinnings of combination immunotherapy, we performed extensive analysis on the tumor and intratumoral immune cells, both numerically and phenotypically, using gene expression analysis and multicolor flow cytometry. Intratumoral analysis revealed increased T-cell numbers in treated mice (Fig. 5a). No distinct changes in myeloid subsets could be found (Fig. S11). However, DC therapy did induced a PD-L1 rich tumor microenvironment (Fig. 5b). To get a more

PART B
Improving the efficacy of
cancer vaccines for solid tumors
by combination immunotherapy

DENDRITIC CELL VACCINATION AND
CD40-AGONIST COMBINATION THERAPY LICENSES
T CELL-DEPENDENT ANTITUMOR IMMUNITY IN
A PANCREATIC CARCINOMA MURINE MODEL

profound insight in the intratumoral immune changes induced by combination therapy, we applied NanoString gene-expression technology on tumors of treated and untreated mice. Unsupervised clustering of significantly different immune-related genes revealed that tumors of untreated or monotherapy-treated mice displayed a distinct gene expression profile as compared to mice treated with the combination therapy (Fig. 5c-d, S12), indicating a unique remodeling of the TME.

Mice treated with combination therapy had consistently lower transcript amounts of a wide range of inhibitory receptors, including Pcd1 (PD-1), Ctla4, Entpd1 (CD39), Vsr (VISTA), Cd244 (2B4), Havcr2 (Tim-3) and Tigit, compared to monotherapy treated

mice (Fig. 6a). Remarkably, both monotherapies induced higher expression of various effector molecules like Prf1 (perforin), Gzma & Gzmb (Granzymes) and IFN γ (Interferon- α). Differential gene expression analysis between monotherapy groups and the combination therapy confirmed significantly higher transcript levels of both inhibitory receptors and effector molecules in tumors of monotherapy treated mice (Fig. S13).

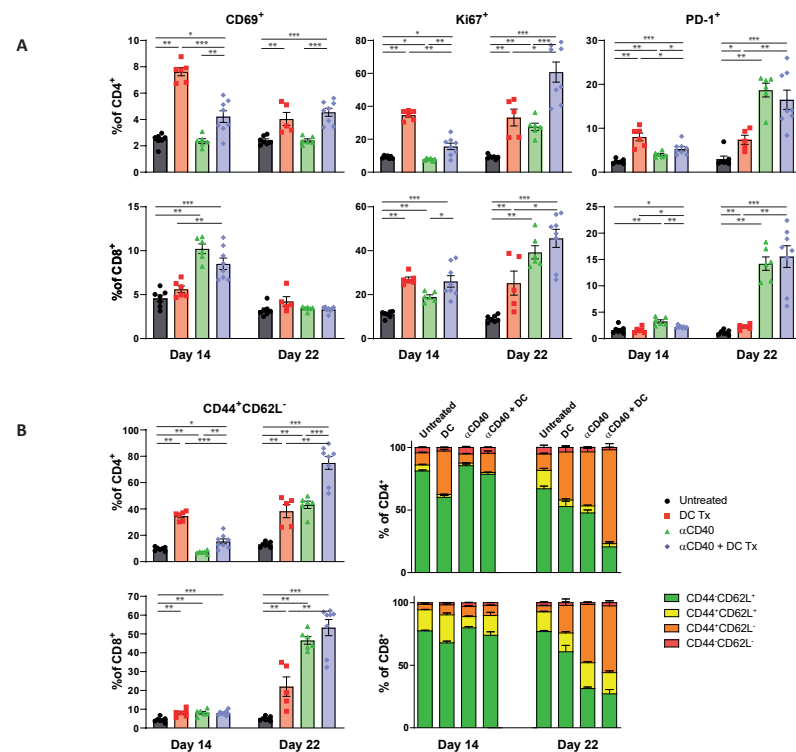


Figure 4. Immune activation in peripheral blood following AE17-lysate DC and FGK45 treatment. (A) Percentage of CD69+, Ki67+ and PD-1+ subsets of CD4+ and CD8+ circulating T cells at day 14 and 22. **(B)** Percentage of CD44+CD62L- effector memory subsets and memory status of CD4+ and CD8+ circulating T cells at day 14 and day 22. N=8 per group. Significance was determined using the non-parametric Mann-Whitney U test. Data presented as the mean \pm s.e.m. *P<0.05, **P<0.01, ***P<0.001.

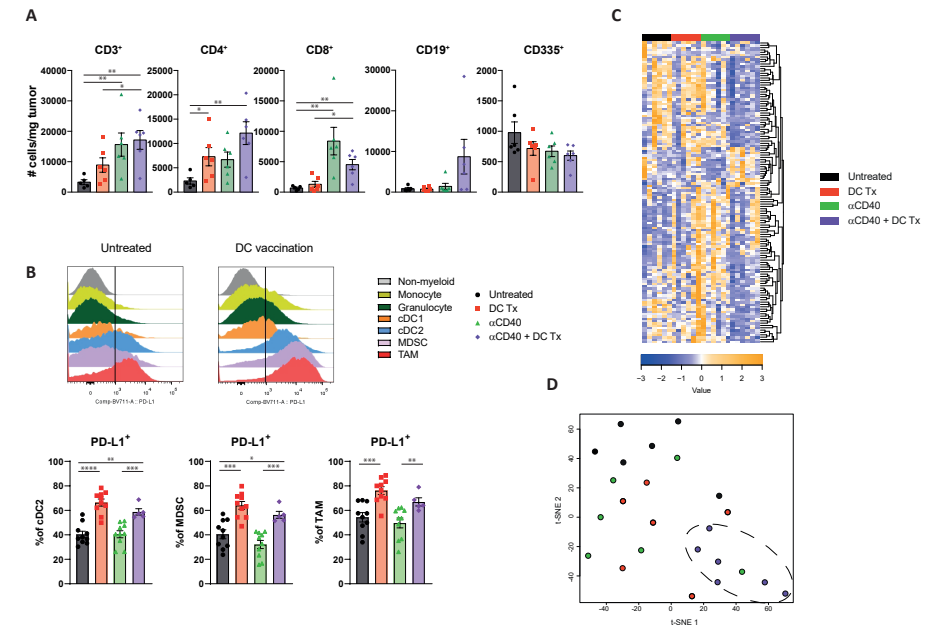


Figure 5. Tumors of combination therapy-treated mice displayed a distinct gene expression profile compared to tumors of untreated or monotherapy-treated mice. (A) Number of CD3+, CD4+, CD8+, CD19+ and CD335+ TILs per mg tumor at end-stage disease. **(B)** PD-L1 MFI of non-myeloid (CD45-), monocyte (CD45+F4/80-CD11b+Ly6C+Ly6G-), granulocyte (CD45+F4/80-CD11b+Ly6C-Ly6G+), cDC1 (CD45+F4/80-CD11b+CD11b-CD11c+MHCII+CD103+), cDC2 (CD45+F4/80-CD11b+CD11c+MHCII+), MDSC (CD45+F4/80-CD11b+Ly6CintLy6Gint) and TAM (CD45+F4/80-CD11b+) population, and percentage of PD-L1+ subset of cDC2s, MDSCs and TAMs. **(C)** Unsupervised clustering of genes significantly different between groups. Downregulated genes are marked blue and upregulated genes are marked yellow. **(D)** t-SNE clustering of individual tumor samples based on genes significant different between groups. N=5-10 per group. Significance was determined using the non-parametric Mann-Whitney U test. Data presented as the mean \pm s.e.m. *P<0.05, **P<0.01, ***P<0.001 ****P<0.0001.

Although the findings of increased effector molecules in the absence of clinical benefit may seem counterintuitive, similar cells displaying high levels of co-inhibitory and effector molecules were recently found to be consistent with a terminally exhausted T-cell phenotype.²⁴⁻²⁸ In line with these findings, gene-set enrichment analysis (GSEA) revealed that gene transcripts associated with T-cell exhaustion were significantly enriched in tumors of α CD40 therapy treated mice compared to combination therapy treated animals

PART B
Improving the efficacy of
cancer vaccines for solid tumors
by combination immunotherapy

DENDRITIC CELL VACCINATION AND
CD40-AGONIST COMBINATION THERAPY LICENSES
T CELL-DEPENDENT ANTITUMOR IMMUNITY IN
A PANCREATIC CARCINOMA MURINE MODEL

(Fig. S14a). This was not observed for DC therapy treated mice. As increased levels of co-inhibitory receptors and effector molecules may be linked to a more exhausted T-cell phenotype, we interrogated markers associated with this state. High expression of Tbx21 (T-Bet) and Klrg1 was found in both monotherapies while high expression of the transcription factor Eomes was only found in α CD40 treated mice (Fig. 6a). Interestingly, combination therapy induced higher expression of Sell (L-selectin) and the chemokine receptor Cxcr5 in the tumor compared to other groups. Furthermore, we also found lower expression of genes related to various collagen markers and "M2" phenotype macrophages after α CD40 therapy indicating TME remodeling. In order to confirm α CD40-induced stromalysis, histochemical staining were performed. Tumors of both α CD40 monotherapy as combination therapy-treated mice showed decreased collagen content (Fig. S15). Strikingly, high mRNA expression of genes related to glycolysis were detected in tumors after combination therapy as compared to α CD40 monotherapy (Fig. 6a). A glycolysis gene set enrichment analysis indeed revealed higher activity in the combination therapy treated mice compared to α CD40 treated mice (Fig. S14b). Combination therapy was also able to significantly upregulate expression of Vegfa, adm and Flt1 compared to α CD40 treated mice (Fig. S13). This is indicative for angiogenesis and vascular formation and may promote immune cell infiltration into the tumor. When immunohistochemically stained for the endothelial marker CD31, tumors of combination therapy-treated mice did express more CD31 compared to untreated or monotherapy-treated mice (Fig. S16).

As gene expression analysis was performed on whole tumor material, inhibitory markers and effector molecules were further validated and quantified at the protein level on both CD4⁺ and CD8⁺ TILs (Fig. 6b-c, S17). Untreated and α CD40 treated mice had the highest frequencies of CD8⁺ TILs expressing various inhibitory receptors (i.e. PD-1, Tim-3, VISTA, CD39, NKG2A) (Fig. 6b). However, only α CD40 treated mice had the highest number of CD8⁺ TILs expressing co-inhibitory receptors. DC therapy was able to reduce the frequencies of PD-1⁺, Tim-3⁺, VISTA⁺, CD39⁺ TILs. A similar trend was also observed when co-expression of multiple inhibitory receptors was assessed (Fig. S17c-d). In addition, DC vaccinated and combination therapy treated mice had the highest frequencies of PD-1/Tim-3 double negative TIL, which have been described to exhibit the highest effector potential, whereas PD-1/TIM-3 double positive T cells are known to be severely dysfunctional.²⁶ α CD40 mediated induction of IFN γ ⁺ and granzyme B⁺ TILs came at the expense of increased numbers of cells producing IL-10 (Fig. 6c). Both the mRNA and protein-expression data point to a preferential induction of effector T-cells expressing less multiple co-inhibitory receptors in the combination immunotherapy treated, as compared to CD40-agonistic monotherapy treated mice.

Recently, targeting NKG2A on T cells has been described as a novel approach to promote anti-tumor immunity and has been linked to T-cell dysfunction.^{29,30} Interestingly,

α CD40 induced the highest numbers of NKG2A⁺ CD8⁺ TILs compared to combination therapy arm (Fig. 6b). Moreover, although α CD40 therapy increased TIL numbers, the frequencies of proliferating TILs were lower compared to untreated mice suggesting that this is not explained by local expansion, but enhanced infiltration (Fig. 6c). Altogether, these findings offer an explanation for the observed efficacy of DC-CD40-agonist combination therapy where an influx of T cells exhibiting low levels of co-inhibitory checkpoints is associated with restricted tumor growth.

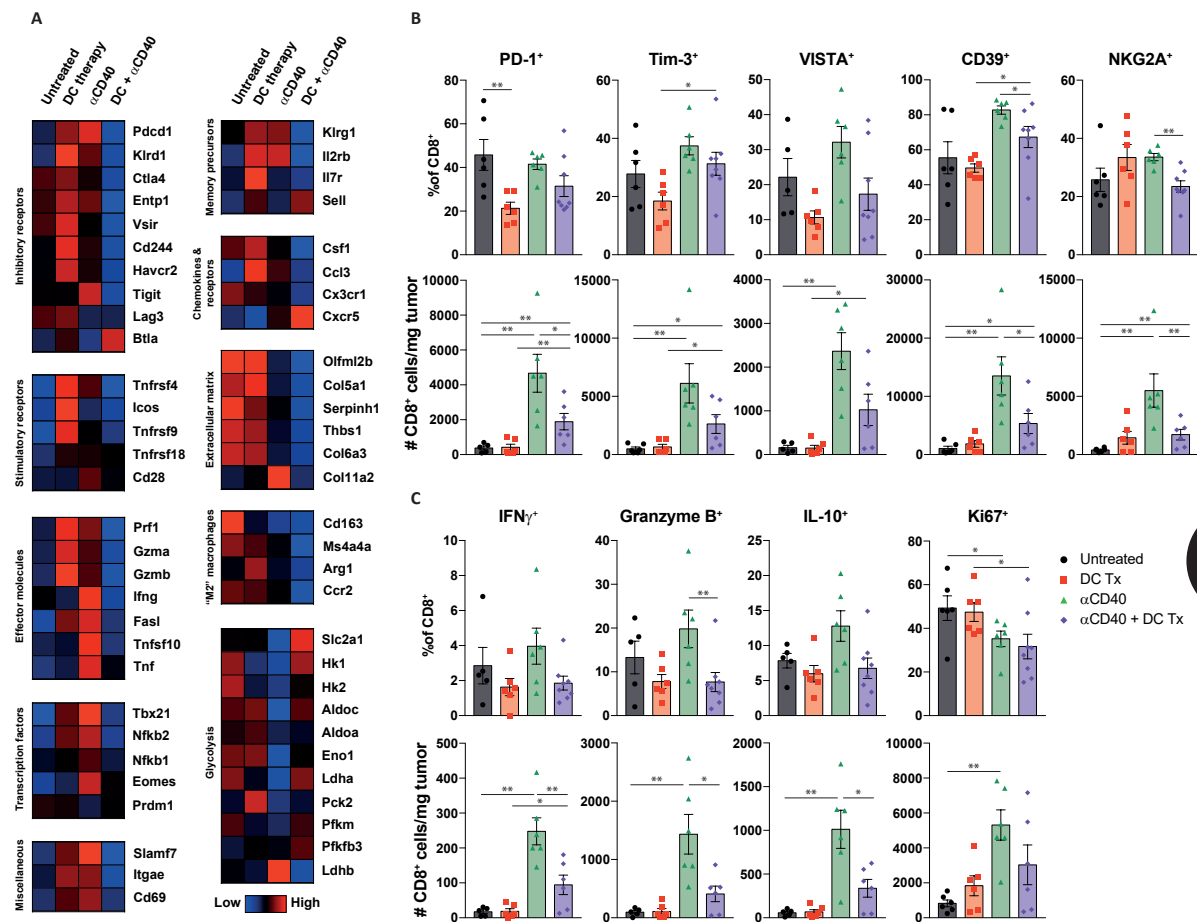


Figure 6. DC vaccination is able to reduce hallmarks of T-cell exhaustion. (A) Heatmap illustrating the average transcript expression of the indicated genes, grouped by function. Rows represent averaged z-scores. (B) Number and percentage of PD-1⁺, Tim-3⁺, VISTA⁺, CD39⁺ and NKG2A⁺ subsets of CD8⁺ TILs. (C) Number and percentage of IFN γ ⁺, Granzyme B⁺, IL-10⁺ and Ki67⁺ subsets of CD8⁺ TILs. N=7-8 per group. Significance was determined using the non-parametric Mann-Whitney U test. Data presented as the mean \pm s.e.m. *P<0.05, **P<0.01, ***P<0.001.

DISCUSSION

Our data highlight that rationally combining immunotherapies in pancreatic cancer can lead to synergistic improvements in anti-tumor T-cell immunity and clinical responses. For these studies, we used immune-competent mice bearing PDAC tumors obtained from *Kras*^{G12D/+}; *Trp53*^{R172H/+}; *Pdx-1-Cre* (KPC) mice. This model mimics (immune) phenotypic features and the aggressiveness of human pancreatic adenocarcinoma.^{16,31} We mainly focused on DC-based therapy to strengthen the tumor-specific effector T-cell response. Previous trials in pancreatic cancer patients utilized single peptide or autologous tumor as a lysate source for DC therapy. We assessed the possibility of loading DCs with mesothelioma lysate based on the rationale that cross-reactive T cells would be generated due to expression of a number of shared TAAs by both mesothelioma and pancreatic cancer. The use of an allogeneic-tumor lysate offers an off-the-shelf approach which is not dependent on the identification of immunodominant epitopes and can be used irrespective of the patient's HLA type and exploits a broad spectrum of TAAs.³² We found that mesothelioma-lysate DC therapy was able to delay pancreatic tumor growth, generate KPC-reactive T cells and induce TIL influx, confirming cross-reactivity. Although some efficacy was observed with non-loaded DCs, possibly by an unspecific inflammatory response that activates bystander T cells or during culture phagocytosed bovine serum proteins, the use of tumor lysate-loaded DCs had significant higher efficacy against the tumor *in vivo* and *in vitro* (Fig. 2). Interestingly, cross-reactivity could also be found *in vitro* when B16F10 lysate was used to load DCs but not to non-loaded DCs (Fig. S4), indicating the involvement of shared antigens (Table S1).

We also investigated if targeting CD40 is able to control tumor growth in established disease. CD40 can be found on B cells, DCs and macrophages and ligation leads to activation.³³ α CD40 therapy may therefore also activate endogenous DCs that present tumor antigens and contribute to a monotherapy effect. Also, *Schoenberger and Bennett et al.* demonstrated that CD40-activated APCs might replace the requirement for CD4⁺ T helper-mediated licensing, thereby lowering the threshold for CD8⁺ effector T-cell priming. This could explain why CD4⁺ T-cell depletion prior combination immunotherapy did not affect efficacy.^{34,35} Alternatively, CD40 ligation may also license delivered DCs, thereby enhancing their capacity to prime CD8⁺ T cells.^{36,37} Indeed, when bone marrow-derived DCs were treated with α CD40, increased IL-12 production could be detected (Fig. S18). Furthermore, α CD40 therapy can also directly modulate the TME: targeting CD40 on macrophages can lead to phenotypic polarization from immunosuppressive "M2" into inflammatory "M1" macrophages, the latter being tumoricidal and capable of ablating tumor stroma.^{16,38} In line with this thought, our mRNA expression data and histochemical staining on tumors confirmed decreased collagen content after α CD40 mono and

combination therapy (Fig. 6a). Also, lower expression of mRNA levels related to M2 macrophages was found in tumors of mice treated with α CD40 (Fig. 6a). Furthermore, it was shown that M2 macrophage-derived granulin contributes to CD8⁺ T cell exclusion and that this process is driven by colony-stimulating factor-1 (CSF-1). It has been found that CSF-1 inhibition leads to desmoplasia depletion and sensitizes pancreatic cancer to immune checkpoint blockade therapy.³⁹ We were able to show lower *Csf1* mRNA levels in tumors after α CD40 therapy and combination therapy (Fig. 6a). A recently reported combination therapy involving α CD40 and α PD-1 therapy showed promising results in preclinical PDAC models, and demonstrated that therapy reprograms the TME resulting in the increase of DCs and decrease of granulocytic-myeloid derived suppressor cells (MDSCs).⁴⁰ As we now focused on the T-cell phenotype responsible for slowing tumor progression following combination treatment, further in-depth studies immediately following α CD40 therapy are likely required to formally dissect its spatiotemporal roles on macrophages and DCs in promoting anti-tumor immune responses.

Interestingly, despite the absence of clinical responses in monotherapy-treated animals in the established tumor model, both monotherapy and combination therapy-treated mice were able to increase total CD3⁺ TIL numbers. The effect of DC therapy was most pronounced on CD4⁺ T cells and less on CD8⁺ T cells whereas α CD40 treatment displayed an inverse pattern. DC and α CD40 treated mice showed improved survival and increased both CD4⁺ and CD8⁺ intratumoral T-cell numbers. However, we demonstrated that the clinical response was primarily driven by CD8⁺ T cells (Fig. 3e-g). The sensitizing role of DC vaccination may be mainly priming of MHC class I-restricted cytotoxic T lymphocytes. Even though CD40 agonistic antibodies significantly increased T-cell infiltration in established pancreatic tumors, clinical efficacy was lacking, prompting further phenotypic analysis of these cells. We observed high expression of various inhibitory receptors and effector molecules on TILs of α CD40 monotherapy treated mice when compared to the other treatment groups. Studies only recently published have associated this phenotype with that of terminally exhausted T cells in both solid cancer and chronic viral infection settings.^{25,41} Although our mRNA expression data also demonstrated the expression of various inhibitory receptors in DC monotherapy treated mice, mRNA analysis was performed on whole tumor tissue, challenging the interpretation of our data as we were not able to assign specific markers to individual immune cell subsets. However, lower amounts of mRNA of various stimulatory receptors (*i.e.* CD28, ICOS, GITR, CD137, OX-40) and high expression of *Tbx21* (T-Bet) and *Eomes* found in α CD40 monotherapy treated mice suggest that this phenotype is primarily restricted to these tumors. In addition, KLRG1^{hi}IL7r^{lo} CD8⁺ T cells have previously been described as dysfunctional.⁴² We found that monotherapy with α CD40 induced higher expression of *Klrg1* but not *Il7r*, whereas DC vaccination increased the levels of both *Klrg1* and *Il7r*. In accordance with the aforementioned phenotype, *Sell* (L-selectin), a marker

PART B
Improving the efficacy of
cancer vaccines for solid tumors
by combination immunotherapy

DENDRITIC CELL VACCINATION AND
CD40-AGONIST COMBINATION THERAPY LICENSES
T CELL-DEPENDENT ANTITUMOR IMMUNITY IN
A PANCREATIC CARCINOMA MURINE MODEL

associated with naïve-like memory T-cells and T-cell homing, was particularly induced in mice treated with combination therapy.^{24,25,28} Finally, the chemokine receptor CXCR5 has been recently found to mark a specific T-cell population capable of responding to PD-1 checkpoint blocking antibodies, which expresses lower levels of co-inhibitory receptors and effector molecules as compared to their CXCR5-negative counterparts.^{25,26,41} We found that combination DC and α CD40 therapy indeed induced higher *Cxcr5* expression in the tumor compared to other groups.

Flow cytometry analysis confirmed the reduced expression of various inhibitory markers on CD8⁺ TILs derived from combination therapy-treated mice compared to α CD40-treated mice. In addition, the lower proliferation rate as evidenced by *ex vivo* measurements of Ki-67 in combination therapy treated animals also matches with an improved T-cell phenotype, as others have previously found these cells to persist in culture longer compared to their Ki-67-high counterparts.²⁵ As human cancers grow at a considerably slower pace than most murine tumor models, it is conceivable that longer T-cell persistence is crucial for durable tumor control.

The presence of low amounts of glycolysis-related gene transcripts following α CD40 monotherapy fits with a more exhausted, terminally differentiated memory T-cell state, as has been proposed by others.^{43,44} Glut-1 (*Slc2a1*) was found to be essential for T-cell activation and *Slc2a1* was highly expressed in combination therapy treated mice.⁴⁵ However, as gene expression was performed on whole tumor material, it's unclear whether glycolysis-related transcripts originated from tumor cells or immune infiltrates. Further functional studies on our combination treated T-cell phenotype are needed to truly assess which factors determine their superior anti-tumor efficacy.

DCs loaded with allogeneic mesothelioma-tumor cell lysate have already proven to be feasible, with clinical efficacy in the absence of toxicity in patients with mesothelioma.²² Following this, a phase II clinical trial examining whether this holds true for macroscopically disease-free, post-resection PDAC patients is currently being conducted (REACTiVe Trial; Netherlands Trial Register NL7432). However, as the majority of pancreatic patients presents with irresectable or metastatic disease, rational and safe treatment combinations are needed to offer perspective for this group of patients too. Currently, several studies with combination strategies incorporating CD40 agonists in PDAC patients are ongoing and recruiting (NCT03214250; NCT02588443; NCT03329950). We have shown that DC-therapy pretreatment allows for proper CD40-agonist efficacy by precluding the formation of T-cells associated with an exhaustion phenotype when administered alone. The lack of DC-therapy toxicity in patients is of particular importance since CD40-agonistic antibodies are associated with serious adverse events leading to premature termination of treatment in some patients.^{16,46} To assess the feasibility and safety of our combinatory approach we are currently in the process of initiating a trial involving DC-CD40-agonist combination

therapy in metastatic disease. Since DC vaccination also induced a PD-L1 rich tumor microenvironment, future combination strategies with immune checkpoint blockers are warranted.

In conclusion, we have found pancreatic cancer and mesothelioma lysate-loaded DCs to be effective in restraining immunologically cold pancreatic tumors when administered prophylactically. In established tumors, effective intratumoral immunity was achieved when DC vaccination was combined with CD40-agonistic antibodies, generating non-redundant immunological effects capable of restraining tumor progression.

PART B
Improving the efficacy of
cancer vaccines for solid tumors
by combination immunotherapy

DENDRITIC CELL VACCINATION AND
CD40-AGONIST COMBINATION THERAPY LICENSES
T CELL-DEPENDENT ANTITUMOR IMMUNITY IN
A PANCREATIC CARCINOMA MURINE MODEL

REFERENCES

- 1 Siegel, R. L., Miller, K. D. & Jemal, A. Cancer statistics, 2018. *CA Cancer J Clin* 68, 7-30 (2018).
- 2 Carioli, G. et al. European cancer mortality predictions for the year 2018 with focus on colorectal cancer. *Annals of Oncology* 29, 1016-1022, doi:10.1093/annonc/mdy033 (2018).
- 3 Rahib, L. et al. Projecting cancer incidence and deaths to 2030: the unexpected burden of thyroid, liver, and pancreas cancers in the United States. *Cancer Res* 74, 2913-2921 (2014).
- 4 Matsumoto, I. et al. Proposed preoperative risk factors for early recurrence in patients with resectable pancreatic ductal adenocarcinoma after surgical resection: A multi-center retrospective study. *Pancreatology* 15, 674-680, doi:https://doi.org/10.1016/j.pan.2015.09.008 (2015).
- 5 Paniccia, A. et al. Characteristics of 10-Year Survivors of Pancreatic Ductal Adenocarcinoma. *JAMA Surg* 150, 701-710, doi:10.1001/jamasurg.2015.0668 (2015).
- 6 Neoptolemos, J. P. et al. Comparison of adjuvant gemcitabine and capecitabine with gemcitabine monotherapy in patients with resected pancreatic cancer (ESPAC-4): a multicentre, open-label, randomised, phase 3 trial. *Lancet (London, England)* 389, 1011-1024, doi:10.1016/s0140-6736(16)32409-6 (2017).
- 7 Weber, J. S. et al. Nivolumab versus chemotherapy in patients with advanced melanoma who progressed after anti-CTLA-4 treatment (CheckMate 037): a randomised, controlled, open-label, phase 3 trial. *Lancet Oncol* 16, 375-384 (2015).
- 8 Robert, C. et al. Nivolumab in previously untreated melanoma without BRAF mutation. *The New England journal of medicine* 372, 320-330, doi:10.1056/NEJMoa1412082 (2015).
- 9 Larkin, J. et al. Combined Nivolumab and Ipilimumab or Monotherapy in Untreated Melanoma. *N Engl J Med* 373, 23-34 (2015).
- 10 Brahmer, J. R. et al. Safety and activity of anti-PD-L1 antibody in patients with advanced cancer. *The New England journal of medicine* 366, 2455-2465, doi:10.1056/NEJMoa1200694 (2012).
- 11 Patnaik, A. et al. Phase I Study of Pembrolizumab (MK-3475; Anti-PD-1 Monoclonal Antibody) in Patients with Advanced Solid Tumors. *Clin Cancer Res* 21, 4286-4293 (2015).
- 12 Jan, N. et al. Systemic treatment with anti-PD-1 antibody nivolumab in combination with vaccine therapy in advanced pancreatic cancer. *Journal of Clinical Oncology* 34, 3092-3092, doi:10.1200/JCO.2016.34.15_suppl.3092 (2016).
- 13 Whatcott CJ, P. R., Von Hoff DD, et al. . Desmoplasia and chemoresistance in pancreatic cancer., (2012).
- 14 Strommes, I. M. et al. Targeted depletion of an MDSC subset unmasks pancreatic ductal adenocarcinoma to adaptive immunity. *Gut* 63, 1769-1781, doi:10.1136/gutjnl-2013-306271 (2014).
- 15 Zhu, Y. et al. CSF1/CSF1R blockade reprograms tumor-infiltrating macrophages and improves response to T-cell checkpoint immunotherapy in pancreatic cancer models. *Cancer Res* 74, 5057-5069 (2014).
- 16 Beatty, G. L. et al. CD40 agonists alter tumor stroma and show efficacy against pancreatic carcinoma in mice and humans. *Science* 331, 1612-1616, doi:10.1126/science.1198443 (2011).
- 17 Long, K. B. et al. IFN γ and CCL2 Cooperate to Redirect Tumor-Infiltrating Monocytes to Degrade Fibrosis and Enhance Chemotherapy Efficacy in Pancreatic Carcinoma. *Cancer Discovery*, doi:10.1158/2159-8290.Cd-15-1032 (2016).
- 18 Beatty, G. L. et al. Exclusion of T Cells From Pancreatic Carcinomas in Mice Is Regulated by Ly6C(low) F4/80(+) Extratumoral Macrophages. *Gastroenterology* 149, 201-210, doi:10.1053/j.gastro.2015.04.010 (2015).
- 19 Tjomsland, V. et al. Pancreatic adenocarcinoma exerts systemic effects on the peripheral blood myeloid and plasmacytoid dendritic cells: an indicator of disease severity? *BMC Cancer* 10, 87, doi:10.1186/1471-2407-10-87 (2010).
- 20 Dallal, R. M. et al. Paucity of dendritic cells in pancreatic cancer. *Surgery* 131, 135-138 (2002).
- 21 Balachandran, V. P. et al. Identification of unique neoantigen qualities in long-term survivors of pancreatic cancer. *Nature* 551, 512, doi:10.1038/nature24462 https://www.nature.com/articles/nature24462#supplementary-information (2017).
- 22 Aerts, J. G. et al. Autologous dendritic cells pulsed with allogeneic tumor cell lysate in mesothelioma: From mouse to human. *Clin Cancer Res* (2017).
- 23 Cheever, M. A. et al. The prioritization of cancer antigens: a national cancer institute pilot project for the acceleration of translational research. *Clin Cancer Res* 15, 5323-5337 (2009).
- 24 Canale, F. P. et al. CD39 Expression Defines Cell Exhaustion in Tumor-Infiltrating CD8(+) T Cells. *Cancer Res* 78, 115-128 (2018).
- 25 Miller, B. C. et al. Subsets of exhausted CD8+ T cells differentially mediate tumor control and respond to checkpoint blockade. *Nature immunology* 20, 326-336, doi:10.1038/s41590-019-0312-6 (2019).
- 26 Kurtulus, S. et al. Checkpoint Blockade Immunotherapy Induces Dynamic Changes in PD-1(-)CD8(+) Tumor-Infiltrating T Cells. *Immunity* 50, 181-194 e186 (2019).
- 27 Li, H. et al. Dysfunctional CD8 T Cells Form a Proliferative, Dynamically Regulated Compartment within Human Melanoma. *Cell* 176, 775-789 e718 (2019).
- 28 Duhen, T. et al. Co-expression of CD39 and CD103 identifies tumor-reactive CD8 T cells in human solid tumors. *Nature communications* 9, 2724-2724, doi:10.1038/s41467-018-05072-0 (2018).
- 29 van Montfoort, N. et al. NKG2A Blockade Potentiates CD8 T Cell Immunity Induced by Cancer Vaccines. *Cell* 175, 1744-1755 e1715 (2018).
- 30 Andre, P. et al. Anti-NKG2A mAb Is a Checkpoint Inhibitor that Promotes Anti-tumor Immunity by Unleashing Both T and NK Cells. *Cell* 175, 1731-1743 e1713 (2018).
- 31 Lee, J. W., Komar, C. A., Bengsch, F., Graham, K. & Beatty, G. L. Genetically Engineered Mouse Models of Pancreatic Cancer: The KPC Model (LSL-Kras(G12D/+);LSL-Trp53(R172H/+);Pdx-1-Cre), Its Variants, and Their Application in Immuno-oncology Drug Discovery. *Current protocols in pharmacology* 73, 14.39.11-14.39.20, doi:10.1002/cpph.2 (2016).
- 32 Neller, M. A., Lopez, J. A. & Schmidt, C. W. Antigens for cancer immunotherapy. *Semin Immunol* 20, 286-295 (2008).
- 33 Vonderheide, R. H. et al. CD40 immunotherapy for pancreatic cancer. *Cancer immunology, immunotherapy : CII* 62, 949-954, doi:10.1007/s00262-013-1427-5 (2013).
- 34 Schoenberger, S. P., Toes, R. E., van der Voort, E. I., Offringa, R. & Melief, C. J. T-cell help for cytotoxic T lymphocytes is mediated by CD40-CD40L interactions. *Nature* 393, 480-483 (1998).
- 35 Bennett, S. R. M. et al. Help for cytotoxic-T-cell responses is mediated by CD40 signalling. *Nature* 393, 478, doi:10.1038/30996 (1998).
- 36 Cella, M. et al. Ligation of CD40 on dendritic cells triggers production of high levels of interleukin-12 and enhances T cell stimulatory capacity: T-T help via APC activation. *J Exp Med* 184, 747-752 (1996).
- 37 Schuurhuis, D. H. et al. Immature dendritic cells acquire CD8(+) cytotoxic T lymphocyte priming capacity upon activation by T helper cell-independent or -dependent stimuli. *J Exp Med* 192, 145-150 (2000).
- 38 Buhtoiarov, I. N. et al. CD40 ligation activates murine macrophages via an IFN-gamma-dependent mechanism resulting in tumor cell destruction in vitro. *J Immunol* 174, 6013-6022 (2005).
- 39 Schmid, M. C. et al. Macrophage-derived granulins drives resistance to immune checkpoint inhibition in metastatic pancreatic cancer. *Cancer Research*, doi:10.1158/0008-5472.can-17-3876 (2018).
- 40 Ma, H. S. et al. A CD40 Agonist and PD-1 Antagonist Antibody Reprogram the Microenvironment of Nonimmunogenic Tumors to Allow T-cell-Mediated Anticancer Activity. *Cancer Immunology Research* 7, 428-442, doi:10.1158/2326-6066.Cir-18-0061 (2019).
- 41 Im, S. J. et al. Defining CD8+ T cells that provide the proliferative burst after PD-1 therapy. *Nature* 537, 417-421 (2016).
- 42 Wherry, E. J. & Kurachi, M. Molecular and cellular insights into T cell exhaustion. *Nature Reviews Immunology* 15, 486, doi:10.1038/nri3862 (2015).
- 43 Siska, P. J. & Rathmell, J. C. T cell metabolic fitness in antitumor immunity. *Trends Immunol* 36, 257-264 (2015).
- 44 Phan, A. T., Goldrath, A. W. & Glass, C. K. Metabolic and Epigenetic Coordination of T Cell and Macrophage Immunity. *Immunity* 46, 714-729 (2017).
- 45 Macintyre, A. N. et al. The glucose transporter Glut1 is selectively essential for CD4 T cell activation and effector function. *Cell Metab* 20, 61-72 (2014).
- 46 Vonderheide, R. H. & Glennie, M. J. Agonistic CD40 Antibodies and Cancer Therapy. *Clinical Cancer Research* 19, 1035-1043, doi:10.1158/1078-0432.Ccr-12-2064 (2013).
- 47 Hos, B. J. et al. Identification of a neo-epitope dominating endogenous CD8 T cell responses to MC-38 colorectal cancer. *Oncimmunology*, 1673125, doi:10.1080/2162402x.2019.1673125 (2019).
- 48 Hegmans, J. P., Hemmes, A., Aerts, J. G., Hoogsteden, H. C. & Lambrecht, B. N. Immunotherapy of murine malignant mesothelioma using tumor lysate-pulsed dendritic cells. *American journal of respiratory and critical care medicine* 171, 1168-1177, doi:10.1164/rccm.200501-0570C (2005).
- 49 Doering, T. A. et al. Network analysis reveals centrally connected genes and pathways involved in CD8+ T cell exhaustion versus memory. *Immunity* 37, 1130-1144 (2012).
- 50 Subramanian, A. et al. Gene set enrichment analysis: A knowledge-based approach for interpreting genome-wide expression profiles. *Proceedings of the National Academy of Sciences* 102, 15545-15550, doi:10.1073/pnas.0506580102 (2005).

PART B
Improving the efficacy of
cancer vaccines for solid tumors
by combination immunotherapy

DENDRITIC CELL VACCINATION AND
CD40-AGONIST COMBINATION THERAPY LICENSES
T CELL-DEPENDENT ANTITUMOR IMMUNITY IN
A PANCREATIC CARCINOMA MURINE MODEL

SUPPLEMENTARY DATA

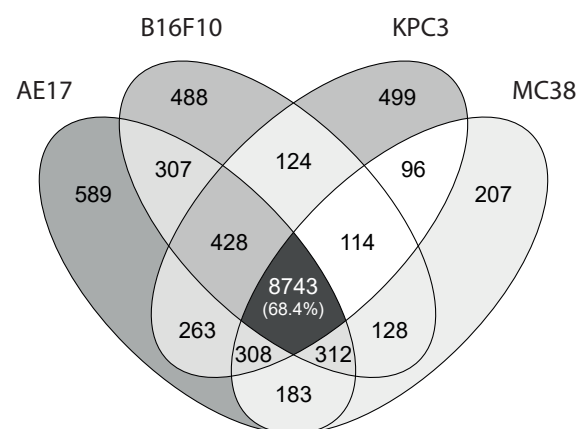


Figure S1. Venn diagram illustrating overlapping and non-overlapping genes of the tumor cell lines KPC3 (pancreatic cancer), AE17 (mesothelioma), B16F10 (melanoma) and MC38 (colon adenocarcinoma).

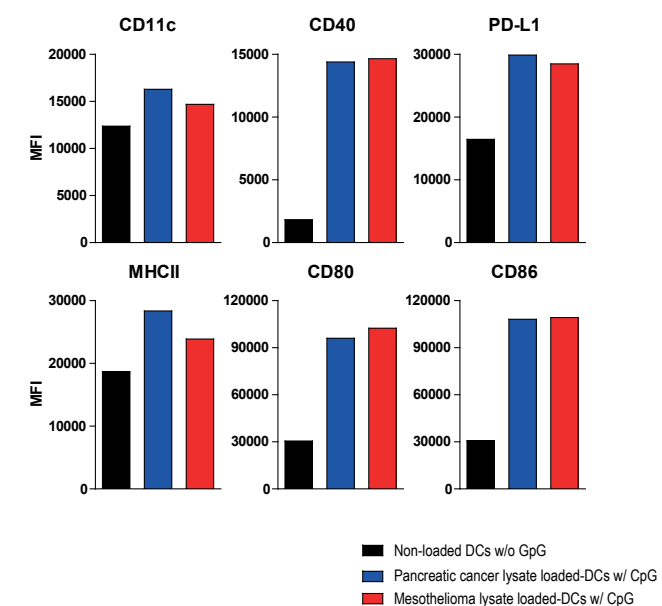


Figure S2. MFI of CD11c, CD40, PD-L1, MHCII, CD80 and CD86 on cultured DCs for vaccination. Control non-loaded DCs were not stimulated with CpG.

PART B
Improving the efficacy of
cancer vaccines for solid tumors
by combination immunotherapy

DENDRITIC CELL VACCINATION AND
CD40-AGONIST COMBINATION THERAPY LICENSES
T CELL-DEPENDENT ANTITUMOR IMMUNITY IN
A PANCREATIC CARCINOMA MURINE MODEL

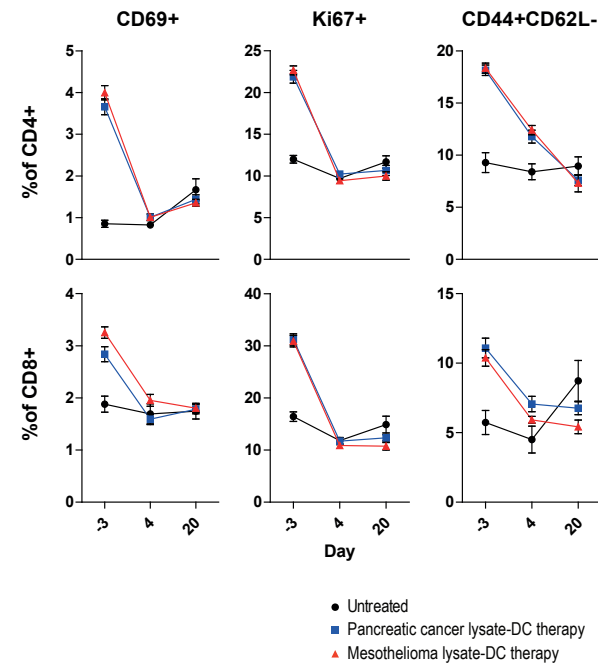


Figure S3. Percentage of CD69+, Ki67+ and CD44+CD62L- subsets of circulating CD4+ and CD8+ T cells at day -3, 4 and 20. N=8 per group. Significance was determined using the non-parametric Mann-Whitney U test. Data presented as the mean \pm s.e.m. *P<0.05.

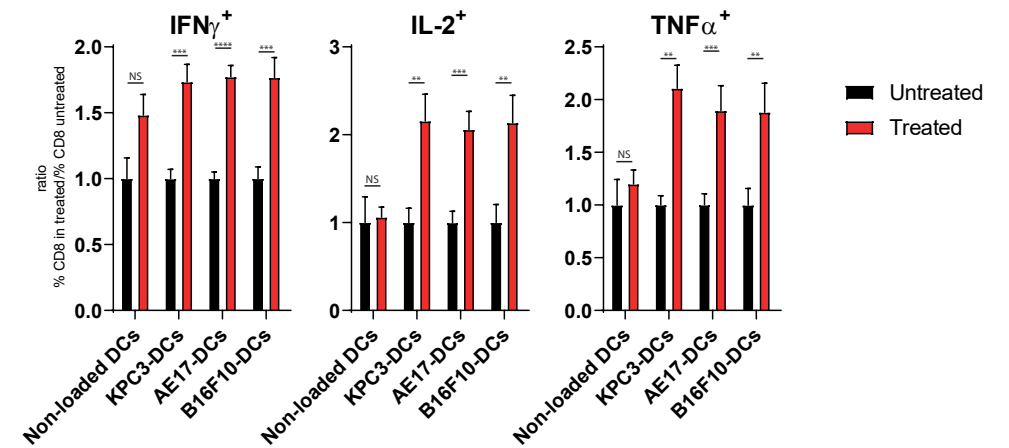


Figure S4. Relative production of IFN γ , IL-2 and TNF α by CD8+ splenocytes of AE17 lysate-DC/αCD40-treated and untreated after stimulation with DCs loaded with KPC3, AE17 or B16F10, or non-loaded DCs, normalized for untreated mice. N=6-10 per group. Significance was determined using the non-parametric Mann-Whitney U test. Data presented as the mean \pm s.e.m. **P<0.01, ***P<0.001, ****P<0.0001.

PART B Improving the efficacy of cancer vaccines for solid tumors by combination immunotherapy

DENDRITIC CELL VACCINATION AND CD40-AGONIST COMBINATION THERAPY LICENSES T CELL-DEPENDENT ANTITUMOR IMMUNITY IN A PANCREATIC CARCINOMA MURINE MODEL

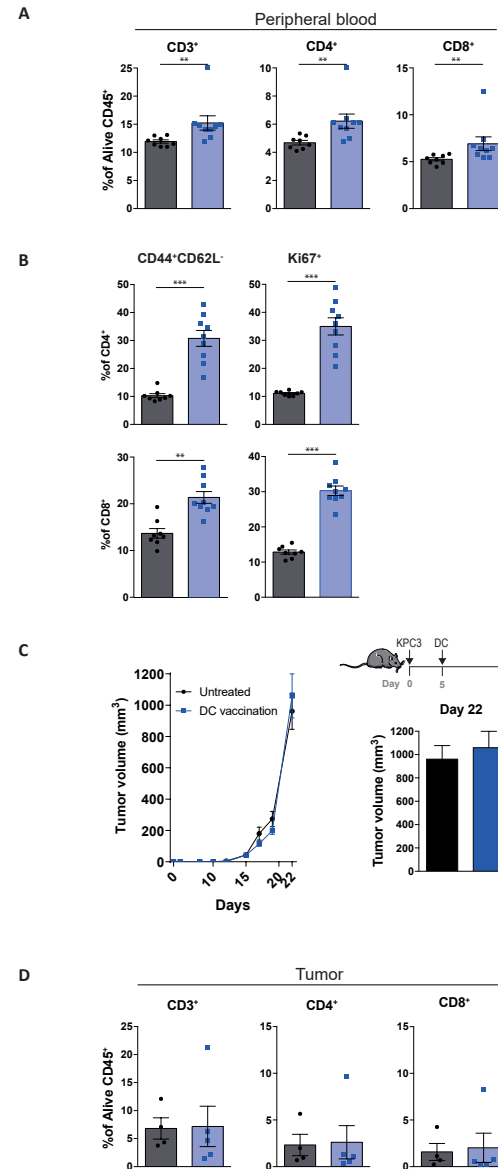


Figure S5. Lysate-DC is not effective as monotherapy in tumor-bearing mice. (A) CD3⁺, CD4⁺ and CD8⁺ circulating T cells as a percentage of alive CD45⁺ cells, four days after DC vaccination. (B) Percentage of CD44⁺CD62L⁻ and Ki67⁺ subsets of CD4⁺ and CD8⁺ circulating T cells, four days after DC vaccination. (C) Tumor volume measured over time, and tumor size at the day of sacrifice (day 22). (D) CD3⁺, CD4⁺ and CD8⁺ TILs as a percentage of alive CD45⁺ cells. N=5-9 per group. Significance was determined using the non-parametric Mann-Whitney U test. Data presented as the mean ± s.e.m. *P<0.05, **P<0.01, ***P<0.001.

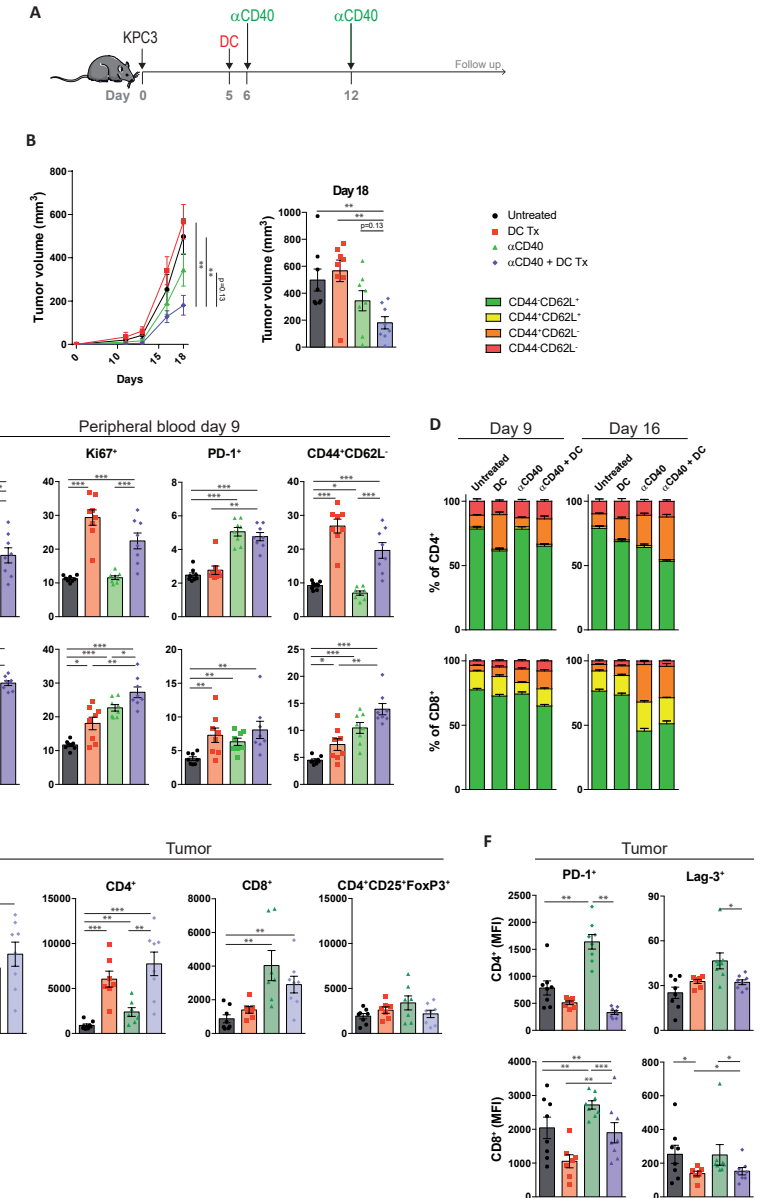


Figure S6. (A) Study setup (B) Tumor volume measured over time, and tumor size at day of sacrifice (day 18). (C) Percentage of CD69⁺, Ki67⁺, PD-1⁺ and CD44⁺CD62L⁻ subsets of CD4⁺ and CD8⁺ circulating T cells, four days after treatment initiation. (D) Memory status of CD4⁺ and CD8⁺ circulating T cells at day 9 and day 16. (E) Number of CD3⁺, CD4⁺, CD8⁺, CD4⁺CD25⁺FoxP3⁺ TILs per mg tumor. (F) MFI of PD-1 and Lag-3 of CD4⁺ and CD8⁺ TILs. N=7-8 per group. Significance was determined using the non-parametric Mann-Whitney U test. Data presented as the mean ± s.e.m. *P<0.05, **P<0.01, *P<0.001.**

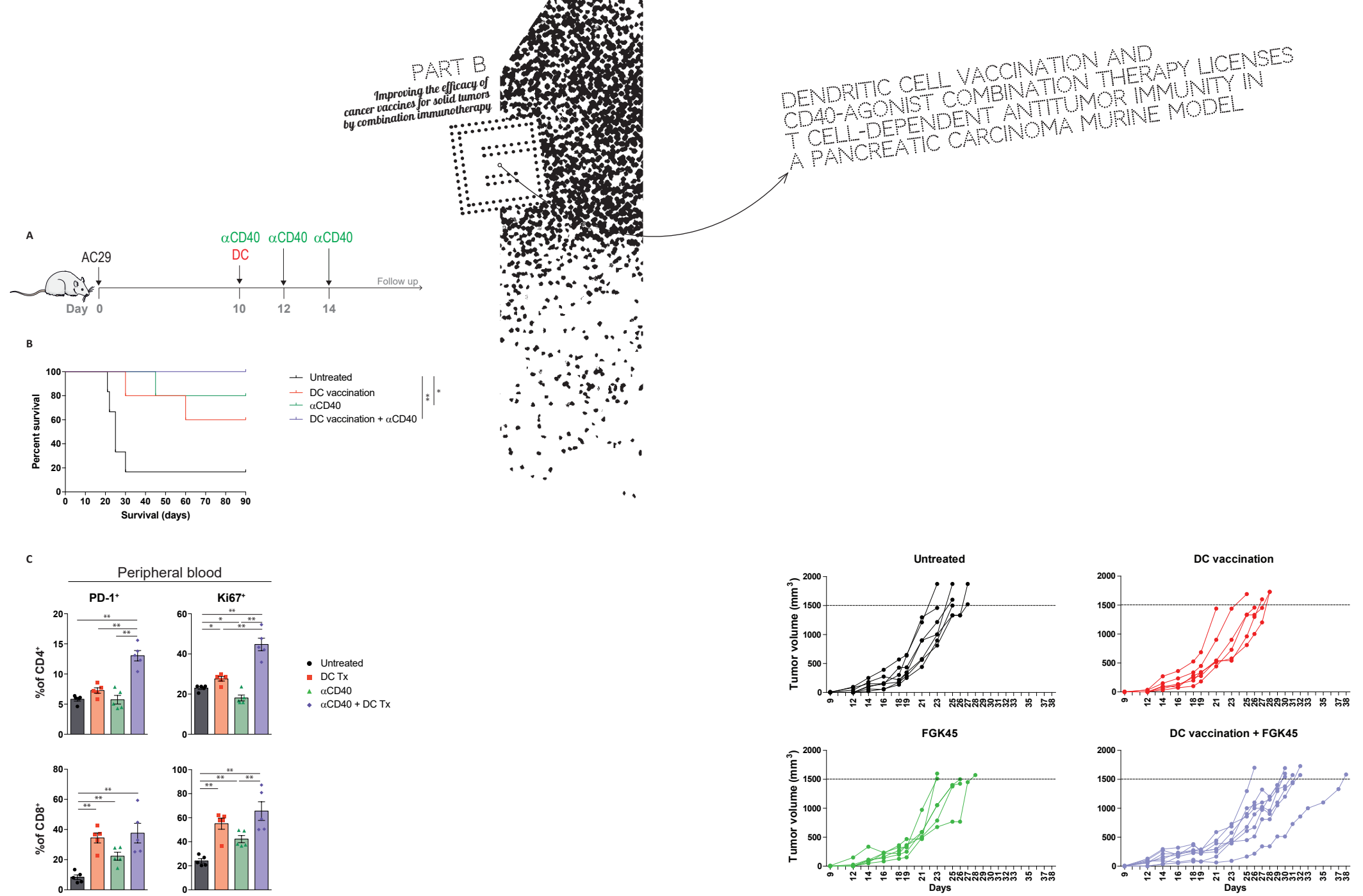
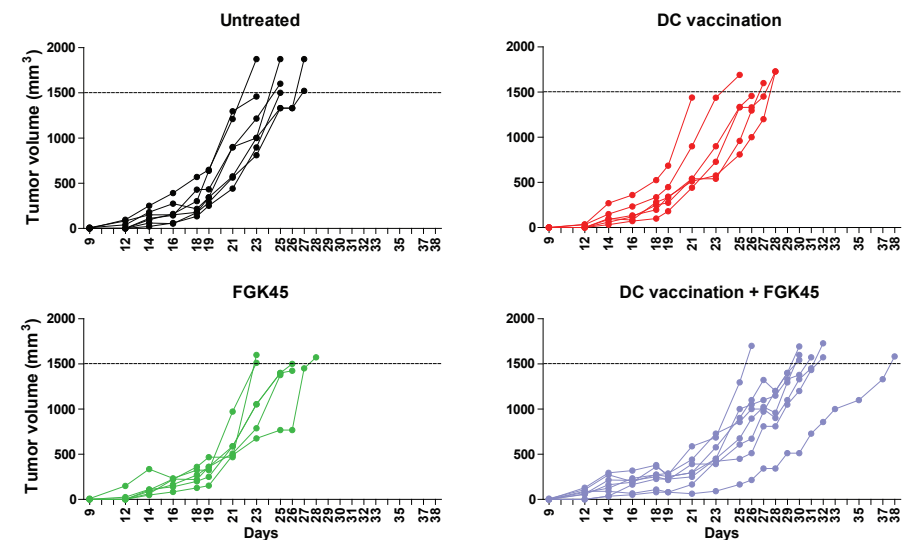


Figure S8. Tumor outgrowth curves of treated and untreated tumor-bearing mice.



PART B
Improving the efficacy of
cancer vaccines for solid tumors
by combination immunotherapy

DENDRITIC CELL VACCINATION AND
CD40-AGONIST COMBINATION THERAPY LICENSES
T CELL-DEPENDENT ANTITUMOR IMMUNITY IN
A PANCREATIC CARCINOMA MURINE MODEL

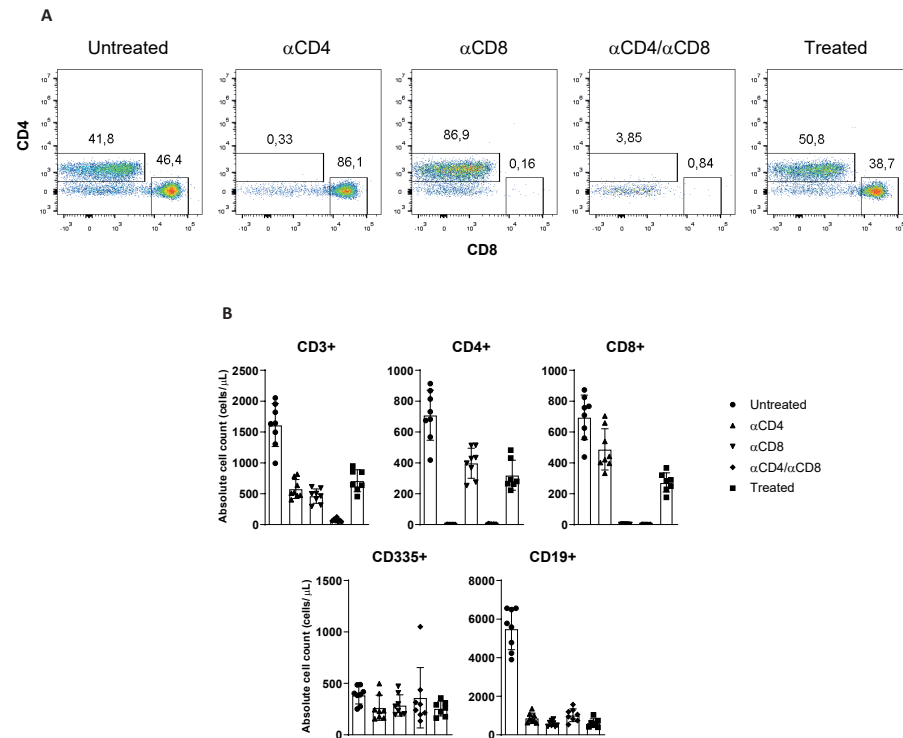


Figure S9. (A) Interim blood analysis on day 14. Percentage of CD4+ and CD8+ of CD3+ T cells. **(B)** Absolute number of CD3+, CD4+, CD8+, CD335+ and CD19+ cells per μ L blood drawn on day 14.

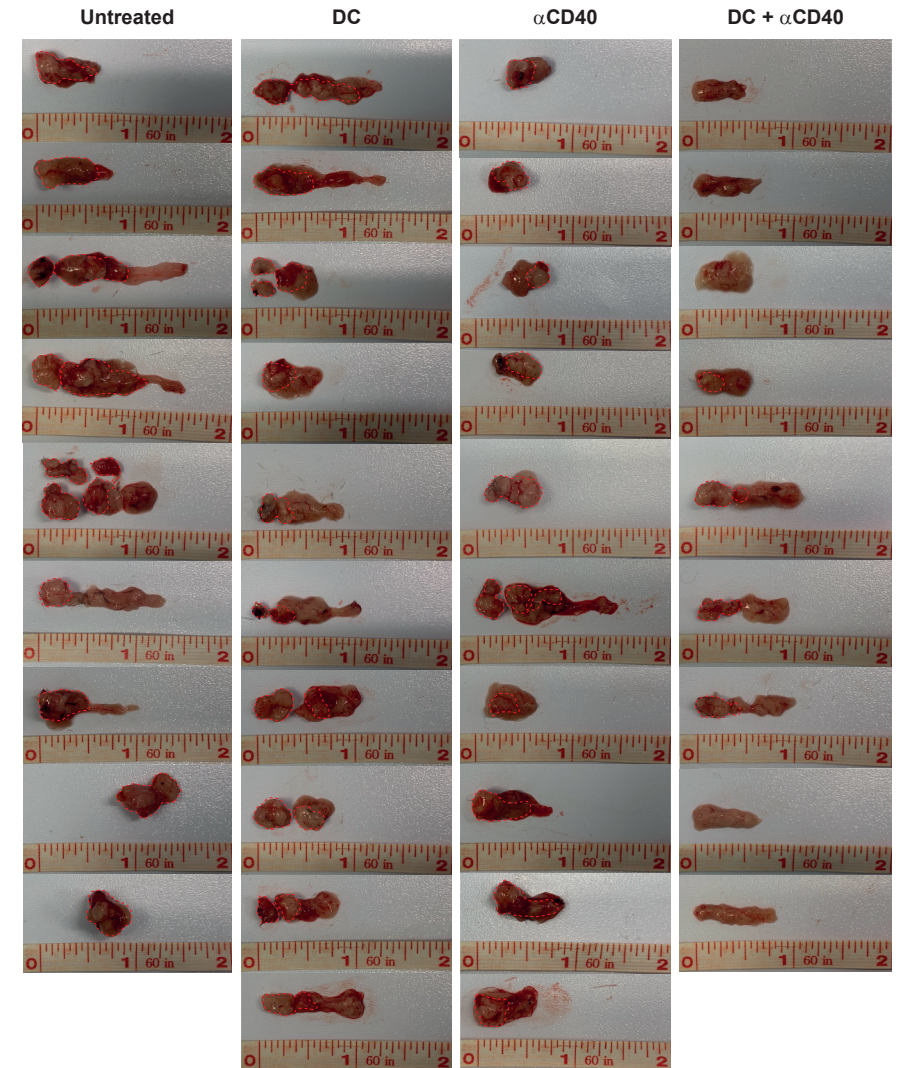


Figure S10. Orthotopic tumors taken out on day 17.

PART B
Improving the efficacy of
cancer vaccines for solid tumors
by combination immunotherapy

DENDRITIC CELL VACCINATION AND
CD40-AGONIST COMBINATION THERAPY LICENSES
T CELL-DEPENDENT ANTITUMOR IMMUNITY IN
A PANCREATIC CARCINOMA MURINE MODEL

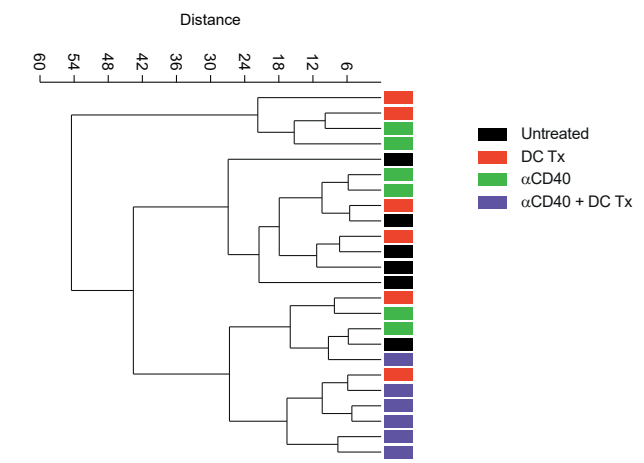
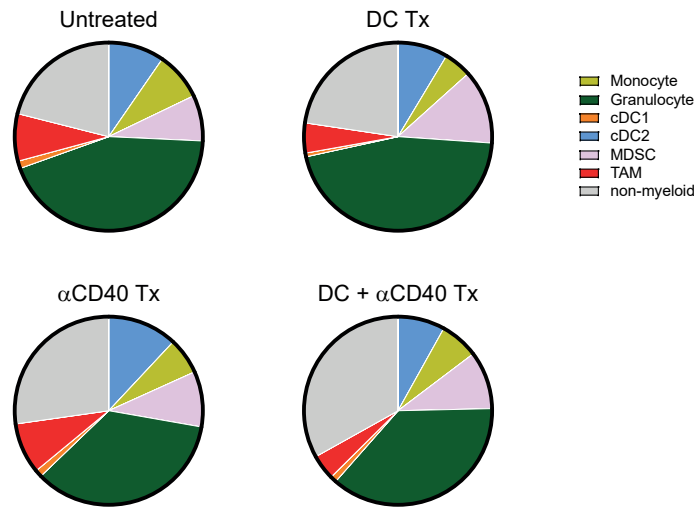


Figure S11. Fraction of non-myeloid (CD45-), monocyte (CD45+F4/80-CD11b+Ly6C+Ly6G-), granulocyte (CD45+F4/80-CD11b+Ly6C-Ly6G+), cDC1 (CD45+F4/80-CD11b+CD11c+MHCII+CD103+), cDC2 (CD45+F4/80-CD11b+CD11c+MHCII+), MDSC (CD45+F4/80-CD11b+Ly6CintLy6Gint) and TAM (CD45+F4/80+CD11b+) as part of a whole of treated and untreated tumors.

Figure S12. Hierarchical clustering of individual tumor samples based on genes significantly different between groups.

PART B
Improving the efficacy of
cancer vaccines for solid tumors
by combination immunotherapy

DENDRITIC CELL VACCINATION AND
CD40-AGONIST COMBINATION THERAPY LICENSES
T CELL-DEPENDENT ANTITUMOR IMMUNITY IN
A PANCREATIC CARCINOMA MURINE MODEL

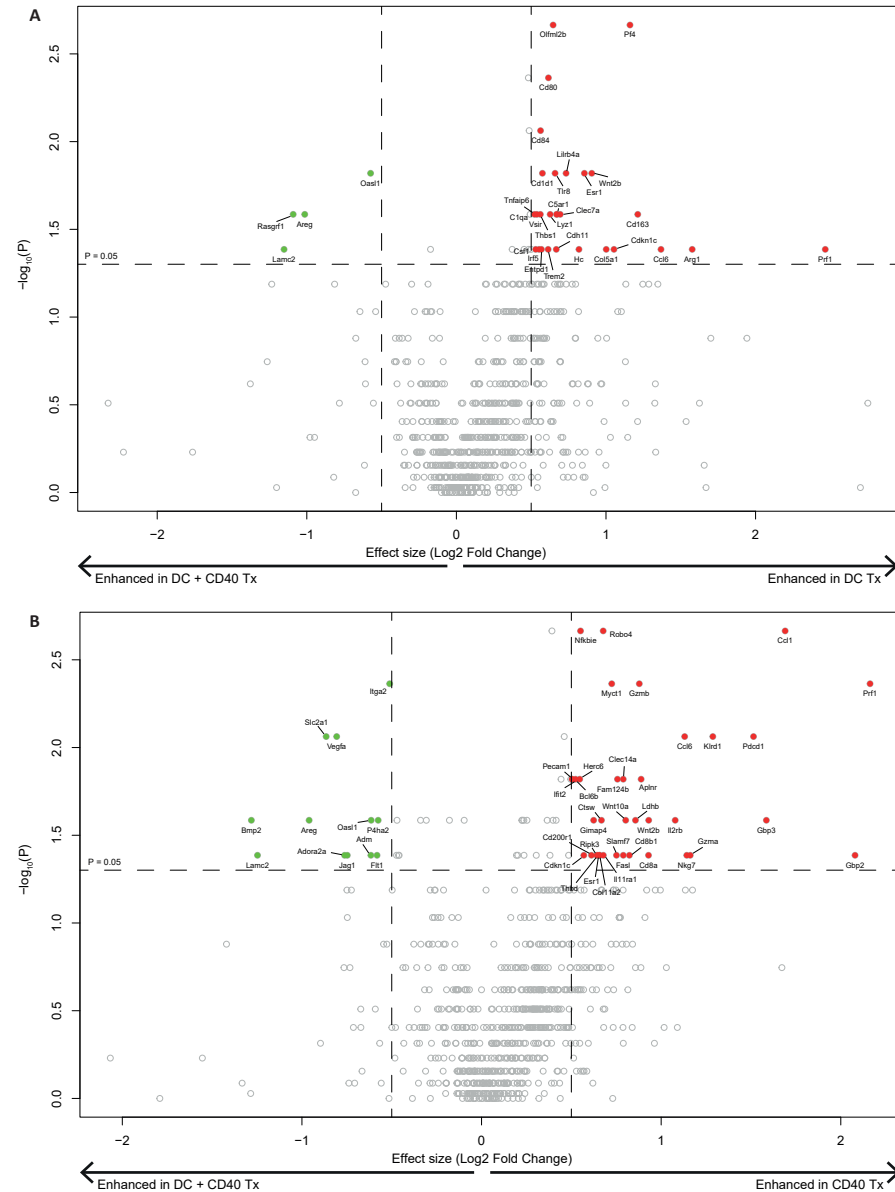


Figure S13. Volcano plots of differentially expressed genes between DC vaccination vs combination therapy (**A**) or α CD40 vs combination therapy (**B**). The X-axis is log2 fold change and the Y-axis is $-\log_{10}$ of the original p-value. Markers with p-values < 0.05 and log2 fold change > 0.5 are marked in red, while markers with p-values < 0.05 and log2 fold change < -0.5 are marked in green. The two vertical lines indicate the log2 fold change threshold of 0.5 and -0.5. The horizontal line indicates the original p-value threshold of 0.05.

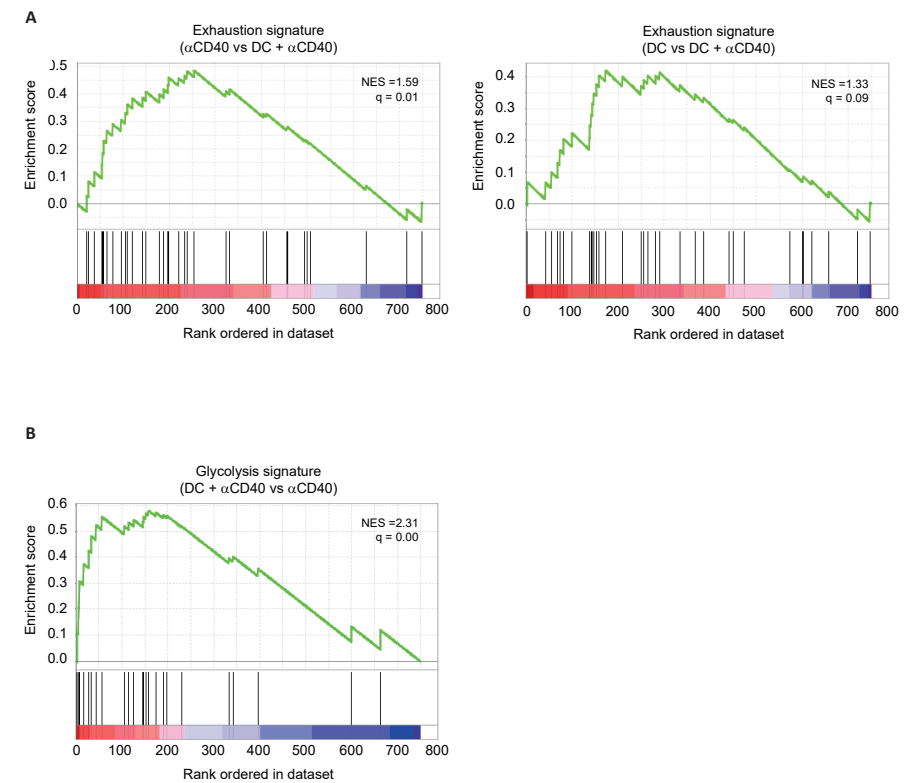


Figure S14. (A) GSEA of T-cell exhaustion gene sets in tumors of α CD40 or DC therapy versus combination therapy treated mice, presented as the normalized enrichment score (NES). (B) GSEA of T-cell exhaustion and glycolysis gene sets in tumors of combination therapy versus α CD40 treated mice, presented as the normalized enrichment score (NES).

PART B
Improving the efficacy of
cancer vaccines for solid tumors
by combination immunotherapy

DENDRITIC CELL VACCINATION AND
CD40-AGONIST COMBINATION THERAPY LICENSES
T CELL-DEPENDENT ANTITUMOR IMMUNITY IN
A PANCREATIC CARCINOMA MURINE MODEL

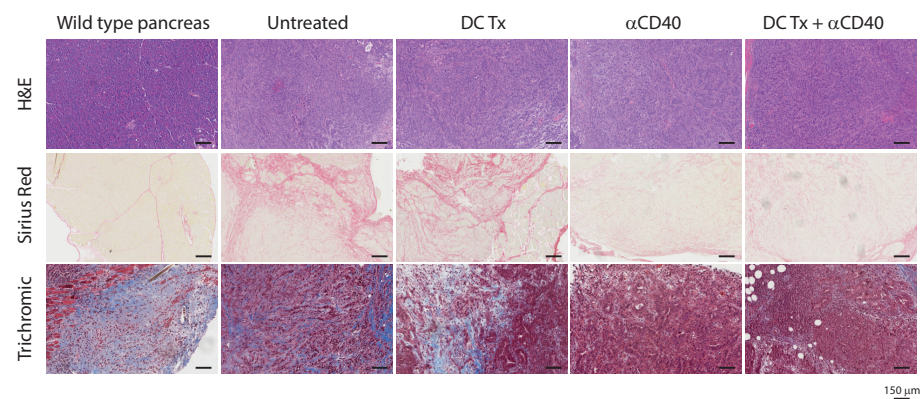


Figure S15. Hematoxylin and Eosin, Sirius Red and Trichromic staining on tumor tissue.

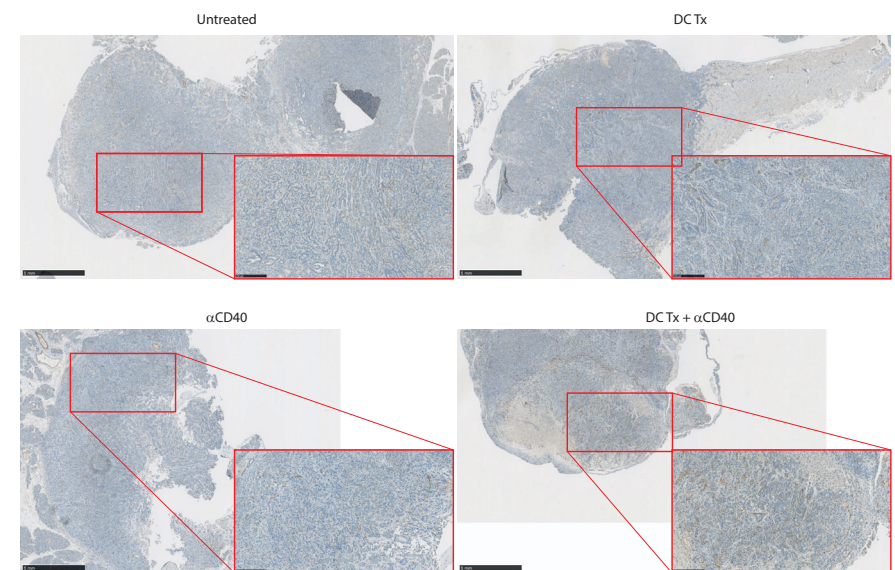


Figure S16. CD31 immunohistochemistry staining on tumor tissue of treated and untreated mice.

PART B
Improving the efficacy of
cancer vaccines for solid tumors
by combination immunotherapy

DENDRITIC CELL VACCINATION AND
CD40-AGONIST COMBINATION THERAPY LICENSES
T CELL-DEPENDENT ANTITUMOR IMMUNITY IN
A PANCREATIC CARCINOMA MURINE MODEL

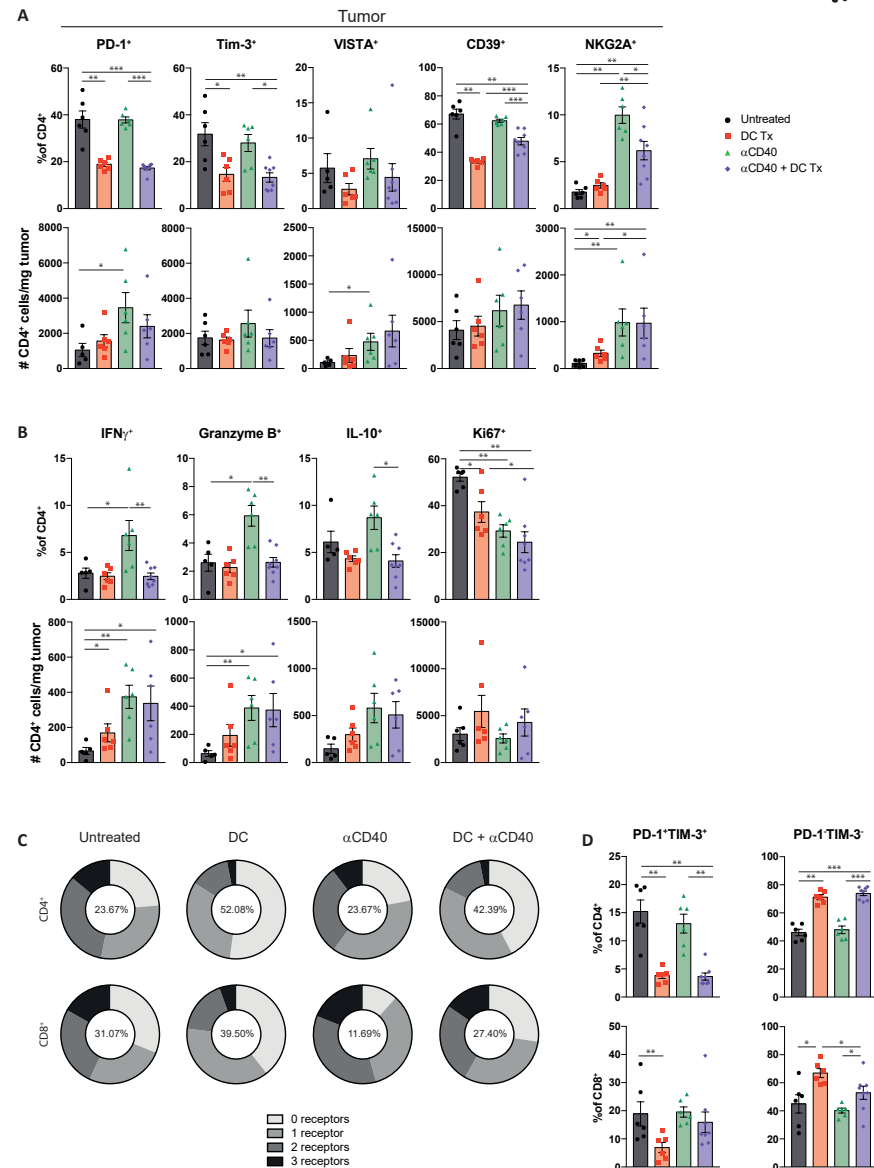


Figure S17. (A) Number and percentage of PD-1+, Tim-3+, VISTA+, CD39+ and NKG2A+ subsets of CD4+ TILs. **(B)** Number and percentage of IFN γ +, Granzyme B+, IL-10+ and Ki67+ subsets of CD4+ TILs. **(C)** Detection of co-expression of inhibitory receptors (PD-1, Tim-3 and CD39) on CD4+ and CD8+ TILs. Numbers within circles represent percentage of TILs with 0 inhibitory receptors. **(D)** Percentage of PD-1/TIM-3 double positive and negative cells of CD4+ and CD8+ TILs. N=7-8 per group. Significance was determined using the non-parametric Mann-Whitney U test. Data presented as the mean \pm s.e.m. *P<0.05, **P<0.01, ***P<0.001.

DC IL-12 production

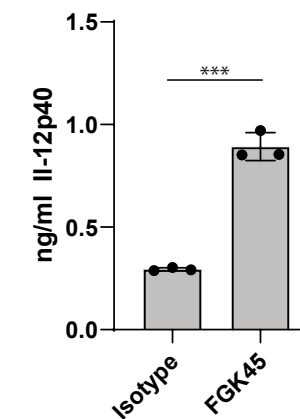


Figure S18. ELISA-based IL-12p40 detection in supernatant of bone-marrow derived DCs stimulated with FGK45 or isotype. Significance was determined using the Student's t-test. Data presented as the mean \pm s.e.m. ***P<0.001.

Table S1. Expression levels of immunogenic tumor antigens as reported by Cheevers et al.²³ translated to murine gene names (Mouse Genome Informatics) in KPC3, AE17 and B16 with a minimal threshold of 1 RPKM (reads per kilo base per million mapped reads).

Tumor antigen (Hu) (Cheevers et al.)	MGI Symbol	KPC3 (RPKM)	AE17 (RPKM)
B7H3	Cd276	10,453	5,128
CarbonicanhydraselX	Car9	0,877	1,723
CyclinB1	Ccnb1	33,524	49,515
CYP1B1	Cyp1b1	0,469	1,83
EGFR	Egfr	15,562	4,443
EphA2	Epha2	13,012	68,084
ETV6-AML	Etv6	7,635	4,272
Fos-relatedantigen1	Fosl1	1,58	14,79
GD2	B4galnt1	2,647	5,119
HER-2/neu	ErbB2	6,633	7,248
hTERT	Tert	0,621	1,516
Legumain	Lgmn	57,026	15,997
LMP2	Psmb9	5,375	0
Mesothelin	Msln	1,613	188,694
MUC1	Muc1	0,187	31,107
p53	Trp53	40,636	72,406
PAP	Acpp	1,667	0,014
PAX3	Pax3	1,097	0,027
PDGFR-β	Pdgfrb	19,265	0,012
Proteinase3(PR1)	Tmem37	12,497	0,511
PSCA	PscA	0,036	6,192
Ras	kras	9,478	7,068
RhoC	Rhoc	59,806	76,701
Sarcomatranslocationbreakpoints	Ewsr1	53,468	65,421
SART3	Sart3	10,381	15,07
SSX2	Rab3ip	8,145	7,677
Survivin	Birc5	33,091	50,658

7

F. Dammeijer
M. van Gulijk
L. Klaase
M. van Nimwegen
R. Bouzid
R. Hoogenboom
M.E. Joosse
R.W. Hendriks
T. van Hall
J.G. Aerts

Submitted.

PART B
Improving the efficacy of
cancer vaccines for solid tumors
by combination immunotherapy

LOW-DOSE JAK3-INHIBITION
IMPROVES ANTI-TUMOR T-CELL IMMUNITY
AND IMMUNOTHERAPY EFFICACY

SUMMARY

Terminal T-cell exhaustion poses a significant barrier to effective anti-cancer immunotherapy efficacy with current drugs aimed at reversing exhaustion being limited. Recent investigations into the molecular drivers of T-cell exhaustion have led to the identification of chronic IL-2 receptor (IL-2R) – STAT5 pathway signaling in mediating T-cell exhaustion. We targeted the key downstream IL-2R-intermediate Janus kinase (JAK) 3 using a clinically relevant highly specific JAK3-inhibitor (JAK3i; PF-06651600) which potently inhibited STAT5-phosphorylation in vitro. Whereas pulsed high-dose JAK3i administration inhibited anti-tumor T-cell immunity, low-dose chronic JAK3i significantly improved T-cell responses and decreased tumor load in mouse models of solid cancer. Low-dose JAK3i combined with cellular and peptide vaccine strategies further decreased tumor load compared to both monotherapies alone. Collectively, these results identify JAK3 as a novel and promising target for combination immunotherapy.

INTRODUCTION

Cancer immunotherapy induces durable anti-tumor immune and clinical responses but only in a minority of patients and tumor types for reasons still incompletely understood¹⁻³. T-cell exhaustion is a major mechanism underlying cancer immunotherapy resistance and current treatment strategies aimed at the prevention or reversal of exhaustion are lacking⁴. T-cell exhaustion arises through chronic antigen stimulation of the T-cell receptor (TCR) in a suppressive tumor microenvironment (TME), decreasing T-cell functionality and persistence^{5,6}. Attempts have been made to prevent T-cell exhaustion by inhibiting key downstream TCR-signaling pathways (e.g. MAPK/ERK, mTOR), yielding varying clinical and preclinical results⁷⁻¹¹. Possible redundancy between different signaling pathways and the existence of exhaustion mechanisms other than chronic TCR-activation could be involved in T-cell exhaustion and immunotherapy resistance.

Besides excessive TCR-stimulation, continuous interleukin 2-receptor (IL-2R)-induced signal transducer and activator of transcription 5 (STAT5)-phosphorylation in T cells has recently been linked to exhaustion in chronic viral infection and cancer, with IL-2^{hi} cancers exhibiting poor prognosis^{12,13}. Despite that IL-2 is required for initial T-cell expansion and survival, excess IL-2 during T-cell priming skews towards a short-lived T-cell effector fate at the expense of memory precursor T cells^{14,15}. Whether temporal downstream IL-2R-inhibition improves antitumor immunity is currently unknown. The IL-2R may be a particularly attractive target as activation of the receptor culminates in MAPK- mTOR- as well as STAT5-signaling, thereby allowing for concomitant targeting of multiple exhaustion-related pathways.

Binding of IL-2 to the high affinity IL-2R $\alpha\beta$ chains CD25 and CD122 activates a downstream cascade initiated by Janus-kinase (JAK) family members JAK1 and JAK3 which in turn phosphorylate STAT5 leading to dimerization and target gene transcription^{16,17}. In contrast to JAK1 associating with various type I and II cytokine receptors, JAK3 is located downstream of the common-gamma chain cytokine receptor family including IL-2R, IL-4R, IL-7R and IL-15R. With the recent development of specific JAK-inhibitors, interrogation of these downstream cytokine-receptors pathways has become feasible with minimal off-target activity¹⁸. This allowed us to investigate JAK3 as novel immunotherapeutic target downstream of the IL-2R using the highly specific JAK3-inhibitor (JAK3i) PF-06651600 (further referred to as PF-06) which was initially developed for treatment of auto-immune disease^{19,20}. In this report, we demonstrate that this JAK3i effectively inhibits IL-2-mediated STAT5-phosphorylation in T cells and when administered at high dose diminishes anti-tumor T-cell immunity. In contrast, at low-dose, PF-06 improves T-cell responses and decreases tumor load in solid tumor mouse models. Moreover, JAK3i potentiated cellular- and peptide vaccine immunotherapies, improving therapeutic efficacy and reducing the exhausted T-cell phenotype. These important potential improvements of current immunotherapy warrant further investigation into the clinical use of low-dose JAK3i in solid tumor patients.

PART B
Improving the efficacy of
cancer vaccines for solid tumors
by combination immunotherapy

LOW-DOSE JAK3-INHIBITION
IMPROVES ANTI-TUMOR T-CELL IMMUNITY
AND IMMUNOTHERAPY EFFICACY

METHODS

Phosphoflow analysis.

Wildtype C57BL/6 mice were euthanized by cervical dislocation and the spleens were isolated and mashed over a 100µm filter establishing a cell suspension in RPMI 1640 containing 2% FCS. 2×10^6 Splenocytes were incubated for 3 hours at 37°C with vehicle (same amount of DMSO as highest concentration of inhibitor as negative control) or Acalabrutinib (10µM, 1µM and 0,1µM in DMSO) or Ibrutinib (10µM, 1µM and 0,1µM in DMSO) or PF-06651600 (10µM, 1µM and 0,1µM in MilliQ, all obtained from Sigma-Aldrich). The cells were stimulated with anti-CD3/CD28 biotin in case of the stimulated samples or RPMI1640 2%FCS for unstimulated samples. Afterwards, the cells were washed with RPMI1640 2% FCS and stained with streptavidin PerCP Cy5.5 to establish receptor cross-linking. After washing, the samples were stimulated at 37°C for 1 minute for pZAP70_{Y319} (pZAP70) and pSLP76_{Y128} (pSLP76), 5 minutes for pITK_{Y180} (pITK₁₈₀) and pERK1/2_{T202/Y204} (pERK), 120 minutes for IκB and pS6_{S240/244} (pS6). Ten minutes before the end of the stimulation a live/death marker was added. At the end of the stimulation, Fix/Perm was added and incubated at 37°C for ten minutes followed by transfer on ice and wash with permeabilization buffer. After permeabilization, the samples were stained for 30 minutes with extracellular surface markers using a monoclonal antibody (mAb) staining mix including Fc-receptor blocking antibodies (aCD16/32; Bioceros). After wash, the samples were stained for one of each of the following phosphoflow targets; pZAP70, pSLP76, pITK180, pERK, and pS6. In case of the unlabeled anti-pS6 antibody, a third staining step containing a PE-labeled anti-Rabbit antibody was necessary. For pIκB a different staining protocol was used by which cells were fixed with paraformaldehyde incubated for 10 minutes at room temperature followed by permeabilization using 0,5% saponin in FACS. Cells were then stained with surface markers and anti-pIκB followed by acquisition for flow cytometry.

IL-2 stimulation and pSTAT5 phosphoflow.

24×10^6 Splenocytes were divided over 12 wells of a 24 wells plate and aCD3/CD28 Dynabeads (Thermofisher) were added in a 1:1 ratio for 72 hours in TCM to induce IL-2R expression as assessed by upregulation of CD25. Dynabeads were extracted by magnet retrieval and 2×10^6 cells were incubated for 3 hours at 37°C with vehicle (same amount of DMSO as highest concentration of inhibitor as negative control) or Acalabrutinib (10µM, 1µM and 0,1µM in DMSO) or Ibrutinib (10µM, 1µM and 0,1µM in DMSO) or PF-06651600 (10µM, 1µM and 0,1µM in MilliQ). After 3 hours, a 500.000/50µL cell suspension was activated for 15 minutes with 10ng/mL IL-2 (R&D Systems) at 37°C. 10 Minutes before the re-stimulation end time, a live/death marker was added (eBioscience) followed by cell fixation using BD Cytofix and incubated for 10 minutes at 37°C. After the cells were fixed,

the cells were washed with MACS buffer (PBS containing 5mM EDTA and 1% BSA) and permeabilized with 150µL permbuffer III (BD) and the cells were incubated for 30 minutes at -20°C. After 30 minutes the cells were washed with MACS buffer and stained with surface markers containing CD25, CD8, CD4, PD-1, CD44, B220 and CD3 and Fc-block for 30 minutes at 4°C followed by wash with MACS buffer and pSTAT5 staining for 30 minutes at room temperature.

Bone marrow derived macrophage (BMDM) cultures.

Bone marrow cells were isolated from the femurs and tibias of naïve CBA/J (Janvier, Hannover, Germany), or C56BL/6 mice (Envigo, Zeist, The Netherlands) mice under sterile conditions. In short, all muscle tissues are removed with gauze from the bones and placed in a 60-mm dish with 70% alcohol for 1 min, washed twice with PBS and transferred into a fresh dish with RPMI 1640. Bones were crushed using a pestle and mortar and subsequently passed through nylon mesh to remove small pieces of bone and debris followed by erythrocyte lysis using ammonium chloride. Bone marrow cells were resuspended in RPMI supplemented with 10% fetal calf serum, 2.5ml gentamicin (10mg/ml) (Gibco, Breda, the Netherlands), 50µM β-mercaptoethanol (SigmaAldrich) and 10ng/ml M-CSF (R&D systems, Oxon, UK) to establish macrophage-TCM. 2×10^5 cells were plated per well in a 24-well Nunc plate with Upcell surface coating, allowing for harvest of cells at low temperatures following a 7-day culture period. Fresh TCM was added on day 3 of culture, and polarizing cytokines with or without a range drug concentrations on day 6 for the final 24 hour remainder of the culture period. M1 macrophages were generated by adding LPS (50ng/ml) and IFNγ (50ng/ml), or IL-4 (10ng/ml) with or without IL-10 (10ng/ml) or IL-13 (10ng/ml) in case of M2 macrophages. Besides the inhibition of JAK3 using the specific JAK3-inhibitor (PF06651600, Sigma Aldrich), cells were alternatively treated with trimeric CD40L (Immunex, 1µg/ml), with a JAK1/JAK3 dual inhibitor (Tofacitinib, Sigma-Aldrich) or associated diluents as negative controls. At the end of the culture, the plates were put on ice and cell suspensions were harvested and prepared for flow-cytometric analysis.

Monocyte derived macrophage cultures.

Monocytes from healthy donors were extracted with magnetic-activated cell sorting (MACS) using anti-CD14 antibody coated microbeads (Milteny Biotec) according to the manufacturer's protocol. Following the MACS-procedure, cells were stained for flow cytometry to guarantee sufficient purity (>98%). Monocytes were then suspended in TCM consisting of RPMI 1640 + Glutamax, 10% normal healthy AB serum and human macrophage colony-stimulating factor (20ng/mL, R&D Systems). Cells were cultured similarly to murine macrophages, with the exception of being an 8-day culture with macrophage polarization occurring in the final 48 hours of culture. Polarization to the M1

or M2 phenotype occurred in the presence of LPS (100ng/mL, Sigma-Aldrich) and IFN γ (20ng/mL, R&D Systems) for M1 or IL-4 (20ng/mL, R&D Systems) with or without IL-13 (20 ng/mL, R&D Systems) for M2 for 2 days.

T-cell cultures.

Venous blood from adult healthy individuals was collected in EDTA tubes and peripheral blood mononuclear cells (PBMCs) were isolated using a Ficoll-Hypaque gradient according to standard protocol (Axis-Shield Diagnostics, Dundee, UK). PBMCs were labelled with CellTrace Violet (ThermoFisher Scientific) and were stimulated with anti-CD3/CD28 Dynabeads at 0.5 bead per mononuclear cell with or without recombinant human IL-2 (1, 10 or 100 IU/ml, R&D Systems) for the indicated time-points. In some conditions, Tofacitinib (200 μ M or 1000 μ M) or PF-06651600 (200 μ M or 1000 μ M) was added to the culture. Cells were cultured in Iscove's modified Dulbecco's medium (ThermoFisher Scientific) supplemented with heat inactivated fetal calf serum, Glutamax (ThermoFisher Scientific), 2-mercaptoethanol, penicillin and streptomycin. Cytokine concentrations in cell supernatants were analyzed using an enzyme-linked immunosorbent assay set for IFN γ (eBioscience) according to the manufacturer's instructions. In case of murine T-cell cultures, proliferation-dye pre-stained wild-type C57BL/6 T-cells were stimulated with anti-CD3/CD28 Dynabeads at 1:1 ratio with various concentrations of PF06651600 (negative control=H $_2$ O) or Tofacitinib (negative control=DMSO) and assessed for proliferation, activation (CD69, CD25) and cytokine (TNF-alpha, Interferon-gamma) production 24 hours later using (intracellular) flow cytometry.

In vivo murine tumor models and experiments.

Female 8-10 week old C57BL/6 mice (Envigo, Zeist, The Netherlands) and CBA/J mice (Janvier, Hannover, Germany) were housed under specific pathogen-free conditions at the animal care facility of the Erasmus MC, Rotterdam. Experiments were approved by the local and central Ethical Committee for Animal Welfare and complied to the Guidelines for the Welfare of Animals in Experimental Neoplasia by the United Kingdom Coordinating Committee on Cancer Research (UKCCCR) and by the Code of Practice of the Dutch Veterinarian Inspection. The AE17 cell and AC29 mesothelioma cell lines were kindly provided by Professor Bruce W.S. Robinson of the Queen Elizabeth II Medical Centre, Nedlands, Australia. Tumor cells were cultured in RPMI 1640 medium containing 25mM HEPES, Glutamax, 50g/ml gentamicin, and 5% (v/v) fetal bovine serum (FBS) (all obtained from Gibco) in a humidified atmosphere and at 5% CO $_2$, in air. For culture, either culture flasks or CellSTACKs (Corning Life Sciences) were used to reach appropriate tumor cell frequencies for injection. AE17 and AC29 cells were passaged once or twice a week to a new flask by treatment with 0.05% trypsin, 0.53 mM EDTA in phosphate buffered

saline (PBS, all Gibco). The cell lines were regularly tested and remained negative for mycoplasma contamination. At the start of the experiment, CBA/J or C57BL/6 mice were i.p or s.c. injected with either 10 7 AC29 cells or 0.5x10 6 AE17 cells respectively, dissolved in PBS, or with PBS as control. Mice were scored using the body condition score, killed if profoundly ill and scored as a death in survival analysis. For DC-therapy experiments, BMDC were generated from wild-type CBA/J mice and loaded with AC29 tumor cell lysate in vitro as described previously. On day 10 following i.p. tumor inoculation, 2-3x10 6 DC were injected i.p. For SLP-vaccination studies in the TC-1 tumor model, TC-1 cells were cultured in 500 ml IMDM medium, 8% FBS (40 ml) and pen/strep plus L-glutamin and following cell harvest were injected in the flank of wild-type C57BL/6 mice. When tumors were established on day 8, mice received s.c. PBS or the SLP HPV16 E743-77 (GQAEPDRAHYNIIVTFCKCDSTLRLCVQSTHVDIR) emulsified at a 1:1 ratio with Incomplete Freund's Adjuvant (IFA; Difco) in the contralateral flank. In case of subcutaneous tumor models, tumors were measured twice weekly using an electronic micro-caliper and mice were euthanized when tumors grew beyond 100mm 2 or became ulcerated.

In vivo treatment with PF-06651600.

Mice were treated with a range of PF-06651600 concentrations dissolved in pre-warmed deionized water (Milli-Q) with all tested concentrations ranging within the solubility spectrum (5mg/ml). Mice were treated with the JAK3-inhibitor or the diluent (MQ) via oral gavage, twice daily with intervals of 12 hours, as reported by the manufacturer for a maximum of 14 days. Alternatively, PF-06651600 was administered in drinking water ad libitum, assuming that 8-week old female mice with an average weight of 20g drink approximately 5ml of water per 24 hours (meaning that for the 5mg/kg dose in drinking water, 10mg of PF-06651600 was dissolved in 1L of MQ, amounting to a ~25 μ M). Drinking water was refreshed every week and bottles were covered with aluminum foil.

Preparation of Single Cell Suspensions from Tissues.

Single cell suspensions were generated from the spleens, blood and tumors of mice from each group. All tissues were either weighed in a microbalance in case of tumors and spleens, or volume determined for blood. Briefly, spleens were aseptically removed and mechanically dispersed over a 100 μ m nylon mesh cell strainer (BD Biosciences) followed by erythrocyte lysis using osmotic lysis buffer (8.3% NH $_4$ Cl, 1% KHCO $_3$, and 0.04% Na $_2$ EDTA in Milli-Q). Blood was collected in EDTA tubes (Microvette CB300, Sarstedt) and subsequently lysed. Tumors were collected, and dissociated using a validated tumor dissociation system (Miltenyi Biotec). Cells suspensions were filtered through a 100 μ m nylon mesh cell strainer (BD Biosciences) and counted in trypan blue with a hemocytometer using the Burkert-Turk method.

Immunomonitoring using Flow Cytometry.

For measurements of cytokine production in lymphoid cells by flow cytometry, cells were restimulated for 4 h at 37°C using PMA and ionomycin supplemented with GolgiStop (BD Biosciences). For assessing cytokine production by myeloid cells, cells were subjected to 4 hours incubation with Golgistop. For cell surface marker staining, cells were washed with FACS-wash (0.05% NaN₃, 2% BSA in PBS) and Fc II/III receptor blocking was performed using anti-mouse 2.4G2 antibody (1:300; kindly provided by L. Boon, Bioceros, Utrecht, The Netherlands). After the blocking procedure, antibodies (all derived from BD Biosciences, Biolegend or ThermoFisher Scientific, titrated to optimal dilutions and used according to the manufacturer's protocol) for cell surface staining were added into each sample and placed on ice for 30 minutes. Cells were washed in FACS-wash followed by a PBS wash, and then stained for viability using fixable LIVE/DEAD aqua cell stain (Thermo-Fisher Scientific, 1:200). After two additional washes with FACS-wash, cells were either measured or in case of intracellular staining; fixed, permeabilized and stained using Fix/Perm buffer (in case of nuclear protein staining, eBioscience) or 4% PFA and 0.5% saponin (in case of cytokine/granzymeB stainings, Sigma-Aldrich). Antibodies were stained for 30 minutes in case of the PFA/Saponin protocol and 60 minutes for the intranuclear staining protocol, on ice in the dark. A fixed number of counting beads (Polysciences Inc.) was added prior to data acquisition to determine the absolute amount of cells. Data were acquired using an LSR II flow cytometer (BD) equipped with three lasers and FACSDiva software (BD) and analyzed by FlowJo (Tree Star Inc., USA) software V10.1.

Tumor cell apoptosis assay.

0.2x10⁶ cells from various murine and human cancer-derived cell lines were cultured in aforementioned appropriate culture conditions in 6-wells plates for 48 hours in the presence of absence of different JAK3i (PF-06651600) concentrations. Following culture, cells were harvested and stained for cell death and apoptosis using the 7-AAD/Annexin V staining kit, according to the manufacturer's protocol (Biolegend).

Statistical Analysis.

Data are expressed as means with SEM. Comparisons between groups were made using the Mann-Whitney U-test for independent samples, or the Wilcoxon signed rank test in case of paired samples. When correlations were depicted, Spearman's rank correlation test was performed to test for statistical significance. A two-tailed value of $p < 0.05$ was considered statistically significant. Survival data were plotted as Kaplan-Meier survival curves, using the log-rank test to determine statistical significance. Data was analyzed using Graphpad Prism software (Graphpad, V5.01)

RESULTS

PF-06 is a potent inhibitor of IL-2 mediated STAT5-phosphorylation in T cells.

Chronic phosphorylation of STAT5 by JAK1/3 in T cells has been recently found to underlie ineffective anti-tumor immunity providing a rational for JAK3i in solid tumors¹². Because JAKs are involved in many pro- and anti-tumor cytokine receptor pathways, off-target specificity of early generation JAK3i could potentially antagonize beneficial outcomes of JAK3-specific inhibition at the expense of increased toxicity¹⁸. In order to evaluate whether the novel compound PF-06 specifically inhibits STAT5-phosphorylation and to which degree, wildtype naive and pre-activated CD25⁺ murine T cells were simulated *in vitro* using anti-CD3/CD28 or IL-2, respectively, and analyzed using Phosphoflow²¹. The broad kinase inhibitor Ibrutinib was applied as a positive control since kinomscan data identified multiple kinases, including JAK3 as targets²². The selective BTK-inhibitor Acalabrutinib was used as a negative control in our studies as BTK is not expressed by T cells^{22,23}. Only PF-06 specifically inhibited IL-2-mediated pSTAT5 in both CD8⁺ and CD4⁺ T cells (Fig. 1)

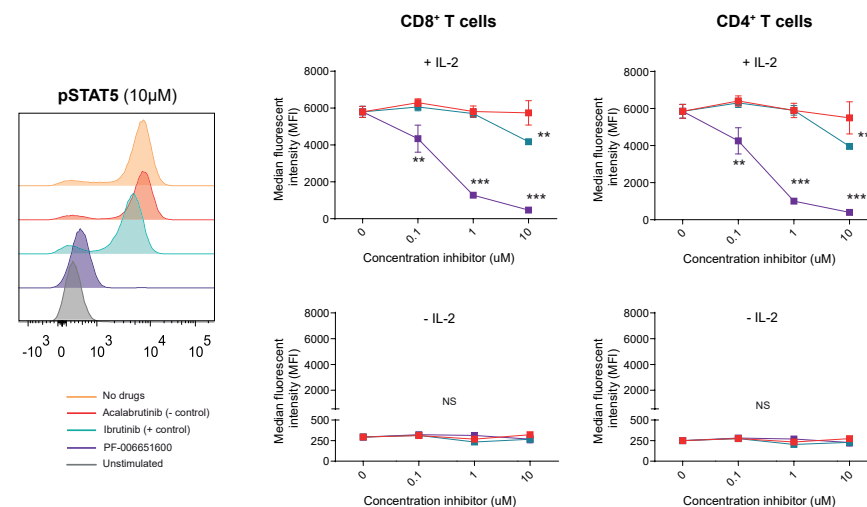


Figure 1. The JAK3-inhibitor PF-06651600 potently inhibits STAT5-phosphorylation in response to IL-2 in T cells. Pre-activated IL-2R α (CD25) expressing murine T cells were stimulated with IL-2 after pre-incubation alone (orange), with the specific JAK3i; PF-06651600 (purple), aspecific JAK3i; Ibrutinib (turquoise) or negative control; Acalabrutinib (red) using Phosphoflow. Histograms are shown displaying the effects of the different inhibitors on pSTAT5-expression at 10µM (left panel) and quantified expression of pSTAT5 in CD8⁺ and CD4⁺ T cells stimulated or unstimulated with IL-2 (right panels). MFI=median fluorescence intensity, * = $p < 0.05$, ** = $p < 0.01$, *** = $p < 0.001$. Means and SEM are shown, n=5/condition.

PART B
Improving the efficacy of
cancer vaccines for solid tumors
by combination immunotherapy

LOW-DOSE JAK3-INHIBITION
IMPROVES ANTI-TUMOR T-CELL IMMUNITY
AND IMMUNOTHERAPY EFFICACY

while leaving other quintessential T-cell signaling pathways (e.g. downstream TCR, NF- κ B, MAPK/ERK) unaltered (Fig. 2, S1). As CD25-expression among CD25⁺ T cells varied, we compared pSTAT5 levels at baseline and in response to JAK3i in CD25-high, intermediate and low-expressing T cells. CD25-high expressing cells displayed increased STAT5-phosphorylation at baseline but also in response to low-dose JAK3i *in vitro* suggesting increased sensitivity to IL-2 in CD25-high expressing cells (Fig. S2A). Regulatory T cells (Tregs) constitutively express CD25 as a means to scavenge IL-2 thereby inhibiting effector T-cell proliferation²⁴. To investigate how Tregs respond to IL-2 and JAK3i we assessed pSTAT5-phosphorylation status in CD44⁺ CD25^{hi} CD4⁺ T cells, a population enriched for Tregs in the naïve spleen (Fig. S2B). As expected, pSTAT5-expression was nearly twice as high in Tregs compared to non-Tregs, with pSTAT5 being completely inhibited only at higher micromolar levels of PF-06 *in vitro* (Fig. S2B). We concluded that the specific JAK3i PF-06 efficiently prevented STAT5 phosphorylation in mouse T cells in a low micromolar range.

PF-06 inhibits T-cell proliferation and effector function at high concentrations in vitro.

To investigate how decreased IL-2-mediated STAT5-phosphorylation translates to T-cell proliferation over time, we stimulated dye-labeled T cells *in vitro* using anti-CD3/CD28 Dynabeads alone or in the context of JAK3i. Head-to-head comparison between PF-06 and the less specific JAK1/3i Tofacitinib showed both drugs to inhibit T-cell proliferation, activation and effector cytokine production but only at high (>1.0 μ M) drug concentrations in mouse (Fig. S3) and human (Fig. S4A-C) T cells. Interestingly, whereas Tofacitinib more potently inhibited T-cell proliferation and cytokine expression in humans compared to PF-06, the opposite was true for mice (Fig. S3-4). In contrast to Tofacitinib, however, PF-06 only modestly inhibited cellular activation and interferon- γ production in healthy-control derived T cells at the micromolar range (Fig. S4C). These findings show PF-06 to be a potent inhibitor of IL-2-mediated pSTAT5 in T cells, with T-cell functions being inhibited only at higher drug concentrations providing a window for STAT5 modulation.

JAK3i decreases tumor progression depending on the dose and mode of administration.

In order to assess the effects of PF-06 *in vivo* and its anti-tumor efficacy we treated AE17 and AC29 immune competent mesothelioma tumor-bearing mice with PF-06 administered by oral gavage twice-daily as described by others¹⁹. Using this treatment scheme, tumor progression was unaltered in these tumor models compared to vehicle treatment (Fig. 3A). The lack of response was accompanied by a reduction in T-cell proliferation monitored in peripheral blood, and decreased activation, proliferation and effector function at the tumor site (Fig. 3B), indicative of suppressed anti-tumor immunity. We postulated that peak PF-06 concentrations following oral administration would approach immune suppressive drug concentrations reminiscent of aforementioned *in vitro* studies (Fig. S3), and that low-

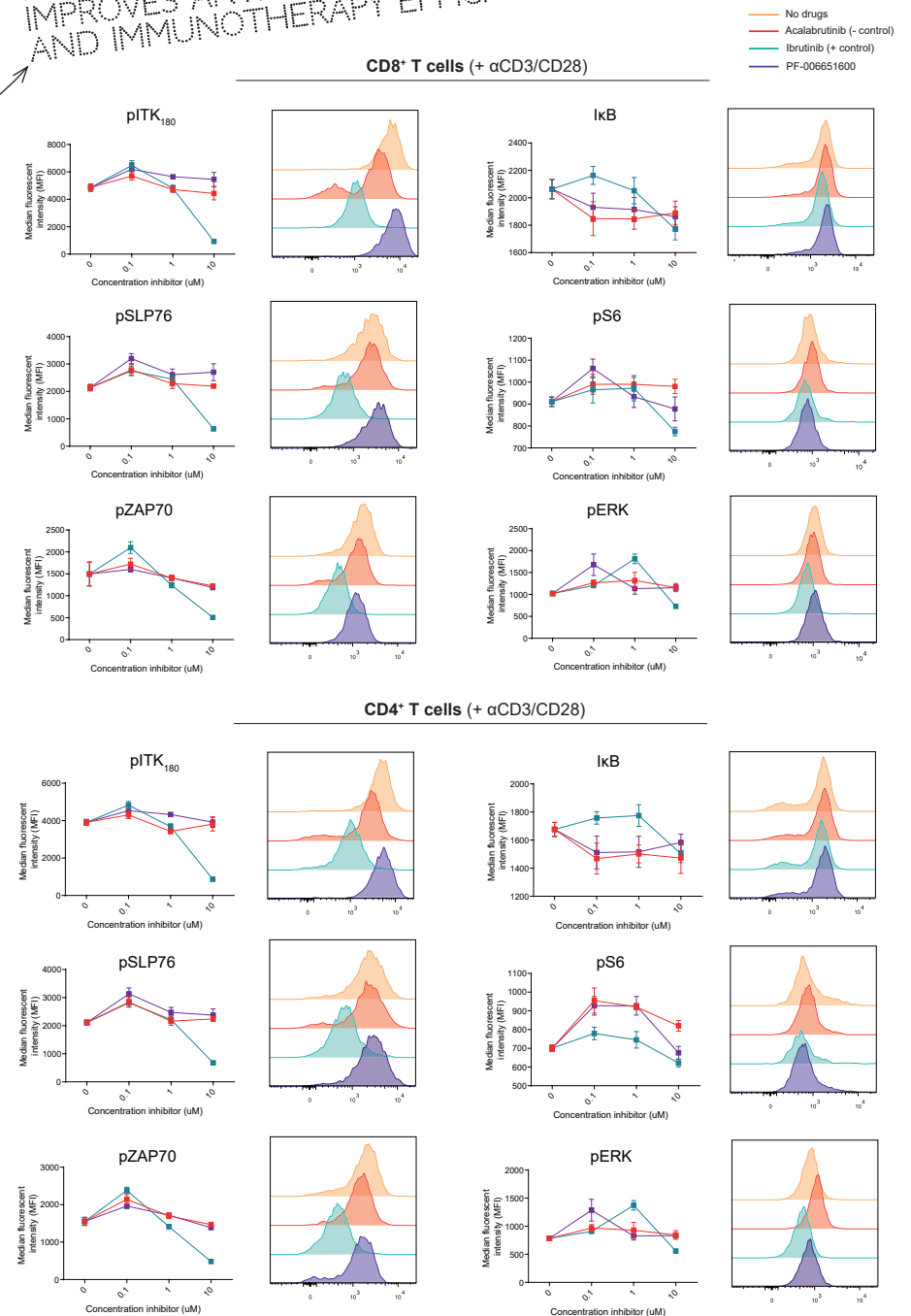
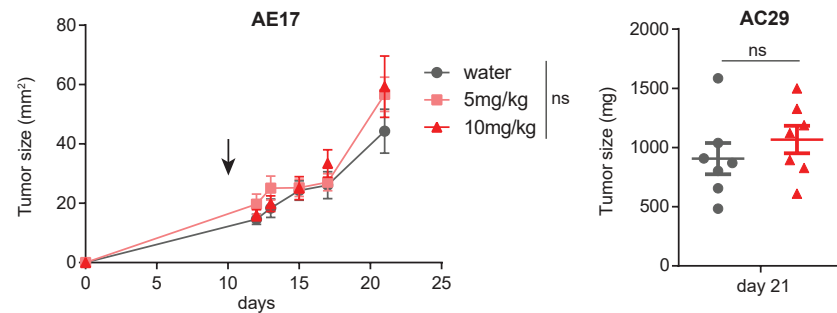


Figure 2. PF-06651600 does not inhibit other T-cell signaling pathways. In order to determine off-target efficacy of PF-06 on other crucial T-cell signaling pathways we assessed phosphorylation of proteins downstream of the T-cell receptor (TCR) (pZAP70, pSLP76, pITK180), PI3K-Akt (pS6), NF- κ B (I κ B) or MAPK-ERK (pERK) pathways following anti-CD3/CD28 stimulation with or without inhibitors using Phosphoflow. Results for both CD8⁺ (upper panels) and CD4⁺ T cells (lower panels) are shown as histograms (10 μ M drug concentration) and line graphs. MFI=median fluorescence intensity, means and SEM are shown, n=5/condition.

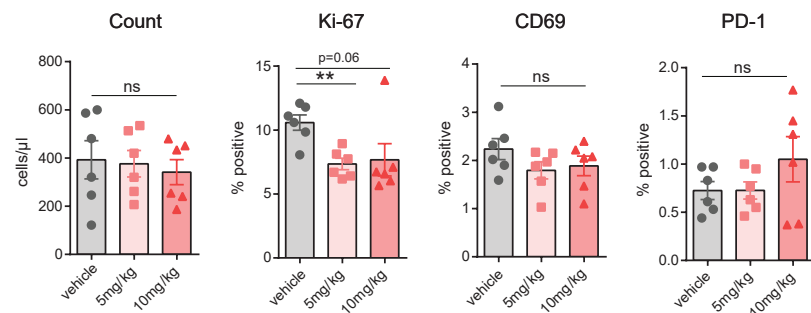
PART B
Improving the efficacy of
cancer vaccines for solid tumors
by combination immunotherapy

LOW-DOSE JAK3-INHIBITION
IMPROVES ANTI-TUMOR T-CELL IMMUNITY
AND IMMUNOTHERAPY EFFICACY

A JAK3i via Oral Gavage



B Peripheral Blood CD8⁺ T cells



Tumor-infiltrating CD8⁺ T cells

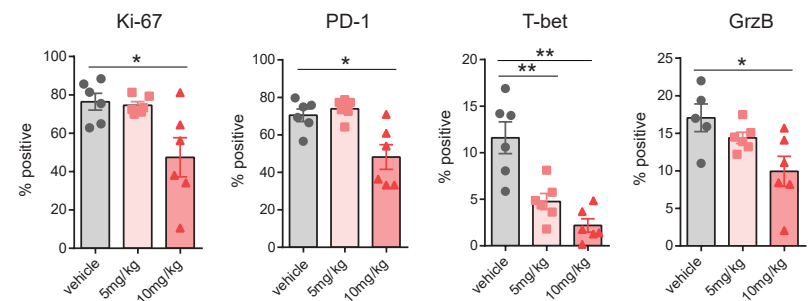
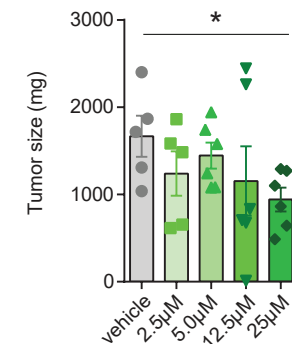


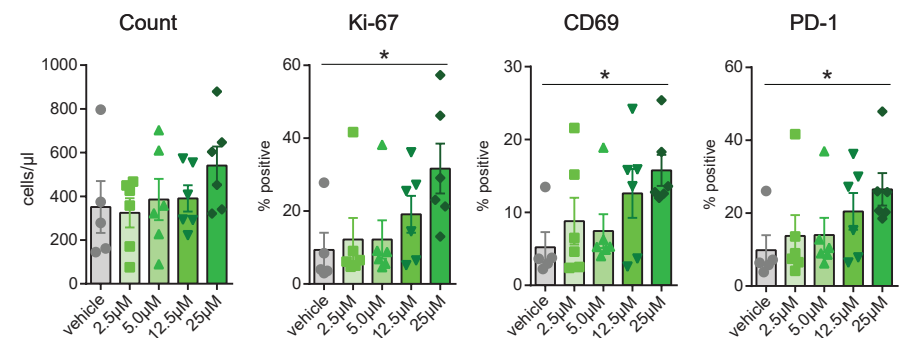
Figure 3. Twice-daily high-dose JAK3i via oral gavage does not impact tumor growth and inhibits T-cell immunity. (A) AE17 subcutaneous and AC29 intraperitoneal tumor-bearing mice were treated with the JAK3i; PF-06651600 via twice-daily oral gavage starting on day 10 and tumor burden was assessed on day 21. **(B)** CD8⁺ T cells in peripheral blood on day 15 or in the tumor at end-stage **(C)** were assessed for proliferation (Ki-67) and activation status using multicolor flow cytometry. Means and SEM are shown with n=6 mice/condition. JAK3i=JAK3-inhibitor, Ns=non-significant, * = p < 0.05, ** = p < 0.01, GrzB=granzyme B.

grade and stable dosing of JAK3i in drinking water would ameliorate this issue. Therefore, we repeated the *in vivo* experiment dissolving PF-06 in drinking water aiming for tonic inhibition of the IL-2R/JAK3/STAT5-axis throughout the anti-tumor immune response. In contrast to oral gavage, continuous low-dose JAK3i suppressed tumor growth in a dose-dependent manner with ~25μM being established as the optimal dose (Fig. 4A). Changes in tumor burden were paralleled by increased T-cell frequency and a more activated and proliferative T-cell compartment as evidenced by increased Ki-67- and PD-1 expression (Fig. 4B). These data show that JAK3i, if provided as a steady continuous administration, impedes tumor progression coinciding with increased T-cell activation.

A JAK3i via drinking water (AC29)



B Peripheral Blood CD8⁺ T cells



PART B
Improving the efficacy of
cancer vaccines for solid tumors
by combination immunotherapy

LOW-DOSE JAK3-INHIBITION
IMPROVES ANTI-TUMOR T-CELL IMMUNITY
AND IMMUNOTHERAPY EFFICACY

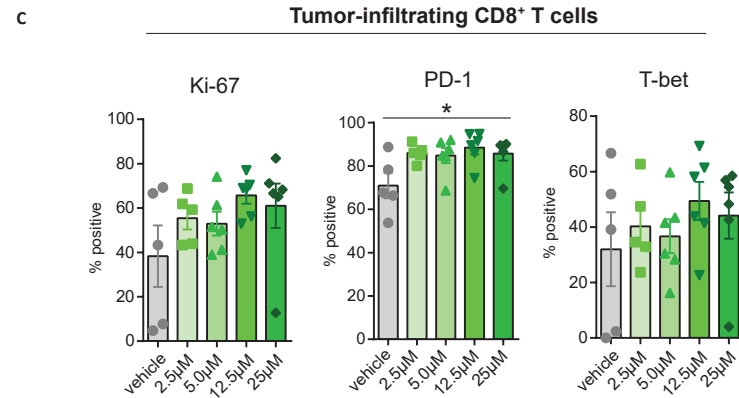
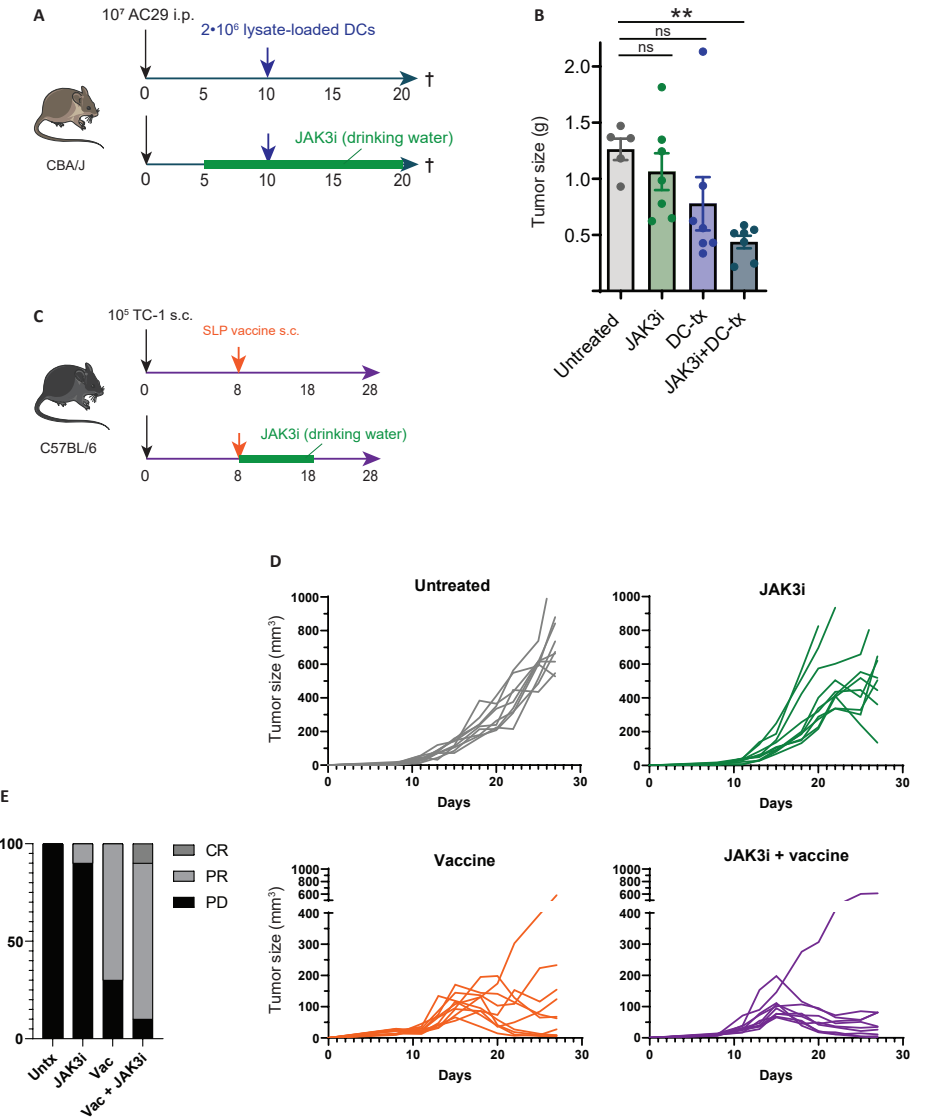


Figure 4. Continuous low-dose JAK3i at 5.0mg/kg significantly decreases tumor weight in AC29-bearing mice and improves anti-tumor T-cell immunity. (A) AC29 intraperitoneal tumor-bearing mice were treated with the JAK3i; PF-06651600 dissolved in drinking water at various pre-specified doses and tumor weight was monitored. (B) CD8⁺ T cells in peripheral blood on day 15 or in the tumor at end-stage (C) were assessed for proliferation (Ki67) and activation status using multicolor flow cytometry. Means and SEM are shown with n=6 mice/condition. JAK3i=JAK3-inhibitor, ns=non-significant, *p<0.05.

In contrast to *in vitro*, macrophage polarization is not altered by JAK3i *in vivo*.

As JAK3 associates with cytokine receptors on other immune cells, treatment efficacy could potentially be explained by inhibition of alternative pathways including IL-4/IL-4R signaling. Indeed, bone-marrow derived macrophages (BMDM) stimulated *in vitro* with IL-4 upregulated the M2 markers CD206, arginase and PD-L1 which could be antagonized by JAK3i (Fig. S5A). This effect could not be rescued by addition of excess IL-13, another M2-inducing cytokine sharing the IL-4R-alpha subunit, or IL-10 (Fig. S5B, *data not shown*)^{25,26}. In contrast to the JAK1/3i Tofacitinib, PF-06 did not alter pro-inflammatory (M1) macrophage differentiation as evaluated by iNOS and MHCII expression (Fig. S5C). Similar findings were obtained using human monocyte-derived macrophages (MoDM) (Fig. S6). Tumor-associated macrophage (TAM) and conventional DC (cDC) frequency and phenotype, however, were largely unaltered by JAK3i in all our investigated models, indicating that IL-4 plays an inferior or redundant role in *in vivo* myeloid cell polarization (Fig. S5D-E). On the same line, JAK3i did not directly affect solid tumor-cell apoptosis *in vitro* (Fig. S7A) or *in vivo* (Fig. S7B), except in case of the JAK3-mutated T-cell lymphoma cell line Hu-78 (Fig. S7A). We concluded that T cells are the most likely direct targets of JAK3i.



PART B

Improving the efficacy of cancer vaccines for solid tumors by combination immunotherapy

LOW-DOSE JAK3-INHIBITION IMPROVES ANTI-TUMOR T-CELL IMMUNITY AND IMMUNOTHERAPY EFFICACY

Although JAK3i as monotherapy is capable of inhibiting tumor progression, combining JAK3i with existing immunotherapies could further enhance efficacy of both modalities. Cellular and peptide cancer vaccines are safe and efficacious in inducing anti-tumor T-cell responses in solid advanced cancer, but durable responses are obtained in a small minority of patients possibly due to the eventual exhaustion of vaccine-elicited T-cell responses²⁷⁻³². In order to improve vaccine-induced T cells and treatment efficacy we treated AC29-bearing mice, at late stage, with tumor-lysate loaded BM-derived dendritic cells (BMDC) in the presence or absence of JAK3i (Fig. 5A). We found JAK3i-DC-combination immunotherapy to effectively reduce tumor load compared to both monotherapies alone (Fig. 5B). Similarly, we combined JAK3i with a synthetic long peptide (SLP) vaccine in the aggressive TC-1 solid tumor model showing similar combination immunotherapy efficacy, improving response rates and reducing heterogeneity in tumor responses observed (Fig. 5C-E).

Further investigations into the immunological mechanisms underlying combination immunotherapy efficacy in end-stage tumors revealed JAK3i to spare CD8⁺ T-cell proliferation and boost TIL activation as indicated by increased CD25 and PD-1- but not CTLA-4 expression (Fig. 6A). In line with an activated rather than exhausted TIL phenotype was a specific increase in single PD-1-expressing TILs (PD-1⁺ CTLA4⁻) rather than inhibitory receptor double-positive TILs known to be exhausted^{33,34}. Recently, the surface molecule CD39 was reported to mark tumor-specific CD8⁺ and CD4⁺ T cells in the TME and this marker was significantly upregulated in combination immunotherapy-treated TILs compared to TILs derived from untreated- or JAK3i-only treated mice^{35,36}. Besides surface molecules, combination immunotherapy-treated TILs displayed highest levels of interferon- γ and granzyme-B (Fig. 6A). These findings were not limited to CD8⁺ T cells, as CD4⁺ T-helper cells were similarly altered in the TME (Fig. 6B). These findings provide a preclinical rationale for JAK3i-combination immunotherapy and inclusion of anti-PD-1 ICI to further increase anti-tumor responses.

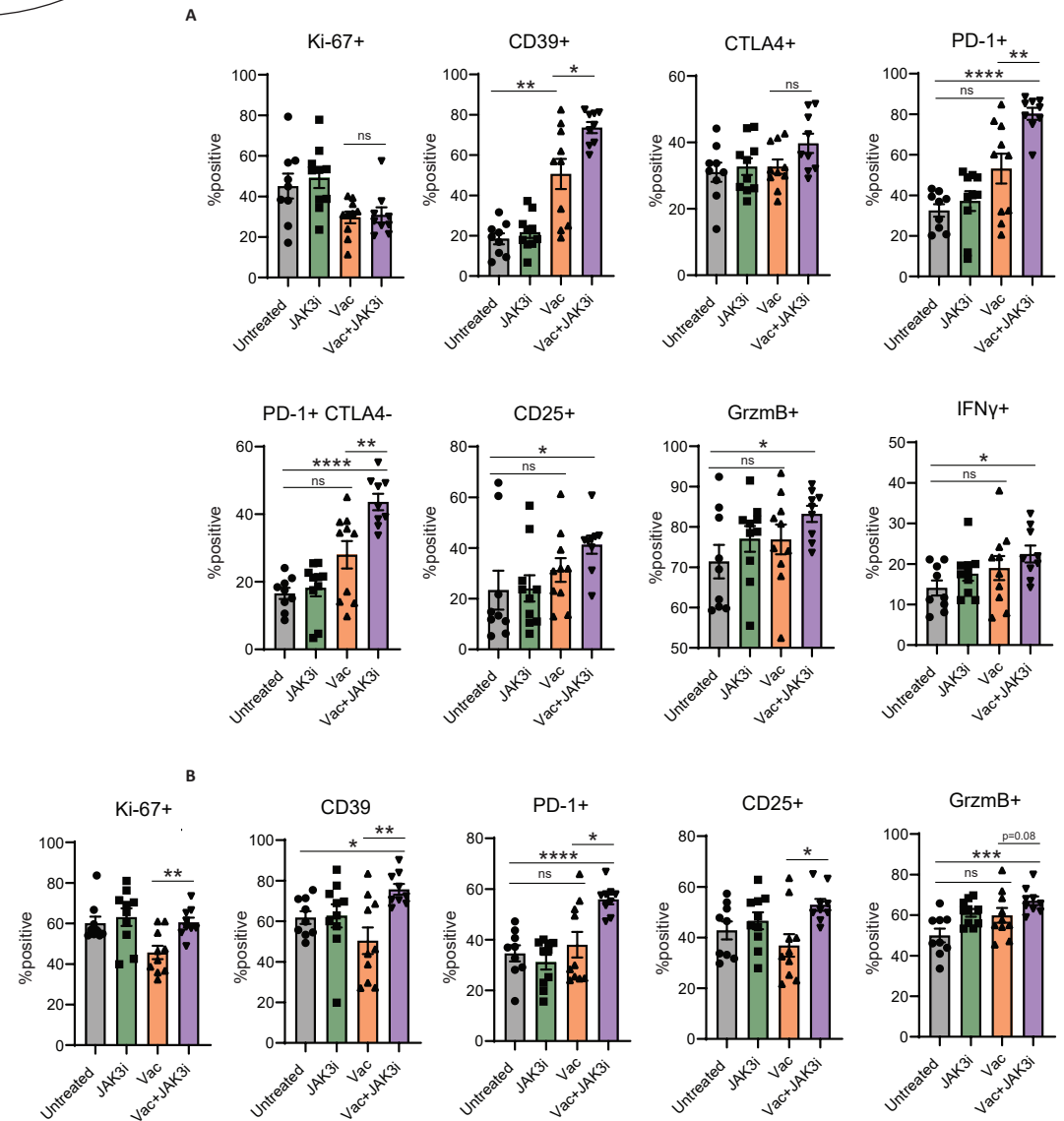


Figure 6. JAK3i improves peptide-vaccine induced CD8⁺ and CD4⁺ T-cell immunity in the tumor microenvironment. CD8⁺ (A) and CD4⁺ T-helper cell (B) proliferation (Ki67), and surface expression of co-inhibitory checkpoints or activation markers was assessed in end-stage tumors of the experiment described in Fig. 4C. Means and SEM are shown with n=9-10 mice/condition JAK3i=JAK3-inhibitor. Vac=SLP-vaccine, GrzmB=granzyme B, IFN γ =interferon-gamma, ns=non-significant, *p<0.05, **p<0.01, ***p<0.001, ****p<0.0001.

PART B
Improving the efficacy of
cancer vaccines for solid tumors
by combination immunotherapy

LOW-DOSE JAK3-INHIBITION
IMPROVES ANTI-TUMOR T-CELL IMMUNITY
AND IMMUNOTHERAPY EFFICACY

DISCUSSION

We are the first to identify JAK3 as a target for cancer immunotherapy *in vivo*. We found low dose JAK3i to decrease pSTAT5 expression while preserving T-cell proliferation *in vitro* and to dose-dependently improve T-cell phenotype and tumor load in solid tumor models as monotherapy, and in combination with cellular and peptide-vaccine approaches. JAK3i-cancer vaccine combination immunotherapy could be a particularly potent anti-cancer strategy with cellular and peptide vaccines inducing novel polyfunctional T-cell clones that are preserved and further boosted by JAK3i. This approach differs from current treatments primarily aimed at amplifying existing and often dysfunctional anti-tumor T-cell responses which are only short-term effective in a proportion of cancer patients^{1,37}. Of note, in a recently described screening assay for T-cell exhaustion reversing compounds, two JAK3i were identified to effectively counter T-cell exhaustion *in vitro*, further solidifying a role for JAK3 in mediating T-cell dysfunction⁴.

With the discovery of more specific JAK3i (e.g. PF-06 and decernotinib³⁸), JAK3 can be specifically targeted limiting unwanted action and toxicity as described for more broad kinase inhibitors such as Tofacitinib and Ibrutinib^{18,39,40}. Specific, small molecule inhibitors hold significant advantages compared to antibody-mediated therapies including route of administration (oral vs. i.v.), lack of anti-drug antibody formation and the possibility of timely and graded target inhibition which may be key in case of pleiotropic targets such as the IL-2R⁴¹. IL-2-IL-2R interaction may be essential or deleterious for T-cell effector function and pool size, depending on the strength, duration and moment of interaction in the anti-tumor immune response^{12,16}. Especially in the setting of vaccination, too early or strong blockade of IL-2R signaling following T-cell priming could suppress proper T-cell expansion thereby limiting therapy efficacy. Although we did not assess early T-cell expansion in peripheral blood (PB) of mice following DC- or SLP-vaccination, the effects of JAK3i monotherapy in PB and the effects on tumor progression indicate that graded JAK3i improves, rather than hampers T-cell activity. Further exploration of JAK3i timing and dosing could further inform about optimal treatment conditions in solid tumor treatment.

Recently, Liu et al demonstrated that chronic IL-2-mediated JAK1/3-pSTAT5 signaling in the TME induced T-cell exhaustion via generation of tryptophan metabolites triggering the aryl hydrocarbon receptor (AhR) in T cells¹². As the authors did not therapeutically target this pathway *in vivo*, our findings with JAK3i complement their findings as JAK3i using PF-06 potently and specifically inhibited STAT5-phosphorylation in T cells and improved T-cell phenotype *in vivo*. Interestingly, Liu et al found that an IL-2^{hi} gene signature in multiple solid cancer types but also AML was associated with poor patient survival, indicating that IL-2R targeting compounds may act on a wide variety of tumor types including solid- and non-solid cancer types¹². Whether our JAK3i acts by limiting

pSTAT5 mediated tryptophan metabolism and subsequent AhR-stimulation remains to be investigated.

JAK3 is located downstream of several (common γ -chain) cytokine receptors besides the IL-2R which may in part explain our *in vivo* efficacy. Although we found a strong effect of JAK3i on IL-4 mediated alternative macrophage polarization *in vitro*, we could not detect this *in vivo* questioning the role of this Th2-related cytokine in the TME. IL-4-mediated M2-polarization and T-cell suppression can be induced, however, following radiotherapy limiting its immunogenic effect on CD8⁺ T cells as documented in a mammary tumor model⁴². IL-15 and IL-7 are two other important cytokines signaling through JAK3-associated receptors whose downstream inhibition could play a role in our tumor models. In contrast to IL-2 which is dynamically upregulated following TCR-stimulation by cognate antigen, IL-7/IL-15 are involved in maintaining survival of naïve and memory T cells during homeostatic conditions⁴³. Liu et al. found IL-15 to be unable to exert the same exhausted profile in CD8⁺ T cells, even though both IL-2 and IL-15 signal through STAT5¹². Besides their known effects on CD8⁺ T cells, common γ -chain cytokines including IL-2 can skew Th-phenotypes, particularly IL-2 mediated Th1-induction⁴³. Although we could not detect changes in IFN γ production by Th-cells following JAK3i *in vivo* (*data not shown*) modulation through Th-subclass differentiation remains a possibility. The same accounts for Treg which constitutively express high levels of the IL-2R and rely on IL-2 for their expansion, survival but not for their suppressive function^{24,43,44}. Interestingly, although effector T-cell phenotype was altered by JAK3i, we did not observe changes in Treg-frequencies of proliferation at the applied JAK3i dose, possibly due to high intrinsic IL-2R expression compensating for decreased downstream signaling in the context of JAK3i (*data not shown*, Fig S2B).

We have shown JAK3 to be a novel and effective target for cancer immunotherapy, improving T-cell phenotype and anti-tumor function depending on the mode of targeting. Our findings lay the groundwork for further efficacy testing in human cancer as monotherapy but more promising in combination with existing immunotherapies.

PART B
Improving the efficacy of
cancer vaccines for solid tumors
by combination immunotherapy

LOW-DOSE JAK3-INHIBITION
IMPROVES ANTI-TUMOR T-CELL IMMUNITY
AND IMMUNOTHERAPY EFFICACY

REFERENCES

- 1 Galon, J. & Bruni, D. Approaches to treat immune hot, altered and cold tumours with combination immunotherapies. *Nat Rev Drug Discov* 18, 197-218, doi:10.1038/s41573-018-0007-y (2019).
- 2 Waldman, A. D., Fritz, J. M. & Lenardo, M. J. A guide to cancer immunotherapy: from T cell basic science to clinical practice. *Nature reviews. Immunology* 20, 651-668, doi:10.1038/s41577-020-0306-5 (2020).
- 3 Dammeijer, F., Lau, S. P., van Eijk, C. H. J., van der Burg, S. H. & Aerts, J. Rationally combining immunotherapies to improve efficacy of immune checkpoint blockade in solid tumors. *Cytokine & growth factor reviews*, doi:10.1016/j.cytogfr.2017.06.011 (2017).
- 4 Marro, B. S. et al. Discovery of Small Molecules for the Reversal of T Cell Exhaustion. *Cell reports* 29, 3293-3302.e3293, doi:https://doi.org/10.1016/j.celrep.2019.10.119 (2019).
- 5 McLane, L. M., Abdel-Hakeem, M. S. & Wherry, E. J. CD8 T Cell Exhaustion During Chronic Viral Infection and Cancer. *Annual review of immunology* 37, 457-495, doi:10.1146/annurev-immunol-041015-055318 (2019).
- 6 Schietinger, A. et al. Tumor-Specific T Cell Dysfunction Is a Dynamic Antigen-Driven Differentiation Program Initiated Early during Tumorigenesis. *Immunity* 45, 389-401, doi:10.1016/j.immuni.2016.07.011 (2016).
- 7 Moore, E. C. et al. Enhanced Tumor Control with Combination mTOR and PD-L1 Inhibition in Syngeneic Oral Cavity Cancers. *Cancer immunology research* 4, 611-620, doi:10.1158/2326-6066.cir-15-0252 (2016).
- 8 Eng, C. et al. Atezolizumab with or without cobimetinib versus regorafenib in previously treated metastatic colorectal cancer (IMblaze370): a multicentre, open-label, phase 3, randomised, controlled trial. *The Lancet Oncology* 20, 849-861, doi:10.1016/S1470-2045(19)30027-0 (2019).
- 9 Verma, V. et al. MEK inhibition reprograms CD8+ T lymphocytes into memory stem cells with potent antitumor effects. *Nature immunology* 22, 53-66, doi:10.1038/s41590-020-00818-9 (2021).
- 10 Ebert, P. J. R. et al. MAP Kinase Inhibition Promotes T Cell and Anti-tumor Activity in Combination with PD-L1 Checkpoint Blockade. *Immunity* 44, 609-621, doi:10.1016/j.immuni.2016.01.024 (2016).
- 11 Diken, M. et al. mTOR inhibition improves antitumor effects of vaccination with antigen-encoding RNA. *Cancer immunology research* 1, 386-392, doi:10.1158/2326-6066.cir-13-0046 (2013).
- 12 Liu, Y. et al. IL-2 regulates tumor-reactive CD8+ T cell exhaustion by activating the aryl hydrocarbon receptor. *Nature immunology*, doi:10.1038/s41590-020-00850-9 (2021).
- 13 Beltra, J.-C. et al. IL2R β -dependent signals drive terminal exhaustion and suppress memory development during chronic viral infection. *Proceedings of the National Academy of Sciences* 113, E5444-E5453, doi:10.1073/pnas.1604256113 (2016).
- 14 Kalia, V. et al. Prolonged interleukin-2R α expression on virus-specific CD8+ T cells favors terminal-effector differentiation in vivo. *Immunity* 32, 91-103, doi:10.1016/j.immuni.2009.11.010 (2010).
- 15 Boyman, O. & Sprent, J. The role of interleukin-2 during homeostasis and activation of the immune system. *Nature reviews. Immunology* 12, 180-190, doi:10.1038/nri3156 (2012).
- 16 Liao, W., Lin, J. X. & Leonard, W. J. Interleukin-2 at the crossroads of effector responses, tolerance, and immunotherapy. *Immunity* 38, 13-25, doi:10.1016/j.immuni.2013.01.004 (2013).
- 17 O'Shea, J. J. et al. The JAK-STAT Pathway: Impact on Human Disease and Therapeutic Intervention. *Annual review of medicine* 66, 311-328, doi:10.1146/annurev-med-051113-024537 (2015).
- 18 Schwartz, D. M. et al. JAK inhibition as a therapeutic strategy for immune and inflammatory diseases. *Nat Rev Drug Discov* 16, 843-862, doi:10.1038/nrd.2017.201 (2017).
- 19 Telliez, J. B. et al. Discovery of a JAK3-Selective Inhibitor: Functional Differentiation of JAK3-Selective Inhibition over pan-JAK or JAK1-Selective Inhibition. *ACS chemical biology* 11, 3442-3451, doi:10.1021/acschembio.6b00677 (2016).
- 20 Thorarensen, A. et al. Design of a Janus Kinase 3 (JAK3) Specific Inhibitor 1-((2S,5R)-5-((7H-Pyrrolo[2,3-d]pyrimidin-4-yl)amino)-2-methylpiperidin-1-yl)prop-2-en-1-one (PF-06651600) Allowing for the Interrogation of JAK3 Signaling in Humans. *Journal of medicinal chemistry* 60, 1971-1993, doi:10.1021/acs.jmedchem.6b01694 (2017).
- 21 Schulz, K. R., Danna, E. A., Krutzik, P. O. & Nolan, G. P. Single-cell phospho-protein analysis by flow cytometry. *Current protocols in immunology* Chapter 8, Unit 8.17, doi:10.1002/0471142735.im0817s78 (2007).
- 22 Herman, S. E. M. et al. The Bruton Tyrosine Kinase (BTK) Inhibitor Acalabrutinib Demonstrates Potent On-Target Effects and Efficacy in Two Mouse Models of Chronic Lymphocytic Leukemia. *Clinical cancer research : an official journal of the American Association for Cancer Research* 23, 2831-2841, doi:10.1158/1078-0432.ccr-16-0463 (2017).
- 23 Pal Singh, S., Dammeijer, F. & Hendriks, R. W. Role of Bruton's tyrosine kinase in B cells and malignancies. *Molecular cancer* 17, 57, doi:10.1186/s12943-018-0779-z (2018).
- 24 Pandiyan, P., Zheng, L., Ishihara, S., Reed, J. & Lenardo, M. J. CD4+CD25+Foxp3+ regulatory T cells induce cytokine deprivation-mediated apoptosis of effector CD4+ T cells. *Nature immunology* 8, 1353-1362, doi:10.1038/ni1536 (2007).
- 25 LaPorte, S. L. et al. Molecular and Structural Basis of Cytokine Receptor Pleiotropy in the Interleukin-4/13 System. *Cell* 132, 259-272, doi:10.1016/j.cell.2007.12.030 (2008).
- 26 Bosurgi, L. et al. Macrophage function in tissue repair and remodeling requires IL-4 or IL-13 with apoptotic cells. *Science* 356, 1072-1076, doi:10.1126/science.aai8132 (2017).
- 27 Dammeijer, F. et al. The Efficacy of Tumor Vaccines and Cellular Immunotherapies in Non-Small Cell Lung Cancer: A Systematic Review and Meta-Analysis. *Journal of clinical oncology : official journal of the American Society of Clinical Oncology*, doi:10.1200/jco.2015.66.3955 (2016).
- 28 Hegmans, J. P. et al. Consolidative dendritic cell-based immunotherapy elicits cytotoxicity against malignant mesothelioma. *American journal of respiratory and critical care medicine* 181, 1383-1390, doi:10.1164/rccm.200909-1465OC (2010).
- 29 Aerts, J. et al. Autologous Dendritic Cells Pulsed with Allogeneic Tumor Cell Lysate in Mesothelioma: From Mouse to Human. *Clinical cancer research : an official journal of the American Association for Cancer Research* 24, 766-776, doi:10.1158/1078-0432.ccr-17-2522 (2018).
- 30 van Poelgeest, M. I. E. et al. HPV16 synthetic long peptide (HPV16-SLP) vaccination therapy of patients with advanced or recurrent HPV16-induced gynecological carcinoma, a phase II trial. *Journal of translational medicine* 11, 88-88, doi:10.1186/1479-5876-11-88 (2013).
- 31 Dammeijer, F. et al. Depletion of Tumor-Associated Macrophages with a CSF-1R Kinase Inhibitor Enhances Antitumor Immunity and Survival Induced by DC Immunotherapy. *Cancer immunology research* 5, 535-546, doi:10.1158/2326-6066.CIR-16-0309 [pii] 10.1158/2326-6066.CIR-16-0309 (2017).
- 32 Ott, P. A. et al. An immunogenic personal neoantigen vaccine for patients with melanoma. *Nature* 547, 217-221, doi:10.1038/nature22991 (2017).
- 33 Duraiswamy, J., Kaluza, K. M., Freeman, G. J. & Coukos, G. Dual blockade of PD-1 and CTLA-4 combined with tumor vaccine effectively restores T-cell rejection function in tumors. *Cancer research* 73, 3591-3603, doi:10.1158/0008-5472.can-12-4100 (2013).
- 34 Fourcade, J. et al. Upregulation of Tim-3 and PD-1 expression is associated with tumor antigen-specific CD8+ T cell dysfunction in melanoma patients. *The Journal of experimental medicine* 207, 2175-2186, doi:10.1084/jem.20100637 (2010).
- 35 Kortekaas, K. E. et al. CD39 Identifies the CD4⁺ Tumor-Specific T-cell Population in Human Cancer. *Cancer immunology research* 8, 1311, doi:10.1158/2326-6066.CIR-20-0270 (2020).
- 36 Duhen, T. et al. Co-expression of CD39 and CD103 identifies tumor-reactive CD8 T cells in human solid tumors. *Nature communications* 9, 2724-2724, doi:10.1038/s41467-018-05072-0 (2018).
- 37 Pai, C. S. et al. Clonal Deletion of Tumor-Specific T Cells by Interferon-gamma Confers Therapeutic Resistance to Combination Immune Checkpoint Blockade. *Immunity* 50, 477-492.e478, doi:10.1016/j.immuni.2019.01.006 (2019).
- 38 Farmer, L. J. et al. Discovery of VX-509 (Decernotinib): A Potent and Selective Janus Kinase 3 Inhibitor for the Treatment of Autoimmune Diseases. *Journal of medicinal chemistry* 58, 7195-7216, doi:10.1021/acs.jmedchem.5b00301 (2015).
- 39 Eberl, H. C. et al. Chemical proteomics reveals target selectivity of clinical Jak inhibitors in human primary cells. *Scientific reports* 9, 14159, doi:10.1038/s41598-019-50335-5 (2019).
- 40 Dunbar, A., Joosse, M. E., de Boer, F., Eefting, M. & Rijnders, B. J. A. Invasive fungal infections in patients treated with Bruton's tyrosine kinase inhibitors. *The Netherlands journal of medicine* 78, 294-296 (2020).
- 41 Oo, C. & Kalbag, S. S. Leveraging the attributes of biologics and small molecules, and releasing the bottlenecks: a new wave of revolution in drug development. *Expert Review of Clinical Pharmacology* 9, 747-749, doi:10.1586/17512433.2016.1160778 (2016).
- 42 Shiao, S. L. et al. TH2-Polarized CD4(+) T Cells and Macrophages Limit Efficacy of Radiotherapy. *Cancer immunology research* 3, 518-525, doi:10.1158/2326-6066.cir-14-0232 (2015).
- 43 Lin, J. X. & Leonard, W. J. The Common Cytokine Receptor γ Chain Family of Cytokines. *Cold Spring Harbor perspectives in biology* 10, doi:10.1101/cshperspect.a028449 (2018).
- 44 Fontenot, J. D., Rasmussen, J. P., Gavin, M. A. & Rudensky, A. Y. A function for interleukin 2 in Foxp3-expressing regulatory T cells. *Nature immunology* 6, 1142-1151, doi:10.1038/ni1263 (2005).

PART B
Improving the efficacy of
cancer vaccines for solid tumors
by combination immunotherapy

LOW-DOSE JAK3-INHIBITION
IMPROVES ANTI-TUMOR T-CELL IMMUNITY
AND IMMUNOTHERAPY EFFICACY

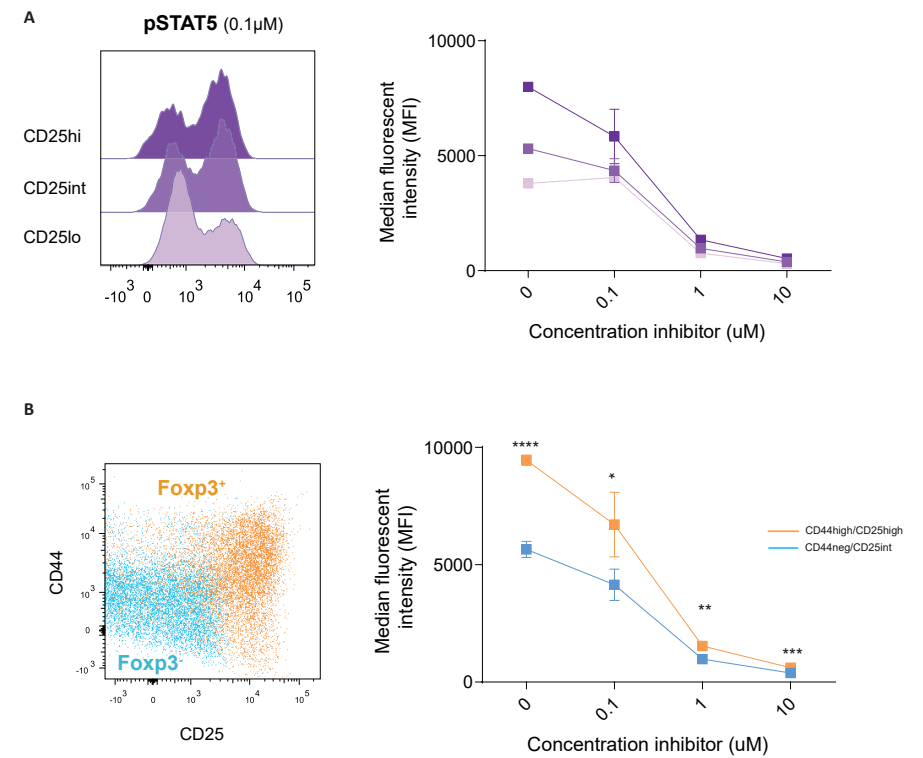
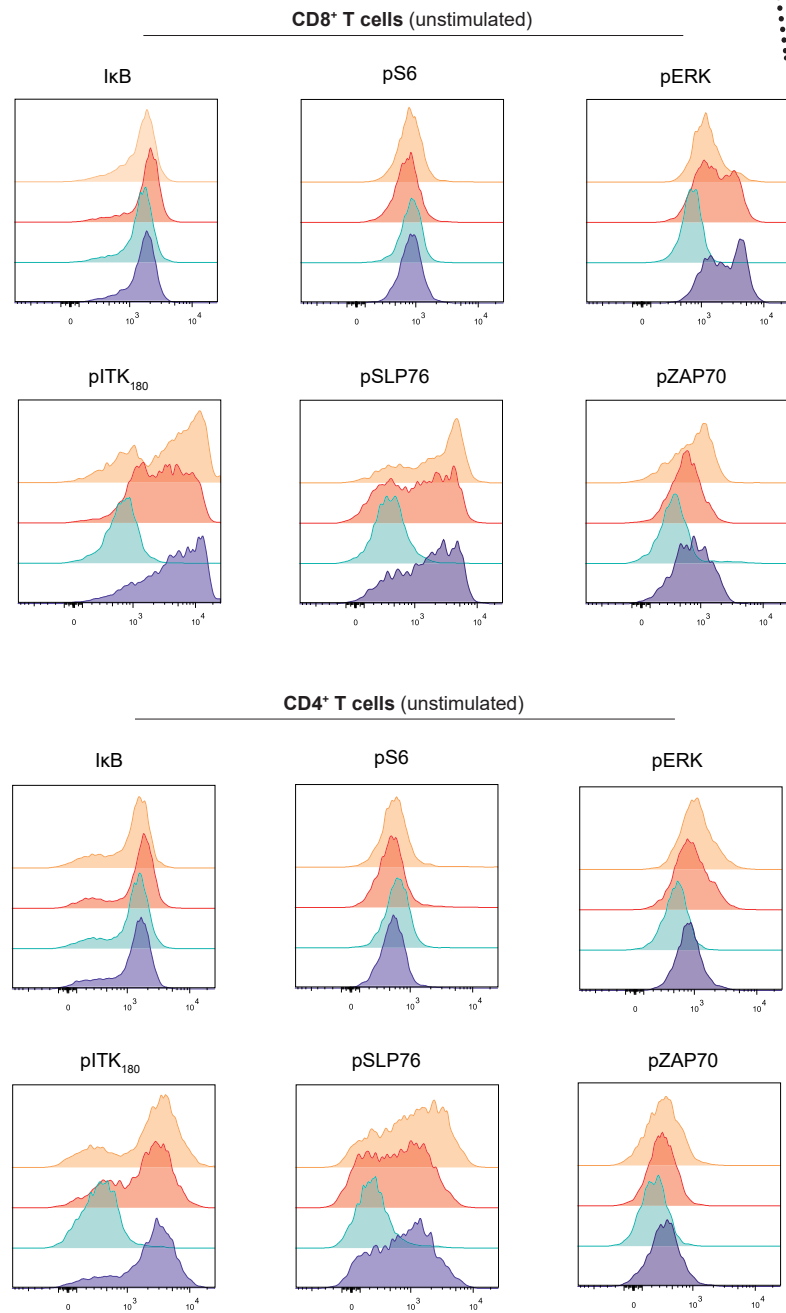


Figure S1. The effects of the different inhibitors used in Figs 1-2 on phosphotargets in different T-cell signaling pathways in the unstimulated setting, for both CD8⁺ (upper panels) and CD4⁺ T cells (lower panels) at the 10 μM concentration.

Figure S2. CD25⁺ CD4⁺ T cells were subdivided into CD25 high/intermediate and low-expressing cells and pSTAT5 expression was assessed for the different subsets (A). Alternatively, as FcγR3 could not be included in the Phosphoflow analysis for technical reasons, CD44⁺ CD25^{int} was chosen as a surrogate for FcγR3⁺ cells (left panel) and compared to CD44⁺ CD25^{int} cells (B). * = p<0.05, ** = p<0.01, *** = p<0.001, **** = p<0.0001, Means and SEM are shown, n=5 mice/condition.

PART B
Improving the efficacy of
cancer vaccines for solid tumors
by combination immunotherapy

LOW-DOSE JAK3-INHIBITION
IMPROVES ANTI-TUMOR T-CELL IMMUNITY
AND IMMUNOTHERAPY EFFICACY

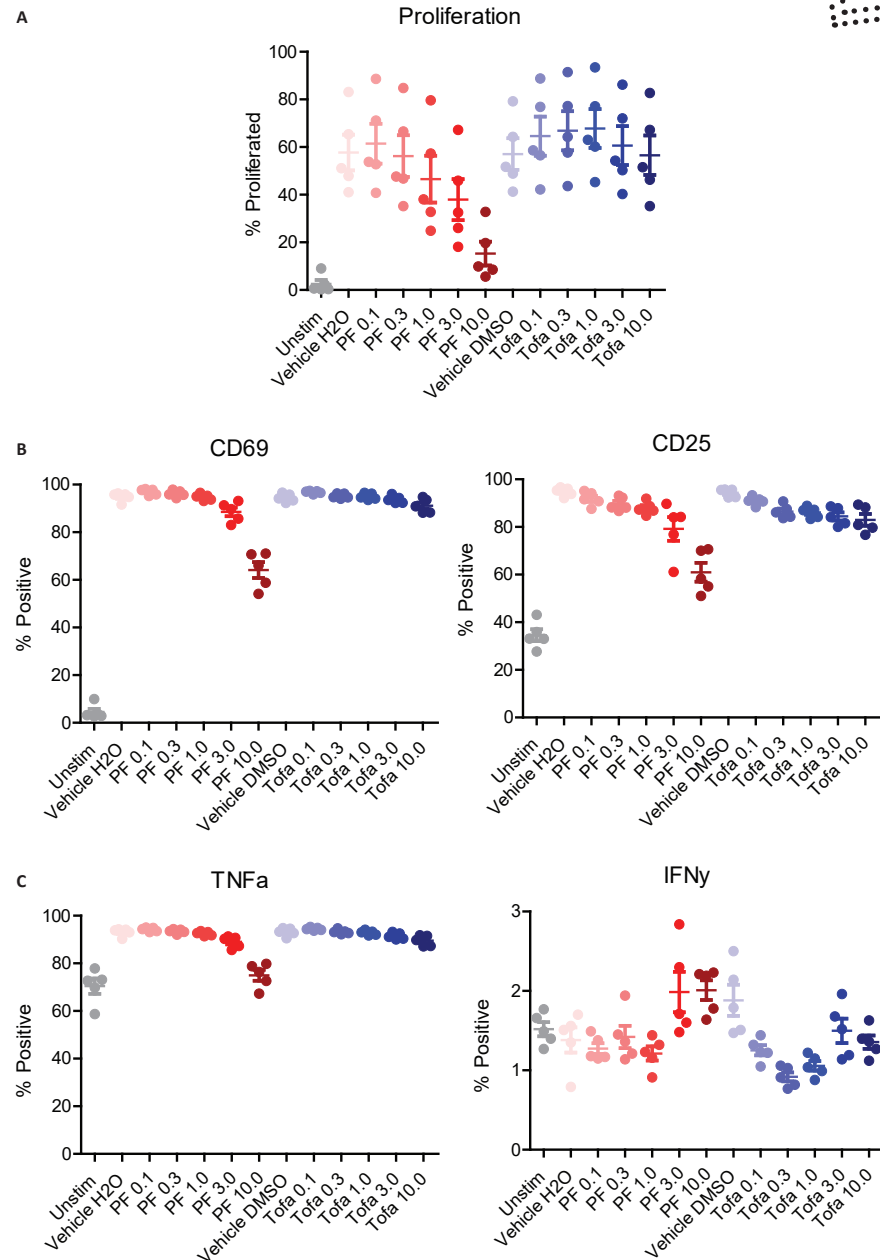


Figure S3. murine wild-type proliferation-dye labeled T cells were stimulated with anti-CD3/CD28 beads in the absence or presence of ascending concentrations of either PF-06651600 (PF) or Tofacitinib (Tofa) and proliferation (A), activation (B) and cytokine production (C) were assessed by multicolor flow cytometry. Means and SEM are shown with n=5 mice/condition IFNγ=interferon gamma, TNFα=tumor-necrosis factor alpha.

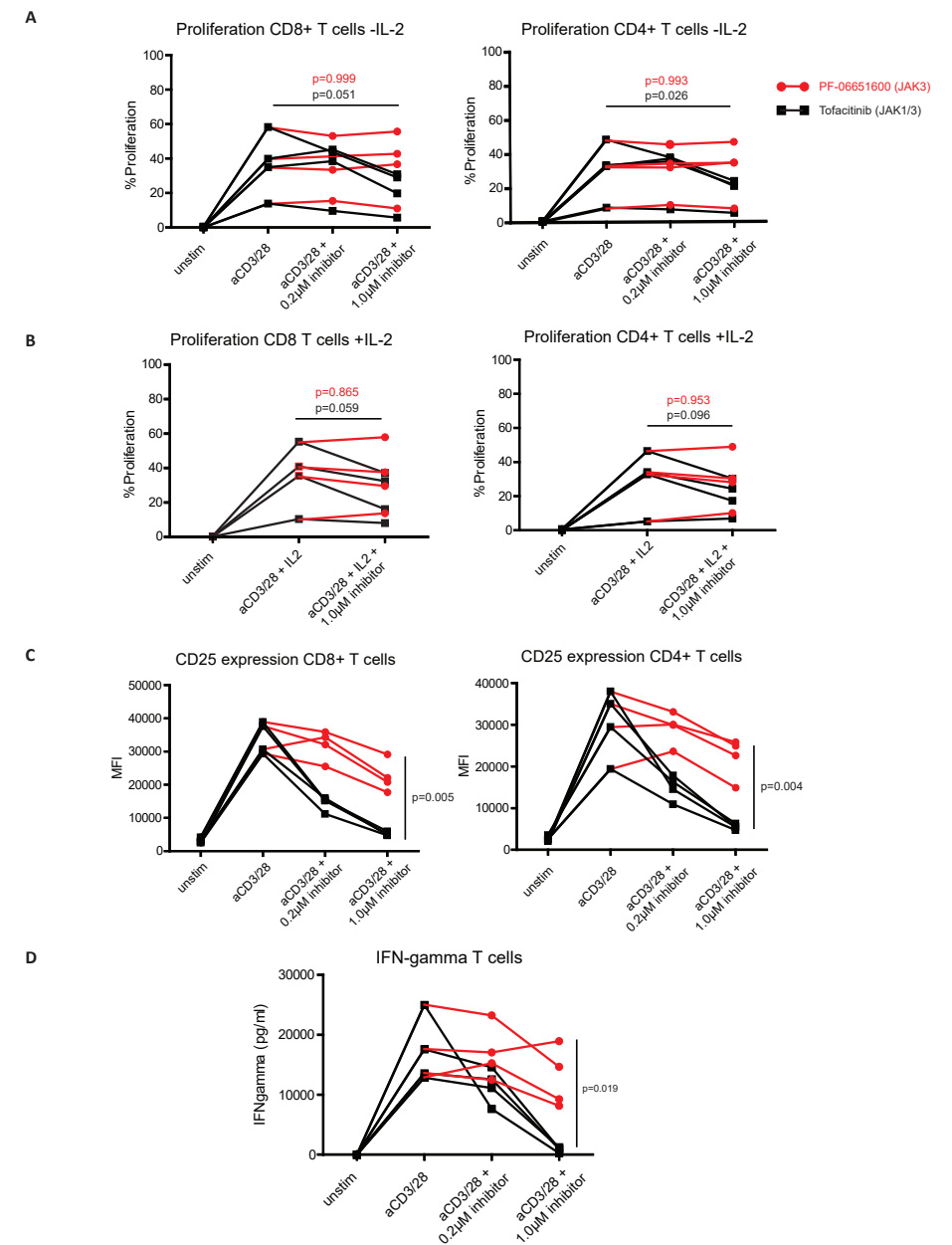


Figure S4. healthy donor-derived T cells were stimulated with anti-CD3/CD28 beads in PF-06651600 or Tofacitinib containing medium without (A) or with (B) exogenous IL-2 added to the culture system. (C) CD4⁺ and CD8⁺ T-cell activation as assessed by CD25-upregulation was quantified by flow cytometry, in addition to interferon-gamma levels in the supernatant using ELISA (D). Means and SEM are shown with n=4 healthy controls/condition, IL-2=interleukin 2, IFNγ=interferon-gamma, MFI=median fluorescence intensity.

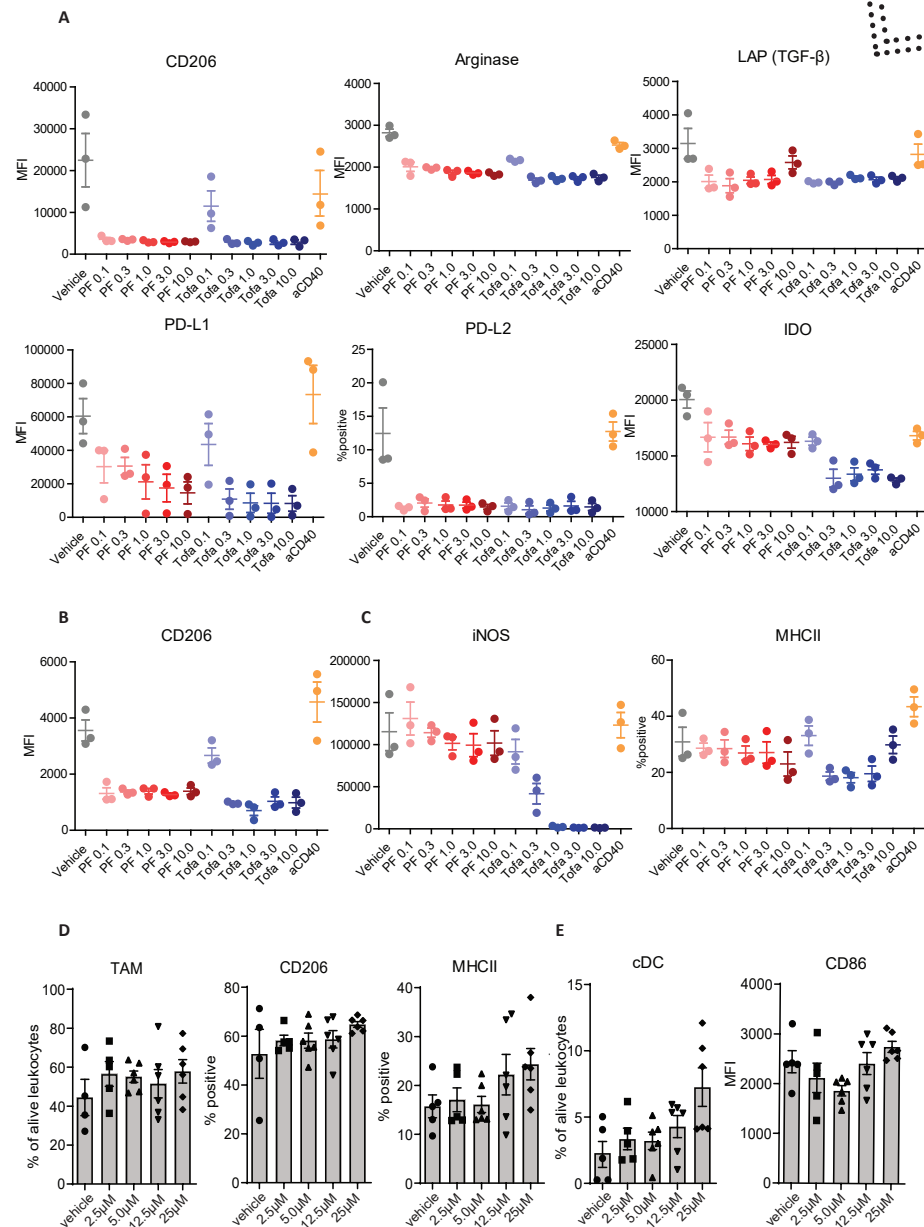


Figure S5. M-CSF generated murine bone-marrow derived macrophages were skewed to the M2 phenotype using IL-4 (**A**) or IL-4+IL-13 (**B**) or to a pro-inflammatory M1 phenotype using LPS and IFN-gamma (**C**) in the presence of PF-06651600 (PF) or Tofacitinib (Tofa) and surface markers were assessed using flow cytometry. a trimeric CD40-agonist (aCD40) was used as a prototypic M1-skewing compound serving as a positive control. (**D-E**) tumor-associated macrophages (TAM) and conventional dendritic cells (cDC) in end-stage tumors from the experiment in Fig. 2 were analyzed for frequency and phenotype. MFI=median fluorescence intensity. Means and SEM are shown.

PART B
Improving the efficacy of cancer vaccines for solid tumors by combination immunotherapy

LOW-DOSE JAK3-INHIBITION IMPROVES ANTI-TUMOR T-CELL IMMUNITY AND IMMUNOTHERAPY EFFICACY

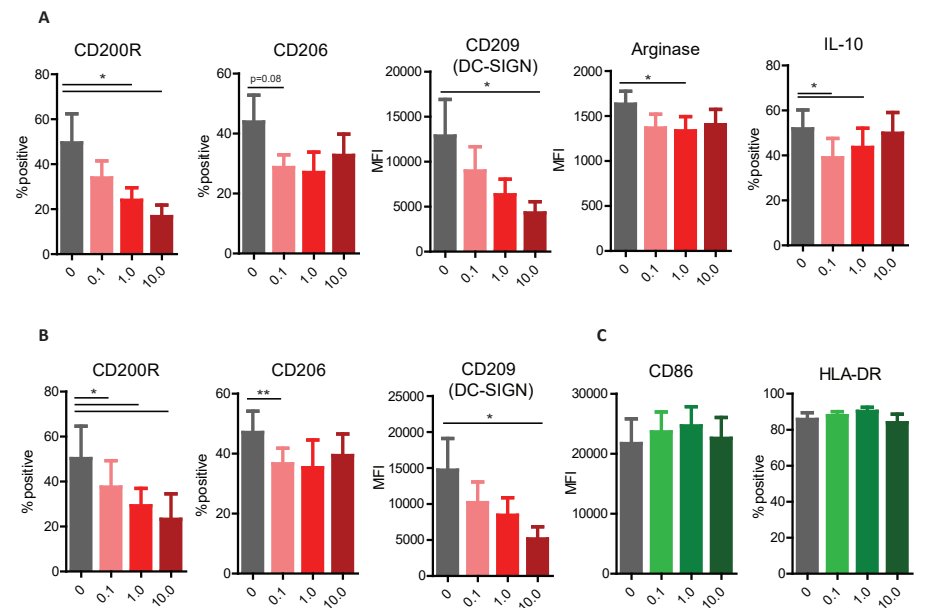


Figure S6. M-CSF generated monocyte-derived macrophages from healthy donors were skewed to M2-macrophages using IL-4 (**A**), IL-4+IL-13 (**B**) or to a pro-inflammatory M1 phenotype using LPS and IFN-gamma (**C**) in the presence of various JAK3i (PF-06651600) concentrations. MFI=median fluorescence intensity. Means and SEM are shown. *=p<0.05, **=p<0.01.

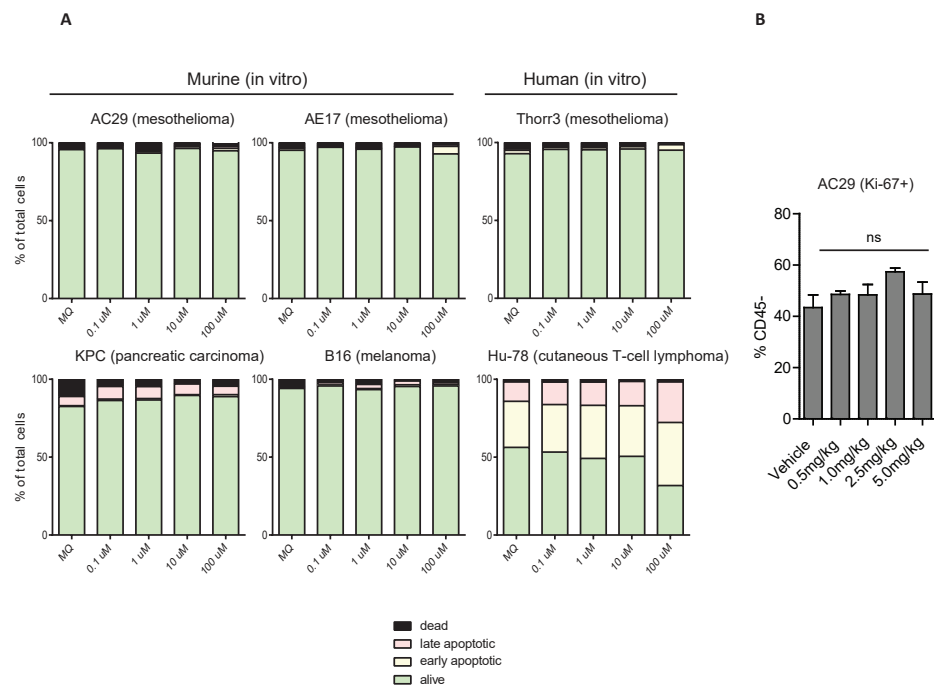
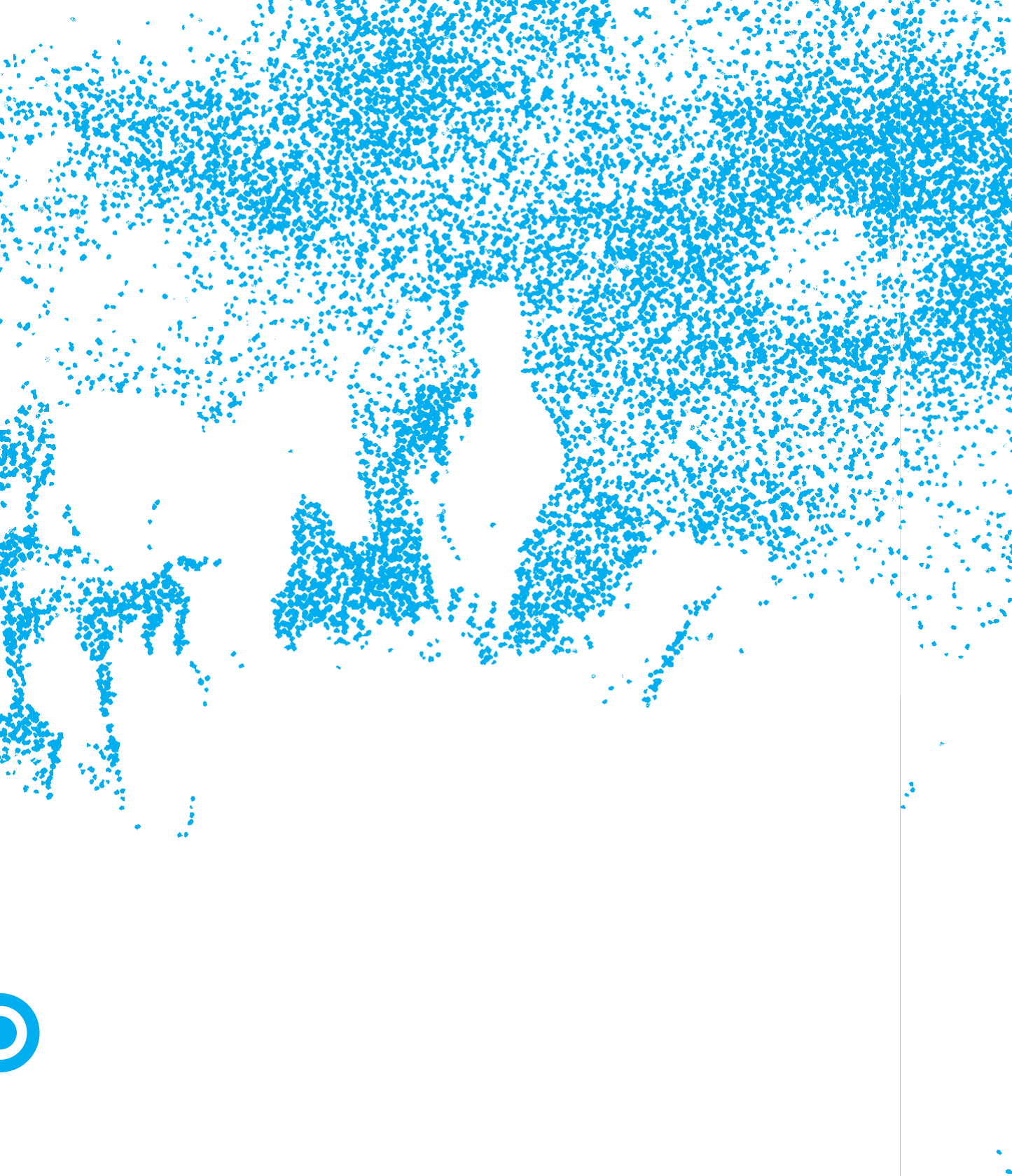


Figure S7. (A) various murine and human tumor cell lines were cultured in the absence or presence of increasing concentrations of JAK3i (PF-06651600) followed by flow-cytometric apoptosis and cell death detection. The T-cell lymphoma cell line Hu78 was used as a positive control as JAK3 is constitutively active and hence responsive to JAK3i. **(B)** CD45⁺ (tumor) cells from the experiment in Fig. 2 were assessed for proliferation (Ki-67) at various doses of PF-06651600 in vivo. Ns= non-significant.



DISCUSSION



Cancer immunotherapy has the potential to durably improve clinical outcome, however, this only occurs in a subgroup of patients and tumor types. Novel insights into what constitutes an effective anti-tumor immune response and how conventional anticancer and immunotherapies can be applied to induce or enhance these responses will be essential for the next generation of cancer immunotherapies. The main goal of this thesis was to investigate whether existing immunotherapies (e.g. ICB and DC-vaccination) have effects beyond their perceived target cell and location, modulating a more broad-acting tumor macroenvironment. Specifically, in **Part A** of this thesis, we hypothesized that anti-PD-L1 immune checkpoint blockade (ICB) and gemcitabine chemotherapy not only affected T cells in the tumor microenvironment (TME), but other cell types at distant sites as well associating with therapy efficacy. In **Chapter 2** we found that in case of anti-PD-L1 immunotherapy, tumor-draining lymph nodes (TDLNs) were critical for treatment efficacy and the degree of PD-1/PD-L1 interaction at this site correlated with survival in melanoma patients. In **Chapter 3**, we discovered that gemcitabine not only decreased myeloid-derived suppressor cells (MDSC) in peripheral blood as was previously known, but significantly altered T- and NK-cell activation correlating with response to treatment in mesothelioma patients. **Part B** focused on cancer vaccines and whether characterization of the tumor macroenvironment in preclinical models could identify novel and synergistic targets for combination immunotherapy. In short, we found cancer vaccines (cellular vaccines in particular) to be moderately effective as monotherapy in non-small cell lung cancer (NSCLC) patients (**Chapter 4**). However, when combined with macrophage-depleting (**Chapter 5**) or repolarizing compounds (**Chapter 6**) as adjuvants, vaccine efficacy was significantly improved. Alternatively, by fine-tuning interleukin 2 receptor (IL-2R)-janus kinase 3 (JAK3) signaling in T cells (**Chapter 7**), T-cell phenotype was systemically enhanced further increasing vaccine efficacy. These findings illustrate the potency of sculpting elements of the tumor macroenvironment improving systemic anti-tumor immunity. How do these findings from this thesis fit in the current tumor immunology and immunotherapy landscape?

Previous research on TME composition has provided us with important knowledge on tumor-infiltrating T-cell (TIL) biology and immune resistance mechanisms but has failed to capture the complete picture of how cancers thwart the immune system. The 'cancer-immunity cycle' model proposed by Chen and Mellman in 2013 provides an idealistic, stepwise approach to anti-tumor T-cell induction and its self-propagation following effective cancer cell lysis in the TME¹. In this model, recently APC-primed tumor-specific T cells migrate through peripheral blood (PB) and infiltrate the TME, where they recognize their cognate tumor antigen and lyse the target cell leading to antigen release, further amplifying the cancer-immunity cycle. Although this model remains valid to date, both preclinical and patient studies point to a more broad-acting, systemic immune response in those experiencing durable clinical benefit from immunotherapy^{2,3}. Contributing to this systemic

DISCUSSION

anti-tumor immune responses are not only primary tumor, TDLN, peripheral blood but also bone-marrow, spleen and the (gut) microbiome, whose roles in modulating systemic immunity have only recently being uncovered⁴⁻⁷. Reciprocally, tumors have been shown to employ a wide variety of local- and distant acting immune-suppressive mechanisms impacting not only TILs, but also myeloid cells and lymphocytes present at extratumoral sites mentioned earlier⁸⁻¹¹. Therefore, the concept of a tumor *macroenvironment* seems to better delineate the complex inter-organ interactions that constitute effective anti-tumor immunity. This thesis provides a basis for further research into key constituents of the tumor macroenvironment (e.g. TDLNs) and support the development of clinical trials investigating combination immunotherapy efficacy (e.g. CD40-agonism and DC-therapy) in patients using tumor macroenvironment principles (Figure 1). Below, the context of these findings and their implications are individually discussed, including potential pitfalls and future areas of discovery to further propel the field of immune-oncology.

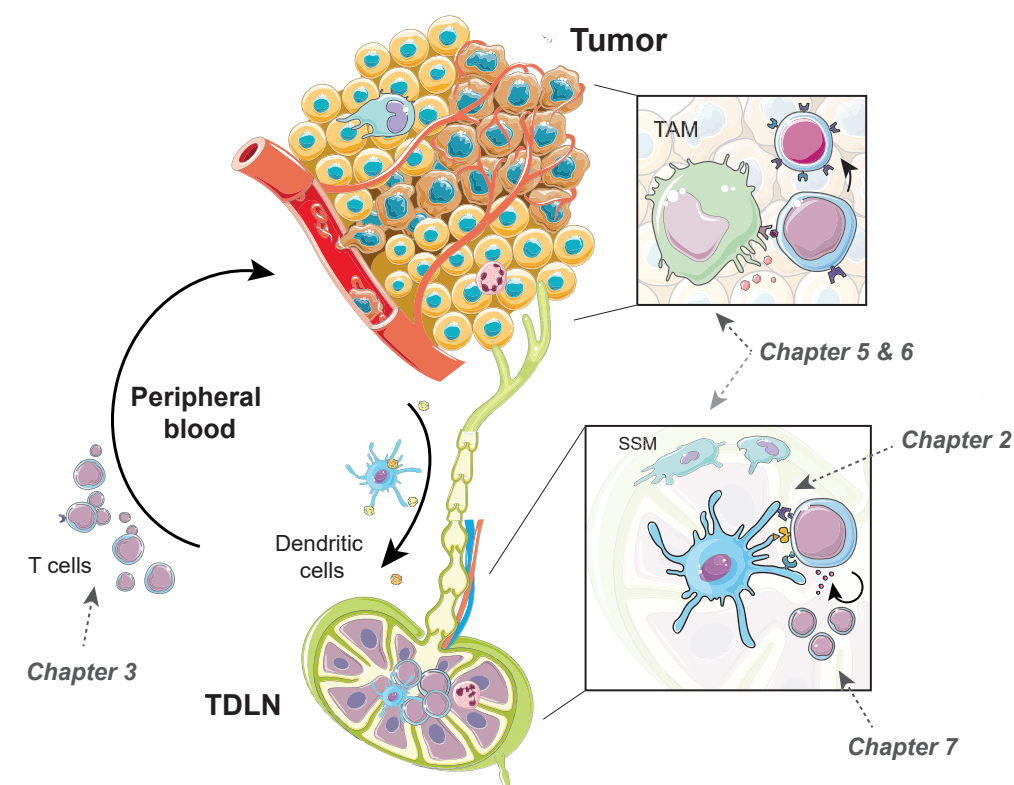


Figure 1. Schematic overview of the tumor macroenvironment and its cell types and locations discussed in this thesis. TAM= tumor-associated macrophage, SSM= subcapsular sinus macrophage, TDLN= tumor-draining lymph node

The TDLN as an effector organ for cancer immunotherapy.

The PD-1/PD-L1-axis as a TDLN-target

Anti-tumor immune responses originate from an APC presenting tumor-antigen to a tumor-specific T cell bearing a cognate TCR in the context of appropriate co-stimulation. This process of priming generally occurs in the TDLN, preferably by tumor-derived (conventional) DCs inducing tumor-antigen specific CD8⁺ T cells that subsequently traffic to the TME exerting their effects^{1,12}. Unfortunately, endogenous anti-tumor responses are often dysfunctional or insufficient to effectively halt cancer progression. In part, this could be due to TDLN corruption by tumors through drainage of immune suppressive molecules or by preventing cDC-maturation or egress completely^{8,13,14}. We questioned whether these processes could be targeted, as this could possibly help to reinstate effective anti-tumor immunity in a larger number of patients. Peptide and cellular (DC-) vaccines are well-known methods to circumvent insufficient T-cell priming in TDLNs. Similar to vaccine approaches, recent clinical data from ICB-treated patients point to novel T-cell clonotypes arising in tumors of patients responding to treatment^{3,15-17}. Based on these data, we hypothesized that ICB-therapy would also act via TDLNs and not merely by targeting T-cell checkpoints in the TME.

In **Chapter 2**, we formally demonstrated that PD-L1-blocking antibodies act, at least in part, by inhibiting PD-L1 on cDCs in TDLNs thereby promoting anti-tumor T-cell responses. How does this finding relate to our current understanding of PD-1/PD-L1- and checkpoint blockade biology? Until recently, the immune-checkpoints CTLA-4 and PD-(L)1 were believed to act largely through separate, non-redundant mechanisms at different sites in the tumor micro or macro-environment¹⁸. Whereas CTLA-4 induced an 'anergic-like' state in T cells through competition for B7-costimulatory molecules in lymphoid organs, PD-1 intercepted down-stream TCR-signaling primarily by PD-L1-expressing tumor cells at the effector site^{19,20}. This latter mechanism was recently challenged showing that PD-1 potentially inhibits downstream CD28-signalling upon ligation by PD-L1, thereby demonstrating that similar to CTLA-4, decreasing co-stimulatory input is a key mechanism of inducing T-cell tolerance^{21,22}. This further implied that for PD-1/PD-L1-blocking antibodies to be effective, PD-1⁺ T cells would have to be in the vicinity of B7-expressing myeloid cells, preferably co-expressing PD-L1. More recent seminal work indicated that PD-L1 on host, non-tumor cells is essential for suppressing PD-1⁺ T cells, with PD-L1 on DCs being particularly important²³⁻²⁸. Where these interactions predominantly occur, however, was largely unknown. Our data complement these findings, showing that cDCs in TDLNs express the highest levels of PD-L1 and B7 molecules in close proximity to PD-1⁺ tumor-specific T cells in the paracortex. More importantly, PD-L1 inhibition specifically in the TDLN restrained tumor-progression and increased TIL frequencies, especially of the TCF-

DISCUSSION

1⁺/SLAMF6-expressing progenitor-exhausted T-cell population (T_{ex}Prog). This is particularly interesting as this T_{ex}Prog population was recently described to mediate anti-PD-1 immunotherapy-efficacy²⁹⁻³¹.

Although the data in **Chapter 2** formally demonstrate that PD-L1-blocking antibodies act, at least in part, by inhibiting PD-L1 on cDCs in TDLNs and thereby promote anti-tumor T-cell responses, there are several questions that remain to be answered regarding the role of TDLNs in PD-1/PD-L1 ICB-therapy. First of all, our TDLN-targeted PD-L1 blockade approach was specific but incomplete, with ~30-40% of PD-L1⁺ cDCs binding the antibody compared to 100% binding efficacy of the antibody with the systemic anti-PD-L1 dose. As a result, it is currently unclear whether the superior therapeutic efficacy of systemic anti-PD-L1 derives from better TDLN-inhibition, or from combined PD-L1 blockade in the tumor. We and others have detected extensive heterogeneity of T cells in the TME, with some populations responding to anti-PD-1 *in vitro* whereas others were too terminally differentiated/exhausted³⁰. Based on these observations, it is tempting to speculate that tumor-infiltrating TDLN-derived T_{ex}Progs are the preferential targets for tumoral PD-1/PD-L1 inhibition, further expanding the anti-tumor T-cell pool, but this has to be further investigated. Unfortunately, we have not been able to study the selective effect of anti-PD-L1 on the tumor *in vivo*, which would be crucial to assess its contribution to immunotherapy efficacy. Implanting recently anti-PD-L1-treated tumors in congenic mice could determine whether sole PD-L1-binding in the TME is sufficient to decrease tumor size, with the obvious limitations of surgery and treating only once. An anti-PD-L1/tumor-antigen bispecific antibody would be an alternative approach to tackle this issue, however, only PD-L1 expressing tumor cells but not PD-L1 expressing APCs will be targeted³². These and other approaches will likely aid in our understanding of how and where effective anti-tumor immunity is generated in response to ICB. This knowledge is pivotal in order to develop novel immunotherapeutic strategies aimed to increase response rates to ICB.

Secondly, it is unclear whether our results can be extrapolated to anti-PD-1-treatment. As we only blocked PD-L1, PD-L2 would still be able to bind the PD-1 receptor thereby silencing proper T-cell activation³³. Interestingly, we could not detect PD-L2 expression by cells in the TDLN, whereas this ligand was abundantly expressed in the TME. Our finding that PD-L1-blockade specifically in the TDLN was sufficient to induce anti-tumor immunity could further underline the relevance of PD-1/PD-L1-axis inhibition in TDLNs compared to the TME. Finally, we could detect frequent PD-1/PD-L1 interactions in melanoma TDLNs, in contrast to the primary tumor, which was associated with early distant disease recurrence following surgery. Current research is aimed at identifying whether the PD-1 expressed by T_{ex}Prog is involved in these PD-1/PD-L1 contacts in patient TDLNs, and whether T_{ex}Prog presence correlates with response to ICB at time of disease relapse.

With PD-1⁺ T_{ex}Prog at the receiving end, which cells provide the PD-L1 signal in the

TDLN? Both TDLN-macrophages as well as cDCs were found to be most numerous and express the highest levels of PD-L1 in TDLN. We could deplete TDLN macrophages with a titrated concentration of clodronate-encapsulated liposomes (CEL), showing that macrophages were dispensable for anti-PD-L1 efficacy, a finding that was recently confirmed by others²⁷. cDC2s, alternatively, were found to co-localize with CD8⁺ T cells in the TDLN whereas cDC1s were scarce and expressed low levels of PD-L1. cDC1s, however, are generally regarded as most optimal CD8⁺ T-cell inducers whereas cDC2s preferably prime CD4⁺ T cells³⁴⁻³⁸. Interestingly, the Krummel lab recently showed that migratory cDC2s proficiently induce CD8⁺ T-cells to a similar extent as resident- and migratory cDC1s³⁹. Furthermore, Maier and colleagues found that cDCs acquire a subtype-independent regulatory program upon apoptotic tumor cell phagocytosis, which caused PD-L1 expression and attenuation of anti-tumor T-cell responses in TDLNs²⁸. These findings challenge the proposed dichotomy in cDC-functionality and suggest that cDC2s are potentially new target for modulation of anti-tumor immune responses.

Targeting other TDLN-constituents to improve anti-tumor immunity

CD8⁺ T-cell priming by DCs takes place amidst a wide variety of LN resident- and migratory cell types that promote, suppress or skew the resultant T-cell phenotype depending on environmental cues. The precise roles of many of these cells in establishing tumor immunity are just now being unraveled and could spark the development of a new wave of immune-stimulatory drugs. As macrophages (TAMs) are among the most numerous cells in the TME displaying high immunosuppressive potential, skewing or depletion of TAMs has gained considerable momentum in the development of effective combination immunotherapy^{40,41}. In **Chapter 5**, we used a clinically applied M-CSFR-inhibitor to deplete TAMs either as monotherapy, or in combination with DC-therapy in TAM-rich mesothelioma tumor models. TAM-depletion significantly improved DC-therapy-induced anti-tumor T-cell responses as indicated by increased T-cell proliferation in PB and improved T-cell phenotype in the TME associating with improved survival. Whether this was mediated by TAM-depletion specifically, or if macrophages at other sites were responsible for the combination therapy efficacy is unknown, but preliminary data indicate that LN subcapsular sinus macrophages (SSMs) were also depleted by M-CSFRi. Crucially, The proportions of proliferating T cells were increased by M-CSFR-inhibition occurring already early following DC-transfer, indicating improved T-cell priming in LNs. Early exploratory analysis using CFSE-labeled DCs showed improved DC-trafficking in the absence of TDLN macrophages which were depleted using TDLN-targeted clodronate encapsulated liposomes (CEL) prior to DC-transfer. Based on these observations, it is interesting to speculate that SSMs could act as a physical barrier to migratory DCs. This idea is reminiscent of other research showing SSMs to shield off tumor-derived exosomes from B cells, thereby preventing the induction

DISCUSSION

of antibodies that would otherwise deposit in the TME and induce TAM-mediated immune suppression⁴². These early findings show that by dissecting the modes and sites of action of commonly applied immune modulatory drugs, novel inhibitory mechanisms can be uncovered providing rationales for combination immunotherapy.

In contrast to depleting macrophages systemically, altering their phenotype to support rather than suppress immune responses could be more beneficial. In **Chapter 6** we repolarized immune suppressive ('M2') macrophages with a CD40-agonist, thereby improving DC-therapy efficacy in mesothelioma and pancreatic ductal adenocarcinoma (PDAC) mouse models. This coincided with enhanced CD40-driven stromal degradation and increased TIL-frequencies with efficacy being dependent on CD8⁺ but not CD4⁺ T cells. Although it has to be noted that both effector- and regulatory T cells are depleted by anti-CD4-antibodies, this could indicate that CD4⁺ T-cell help may be redundant in case of CD40-agonistic antibodies. Also, it is unclear whether combination therapy efficacy manifests by enhanced DC-priming capacity in the context of CD40-stimulation (e.g. as demonstrated by increased T-cell proliferation and effector-memory generation in PB) or by effects in the TME. Experiments in which CD40 knock-out or inversely *in vitro* anti-CD40 antibody-stimulated DCs are injected could shed light on the mechanisms underlying the efficacy of combination immunotherapy. The aforementioned results provide a preclinical rationale for a current clinical trial investigating the efficacy of CD40-agonist/DC-combination immunotherapy in metastatic PDAC patients from which safety and early efficacy data are eagerly anticipated.

CD4⁺ T cells as effectors and suppressors in the tumor macroenvironment.

Depletion of CD4⁺ T cells during CD40-agonist/DC-combination immunotherapy did not abrogate therapy efficacy in PDAC-bearing mice as mentioned above. How do CD4⁺ T cells contribute to anti-tumor immunity? CD8⁺ T cells are believed to be the primary anti-tumor effector cells, but the relevance of CD4⁺ T cells in tumor immunity is becoming more apparent. Recent data from the Schreiber group showed that CD4⁺ T cells were critical mediators of ICB-efficacy, as CD4-depleting antibodies and genetic loss of MHCII-antigens abrogated treatment benefit in topical carcinogen-induced (MCA) tumors^{43,44}. Additionally, baseline CD4⁺ effector T-cell frequencies in PB have been found to correlate with ICB-response in patients^{45,46}. Besides their previously unappreciated direct cytotoxic functions⁴⁷, CD4⁺ T-helper cells are critical in providing T-cell help to DCs in the TDLN in a process called DC-licensing⁴⁸. Through a set of bidirectional co-stimulatory signaling pathways including CD40-CD40L and CD27-CD70, CD4⁺ T cells increase the capacity of DCs to induce potent effector T-cell responses⁴⁹⁻⁵². 'Helped' CD8⁺ T cells, in turn, displayed enhanced memory-potential, decreased expression of co-inhibitory checkpoints and increased tumor invasiveness⁴⁸. Despite the predicted role of CD4⁺ T cells in ICB-efficacy,

it remains to be investigated whether insufficient T-cell help contributes to CD8⁺ T-cell dysfunction in ICB non-responding patients.

In contrast to CD4⁺ effector T cells, regulatory T cells are potent suppressors of anti-tumor immunity through a wide variety of mechanisms including the scavenging of B7-signals and IL-2 by CTLA-4 and constitutive CD25-expression, respectively⁵³. The role of Tregs has been especially described in the TME where they inhibit CD8⁺ effector T-cell responses and correlate with worse prognosis and decreased ICB-efficacy and LN-metastasis⁵⁴⁻⁵⁶. In addition to affecting anti-tumor CD8⁺ T-cell responses locally in the TME, tumor-resident Tregs may indirectly alter CD4⁺ effector T-cell priming in TDLNs. It has been shown that Tregs in the TME induce a tolerogenic cDC2 subset which resultantly failed to induce effective anti-tumor immunity¹³. As tolerogenic TDLN DCs were found to preferentially induce anergic and regulatory CD4⁺ T cells in the TDLN of a spontaneous lung adenocarcinoma model, this could point to a vicious cycle fueling tumor progression⁵⁷. Blocking CTLA-4 on Tregs using anti-CTLA-4 ICB effectively abrogated Treg-induced CD8⁺ effector T-cell suppression and prevented DC phenotype alteration in mice¹³. As anti-CTLA-4 depletes Tregs in mice but not in humans, this contribution of anti-CTLA-4 ICB in patients remains to be investigated⁵⁸. Although Tregs have been found to suppress anti-PD-(L)1 induced anti-tumor immune responses in mice, their relative contribution to ICB in the patient setting was unknown^{59,60}. Future research will have to focus on the role of Tregs in antagonizing ICB-induced anti-tumor immunity and treatments aimed at the skewing or depletion of Tregs in the tumor macroenvironment.

Discovering novel modes of action of existing anticancer drugs for combination immunotherapy.

Utilizing off-target effects of chemotherapy and small-molecule inhibitors

Novel and rational combination-treatment approaches including both conventional- and immune-based therapies will be needed to increase response rates to immunotherapy. Chemo- and targeted therapies are particularly suited treatments for combination immunotherapy because of the extensive clinical experience and availability of these drugs. The majority of current anticancer drugs including chemo-, targeted- (e.g. small molecule inhibitors) and immunotherapies were initially developed to induce cell death by targeting tumor cell vulnerabilities (e.g. increased cell division, oncogene-addiction or PD-L1 expression). In the last two decades researchers have begun to dissect the precise cellular and molecular underpinnings of how these drugs constitute their effect. For example, experiments in mice have shown chemotherapeutic agents including doxorubicin, oxaliplatin and gemcitabine to depend on the presence of a functional immune system in order to be effective^{61,62}. The immune-stimulatory capacity

DISCUSSION

of these drugs and associated clinical responses in patients, however, are incompletely understood. To obtain insight in the effect of chemotherapeutics on the immune system, in **Chapter 3**, we analyzed circulating immune cells of malignant mesothelioma patients treated with the commonly used chemotherapeutic drug gemcitabine. Although second-line maintenance gemcitabine significantly increased time to disease progression in mesothelioma patients, survival was only prolonged in a subset of patients, warranting improved mechanistic insight and biomarkers that predict clinical benefit⁶³. We found gemcitabine to decrease frequencies of known immune suppressive cell types including MDSCs and to halt proliferation of Tregs while concurrently stimulating NK- and effector T cells in PB, as evidenced by increased proliferation and expression of co-stimulatory receptors. The majority of these immunomodulatory effects only occurred in gemcitabine-treated patients and not in the untreated control arm. Moreover, parameters such as increased NK-cell proliferation correlated with improved overall survival following chemotherapy identifying a potential on-treatment biomarker which should be further validated. Tumor samples pre- and post-treatment are needed to investigate whether the alterations in circulating immune cell composition are associated with an enhanced anti-tumor effect and impact patient survival through this mechanism. Unfortunately, we could not answer this question, because tumor samples pre- and post-treatment were lacking in this trial. The observed gemcitabine-associated increases in inhibitory (e.g. PD-1) and stimulatory receptors (e.g. ICOS) do provide a treatment rationale to combine gemcitabine with antagonistic- or agonistic antibodies to these receptors, respectively. In accordance with these findings, preclinical data in mice and two chemotherapy- and ICB-refractory mesothelioma patients treated with gemcitabine + anti-PD-1 showed potential synergy between the two therapies⁶⁴. These findings highlight the opportunities of performing comprehensive immunomonitoring in PB in order to rationally design combination immunotherapy in solid tumor patients.

Instead of promoting anti-tumor immunity directly (e.g. increasing immunogenicity) or indirectly (e.g. MDSC depletion), off-target effects of anticancer drugs can also potentially negate beneficial anti-tumor efficacy. E.g., in addition to the immune-stimulatory effects observed with gemcitabine in PB, gemcitabine has been reported to increase IL-1 β secretion by MDSCs, leading to IL-17 secretion by CD4⁺ T cells curtailing anti-tumor efficacy⁶⁵. Whether this mechanism plays a role in resistance to gemcitabine in patients remains to be investigated, but could be assessed by measuring IL-1 β and IL-17 cytokine levels in patient serum⁶³. Another example of a drug with pleiotropic properties is the focal-adhesion kinase (FAK) inhibitor Defactinib which was developed to target FAK-dependent cellular invasion and pro-survival signaling in cancer (stem) cells⁶⁶. Especially NF2-mutated cancers such as malignant mesothelioma were found to be particularly sensitive to FAK-inhibition both *in vitro* and in immunodeficient xenograft models⁶⁷.

Unexpectedly, a randomized controlled trial in malignant mesothelioma failed to show any survival benefit of Defactinib, independent of NF2-mutation status⁶⁸. Besides limiting tumor-cell migration, FAK-mediated cytoskeletal rearrangement could be essential in DCs for their migratory and antigen-presentation capacity (Fig. 2A). Exploratory analyses revealed that concurrent administration of a FAK-inhibitor together with tumor-lysate loaded DCs completely abrogated DC-efficacy in mesothelioma-bearing mice (Fig. 2B-D). This coincided with decreased T-cell proliferation in PB and in the TME. DC-T-cell cultures further showed decreased proliferation *in vitro*, illustrating that FAK-inhibition negatively impacts DC-T-cell interaction thereby potentially negating effective anti-tumor immunity. Interestingly, when others combined FAK-inhibition with PD-1 checkpoint blockade therapy in PDAC models, synergy was noted showing that dependency of FAK might rely on the model and the context and kinetics of the immune response⁶⁹. These data further emphasize the importance of using multiple translational immune-competent models in order to fully understand the net result of both target and off-target drug effects on the tumor macroenvironment.

Drug dose, specificity and partner dictate combination immunotherapy efficacy and toxicity

In addition to the identification of novel immunotherapeutic targets, appropriate drug selection, specificity, dose, timing and type of combined immunotherapy modality are crucial to achieve effective combination immunotherapy. Although anti-CTLA-4 and anti-PD-1 ICB are often combined because of their perceived non-redundancy, synergism is only established in some cancer types, whereas in others efficacy is limited at the expense of significant toxicity⁷⁰⁻⁷². Recently, anti-PD-1/CTLA-4 combination ICB was shown to inflict activation-induced cell death (AICD) in tumor-specific T cells, suggesting that approaches other than combination ICB are needed to safely and effectively improve cancer immunotherapy⁷³. One of these methods includes the use of low-dose immunosuppressive drugs such as mTOR- and MAPK-pathway inhibitors in order to improve immunotherapy efficacy. Opposite to merely amplifying T-cell driven responses through combination ICB, modulation of downstream signaling pathways could fine-tune anti-tumor T-cell responses and increase response durability. For instance, Sahin and colleagues have shown that combining an RNA-vaccine with the mTOR-inhibitor rapamycin skewed vaccine-elicited T-cells to a long-lived memory-precursor IL-7R^{hi} phenotype at the expense of short-lived (IL-7R^{lo} KLRG1⁺) effector T-cells, thereby improving vaccine efficacy⁷⁴. Similarly, MEK-inhibition (MEKi) was found to decrease T-cell exhaustion and induce a memory-precursor/TexProgl-like phenotype through increased fatty-acid oxidation, improving adoptive T-cell transfer and PD-L1-ICB efficacy in melanoma mouse models^{75,76}. Timing and dosing of these immunomodulatory drugs is essential, as early administration of MEKi and rapamycin

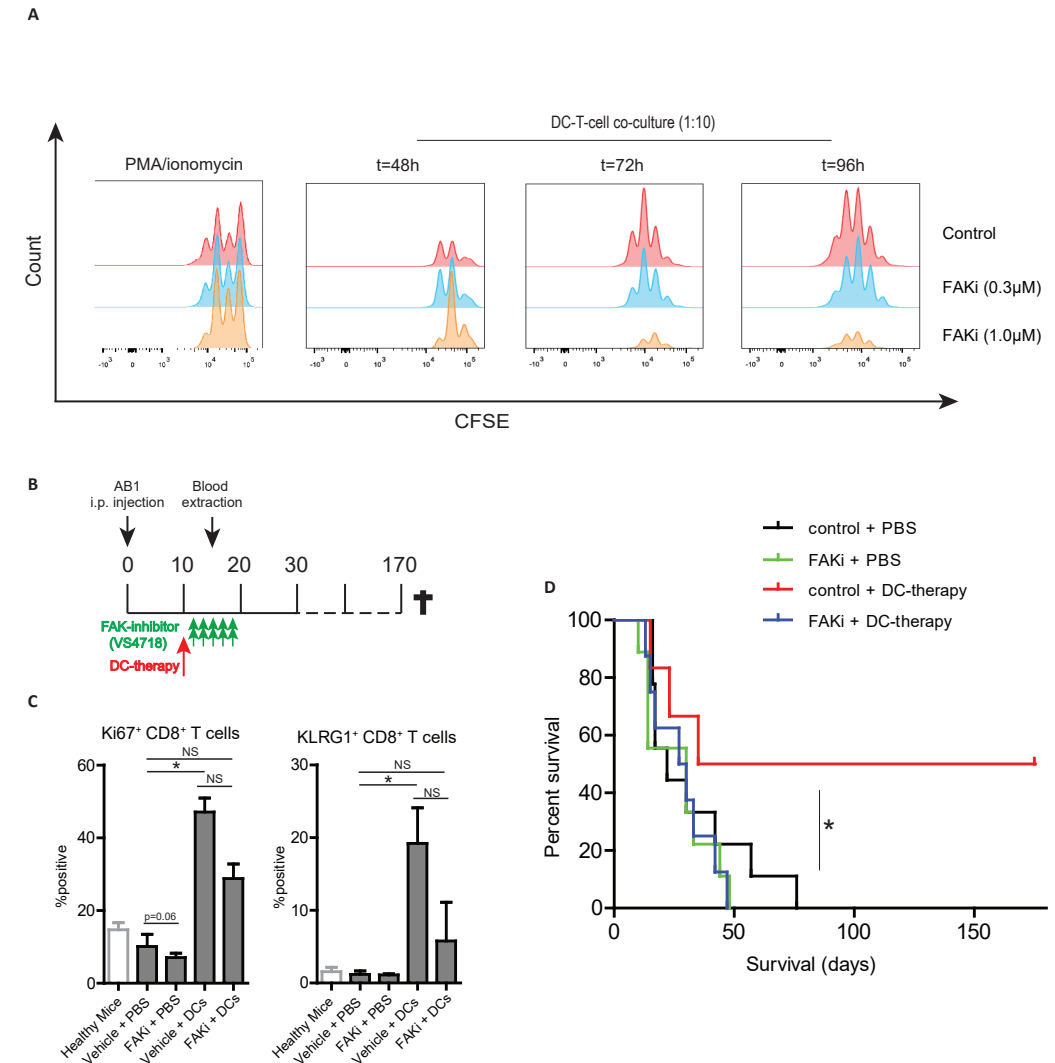


Figure 2. Inhibition of focal-adhesion kinase (FAK) abrogates dendritic cell (DC-) immunotherapy efficacy in mice. (A) Wild type OT-I T cells were either stimulated with PMA-ionomycin (left) or with bone-marrow derived dendritic cells (BMDCs) loaded with cognate peptide in the absence or presence of different doses of FAK-inhibitor (FAKi). T-cell apoptosis was not affected by FAKi as assessed by 7-AAD/Annexin V staining (not shown) (B) BALB/c mice were injected with AB-1 tumor cells and either treated with AB-1-lysate loaded BMDCs (DC-therapy) and/or FAKi administered twice daily via oral gavage. (C) Peripheral blood was analyzed on day 15 following tumor implantation and CD8⁺ T cell proliferation (Ki-67) and effector-cell differentiation (KLRG-1) was assessed using flow cytometry (D) Kaplan-Meier curve showing survival of the individual treatment groups. NS= non-significant, *= p<0.05, CFSE= Carboxyfluoresceine succinimidyl ester, PMA= phorbol myristate acetate.

was found to suppresses T-cell priming in TDLNs⁷⁵ and to generate Tregs, respectively, antagonizing therapy efficacy⁷⁷.

In **Chapter 7**, we adopted an alternative strategy inhibiting the downstream IL-2R-target JAK3 with a novel highly specific tyrosine kinase inhibitor (TKI; PF-06651600) aimed to modulate T-cell responses in the tumor macroenvironment^{78,79}. JAK3 was identified as a promising target based on earlier studies of Ibrutinib, a non-specific BTK-inhibitor used in the treatment of B-cell malignancies⁸⁰. At that time, BTK was identified as a master regulator of M2-polarization in TAMs based on Ibrutinib experiments in mice, which prompted us to investigate the efficacy of the highly specific BTK-inhibitor Acalabrutinib in skewing of the TAM-phenotype⁸¹⁻⁸³. Interestingly, BTK-knock out mice and treatment with Acalabrutinib did not alter TAM-polarization nor was survival of mesothelioma-bearing mice prolonged (Fig 3A-C). Treatment with the less-specific TKI Ibrutinib did, however, modestly improve survival (Fig 3D).

Based on these results, we hypothesized that an alternative molecular target of Ibrutinib was responsible for the observed effects by us and others, pointing to JAK3 (also in addition to SRC- and TEC-kinase family members) as a potent target of Ibrutinib based on previously published Kinomescan data⁸². *In vitro* human and murine macrophage polarization was potently inhibited by JAK3i, presumably by inhibition of downstream IL-4R-signaling known to induce the M2-phenotype^{84,85}. The importance of a careful selection of drug dose and route of administration was illustrated by JAK3i treatment in mesothelioma mouse models causing overt T-cell suppression and lack of clinical efficacy when administered at high dose via twice-daily oral gavage (**Chapter 7**). Also, TAM phenotype was unaltered *in vivo* suggesting that IL-4/IL4R-signaling may not be involved or may be functionally redundant during *in vivo* TAM polarization. At low dose continuous JAK3i administration in drinking water, however, T-cell activation was enhanced, as shown by increased TIL proliferation and PD-1-expression which was associated with decreased tumor load. Moreover, JAK3i improved DC- and peptide-vaccine efficacy providing a preclinical rationale for clinical combination immunotherapy. How does JAK3i modulate anti-tumor T-cell immunity and responses? JAK3 associates with the common-gamma chain family of cytokine receptors including the IL-2R, which is indispensable for early T-cell proliferation and survival following priming⁸⁶. However, recent findings by Liu *et al.* indicate that chronic IL-2R-JAK1/3-STAT5 signaling induces TIL-exhaustion through tryptophan metabolites activating the aryl hydrocarbon receptor in T cells^{87,88}. Moreover, excess IL-2 during priming skews T-cells to the short-lived effector T-cell (SLEC) fate, which is reminiscent of the aforementioned finding that inhibition of the mTOR and MAPK-pathways prevents SLEC development^{89,90}. In addition to STAT5, mTOR and MAPK-pathways are also activated by IL-2R-JAK1/3-signaling, suggesting that JAK3i could have widespread effects on intracellular

DISCUSSION

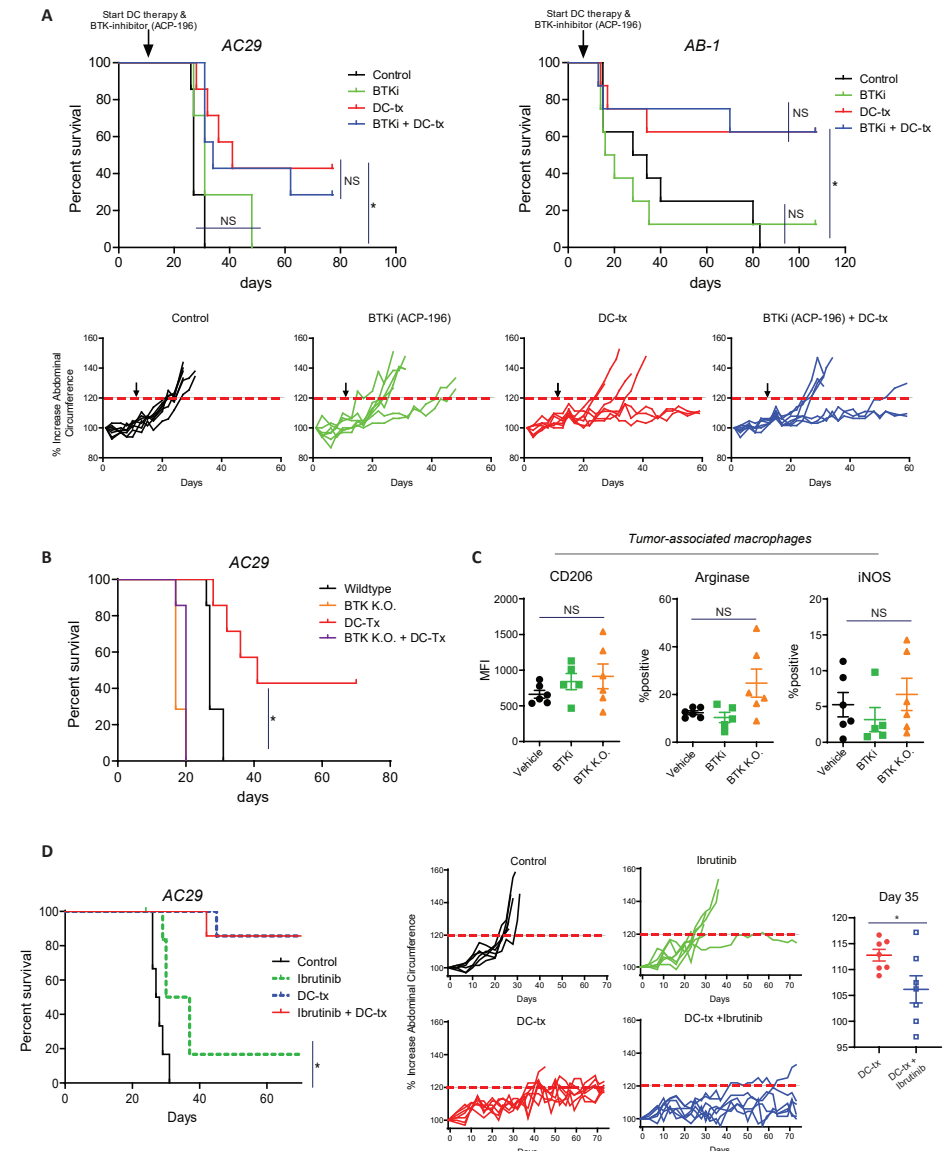


Figure 3. Inhibition or lack of Bruton's tyrosine kinase (BTK) does not impact survival or macrophage phenotype in mesothelioma murine tumors. (A) CBA/J and BALB/c mice were injected with AC-29 or AB-1 tumor cells, respectively, and either treated with AB-1-lysate loaded BMDCs (DC-therapy) and/or ACP-196, a highly specific BTK-inhibitor (BTKi) in drinking water. Survival was monitored and plotted in Kaplan-Meier curves and in case of CBA/J mice, abdominal circumference was measured as a proxy for ascites volume. (B) BTK wild-type (CBA/J) or knock-out (K.O.; CBA/N) mice were injected with AC29 tumor cells followed by DC-therapy at day 10 and survival was monitored. (C) In end-stage tumor tissue, tumor-associated macrophages (TAM) phenotype was assessed using M2 (arginase, CD206) and M1 (iNOS) markers. (D) Alternatively, AC29-bearing CBA/J mice were treated with Ibrutinib and/or DC-therapy and survival and abdominal circumference was noted. NS= non-significant, * = p < 0.05

signaling culminating in an improved T-cell phenotype⁹⁰. Whether these mechanisms account for the beneficial effects of chronic low-dose JAK3i or Ibrutinib *in vivo* remains to be investigated. These findings illustrate the potency but also complexity of using small molecule TKI as immunomodulatory agents in cancer immunotherapy.

Concluding remarks and prospects for future investigation

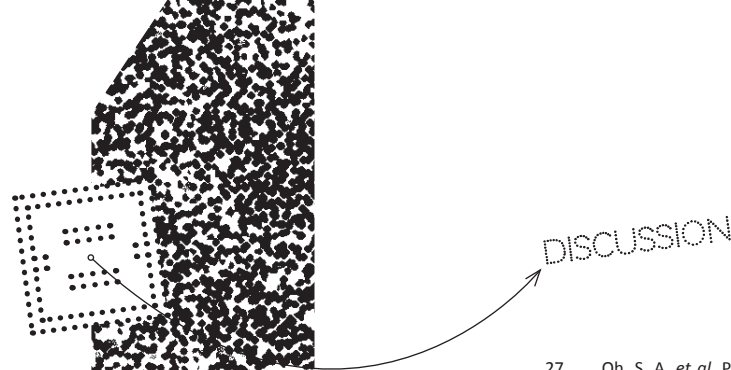
This thesis provides novel insights into the role of the tumor macroenvironment in tumor immunology and cancer immunotherapy, however, much remains to be explored in order to optimally treat solid tumor patients. **Part A** of this thesis encompasses novel insights into the mechanisms underlying conventional- and immunotherapy efficacy, with the identification of TDLNs as key actors in the tumor macroenvironment. Current and future research will be aimed at the further characterization of the TDLN-environment in solid tumor patients, focusing on APC-T-cell interactions, the development of T_{ex} Prog and the contribution of checkpoints other than PD-1/PD-L1 in TDLN-homeostasis. Although T-cell immunosurveillance of primary tumors is frequently studied, the role of T cells in curtailing LN metastasis is largely unknown and could offer novel targets for immunotherapy. To these ends, novel tools will be employed allowing spatial discrimination of cells in the architecturally complex TDLN including imaging mass-cytometry, multicolor chromogenic multiplex staining and Nanostring digital spatial profiling (DSP). Several tumor types such as PDAC, NSCLC and melanoma will be included in order to assess the role of TDLNs in tumors differing in immunogenicity and ICB-responsiveness. Concerning melanoma, the increased abundance of PD-1/PD-L1 interactions in the TDLN associating with poor clinical outcome deserves further validation and improved (automated) quantification in larger cohorts. As non-metastatic stage II-III melanoma patients are increasingly being treated with (neo-)adjuvant ICB in clinical studies and daily practice, a biomarker predicting benefit to ICB treatment is anticipated^{91,92}. These studies will further improve insight into the dynamic interaction between our immune system and (metastatic) cancer, yielding novel biomarkers and targets for immunotherapy.

In **Part B**, characterization of the mesothelioma and PDAC microenvironment allowed for rational design of cellular (DC) and peptide vaccine combination immunotherapy, primarily by targeting immunosuppressive macrophages in the tumor macroenvironment. These studies form the preclinical basis for current phase I-II clinical trials in PDAC in which DC-therapy is investigated as monotherapy following surgical resection or in combination with a CD40-agonistic antibody in the metastatic setting. By increasing T-cell infiltration of PDAC and mesothelioma tumors, DC-therapy (+/- anti-CD40) could subsequently sensitize these tumors to anti-PD-(L)1 ICB to which they are inherently resistant⁹³⁻⁹⁵. Exploratory analysis (not included in this thesis) point to potential synergy between concurrent anti-PD-L1 and DC-therapy administration in mice, significantly increasing T-cell activation

DISCUSSION

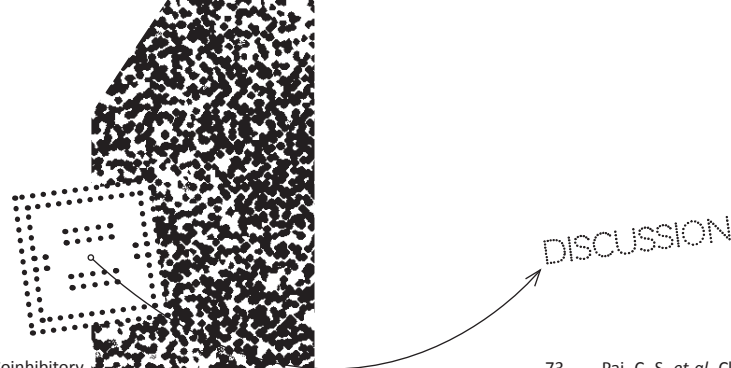
and proliferation in PB following treatment. This effect was derived in part from blockade of PD-L1 in the DC- and tumor-DLN, because LN-targeted PD-L1 blockade was nearly as effective as systemic anti-PD-L1 administration. As both endogenous and exogenous *in vitro* stimulated DCs express high levels of PD-L1, ICB could promote DC-therapy efficacy by improving both T-cell priming and TIL-effector function in the TME. This illustrates that by comprehensive characterization of not only the TME, but the tumor macroenvironment, novel interactions between immune, stromal and tumor cells can be uncovered and redirected to mount effective anti-tumor immunity in patients.

Essential to the development of novel combination immunotherapies are innovative trial designs with comprehensive multi-tissue immunomonitoring allowing for the study of anti-tumor immune responses directly *in vivo*. As timing of chemo- or radiation therapy in combination with immunotherapy may elicit widely different responses^{96,97}, early-phase clinical trials including multiple smaller-armed patient cohorts could reveal potent synergies which could be then confirmed on a larger scale⁹⁸. Translating these findings back to appropriate pre-clinical models rather than vice-versa will aid in an improved understanding of the molecular mechanisms underlying treatment efficacy and provide rationales for novel immunotherapies⁹⁹. As current forms of immunotherapy (including immunogenic forms of chemo- and radiotherapy) act at different steps of the anti-tumor immune response (Figure 1), rational combination immunotherapy efficacy at the offset of treatment (e.g. ICB + cellular therapies, rather than combination ICB) may be most effective in rendering durable treatment responses. Careful pre- but also on-treatment biomarkers should be used to optimally stratify patients for individual treatment combinations and adjust treatment when secondary/acquired immune resistance ensues, respectively. For example, patients exhibiting a lack of a pre-existing anti-tumor immune response could benefit from a cellular or peptide vaccine, combined with (anti-PD-1/PD-L1) ICB to amplify immune priming in lymphoid organs. If disease relapse occurs, tissue or liquid biomarkers could inform on the mode of resistance. In case of a defect in tumor cell antigen-processing machinery an approach could be an individualized T-cell therapy approach (e.g. chimeric antigen receptor [CAR] T-cells), vaccination with alternative antigens (e.g. T cell epitopes associated with impaired peptide processing; TEIPP) or a different conventional anticancer agent¹⁰⁰⁻¹⁰². Such a dynamic and personalized application of cancer immunotherapy guided by biomarkers informing about tumor macroenvironment status will improve cancer immunotherapy allocation and efficacy in the future.



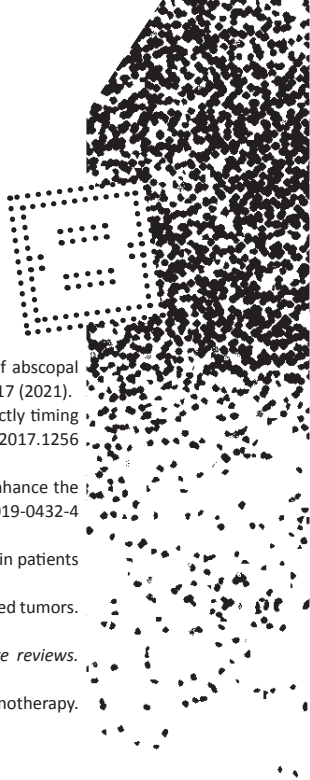
REFERENCES

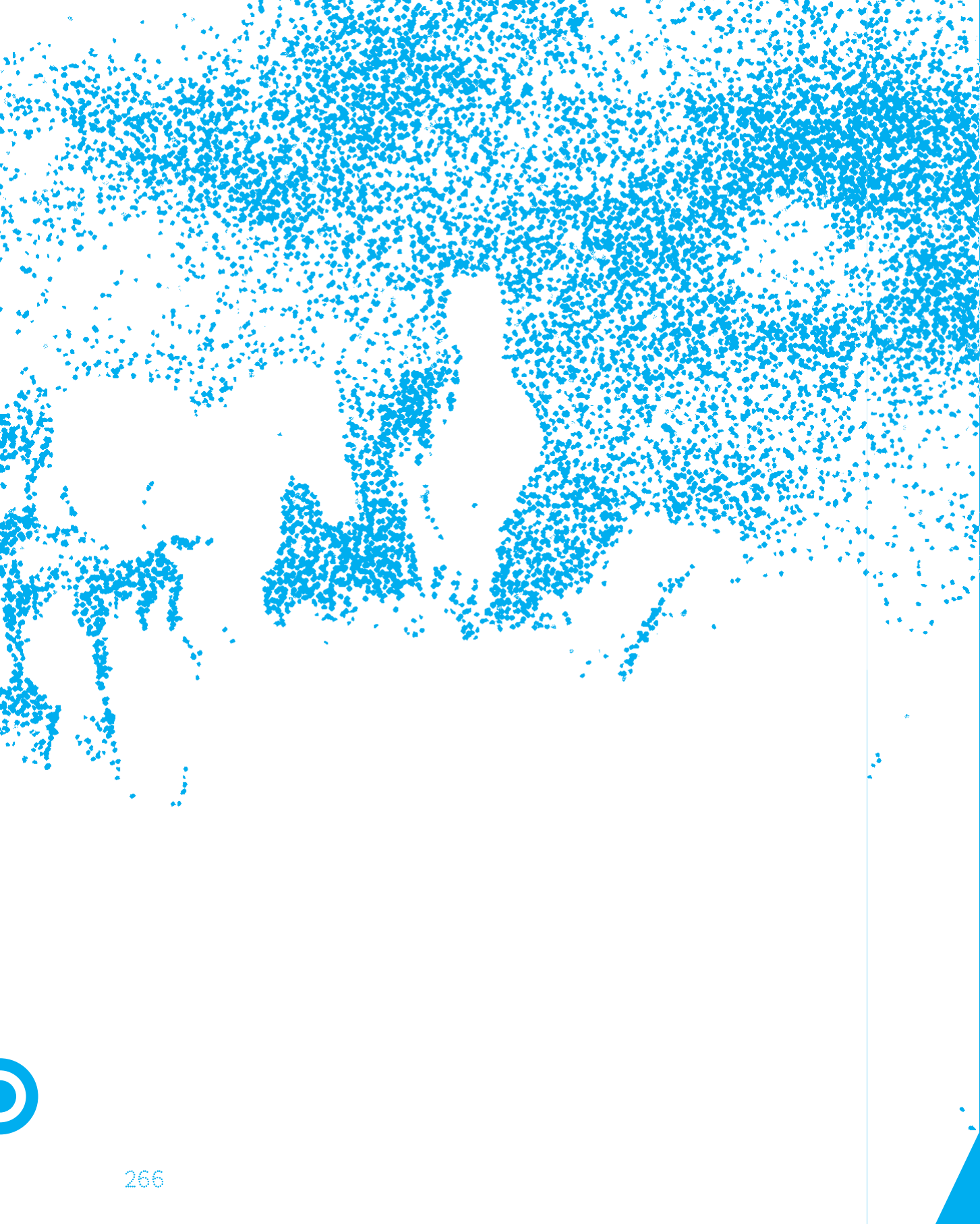
- 1 Chen, D. S. & Mellman, I. Oncology meets immunology: the cancer-immunity cycle. *Immunity* **39**, 1-10, doi:10.1016/j.immuni.2013.07.012 (2013).
- 2 Spitzer, M. H. *et al.* Systemic Immunity Is Required for Effective Cancer Immunotherapy. *Cell* **168**, 487-502. e415, doi:10.1016/j.cell.2016.12.022 (2017).
- 3 Wu, T. D. *et al.* Peripheral T cell expansion predicts tumour infiltration and clinical response. *Nature* **579**, 274-278, doi:10.1038/s41586-020-2056-8 (2020).
- 4 Gopalakrishnan, V., Helmink, B. A., Spencer, C. N., Reuben, A. & Wargo, J. A. The Influence of the Gut Microbiome on Cancer, Immunity, and Cancer Immunotherapy. *Cancer cell* **33**, 570-580, doi:10.1016/j.ccell.2018.03.015 (2018).
- 5 Zitvogel, L., Ma, Y., Raoult, D., Kroemer, G. & Gajewski, T. F. The microbiome in cancer immunotherapy: Diagnostic tools and therapeutic strategies. *Science* **359**, 1366-1370, doi:10.1126/science.aar6918 (2018).
- 6 Davar, D. *et al.* Fecal microbiota transplant overcomes resistance to anti-PD-1 therapy in melanoma patients. *Science* **371**, 595, doi:10.1126/science.abf3363 (2021).
- 7 Baruch, E. N. *et al.* Fecal microbiota transplant promotes response in immunotherapy-refractory melanoma patients. *Science* **371**, 602, doi:10.1126/science.abb5920 (2021).
- 8 Cochran, A. J. *et al.* Tumour-induced immune modulation of sentinel lymph nodes. *Nature reviews. Immunology* **6**, 659-670, doi:10.1038/nri1919 (2006).
- 9 Chongsathidkiet, P. *et al.* Sequestration of T cells in bone marrow in the setting of glioblastoma and other intracranial tumors. *Nature medicine* **24**, 1459-1468, doi:10.1038/s41591-018-0135-2 (2018).
- 10 Garner, H. & de Visser, K. E. Immune crosstalk in cancer progression and metastatic spread: a complex conversation. *Nature reviews. Immunology* **20**, 483-497, doi:10.1038/s41577-019-0271-z (2020).
- 11 Bronte, V. & Pittet, M. J. The spleen in local and systemic regulation of immunity. *Immunity* **39**, 806-818, doi:10.1016/j.immuni.2013.10.010 (2013).
- 12 Roberts, E. W. *et al.* Critical Role for CD103⁺/CD141⁺ Dendritic Cells Bearing CCR7 for Tumor Antigen Trafficking and Priming of T Cell Immunity in Melanoma. *Cancer cell* **30**, 324-336, doi:10.1016/j.ccell.2016.06.003 (2016).
- 13 Binnewies, M. *et al.* Unleashing Type-2 Dendritic Cells to Drive Protective Antitumor CD4⁺ T Cell Immunity. *Cell* **177**, 556-571.e516, doi:10.1016/j.cell.2019.02.005 (2019).
- 14 Wculek, S. K. *et al.* Dendritic cells in cancer immunology and immunotherapy. *Nature reviews. Immunology* **20**, 7-24 (2020).
- 15 Carreno, B. M. *et al.* A dendritic cell vaccine increases the breadth and diversity of melanoma neoantigen-specific T cells. *Science* **348**, 803-808, doi:10.1126/science.aaa3828 (2015).
- 16 Yost, K. E. *et al.* Clonal replacement of tumor-specific T cells following PD-1 blockade. *Nature medicine* **25**, 1251-1259, doi:10.1038/s41591-019-0522-3 (2019).
- 17 Cha, E. *et al.* Improved survival with T cell clonotype stability after anti-CTLA-4 treatment in cancer patients. *Science translational medicine* **6**, 238ra270-238ra270, doi:10.1126/scitranslmed.3008211 (2014).
- 18 Ribas, A. & Wolchok, J. D. Cancer immunotherapy using checkpoint blockade. *Science* **359**, 1350-1355 (2018).
- 19 Yokosuka, T. *et al.* Programmed cell death 1 forms negative costimulatory microclusters that directly inhibit T cell receptor signaling by recruiting phosphatase SHP2. *The Journal of experimental medicine* **209**, 1201-1217, doi:10.1084/jem.20112741 (2012).
- 20 Schildberg, F. A., Klein, S. R., Freeman, G. J. & Sharpe, A. H. Coinhibitory Pathways in the B7-CD28 Ligand-Receptor Family. *Immunity* **44**, 955-972, doi:10.1016/j.immuni.2016.05.002 (2016).
- 21 Hui, E. *et al.* T cell costimulatory receptor CD28 is a primary target for PD-1-mediated inhibition. *Science* **355**, 1428-1433 (2017).
- 22 Kamphorst, A. O. *et al.* Rescue of exhausted CD8 T cells by PD-1-targeted therapies is CD28-dependent. *Science* **355**, 1423-1427 (2017).
- 23 Kleinovink, J. W. *et al.* PD-L1 expression on malignant cells is no prerequisite for checkpoint therapy. *Oncoimmunology* **6**, e1294299, doi:10.1080/2162402x.2017.1294299 (2017).
- 24 Tang, H. *et al.* PD-L1 on host cells is essential for PD-L1 blockade-mediated tumor regression. *The Journal of clinical investigation* **128**, 580-588 (2018).
- 25 Lau, J. *et al.* Tumour and host cell PD-L1 is required to mediate suppression of anti-tumour immunity in mice. *Nature communications* **8**, 14572, doi:10.1038/ncomms14572 (2017).
- 26 Lin, H. *et al.* Host expression of PD-L1 determines efficacy of PD-L1 pathway blockade-mediated tumor regression. *The Journal of clinical investigation* **128**, 1708 (2018).
- 27 Oh, S. A. *et al.* PD-L1 expression by dendritic cells is a key regulator of T-cell immunity in cancer. *Nature Cancer* **1**, 681-691, doi:10.1038/s43018-020-0075-x (2020).
- 28 Maier, B. *et al.* A conserved dendritic-cell regulatory program limits antitumour immunity. *Nature* **580**, 257-262, doi:10.1038/s41586-020-2134-y (2020).
- 29 Siddiqui, I. *et al.* Intratumoral Tcf1+PD-1+CD8⁺ T Cells with Stem-like Properties Promote Tumor Control in Response to Vaccination and Checkpoint Blockade Immunotherapy. *Immunity* **50**, 195-211.e110, doi:https://doi.org/10.1016/j.immuni.2018.12.021 (2019).
- 30 Miller, B. C. *et al.* Subsets of exhausted CD8⁺ T cells differentially mediate tumor control and respond to checkpoint blockade. *Nature immunology* **20**, 326-336, doi:10.1038/s41590-019-0312-6 (2019).
- 31 Sade-Feldman, M. *et al.* Defining T Cell States Associated with Response to Checkpoint Immunotherapy in Melanoma. *Cell* **175**, 998-1013.e1020, doi:https://doi.org/10.1016/j.cell.2018.10.038 (2018).
- 32 Koopmans, I. *et al.* A novel bispecific antibody for EGFR-directed blockade of the PD-1/PD-L1 immune checkpoint. *Oncoimmunology* **7**, e1466016, doi:10.1080/2162402X.2018.1466016 (2018).
- 33 Latchman, Y. *et al.* PD-L2 is a second ligand for PD-1 and inhibits T cell activation. *Nature immunology* **2**, 261-268, doi:10.1038/85330 (2001).
- 34 Spranger, S., Dai, D., Horton, B. & Gajewski, T. F. Tumor-Residing Batf3 Dendritic Cells Are Required for Effector T Cell Trafficking and Adoptive T Cell Therapy. *Cancer cell* **31**, 711-723.e714, doi:10.1016/j.ccell.2017.04.003 (2017).
- 35 Salmon, H. *et al.* Expansion and Activation of CD103⁺ Dendritic Cell Progenitors at the Tumor Site Enhances Tumor Responses to Therapeutic PD-L1 and BRAF Inhibition. *Immunity* **44**, 924-938, doi:10.1016/j.immuni.2016.03.012 (2016).
- 36 Roberts, E. W. *et al.* Critical Role for CD103⁺/CD141⁺ Dendritic Cells Bearing CCR7 for Tumor Antigen Trafficking and Priming of T Cell Immunity in Melanoma. *Cancer cell*, doi:10.1016/j.ccell.2016.06.003 (2016).
- 37 Binnewies, M. *et al.* Unleashing Type-2 Dendritic Cells to Drive Protective Antitumor CD4⁺ T Cell Immunity. *Cell* **177**, 556-571.e516, doi:https://doi.org/10.1016/j.cell.2019.02.005 (2019).
- 38 Eisenbarth, S. C. Dendritic cell subsets in T cell programming: location dictates function. *Nature reviews. Immunology* **19**, 89-103, doi:10.1038/s41577-018-0088-1 (2019).
- 39 Ruhland, M. K. *et al.* Visualizing Synaptic Transfer of Tumor Antigens among Dendritic Cells. *Cancer cell* **37**, 786-799.e785 (2020).
- 40 Coussens, L. M., Zitvogel, L. & Palucka, A. K. Neutralizing tumor-promoting chronic inflammation: a magic bullet? *Science* **339**, 286-291, doi:10.1126/science.1232227 (2013).
- 41 Mantovani, A., Marchesi, F., Malesci, A., Laghi, L. & Allavena, P. Tumour-associated macrophages as treatment targets in oncology. *Nature reviews. Clinical oncology* **14**, 399-416, doi:10.1038/nrclinonc.2016.217 (2017).
- 42 Pucci, F. *et al.* SCS macrophages suppress melanoma by restricting tumor-derived vesicle-B cell interactions. *Science* **352**, 242-246, doi:10.1126/science.aaf1328 (2016).
- 43 Gubin, M. M. *et al.* Checkpoint blockade cancer immunotherapy targets tumour-specific mutant antigens. *Nature* **515**, 577-581, doi:10.1038/nature13988 (2014).
- 44 Alspach, E. *et al.* MHC-II neoantigens shape tumour immunity and response to immunotherapy. *Nature* **574**, 696-701, doi:10.1038/s41586-019-1671-8 (2019).
- 45 Kagamu, H. *et al.* CD4⁺ T-cell Immunity in the Peripheral Blood Correlates with Response to Anti-PD-1 Therapy. *Cancer immunology research* **8**, 334, doi:10.1158/2326-6066.CIR-19-0574 (2020).
- 46 Zuazo, M. *et al.* Functional systemic CD4 immunity is required for clinical responses to PD-L1/PD-1 blockade therapy. *EMBO molecular medicine* **11**, e10293, doi:10.15252/emmm.201910293 (2019).
- 47 Oh, D. Y. *et al.* Intratumoral CD4⁺ T Cells Mediate Anti-tumor Cytotoxicity in Human Bladder Cancer. *Cell* **181**, 1612-1625.e1613, doi:https://doi.org/10.1016/j.cell.2020.05.017 (2020).
- 48 Borst, J., Ahrends, T., Bąbala, N., Melief, C. J. M. & Kastenmüller, W. CD4⁺ T cell help in cancer immunology and immunotherapy. *Nature reviews. Immunology* **18**, 635-647, doi:10.1038/s41577-018-0044-0 (2018).
- 49 Schoenberger, S. P., Toes, R. E., van der Voort, E. I., Offringa, R. & Melief, C. J. T-cell help for cytotoxic T lymphocytes is mediated by CD40-CD40L interactions. *Nature* **393**, 480-483, doi:10.1038/31002 (1998).
- 50 Dolfi, D. V. *et al.* Late signals from CD27 prevent Fas-dependent apoptosis of primary CD8⁺ T cells. *Journal of immunology (Baltimore, Md. : 1950)* **180**, 2912-2921, doi:10.4049/jimmunol.180.5.2912 (2008).
- 51 Hendriks, J. *et al.* CD27 is required for generation and long-term maintenance of T cell immunity. *Nature immunology* **1**, 433-440, doi:10.1038/80877 (2000).



DISCUSSION

- Ahrends, T. *et al.* CD4(+) T Cell Help Confers a Cytotoxic T Cell Effector Program Including Coinhibitory Receptor Downregulation and Increased Tissue Invasiveness. *Immunity* **47**, 848-861.e845, doi:10.1016/j.immuni.2017.10.009 (2017).
- Togashi, Y., Shitara, K. & Nishikawa, H. Regulatory T cells in cancer immunosuppression - implications for anticancer therapy. *Nature reviews. Clinical oncology* **16**, 356-371, doi:10.1038/s41571-019-0175-7 (2019).
- Fridman, W. H., Zitvogel, L., Sautès-Fridman, C. & Kroemer, G. The immune contexture in cancer prognosis and treatment. *Nature Reviews Clinical Oncology* **14**, 717-734, doi:10.1038/nrclinonc.2017.101 (2017).
- Kumagai, S. *et al.* The PD-1 expression balance between effector and regulatory T cells predicts the clinical efficacy of PD-1 blockade therapies. *Nature immunology*, doi:10.1038/s41590-020-0769-3 (2020).
- Núñez, N. G. *et al.* Tumor invasion in draining lymph nodes is associated with Treg accumulation in breast cancer patients. *Nature communications* **11**, 3272, doi:10.1038/s41467-020-17046-2 (2020).
- Alonso, R. *et al.* Induction of anergic or regulatory tumor-specific CD4+ T cells in the tumor-draining lymph node. *Nature communications* **9**, 2113, doi:10.1038/s41467-018-04524-x (2018).
- Sharma, A. *et al.* Anti-CTLA-4 Immunotherapy Does Not Deplete FOXP3⁺ Regulatory T Cells (Tregs) in Human Cancers. *Clinical Cancer Research* **25**, 1233-1238, doi:10.1158/1078-0432.ccr-18-0762 (2019).
- Arce Vargas, F. *et al.* Fc-Optimized Anti-CD25 Depletes Tumor-Infiltrating Regulatory T Cells and Synergizes with PD-1 Blockade to Eradicate Established Tumors. *Immunity* **46**, 577-586, doi:10.1016/j.immuni.2017.03.013 (2017).
- Kamada, T. *et al.* PD-1⁺ regulatory T cells amplified by PD-1 blockade promote hyperprogression of cancer. *Proceedings of the National Academy of Sciences* **116**, 9999-10008, doi:10.1073/pnas.1822001116 (2019).
- Galluzzi, L., Humeau, J., Buqué, A., Zitvogel, L. & Kroemer, G. Immunostimulation with chemotherapy in the era of immune checkpoint inhibitors. *Nature Reviews Clinical Oncology*, doi:10.1038/s41571-020-0413-z (2020).
- Suzuki, E., Sun, J., Kapoor, V., Jassar, A. S. & Albelda, S. M. Gemcitabine has significant immunomodulatory activity in murine tumor models independent of its cytotoxic effects. *Cancer biology & therapy* **6**, 880-885 (2007).
- de Gooijer, C. J. *et al.* Switch-maintenance gemcitabine after first-line chemotherapy in patients with malignant mesothelioma (NVALT19): an investigator-initiated, randomised, open-label, phase 2 trial. *Lancet Respir Med*, doi:10.1016/s2213-2600(20)30362-3 (2021).
- Tallón de Lara, P. *et al.* Gemcitabine Synergizes with Immune Checkpoint Inhibitors and Overcomes Resistance in a Preclinical Model and Mesothelioma Patients. *Clinical Cancer Research* **24**, 6345, doi:10.1158/1078-0432.CCR-18-1231 (2018).
- Bruchard, M. *et al.* Chemotherapy-triggered cathepsin B release in myeloid-derived suppressor cells activates the Nlrp3 inflammasome and promotes tumor growth. *Nature medicine* **19**, 57-64, doi:10.1038/nm.2999 (2013).
- Murphy, J. M., Rodriguez, Y. A. R., Jeong, K., Ahn, E.-Y. E. & Lim, S.-T. S. Targeting focal adhesion kinase in cancer cells and the tumor microenvironment. *Experimental & Molecular Medicine* **52**, 877-886, doi:10.1038/s12276-020-0447-4 (2020).
- Shapiro, I. M. *et al.* Merlin deficiency predicts FAK inhibitor sensitivity: a synthetic lethal relationship. *Science translational medicine* **6**, 237ra268, doi:10.1126/scitranslmed.3008639 (2014).
- Fennell, D. A. *et al.* Maintenance Defactinib Versus Placebo After First-Line Chemotherapy in Patients With Merlin-Stratified Pleural Mesothelioma: COMMAND-A Double-Blind, Randomized, Phase II Study. *Journal of clinical oncology : official journal of the American Society of Clinical Oncology* **37**, 790-798, doi:10.1200/jco.2018.79.0543 (2019).
- Jiang, H. *et al.* Targeting focal adhesion kinase renders pancreatic cancers responsive to checkpoint immunotherapy. *Nature medicine* **22**, 851-860, doi:10.1038/nm.4123 (2016).
- Rizvi, N. A. *et al.* Durvalumab With or Without Tremelimumab vs Standard Chemotherapy in First-line Treatment of Metastatic Non-Small Cell Lung Cancer: The MYSTIC Phase 3 Randomized Clinical Trial. *JAMA oncology* **6**, 661-674, doi:10.1001/jamaoncol.2020.0237 (2020).
- Hellmann, M. D. *et al.* Nivolumab plus Ipilimumab in Advanced Non-Small-Cell Lung Cancer. *New England Journal of Medicine* **381**, 2020-2031, doi:10.1056/NEJMoa1910231 (2019).
- Larkin, J. *et al.* Five-Year Survival with Combined Nivolumab and Ipilimumab in Advanced Melanoma. *New England Journal of Medicine* **381**, 1535-1546, doi:10.1056/NEJMoa1910836 (2019).
- Pai, C. S. *et al.* Clonal Deletion of Tumor-Specific T Cells by Interferon- γ Confers Therapeutic Resistance to Combination Immune Checkpoint Blockade. *Immunity* **50**, 477-492.e478, doi:10.1016/j.immuni.2019.01.006 (2019).
- Diken, M. *et al.* mTOR inhibition improves antitumor effects of vaccination with antigen-encoding RNA. *Cancer immunology research* **1**, 386-392, doi:10.1158/2326-6066.cir-13-0046 (2013).
- Ebert, P. J. R. *et al.* MAP Kinase Inhibition Promotes T Cell and Anti-tumor Activity in Combination with PD-L1 Checkpoint Blockade. *Immunity* **44**, 609-621, doi:10.1016/j.immuni.2016.01.024 (2016).
- Verma, V. *et al.* MEK inhibition reprograms CD8(+) T lymphocytes into memory stem cells with potent antitumor effects. *Nature immunology* **22**, 53-66, doi:10.1038/s41590-020-00818-9 (2021).
- Vanneman, M. & Dranoff, G. Combining immunotherapy and targeted therapies in cancer treatment. *Nature reviews. Cancer* **12**, 237-251, doi:10.1038/nrc3237 (2012).
- Telliez, J. B. *et al.* Discovery of a JAK3-Selective Inhibitor: Functional Differentiation of JAK3-Selective Inhibition over pan-JAK or JAK1-Selective Inhibition. *ACS chemical biology* **11**, 3442-3451, doi:10.1021/acscchembio.6b00677 (2016).
- Thorarensen, A. *et al.* Design of a Janus Kinase 3 (JAK3) Specific Inhibitor 1-((2S,5R)-5-((7H-Pyrrolo[2,3-d]pyrimidin-4-yl)amino)-2-methylpiperidin-1-yl)prop-2-en-1-one (PF-06651600) Allowing for the Interrogation of JAK3 Signaling in Humans. *Journal of medicinal chemistry* **60**, 1971-1993, doi:10.1021/acs.jmedchem.6b01694 (2017).
- Pal Singh, S., Dammeijer, F. & Hendriks, R. W. Role of Bruton's tyrosine kinase in B cells and malignancies. *Molecular cancer* **17**, 57, doi:10.1186/s12943-018-0779-z (2018).
- Gunderson, A. J. *et al.* Bruton's Tyrosine Kinase (BTK)-dependent immune cell crosstalk drives pancreas cancer. *Cancer Discov* (2015).
- Herman, S. E. M. *et al.* The Bruton Tyrosine Kinase (BTK) Inhibitor Acalabrutinib Demonstrates Potent On-Target Effects and Efficacy in Two Mouse Models of Chronic Lymphocytic Leukemia. *Clinical cancer research : an official journal of the American Association for Cancer Research* **23**, 2831-2841, doi:10.1158/1078-0432.ccr-16-0463 (2017).
- Byrd, J. C. *et al.* Acalabrutinib (ACP-196) in Relapsed Chronic Lymphocytic Leukemia. *The New England journal of medicine* (2015).
- Shiao, S. L. *et al.* TH2-Polarized CD4(+) T Cells and Macrophages Limit Efficacy of Radiotherapy. *Cancer immunology research* **3**, 518-525, doi:10.1158/2326-6066.cir-14-0232 (2015).
- Bosurgi, L. *et al.* Macrophage function in tissue repair and remodeling requires IL-4 or IL-13 with apoptotic cells. *Science* **356**, 1072-1076, doi:10.1126/science.aai8132 (2017).
- Spolski, R., Li, P. & Leonard, W. J. Biology and regulation of IL-2: from molecular mechanisms to human therapy. *Nature Reviews Immunology* **18**, 648-659, doi:10.1038/s41577-018-0046-y (2018).
- Liu, Y. *et al.* IL-2 regulates tumor-reactive CD8+ T cell exhaustion by activating the aryl hydrocarbon receptor. *Nature immunology*, doi:10.1038/s41590-020-00850-9 (2021).
- Beltra, J.-C. *et al.* IL2R β -dependent signals drive terminal exhaustion and suppress memory development during chronic viral infection. *Proceedings of the National Academy of Sciences* **113**, E5444-E5453, doi:10.1073/pnas.1604256113 (2016).
- Kalia, V. *et al.* Prolonged Interleukin-2R α Expression on Virus-Specific CD8+ T Cells Favors Terminal-Effector Differentiation In Vivo. *Immunity* **32**, 91-103, doi:https://doi.org/10.1016/j.immuni.2009.11.010 (2010).
- Boyman, O. & Sprent, J. The role of interleukin-2 during homeostasis and activation of the immune system. *Nature Reviews Immunology* **12**, 180-190, doi:10.1038/nri3156 (2012).
- Eggermont, A. M. M., Robert, C. & Ribas, A. The new era of adjuvant therapies for melanoma. *Nature reviews. Clinical oncology* **15**, 535-536, doi:10.1038/s41571-018-0048-5 (2018).
- Rozeman, E. A. *et al.* Survival and biomarker analyses from the OpACIN-neo and OpACIN neoadjuvant immunotherapy trials in stage III melanoma. *Nature medicine*, doi:10.1038/s41591-020-01211-7 (2021).
- Brahmer, J. R. *et al.* Safety and Activity of Anti-PD-L1 Antibody in Patients with Advanced Cancer. *New England Journal of Medicine* **366**, 2455-2465, doi:10.1056/NEJMoa1200694 (2012).
- Popat, S. *et al.* A multicentre randomised phase III trial comparing pembrolizumab versus single-agent chemotherapy for advanced pre-treated malignant pleural mesothelioma: the European Thoracic Oncology Platform (ETOP 9-15) PROMISE-meso trial. *Annals of Oncology* **31**, 1734-1745, doi:10.1016/j.annonc.2020.09.009 (2020).
- S.P. Lau, F. D., C.H.J. van Eijck. HET PANCREASCARCINOOM: TOCH NIET IMMUUN VOOR THERAPIE? ONTWIKKELINGEN IN DE IMMUUNTHERAPIE VOOR DUCTAAL ADENOCARCINOOM VAN HET PANCREAS. *Nederlands Tijdschrift voor de Oncologie* **16** (2020).

- 
- 96 Wei, J. *et al.* Sequence of α PD-1 relative to local tumor irradiation determines the induction of abscopal antitumor immune responses. *Science Immunology* **6**, eabg0117, doi:10.1126/sciimmunol.abg0117 (2021).
- 97 Beyranvand Nejad, E., Welters, M. J. P., Arens, R. & van der Burg, S. H. The importance of correctly timing cancer immunotherapy. *Expert Opinion on Biological Therapy* **17**, 87-103, doi:10.1080/14712598.2017.1256388 (2017).
- 98 Voorwerk, L. *et al.* Immune induction strategies in metastatic triple-negative breast cancer to enhance the sensitivity to PD-1 blockade: the TONIC trial. *Nature medicine* **25**, 920-928, doi:10.1038/s41591-019-0432-4 (2019).
- 99 Gao, J. *et al.* VISTA is an inhibitory immune checkpoint that is increased after ipilimumab therapy in patients with prostate cancer. *Nature medicine* **23**, 551-555, doi:10.1038/nm.4308 (2017).
- 100 Doorduijn, E. M. *et al.* TAP-independent self-peptides enhance T cell recognition of immune-escaped tumors. *The Journal of clinical investigation* **126**, 784-794, doi:10.1172/jci83671 (2016).
- 101 Brown, C. E. & Mackall, C. L. CAR T cell therapy: inroads to response and resistance. *Nature reviews. Immunology* **19**, 73-74, doi:10.1038/s41577-018-0119-y (2019).
- 102 Snyder, A., Morrissey, M. P. & Hellmann, M. D. Use of Circulating Tumor DNA for Cancer Immunotherapy. *Clinical Cancer Research* **25**, 6909, doi:10.1158/1078-0432.CCR-18-2688 (2019).

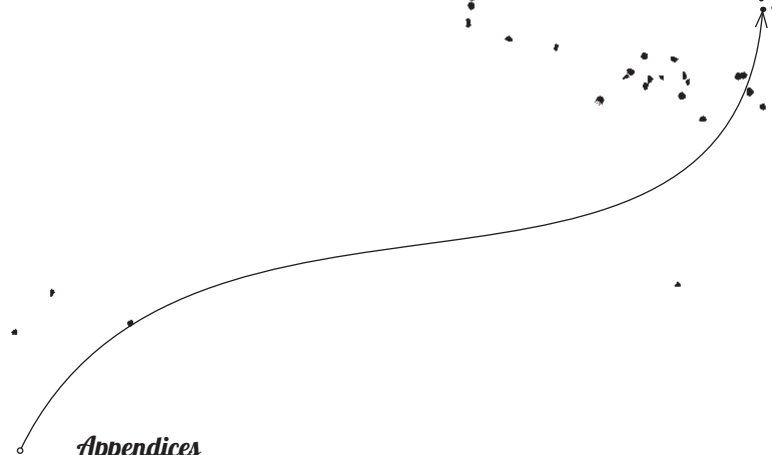


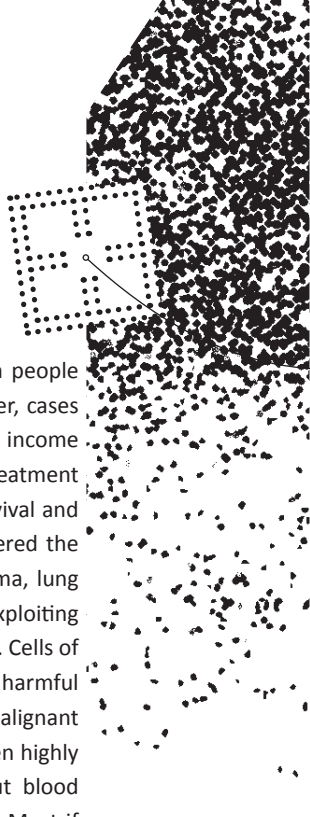
ENGLISH SUMMARY	269
NEDERLANDSE SAMENVATTING	277
DANKWOORD	285
LIST OF PUBLICATIONS	291
ABOUT THE AUTHOR	295
ABOUT THE COVER	301





ENGLISH SUMMARY





Cancer is one of the leading causes of death worldwide with nearly 20 million people being diagnosed with cancer causing almost 10 million deaths in 2020. Moreover, cases are expected to increase by 50% in the next 20 years especially in low- to middle income countries. When cancer is diagnosed at an advanced disease stage, conventional treatment options often include radio-, chemo or molecular therapy to extend patient survival and improve cancer-related symptoms. In the last decade, immunotherapy has entered the stage as a promising treatment for a wide variety of cancers including melanoma, lung cancer and leukemia. Whereas radio-, chemo and molecular therapies work by exploiting enhanced cell division or growth in tumor cells, immunotherapy works differently. Cells of our immune system called T cells patrol our body for potential threats including harmful bacteria or viruses, but also tumor cells which differ slightly from healthy non-malignant cells. However, when T cells reach the tumor, they encounter a complex and often highly immune suppressive ‘microenvironment’ containing not only cancer cells, but blood vessels and other immune cells that prevent T cells from destroying the tumor. Most if not all immunotherapies convalesce at an improved capacity of T cells to recognize and lyse tumor cells. Of the many different immunotherapeutic approaches that are currently being employed, immune-checkpoint blockade (ICB) is most frequently used in the clinic. In short, ICB regimens consist of blocking antibodies to key ‘checkpoint’ proteins on the T cell surface that function as molecular brakes to keep these cells in check. Blocking the checkpoints causes T cells to become increasingly activated and destroy tumor cells. Alternatively, anti-tumor T cells can be generated by cancer vaccines (similar to e.g. a vaccine directed against COVID-19) or modified and cultured in the laboratory to be infused in patients. Although a proportion of patients display significant reduction or even complete eradication of disease following immunotherapy, the majority become resistant and relapse. An improved mechanistic insight into how and where immunotherapies act, and how efficacy may be increased by combining different treatment modalities (e.g. ICB and specific chemotherapy) will likely improve survival of cancer patients. In this thesis, we have attempted to elucidate the working mechanisms of several immunotherapies which are summarized below.

In **Chapter 1**, key concepts in basic oncology and immunology are introduced. For cancers to occur, several demands need to be met, including unperturbed cell growth, increased survival, and sufficient blood vessel formation. These ‘hallmarks’ of cancer biology also include evasion from the immune system and chronic inflammation which further fuels tumor growth. Research from the last decade has shown that instead of contributing to one process individually, one hallmark can influence several others at the same time (e.g. one mutation causing relentless growth of tumor cells may also prevent T cells from properly infiltrating the tumor). These insights have improved our understanding of how

ENGLISH SUMMARY

cancers thwart the immune system and how we can manipulate these processes to our advantage (e.g. by combining immunotherapy with drugs preventing excessive cell growth or blood vessel formation). The second concept crucial to our understanding of cancer evolves around the notion of cancer being a systemic disease affecting the entire body rather than a tumor within a particular organ. In this model of a tumor *macro*-, rather than microenvironment, tumors influence not only the immune cells within the tumor itself but more extensively corrupt connected lymph nodes, bone marrow and even prime immune cells in distant organs for future metastasis. Therefore, in order to combat cancer, an effective and systemic immune response is needed to ensure durable cancer remissions. An improved insight into the role of the tumor macroenvironment in regulating systemic antitumor immunity will be essential to understand resistance and design novel therapies for cancer patients.

In the following chapters, novel insights and approaches aimed at promoting effective systemic immunity are discussed in two parts. In **Part A**, new mechanisms of action of two frequently used anticancer therapies are elucidated, namely anti-PD-L1 ICB (Chapter 2) and gemcitabine chemotherapy (Chapter 3). As mentioned above, ICB antibodies have long been thought to activate T cells in the tumor microenvironment, thereby leading to tumor destruction in patients. The majority of patients, however, do not respond or respond only temporarily to these drugs. Lymph nodes are key organs in the tumor macroenvironment by facilitating an environment where T cells can be primed and expand before they infiltrate the tumor. In **Chapter 2** we assessed lymph nodes most proximal to the tumor (tumor-draining lymph nodes; TDLNs) and investigated whether they could be involved in ICB-efficacy. We found anti-tumor T cells in TDLNs to express high levels of inhibitory checkpoint proteins on the cell surface acting as molecular brakes preventing them from reaching the tumor and having effect. To assess whether these cells are responsive to ICB immunotherapy we developed a method to specifically target T cells in the TDLN with ICB antibodies. Using this approach, we could show that ICB antibodies work, in part, by activating T cells in TDLNs that in turn migrate to tumors where they have their effect. Blocking T-cell egress from TDLNs, abrogated immunotherapy responses, showing TDLNs are essential targets for ICB immunotherapy. Lastly, we discovered that melanoma patients harboring high levels of immune checkpoints on T cells in their TDLNs were more likely to have metastatic disease in the future, indicating that these patients might benefit from ICB therapy after surgery.

Chemotherapies are thought to act primarily by inhibiting tumor cell growth leading to cell death. How chemotherapies affect the immune system of cancer patients is largely unclear. In **Chapter 3** we studied the effects of gemcitabine chemotherapy on the circulating

immune cells in mesothelioma cancer patients. Compared with patients not receiving gemcitabine therapy, immune suppressive cells (including myeloid-derived suppressor cells, regulatory T cells) were found to be decreased in frequency or proliferation rate following gemcitabine. On the other hand, anti-tumor immune cells including T cells and natural killer (NK) cells showed increased cell division compared to non-gemcitabine-treated patients. Furthermore, activation status of T and NK cells was increased following gemcitabine treatment as was indicated by elevated expression of co-stimulatory molecules on the cell surface. Concurrently, expression of the PD-1 checkpoint was also increased suggesting potential combination treatment efficacy with gemcitabine and ICB antibodies. Lastly, some of the aforementioned dynamics in T- and NK-cell phenotype correlated with improved response to gemcitabine treatment, suggesting that gemcitabine-related immune alterations could directly affect patient outcome. This study shows that in addition to targeting tumor cell directly, gemcitabine is highly immunomodulatory which is important for future studies assessing the effect of gemcitabine-immunotherapy combination treatment in patients.

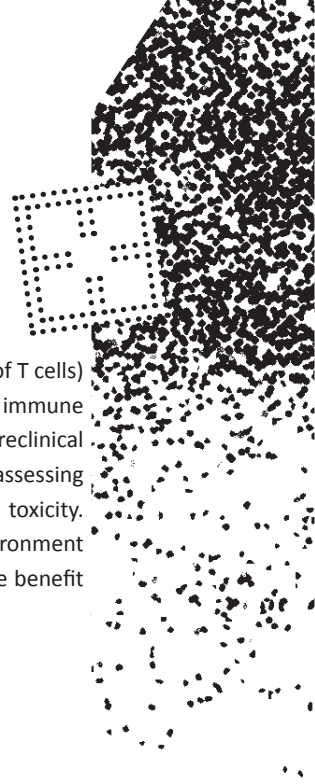
Besides ICB antibodies and immunogenic chemotherapy, cancer vaccination is another potent strategy to induce immune responses to cancer with the aim of decreasing tumor burden. In contrast to previously highlighted cancer therapies, vaccines are often highly specific to faulty or overly abundant proteins on the tumor cell surface (so called 'tumor-antigens'), resulting in few off-target side effects. Cancer vaccines can be subdivided into peptide vaccines or cellular vaccines including dendritic cell (DC) therapy. DCs are potent antigen presenting cells meaning that they pick up antigen (e.g. foreign particles) and present these to T cells in lymph nodes thereby activating them to neutralize existing threats. In the case of DC-therapy, DCs are cultured or extracted from patient blood, followed by a loading step with peptide or tumor material in the culture medium, activation with an adjuvant and infusion into the patient. The response to cancer vaccines can be highly variable depending on the design, target and adjuvant included in the vaccine but often patients respond only temporarily. In **Part B** of this thesis, new cancer vaccine strategies were investigated by targeting key modes of resistance in the tumor macroenvironment that could hamper clinical vaccine efficacy. First, to assess which vaccines hold promise in cancer treatment, Part B commences with a systematic analysis of the efficacy of cancer vaccines in the treatment of lung cancer (**Chapter 4**). By collecting and combining a multiple vaccine trials, improved efficacy over best supportive care of placebo could be demonstrated. By comparing cellular and peptide vaccine approaches, we demonstrated improved efficacy of cellular vaccines over peptide vaccines.

ENGLISH SUMMARY

Vaccine efficacy may be compromised at several steps in the formation of a systemic immune response. T cells induced by vaccines need to migrate from lymph nodes into the tumor where they have the capacity to kill unless perturbed by immune suppressive cells. One major and potent immune suppressive immune cell is the macrophage. In **Chapter 5**, we tested whether depletion of macrophages using a specific drug could render DC-therapy more effective in mouse models of cancer. To this end we studied the effect of macrophage depletion and DC-therapy in mesothelioma tumor models, as these tumors are notoriously rich in macrophages, also in patients. Similar to the patient setting, DC-therapy prolonged survival in tumor mice but eventually nearly all mice died from their mesotheliomas. Depletion of macrophages had no effect by itself, but when combined with DC-therapy, survival was significantly improved with a majority of mice being cured. Macrophages have the ability to change from immune suppressive to immune stimulatory (or vice versa) depending on signals from their environment. Switching macrophages to an immune stimulatory phenotype rather than depleting them could be even more potent in improving cancer vaccine efficacy. We tested this hypothesis in **Chapter 6**, by using an antibody to activate a stimulatory molecule called CD40 which is expressed on both macrophages and DCs. We found that activation of this molecule was capable of skewing previously immune-suppressive macrophages to immune-stimulatory ones, thereby improving mesothelioma survival in mice. Also, treatment with activating antibodies to CD40 sensitized mice with aggressive immunotherapy-resistant pancreatic cancer to the effects of DC-therapy. This finding uncovered a novel potent treatment strategy, which is currently tested in patients. In **Chapter 7** we investigated a novel target potentially involved in macrophage skewing called Janus Kinase 3 (JAK3), which is a critical signal transducer downstream from various cytokine receptors. Besides being expressed in macrophages, JAK3 is expressed by many other immune cells including T cells. Whereas JAK3 was capable of altering macrophages in culture plates, treatment in mice did not result in macrophage skewing. Because JAK3-inhibition at the correct dosing regimen did decrease tumor size, we further investigated its mode of action. We found that T cells were positively affected by JAK3-inhibition in tumors, with T cells displaying a more activated profile. Although monotherapy with JAK3-inhibition was modestly effective, combination therapy with a peptide or DC-vaccine further improved responses in mouse tumor models. Where in the tumor macroenvironment and how JAK3-inhibition specifically stimulates T cells and whether cancer patients will benefit remains to be further investigated.

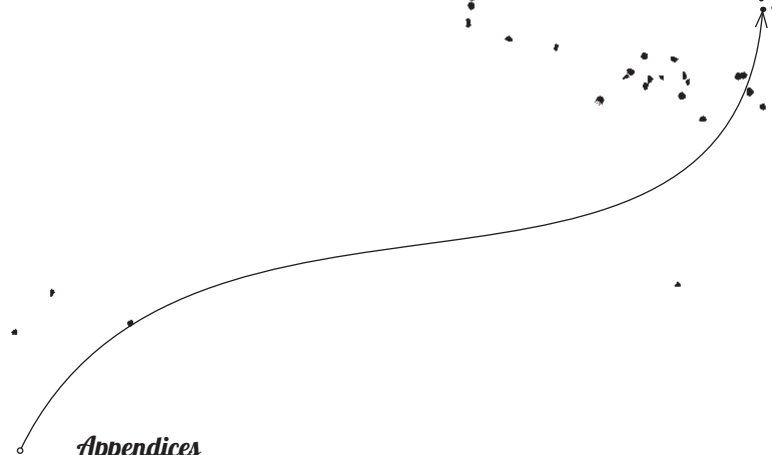
This thesis concludes with a discussion in **Chapter 8**, where the findings are put into context. In addition, novel research aims and perspectives are put forward to further increase our understanding of effective anti-tumor immunity and immunotherapy. These include a comprehensive analysis of key hubs in the tumor macroenvironment (focusing

on TDLNs and colonizing immune cells such as macrophages and different types of T cells) using novel techniques to determine why some patients form proper anti-tumor immune responses and others do not. In addition, aforementioned results obtained from preclinical models should be extrapolated to carefully designed clinical trials in patients, assessing whether responses to immunotherapy can be improved without increased toxicity. 'Unchaining immunity' through rational modulation of the tumor macroenvironment might prove pivotal in launching the next generation of immunotherapies for the benefit of patient care.





NEDERLANDSE SAMENVATTING



Appendices

Kanker is een van de meest voorkomende oorzaken van sterfte wereldwijd met bijna 20 miljoen nieuwe patiënten en 10 miljoen doden in 2020. Daarnaast wordt er een stijging van 50% aan nieuwe patiënten over de komende 20 jaar verwacht, met name in laag- en middeninkomen landen. Indien kanker zich in een gevorderd stadium bevindt, bestaan de huidige conventionele behandelingen meestal uit chemotherapie, bestraling en moleculaire therapieën om zo overleving en kanker-gerelateerde klachten te verbeteren. In de laatste jaren is immuuntherapie erbij gekomen als een veelbelovende behandeling voor een groot aantal type kankers waaronder longkanker, melanoom en leukemie. De eerder genoemde conventionele therapieën werken door in te grijpen op de celdeling van kankercellen. Immuuntherapie grijpt niet direct op de celdeling aan, maar heeft als doel het afweersysteem te 'ontketenen' en te richten tegen de tumor zelf. Een specifieke cel van ons afweersysteem genaamd de 'T cel' is cruciaal in dit proces en vrijwel alle immuuntherapieën hebben als gedeelde noemer het activeren van T cellen die zich vervolgens tot de tumor richten. Een veelgebruikte methode is immuun-checkpointblokkade (ICB) waarbij blokkerende antistoffen gericht tegen zogenaamde 'checkpoints' op de T cel zorgen voor verhoogde T-celactiviteit en dus tumorafbraak. Een alternatieve methode is het induceren van anti-tumor T cellen door vaccins te geven die een afweerrespons gericht tegen eiwitten op de kankercel aanwakkeren. Dit kan zowel via een vaccin dat tumoreiwitten en immuun-activerende stoffen bevat (lijkend op bijv. het COVID-19 vaccin) of via gekweekte afweerellen uit het laboratorium die T cellen instrueren de kanker aan te vallen (dendritische-cel therapie). Ondanks dat een deel van de patiënten reageert of zelfs geneest dankzij immuuntherapie, treedt vaak resistentie op en groeit de tumor door of komt deze terug ondanks therapie. Een beter inzicht in hoe verschillende immuuntherapieën werken, en hoe effectiviteit versterkt kan worden door therapieën met elkaar te combineren (bijv. immuuntherapie en chemotherapie) kan de overleving van patiënten met kanker verbeteren.

In **hoofdstuk 1** worden sleutelbegrippen uit de oncologie en immunologie geïntroduceerd. Voordat kanker ontstaat moet een tumor aan enkele basisbehoeften voldoen zoals ongelimiteerde celgroei, verbeterde overleving en voldoende bloedvoorziening. Inzichten aan het begin van deze eeuw hebben aangetoond dat naast deze reeds bekende basisbehoeften, het ontwijken van ons immuunsysteem ook essentieel is om kanker te ontwikkelen. De laatste jaren is steeds meer duidelijk geworden hoe tumoren hiertoe in staat zijn. Het blijkt dat dezelfde genetische afwijkingen die zorgen voor ongestoorde celgroei, tegelijkertijd kunnen zorgen dat bijvoorbeeld T cellen minder goed de tumor kunnen bereiken. Dit betekent dat het wellicht wenselijk is om middels combinatiebehandelingen te interveniëren in meerdere processen die leiden tot tumorprogressie om zo de kans op genezing te verbeteren. Het tweede concept cruciaal voor ons begrip van de relatie

NEDERLANDSE SAMENVATTING

tussen kanker en het immuunsysteem centreert zich om de bevinding dat kanker (zelfs in niet-uitgezaaide vorm) een systemische ziekte is in plaats van een orgaan specifieke ziekte. In dit model van een *macro*- in plaats van *micro*-omgeving ('environment') beïnvloed de tumor niet enkel cellen in zijn directe omgeving (micro) maar organen in de buurt (bijv. lymfeklieren) en op afstand (bijv. de milt of de longen, zelfs voordat er uitzaaiingen zijn). Daarom zal een effectieve *systemische* immuunrespons tegen de kanker onontbeerlijk zijn om langdurige controle van ziekte te bereiken. Een verbeterd inzicht in de betrokken elementen van de tumor macro-omgeving en hoe zij bijdragen aan de systemische anti-tumorrespons kan hier verder aan bijdragen.

In de volgende hoofdstukken zullen nieuwe inzichten en aangrijpingspunten voor een effectieve immuunrespons tegen kanker besproken worden in twee delen. In **deel A** worden nieuwe werkingsmechanismen van twee veelgebruikte anti-tumor therapieën besproken, zijnde (anti-PD-L1) ICB (hoofdstuk 2) en chemotherapie middels gemcitabine (hoofdstuk 3). Zoals eerder benoemd werken ICB antistoffen door het remmen van checkpoints op T cellen waarbij de T cel zich vervolgens tegen de tumor richt. Voor lange tijd werd gedacht dat dit met name T cellen in de tumor micro-omgeving betrof. Uit voorgaande studies blijkt dat de aanwezigheid van checkpoints in de tumor echter maar matig voorspelt of iemand baat gaat hebben bij ICB of niet. In **hoofdstuk 2** hebben we ons daarom gericht op lymfeklieren dicht gelegen bij de tumor (tumor-drainerende lymfeklieren) gezien deze klieren belangrijk zijn voor het initieel activeren van anti-tumor T cellen. Hiervoor werd gebruik gemaakt van meerdere muismodellen voor kanker. We vonden dat T cellen in tumor-drainerende lymfeklieren onder controle stonden van checkpoints, in tegenstelling tot T cellen in klieren op afstand. Door het specifiek blokkeren van deze checkpoints in tumor-drainerende lymfeklieren met ICB antistoffen konden we aantonen dat deze T cellen vervolgens meer effectief werden en meer aanwezig waren in de tumor. Wanneer T cellen de lymfeklier niet konden verlaten, doordat we het vertrek uit de lymfeklier blokkeerden, zagen we dat het anti-tumor effect van ICB antistoffen verloren ging. Deze en andere proeven tonen dat tumor-drainerende lymfeklieren essentiële organen zijn in de systemische anti-tumor respons na ICB-immunotherapie. Dat dit mogelijk ook relevant voor patiënten is blijkt uit analyses van tumor-drainerende lymfeklieren in de buurt van melanomen. Patiënten die na een operatie alsnog uitzaaiingen ontwikkelden hadden T cellen in de lymfeklier die sterk onder controle stonden van checkpoints. Patiënten die geen uitzaaiingen kregen hadden dit niet of in mindere mate. Deze eerste groep patiënten zou potentieel baat kunnen hebben bij ICB na de operatie om zo een later recidief van het melanoom te voorkomen.

Naast immuuntherapie wordt chemotherapie nog steeds veelvuldig toegepast. Hoe verschillende chemotherapieën het immuunsysteem van patiënten met kanker beïnvloeden is nog grotendeels onbekend. In **hoofdstuk 3** hebben we immuuncellen in het bloed van mesotheliom (asbestkanker) patiënten bestudeerd die behandeld werden met gemcitabine chemotherapie. Hierbij vonden we dat patiënten behandeld met gemcitabine een daling van afweerremmende cellen in het bloed toonden in tegenstelling tot onbehandelde patiënten. Tegelijkertijd waren cellen betrokken bij een afweerreactie tegen de tumor (T-cellen en natuurlijke killer [NK] cellen) juist meer aan het delen en geactiveerd. Daarnaast was dezelfde checkpoint die op T cellen werd bestudeerd in hoofdstuk 2 sterker aanwezig op T cellen na gemcitabine behandeling wat mogelijk impliceert dat ICB samen met gemcitabine een potentiële combinatiebehandeling zou kunnen zijn. Tevens konden we aantonen dat meerdere veranderingen op immuuncellen correleerden met de overlevingsduur van patiënten na gemcitabine wat zou kunnen wijzen op directe betrokkenheid van deze cellen in de anti-tumor respons. Toekomstige studies zijn nodig om bovenstaande associaties te bevestigen en de effectiviteit van gemcitabine-ICB antistof combinatietherapie te onderzoeken.

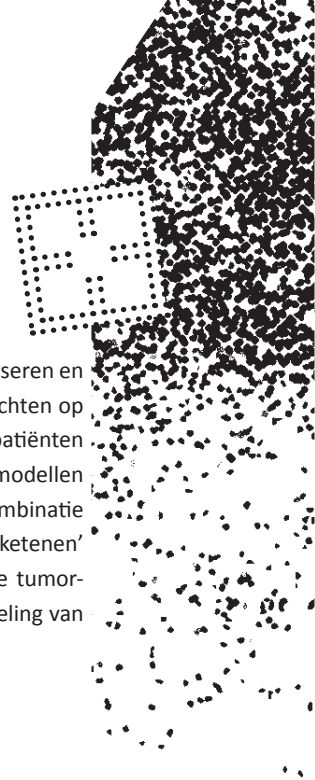
Een andere potente strategie om anti-tumor immuniteit te induceren is het gebruik van tumor vaccins. Anders dan voorgaande therapieën, wekken vaccins een afweerrespons op die uitermate specifiek is voor hetgeen waartegen ze gericht zijn (bijv. een eiwit dat op de tumor maar niet elders aanwezig is) met hierdoor weinig bijwerkingen. Vaccins zijn onder te verdelen in peptide vaccins en cellulaire vaccins waaronder dendritische celtherapie (DC-therapie). DCs zijn in staat om vreemd materiaal (bijvoorbeeld eiwitten uit de tumor) op te nemen en te presenteren aan T cellen waarna deze zich vermenigvuldigen om vervolgens het doel te elimineren. Met DC-therapie worden DCs direct gewonnen of gekweekt uit bloed van patiënten, in een kweekplaat blootgesteld aan tumoreiwitten en na activatie met een adjuvans weer terug gegeven aan de patiënt. De effectiviteit van kankervaccins is wisselend en is waarschijnlijk afhankelijk van het ontwerp, de target en het type adjuvans dat is toegevoegd aan het vaccin. Toch reageert maar een deel van de patiënten op kankervaccins voor nog onduidelijke redenen. In **deel B** van dit proefschrift hebben we kankervaccins verder bestudeerd in de context van de tumor macro-omgeving en vervolgens rationele combinatiestrategieën onderzocht om de werking van kankervaccins te verhogen. Deel B begint met een systematische analyse van de effectiviteit van verschillende kankervaccins bij longkanker patiënten (**hoofdstuk 4**). Door meerdere studies met elkaar te combineren konden we een klinisch voordeel van kankervaccins aantonen boven placebobehandeling. Tevens vonden we verhoogde effectiviteit van cellulaire vaccins vergeleken met peptide vaccins.

NEDERLANDSE SAMENVATTING

Uit voorgaande studie bleek dat cellulaire vaccins effectief konden zijn in patiënten met longkanker, maar dat een deel van de patiënten niet of onvoldoende lijkt te reageren. In de volgende hoofdstukken is getracht om effectieve combinatiebehandelingen te ontdekken om zo kankervaccinatie voor een bredere groep patiënten effectief te maken. Het induceren van een anti-tumor T cel reactie middels vaccinatie kan op meerdere momenten en plekken in de tumor-macro omgeving verstoord worden. Een belangrijk en frequent aanwezig celtype in de tumor en daarbuiten is de macrofaag. Macrofagen zijn betrokken bij meerdere processen in het lichaam, zoals het opruimen van dood celmateriaal en het in gang zetten van een ontstekingsreactie. Ook zijn ze potentieel afweerremmend waarbij eerder onderzoek heeft aangetoond dat dit een rol kan spelen in het teniet doen van een effectieve anti-tumor respons in patiënten. In **hoofdstuk 5** hebben we onderzocht of het verwijderen (depletieren) van macrofagen voor een sterkere immuunreactie zorgt in combinatie met DC-therapie in muizen. Net als in patiënten was DC-therapie effectief in een deel van de muizen, maar trad uiteindelijk toch tumorgroei op. Macrofaagdepletie leidde tot een duidelijk verbeterde vaccinatie respons waarbij vrijwel alle muizen genezen waren van hun tumoren. Zoals eerder genoemd kunnen macrofagen ook een ontstekingsreactie in gang zetten. In **hoofdstuk 6** hebben we onderzocht of we in plaats van het verwijderen van macrofagen, ze kunnen aanzetten tot ondersteuning van de anti-tumor T cel respons. Hiervoor werd gebruik gemaakt van een activerend antistof tegen het molecuul CD40, wat zowel op macrofagen als DCs aanwezig is. We vonden dat deze aanpak evenals het verwijderen van macrofagen uiterst effectief in muismodellen van kanker was. Tevens was het in staat om de overleving van muizen met een moeilijk te behandelen vorm van alveolairkanker te verbeteren; dit in tegenstelling tot alleen anti-CD40 behandeling of DC-therapie. Deze vorm van behandeling zal binnenkort in patiënten onderzocht worden. Ten slotte werd er in **hoofdstuk 7** een nieuwe target onderzocht in macrofagen; Janus-kinase 3 ofwel JAK3. Waarbij macrofagen in kweekplaten goed reageerden op JAK3-remming en verminderd afweerremmend leken kon dit effect in muismodellen niet aangetoond worden. Toch leefden muizen bij de juiste dosering en toedieningswijze langer met JAK3-remming dan zonder. Uiteindelijk bleek directe modulering van T cellen bij te dragen aan het therapeutische effect van dit nieuwe middel. Tevens kon zowel de werkzaamheid van peptide- als DC-vaccinatie verbeterd worden in muizen. Aanvullende studies in muizen gevolgd door patiëntstudies zullen de werkzaamheid van dit middel verder moeten bevestigen.

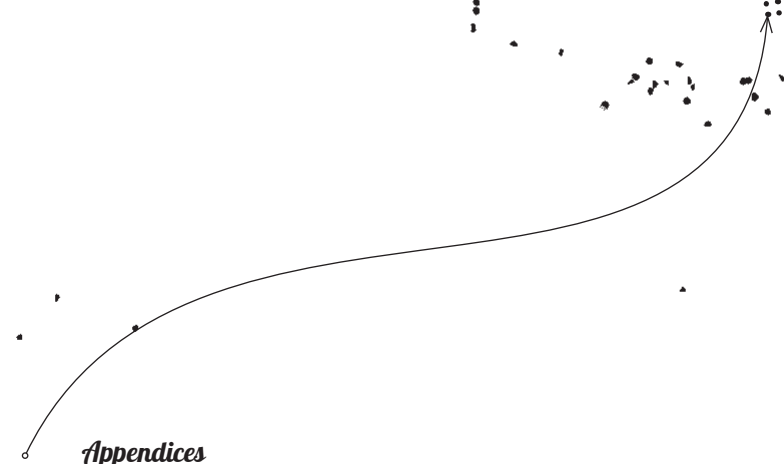
Dit proefschrift sluit af met een samenvatting van de bevindingen en het plaatsen van deze in de huidige literaire context in **hoofdstuk 8**. Daarnaast worden nieuwe onderzoeksvragen uitgezet die onze kennis van anti-tumor immuniteit en immuuntherapie verder kunnen verbeteren. Belangrijk hiervoor is het gebruik van nieuwe technieken die men in staat stelt

om de complexe architectuur van organen in de tumor macro-omgeving te visualiseren en te analyseren. Op basis van bovenstaande bevindingen zal deze zich allereerst richten op T cellen, macrofagen en DCs in tumoren en tumor-drainerende lymfeklieren in patiënten met verschillende kankersoorten. Daarnaast zullen opgedane inzichten uit muismodellen in studieverband bij patiënten onderzocht moeten worden om vast te stellen of combinatie immuuntherapie veilig is en meerwaarde heeft boven monotherapie. Het 'ontketenen' van het immuunsysteem door op een rationele, veilige en effectieve manier de tumor-macro omgeving te moduleren kan zo een nieuwe impuls brengen in de behandeling van patiënten met kanker.





DANKWOORD



Appendices

Mijn wetenschappelijke carrière, tot heden vertaald in dit proefschrift, heb ik aan vele bijzondere mensen te danken. Hun bijdrage; groot of klein, in het Erasmus MC of daarbuiten, in het verleden, het nu en in de nabije toekomst is niet te onderschatten. Graag zou ik een aantal personen specifiek willen uitlichten, om maar te beginnen bij het begin.

Waar vele dankwoorden eindigen met de belangrijkste persoon in je leven zal deze er mee starten, ook omdat met haar ontmoeting mijn wetenschappelijke avontuur begon. Lieve Linda, toen wij elkaar ontmoetten tijdens de Infection & Immunity Research Master 8 jaar geleden vond je me maar een eigenwijze knurft. Toch sloeg de vonk over. Snel werd duidelijk dat we tegen elkaar waren opgewassen, maar nog belangrijker dat we echt synergetisch waren en nog steeds zijn. Samen jonge ambitieuze dokters en promovendi in het lab zijn vroeg geregeld om 'gecondenseerd genieten' waarin we onze passies voor cultuur (lang weekend impressionisten in Parijs), haute cuisine (voor Hiša Franko naar Slovenië) en ontspanning (Bounty-eiland Mauritius) samen deelden. Trots was ik op je toen je in 2019 *cum laude* promoveerde en aangenomen werd als internist in opleiding maar nog trotser was ik hoe je met het verlies van Felix om ging in datzelfde najaar. De kruisbestuivingen tussen onze werelden werpen nog dagelijks zijn vruchten af en met jouw toekomst als internist-oncoloog kunnen we als droomteam kankerzorg en onderzoek verder verbeteren. Kruisbestuiving anderszins leidde in 2020 tot de geboorte van ons grootste meesterwerk; Caspar. Lieve Caspar, de compensatiedagen waarin ik mijn discussie zat te schrijven met jou en *Dora the Explorer* tegenover mij waren magisch. Menig typo in dit boekje is het gevolg van onze tussentijdse knuffelpartijen waarvoor excuses aan de lezer.

Ik wil graag mijn promotoren bedanken voor hun bijdrage aan dit boekje en mijn ontwikkeling als wetenschapper. Prof. Aerts, beste Joachim, al vroeg keek ik bij je af wat de uitdagingen zijn van een bestaan als medisch specialist en wetenschapper. Toch liet jij me inzien wat de mogelijkheden zijn, en het feit dat ik mijn coschappen ben gaan doen en uiteindelijk voor longgeneeskunde heb gekozen is jou dan ook ten dele aan te rekenen. Ik heb geen minuut spijt gehad van deze keuze, waar ik dagelijks de voordelen zie van een dokter met een poot in de kliniek, en de ander in het lab om zo niet alleen op micro- maar ook op macroniveau het verschil te kunnen maken voor de patiënt. Niet geheel toevallig is dan ook dat de term *tumor macroenvironment* jouw vinding was in een van onze vele brainstormsessies. Jij hebt me altijd het volle vertrouwen en de financiële ruimte gegeven om onze ideeën tot uitvoering te kunnen brengen, met de artikelen in dit boekje als resultaat. Ik hoop onze samenwerking nog vele jaren te kunnen continueren als postdoc aan je afdeling. Prof. Hendriks, beste Rudi. Jij hebt mij onder je vleugels genomen tijdens de turbulente tijden in het lab en de 'tricks of the trade' als wetenschapper

DANKWOORD

bijgebracht. Jouw integriteit, betrouwbaarheid, maar boven alles brede immunologische basiskennis hebben mij gevormd tot de immunoloog die ik nu ben. Jouw ondersteuning en kennisoverdracht bij methodologische vraagstukken en het presenteren en opschrijven van data zullen mij immer bijblijven waarvoor dank. Prof. Van Hall, beste Thorbald. Alle goede dingen bestaan in drieën, zo ook mijn promotieteam. Ik herinner me nog onze eerste ontmoeting in Leiden, waarin ik met jou mocht stoeien over macrofagen en hun bijdrage in tumoren en daarbuiten. In plaats van argwaan, scepsis of verveling ontving je mij en mijn ideeën met open armen en nam je vaak uitgebreid de tijd onder het genot van een kopje bonenkoffie (hint: Erasmus MC). Jouw ervaring en internationale erkenning als tumor-immunoloog heeft diepgang gebracht in onze artikelen en ik ben trots op onze samenwerking. Tevens wil ik graag de leden van mijn kleine commissie bedanken voor het kritisch bestuderen en becommentariëren van mijn thesis, my sincere gratitude to Prof. Tanja de Gruijl, Prof. Reno Debets en Dr. Prasad Adusumilli. Ik wil graag de leden van de promotiecommissie bedanken voor het kritisch lezen van mijn proefschrift en de bereidwilligheid om deel te nemen aan mijn verdediging. Ik hoop op een uitdagende discussie en een mooie verdediging van mijn proefschrift.

Het laboratorium Longgeneeskunde is voor vele jaren mijn thuishaven geweest, mede dankzij de vele charmante collega's. Per enig toeval belandde ik in 2015 op de afdeling op zoek naar tumor-immunologisch onderzoek. Dr. Joost Hegmans stond aan de wieg van de *Thoracic Oncology Rotterdam Research Group (THORR)* met zijn baanbrekende onderzoek naar dendritische cel (DC) therapie bij asbestkanker. Beste Joost, dank voor je vrijgevigheid en je ondersteuning in mijn vroege fase als onderzoeker in opleiding. Beste Sanne, ik had uit geen beter nest kunnen komen. Dank voor de begeleiding en de gezelligheid, ik hoop dat we elkaar nog veel tegen gaan komen in ons mooie vakgebied. Zonder het analistenteam op de afdeling was dit boekje niet tot stand gekomen. Beste Menno, al snel waren wij twee handen op een (harige) buik met onze gedeelde interesses voor schilderkunst, film, en zo nu en dan een potje golf. Jij als geen ander begreep dat werken op het lab als een harmonica was; ten tijden van drukte en deadlines gingen we tot het gaatje maar konden we in incubatietijd ook prima naar musea, het terras en als stilistisch duo bureaulampen maken. Je hebt vele mensen op het lab zien komen en gaan, ik hoop dat onze vriendschap blijft. Dank dat je mijn paranimf wilt zijn. Dank ook aan de overige leden van het illustere *Bon Vivants*, Peter en Thomas, bedankt voor de mooie momenten die zijn geweest en nog gaan komen. Koen, bedankt voor mij op sleptouw nemen als jong broekie en je geduld tijdens het orde scheppen in de chaos die heette mijn labjournaal. Margaretha, Cynthia, Melanie en Larissa, dank voor jullie onuitputbare hulp met de experimenten en passie voor gedegen en hoogkwalitatief proefdieronderzoek. Dank Ralph en Anneloes voor jullie input en waardevolle bijdragen op het gebied van bio-informatica. Dank aan alle andere

analisten, PhD-studenten en Postdocs die zijn gekomen, weer gegaan en nog bezig zijn! Tevens dank aan alle mensen buiten afdeling longgeneeskunde en het Erasmus MC met wie ik met veel plezier heb samengewerkt en nog steeds doe; Prof. Peter Katsikis en Dr. Yvonne Mueller (Immunologie), Dr. Thierry van den Bosch en Dr. Jan von der Thüßen (Pathologie), Evalyn Mulder, Dr. Dirk Grünhagen en Prof. Kees Verhoef (Oncologische chirurgie), Dr. Sjaak Burgers en Dianne de Gooijer (Longgeneeskunde NKI-AVL), Dr. Sjoerd Schetters (VIB Gent) en Prof. Lidia Arends (Statistiek, Erasmus Universiteit Rotterdam). Beste Prof. Arends, dank voor uw durf en welwillendheid om samen te werken bij mijn eerste artikel.

Tijdens mijn promotieonderzoek heb ik een aantal super gemotiveerde en veelbelovende studenten mogen begeleiden, die op hun beurt een essentiële bijdrage hebben geleverd aan dit proefschrift. Te beginnen met Mandy. Beste Mandy, als een geschenk van boven mailde je mij via-via of je een afstudeerstage aan onze afdeling kon komen doen gericht op DC-therapie. Wat begon met intensief samenwerken en zo nu en dan schermutselingen groeide uit tot een duurzame, waardevolle en fijne samenwerking die hopelijk nog lang zal voortbestaan. Ik geniet van je humor, je arbeidsethos en de groei die we samen hebben doorgemaakt. Op naar het volgende hoofdstuk! Rachid, bedankt voor je harde werk en je gezelligheid tijdens onze reisjes, met als hoogtepunt Keystone in Whistler Canada waar jij je snowboardtalent demonstreerde. Vivian, jouw talent en zelfstandigheid voorspellen nog veel goeds voor de toekomst, ik hoop dat we dit samen verder kunnen gaan ontwikkelen en exploreren! Dank ook aan de mensen van Infection & Immunity die de nieuwe generatie immunologen van het Erasmus MC mede mogelijk maken; dank Jan en Astrid. Bedankt Frank voor je heerlijke can-do mentaliteit en je pragmatisme. Je hebt mij en Linda altijd ondersteund tijdens I&I en daarbuiten, met o.a. een prachtige cursus die we nu verder door ontwikkelen.

Naast wetenschap ligt mijn hart in de kliniek, waar ik geniet van een prachtige opleiding tot longarts. Dank aan Leon van den Toorn voor het vertrouwen door mij aan te nemen voor de opleiding tot longarts. Bedankt Prewesh Chandoesing voor het aanwakkeren van het vuur in mij dat me drijft een goede (generalistische) dokter te worden. Op diezelfde noot, dank aan alle dokters die mij tijdens mij coschappen de kunsten van het vak hebben geleerd, en altijd vol interesse naar mijn onderzoek vroegen en dit faciliteerden. Dank aan alle stafleden en assistenten maar ook verpleegkundigen die de afdeling Longgeneeskunde in het EMC tot de mooiste van Nederland maken. Ook wil ik het warme bad Ikazia bedanken, met name Dr. Felix de Jongh en Dr. Marieke Wabbijn als opleiders die me meteen thuis lieten voelen. Beste Dr. de Jongh, uw kennis en betrokkenheid bij uw patiënten zijn een inspiratiebron voor mij, ik hoop nog veel van u te mogen leren. Beste Dr. Wabbijn, bedankt

DANKWOORD

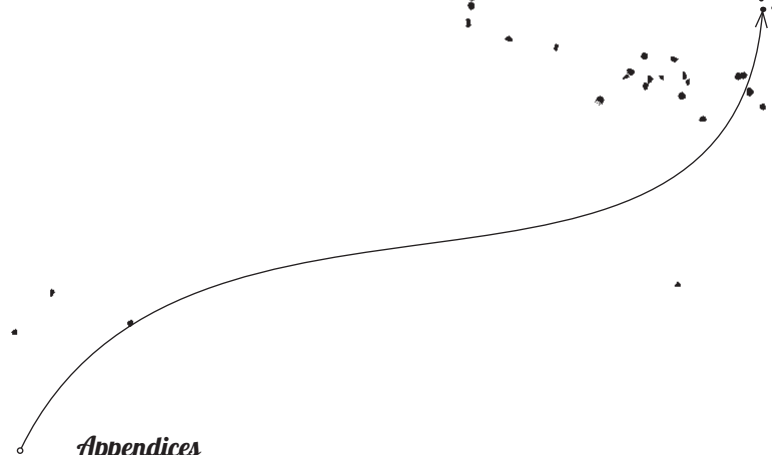
voor uw betrokkenheid bij ons als arts-assistenten en in het bijzonder bij mij in Linda in moeilijke tijden.

Er is ook een leven naast het lab, de kliniek en mijn gezin wat verder kleur krijgt door een trouwe groep vrienden met wie menig etentje, terrasje of stapavondje voor een goede afleiding zorgde tijdens dit promotieonderzoek. Bedankt Sai Ping voor de trouwe vriendschap de afgelopen jaren. Ik had nooit kunnen bedenken dat ons begin met I&I ons hier zou brengen, samen onderzoek doen en publiceren, niet te vergeten jouw gouden tijd in New York waar we elkaar meermaals ontmoet hebben. De vrienden van thuis, met name Bas, Daniele en Jeroen, dank voor jullie onvoorwaardelijke steun in dit proces. Lieve Elke, samen geneeskunde doorlopen en een promotieonderzoek was een genot, succes met je opleiding tot anesthesioloog! Lieve Sanne, soms lijkt mijn leven een blauwdruk van het jouwe. Jouw wetenschappelijke ambitie en verdiensten zijn bewonderingswaardig maar daarnaast ben en blijf je dezelfde vriendin van 15 jaar geleden. Heren van wijnclub *Vin du Roffa* en JC Taurus, bedankt voor de mooie avonden!

Van waar mijn promotie eindigt tot waar het ooit allemaal begon; bij mijn familie. Ten eerste mijn schoonfamilie, Cees, Marlies, Kevin en Mark. Ik kan me geen fijnere schoonfamilie wensen, van B&B tijdens mijn coschappen in Zeeland, tot weekendjes op de Waddeneilanden of een afzakkertje bij Schele Lau; bij jullie is het altijd feest en vertrouwd. Dank voor de mooie momenten en voor de velen die nog komen gaan. Voor mijn grootouders in Goirle en oma in Venlo, dank voor de interesse in mijn onderzoek en jullie steun. Beste Olaf, wat bof ik met jou als zwager! Lieve Maud, in goede of slechte tijden ben jij er altijd voor ons geweest. Wat een genot is het geweest om jou te zien groeien tot de succesvolle powervrouw die je nu geworden bent; ik ben trots op jou als paranimf. Lieve Joost, al vanaf jongs af aan trokken we samen op en dat is tijdens mijn promotie niet anders geweest. Het duurde even voor je je draai gevonden had in Rotterdam, maar oh wat ben ik jaloers op je nieuwe baan! Daarnaast ben je de beste vriend van Caspar en kan ik me zelf geen betere wensen. Lieve mam, de rol van powervrouw heeft Maud bij je afgekeken. Jij bent de lijm die ons gezin bij elkaar houdt en degene die een warm nest biedt voor de hele familie en iedereen daarbuiten. Jouw kracht en maatschappelijke engagement maken mij een trotse zoon. Ten slotte lieve pap, ik kan me jouw promotieonderzoek nog goed herinneren. De vakantie in Frankrijk waarbij jij in een aftands internetcafé een artikel moest indienen deed opvallend denken aan mijn laatste vakantie in Frankrijk waar ik bij 30 graden op een parkeerplaatsje zat te skypen in de auto met mijn promotoren. Je had me kunnen waarschuwen voor wat we me stond te wachten, maar je steunde me all the way. Je bent een voorbeeld voor mij als de hardwerkende betrokken medisch specialist die je bent, die toch nieuwsgierig en breed georiënteerd blijft. Samen zijn wij team Dammeijer op Pubmed, en dat maakt me trots!



LIST OF PUBLICATIONS





LIST OF PUBLICATIONS

Comments on 'High-intensity statins are associated with improved clinical activity of programmed cell death protein 1 inhibitors in malignant pleural mesothelioma and advanced non-small cell lung cancer patients'.

Cantini L, Pecci F, **Dammeijer F**, Aerts JGJV, Berardi R. European Journal of Cancer. 2021 Jun 18;S0959-8049(21)00325-7. doi: 10.1016/j.ejca.2021.05.016.

Immune monitoring in mesothelioma patients identifies novel immune-modulatory functions of gemcitabine associating with clinical response.

Dammeijer F, De Gooijer CJ, van Gulijk M, Lukkes M, Klaase L, Lieveense LA, Waasdorp C, Jebbink M, Bootsma GP, Stigt JA, Biesma B, Kaijen-Lambers MEH, Mankor J, Vroman H, Cornelissen R, Baas P, Van der Noort V, Burgers JA, Aerts JG. EBioMedicine. 2021 Feb;64:103160. doi: 10.1016/j.ebiom.2020.103160.

Switch-maintenance gemcitabine after first-line chemotherapy in patients with malignant mesothelioma (NVALT19): an investigator-initiated, randomised, open-label, phase 2 trial.

de Gooijer CJ, van der Noort V, Stigt JA, Baas P, Biesma B, Cornelissen R, van Walree N, van Heemst RC, Soud MY, Groen HJM, den Brekel AJS, Buikhuisen WA, Bootsma GP, **Dammeijer F**, van Tinteren H, Lalezari F, Aerts JG, Burgers JA; NVALT19 study group. Lancet Respiratory Medicine. 2021 Jun;9(6):585-592. doi: 10.1016/S2213-2600(20)30362-3

The PD-1/PD-L1-Checkpoint Restrains T cell Immunity in Tumor-Draining Lymph Nodes.

Dammeijer F, van Gulijk M, Mulder EE, Lukkes M, Klaase L, van den Bosch T, van Nimwegen M, Lau SP, Latupeirissa K, Schetters S, van Kooyk Y, Boon L, Moyaart A, Mueller YM, Katsikis PD, Eggermont AM, Vroman H, Stadhouders R, Hendriks RW, Thüsen JV, Grünhagen DJ, Verhoef C, van Hall T, Aerts JG. Cancer Cell. 2020 Nov 9;38(5):685-700.e8. doi: 10.1016/j.ccell.2020.09.001.

Dendritic cell vaccination and CD40-agonist combination therapy licenses T cell-dependent antitumor immunity in a pancreatic carcinoma murine model.

Lau SP, van Montfoort N, Kinderman P, Lukkes M, Klaase L, van Nimwegen M, van Gulijk M, Dumas J, Mustafa DAM, Lieveense SLA, Groeneveldt C, Stadhouders R, Li Y, Stubbs A, Marijt KA, Vroman H, van der Burg SH, Aerts J, van Hall T, van Eijck CHJ, **Dammeijer F**. Journal of Immunotherapy of Cancer. 2020 Jul;8(2):e000772. doi: 10.1136/jitc-2020-000772.

Het pancreascarcinoom: toch niet immuun voor therapie? Ontwikkelingen in de immuuntherapie voor ductaal adenocarcinoom van het pancreas.

Lau SP, **Dammeijer F**, van Eijck CHJ. Nederlands Tijdschrift voor Oncologie 2019;16:309–16

Combination Strategies to Optimize Efficacy of Dendritic Cell-Based Immunotherapy.

van Gulijk M, **Dammeijer F**, Aerts JGJV, Vroman H. Frontiers in Immunology. 2018 Dec 5;9:2759. doi: 10.3389/fimmu.2018.02759.

Current State of Dendritic Cell-Based Immunotherapy: Opportunities for in vitro Antigen Loading of Different DC Subsets?

Huber A, **Dammeijer F**, Aerts JGJV, Vroman H. Frontiers in Immunology. 2018 Dec 3;9:2804. doi: 10.3389/fimmu.2018.02804.

Role of Bruton's tyrosine kinase in B cells and malignancies.

Pal Singh S, **Dammeijer F**, Hendriks RW. Molecular Cancer. 2018 Feb 19;17(1):57. doi: 10.1186/s12943-018-0779-z.

Rationally combining immunotherapies to improve efficacy of immune checkpoint blockade in solid tumors.

Dammeijer F, Lau SP, van Eijck CHJ, van der Burg SH, Aerts JGJV. Cytokine Growth Factor Reviews. 2017 Aug;36:5-15. doi: 10.1016/j.cytogfr.2017.06.011.

Depletion of Tumor-Associated Macrophages with a CSF-1R Kinase Inhibitor Enhances Antitumor Immunity and Survival Induced by DC Immunotherapy.

Dammeijer F, Lieveense LA, Kaijen-Lambers ME, van Nimwegen M, Bezemer K, Hegmans JP, van Hall T, Hendriks RW, Aerts JG. Cancer Immunology Research. 2017 Jul;5(7):535-546. doi: 10.1158/2326-6066.CIR-16-0309

Immunotherapeutic strategies in non-small-cell lung cancer: the present and the future.

Steendam CM, **Dammeijer F**, Aerts JGJV, Cornelissen R. Immunotherapy. 2017 May;9(6):507-520. doi: 10.2217/imt-2016-0151.

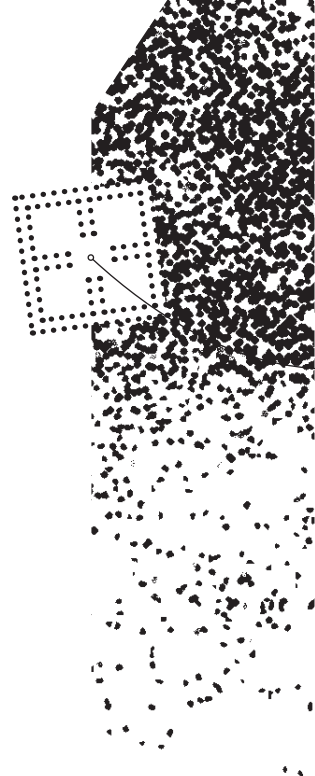
Efficacy of Tumor Vaccines and Cellular Immunotherapies in Non-Small-Cell Lung Cancer: A Systematic Review and Meta-Analysis.

Dammeijer F, Lieveense LA, Veerman GD, Hoogsteden HC, Hegmans JP, Arends LR, Aerts JG. Journal of Clinical Oncology. 2016 Sep 10;34(26):3204-12. doi: 10.1200/JCO.2015.66.3955.



ABOUT THE AUTHOR





ABOUT THE AUTHOR

Floris Dammeijer was born on the 7th of September 1992 in Maastricht, the Netherlands. In 1995 he moved with his parents to the city of Venlo where he spent a happy childhood with hobbies such as playing the piano and playing hockey. He completed his bilingual secondary school education (Athenaeum, International Baccalaureate English Higher Level, cum laude) at College Den Hulster Venlo in 2010. In the same year he moved to Rotterdam to start his medical training at the medical faculty of the Erasmus Medical Center in Rotterdam. He received his Bachelor of Science in Medicine in 2013. He postponed his further medical training as he first enrolled in the Master of Science program Infection and Immunity (Molecular Medicine Postgraduate School, Erasmus University Rotterdam). He graduated in 2015 (cum laude) with his thesis on *'Targeting macrophages in malignant mesothelioma to improve cancer immunotherapy'* for which he received the Nijbakker-Morra prize (best master thesis in oncology) in 2015.



In 2015 he commenced with the Master of Science program in Medicine from which he graduated and obtained his Dutch medical degree in August 2019 (cum laude). In 2015 he also started with a PhD project at the Department of Pulmonary Medicine Erasmus MC Rotterdam, Thoracic Oncology Research Group (group leader Prof. Dr. Joachim Aerts) of which the results are presented in this thesis.

In 2019 he started his residency training in pulmonary medicine whilst keeping a position as researcher at the Thoracic Oncology Research Group. He strives to become a pulmonologist being able to combine clinical work with conducting research in the field of immuno-oncology. Floris presently lives in Rotterdam, together with his wife Linda and their son Caspar.

PhD PORTFOLIO

Summary of PhD training, teaching activities and awards/funding

Name: F.H.W.P. Dammeijer
 Department: Dept. of Pulmonary Medicine, Erasmus Medical Center Rotterdam
 Research School: Molecular Medicine Postgraduate School
 PhD-period: 2015-2021
 Promotors: Prof. J.G. Aerts, Prof. R.W. Hendriks, Prof. T. van Hall

1. PhD training	Year	Workload (ECTS)
Courses		
Animal Article 9 Course on Animal Experimentation	2015	3.5
Scientific Integrity Course	2016	0.3
Good Clinical Practice (BROK)	2019	1.5
Presentations & Conferences		
Annual Cancer Immunology & Immunotherapy Conference CICON (AACR/CIMT/CRI/EATI), September 25-27, Paris France (Poster presentations)	2019	1.0
Annual Cancer Immunology & Immunotherapy Conference (AACR/CIMT/CRI/EATI), October 30- November 3, NYC, USA (poster presentation)	2018	1.2
Keystone Meeting Cancer immunology & Immunotherapy, March 20-23, Whistler, Canada. (poster presentation)	2017	1.2
European Asbestos Forum 2016, September 30, Amsterdam NL (invited speaker)	2017	0.6
IMIG 13th International Conference of the International Mesothelioma Interest Group (iMig) May 1-4, Birmingham UK (oral presentation)	2016	2.0
NVVI-BSI Joint Meeting, Liverpool, UK, December 6-9 (poster presentation)	2016	1.2
NVVI: Winter meeting 2015, December 16-17 (poster presentation)	2015	0.6
Annual MolMed day, Rotterdam	2015-2019	1.2
2. Teaching		
Supervisor of I&I Research Master Student: 9-month internship R. Bouzid, project entitled: Enhancing immunotherapeutic responses by targeting the tumor microenvironment: To BTK or not to BTK	2016-2017	5.0
Supervisor Biomedical Sciences Research Student: 9-month internship M. van Gulijk, project entitled: Investigating the Role of Myeloid Cells in Modulating Anti-Tumor T-cell Immunity	2017-2018	5.0
Supervisor I&I Research Master Student: 9-month internship K. Latupeirissa, project entitled: Identifying exhausted-T-cell precursor cells in tumor-draining lymph nodes	2019-2020	5.0
Supervisor I&I Research Master Student: 9-month internship V. Gerretsen, project entitled: Automatic quantification and prognostic relevance of exhausted-T-cell precursor cells in tumor-draining lymph nodes	2020-2021	5.0
Co-promotor PhD-student M. van Gulijk, on the subject of dissecting novel modes of anti-PD-1/PD-L1 checkpoint immunotherapy	2018-	5.0
Teacher at Skillslab. Course: 'Anatomy, Physiology and Immunology of the Skin'	2014-2016	1.0
Guest teacher Secondary School (Goes): the origins of cancer	2015-2018	1.2
Co-founder USMLE S.O.S., teacher and organizer USMLE Step 1 preparation course	2016-2020	3.0
Total ECTS		44.5


ABOUT THE AUTHOR

3. Awards and funding	Year	Amount
van Herk Fellowship, The fellowships are awarded in a very competitive selection to highly motivated professionals who are in a position to introduce the newly-acquired skills and knowledge into their research and PhD program)	2016	€ 180.000
Young Investigator Award at the IMIG 13th International Conference of the International Mesothelioma Interest Group (iMig 2016) 1-4th of May, Birmingham UK.	2016	£ 500
Nijbakker-Morra Thesis award: Enhancing Dendritic Cell Immunotherapy by Modulating the Tumor Microenvironment in a Mesothelioma Mouse Model; best thesis in oncology (NL)	2015	€ 1600



ABOUT THE COVER





For long, tumor immunology was considered a niche with only a few determined scientists pioneering a field that would later turn out to become the next frontier in cancer research. Stemming from earlier discoveries on the role and function of immune cells in cancer came drugs targeting surface molecules on T cells, thereby 'unchaining' them from their engaged existence. Both scientists and physicians try and direct these unchained T cells towards the cancer, while at the same time preventing collateral damage as toxicity. Still, only a minority of patients benefit durably from these efforts. Currently, a Wild West of clinical trials in patients has emerged where various treatments are combined in multiple cancer types with often little scientific rationale. By studying not only the cancer but its entire macroenvironment, novel and safe combination treatments can be designed with the aim of improving patient outcome.

Immunity Unchained

IMPROVING CANCER
IMMUNOTHERAPY
BY TARGETING THE TUMOR
MACRO-ENVIRONMENT